DELAYED FISSION NEUTRONS

PROCEEDINGS OF A PANEL, VIENNA, 24-27 APRIL 1967

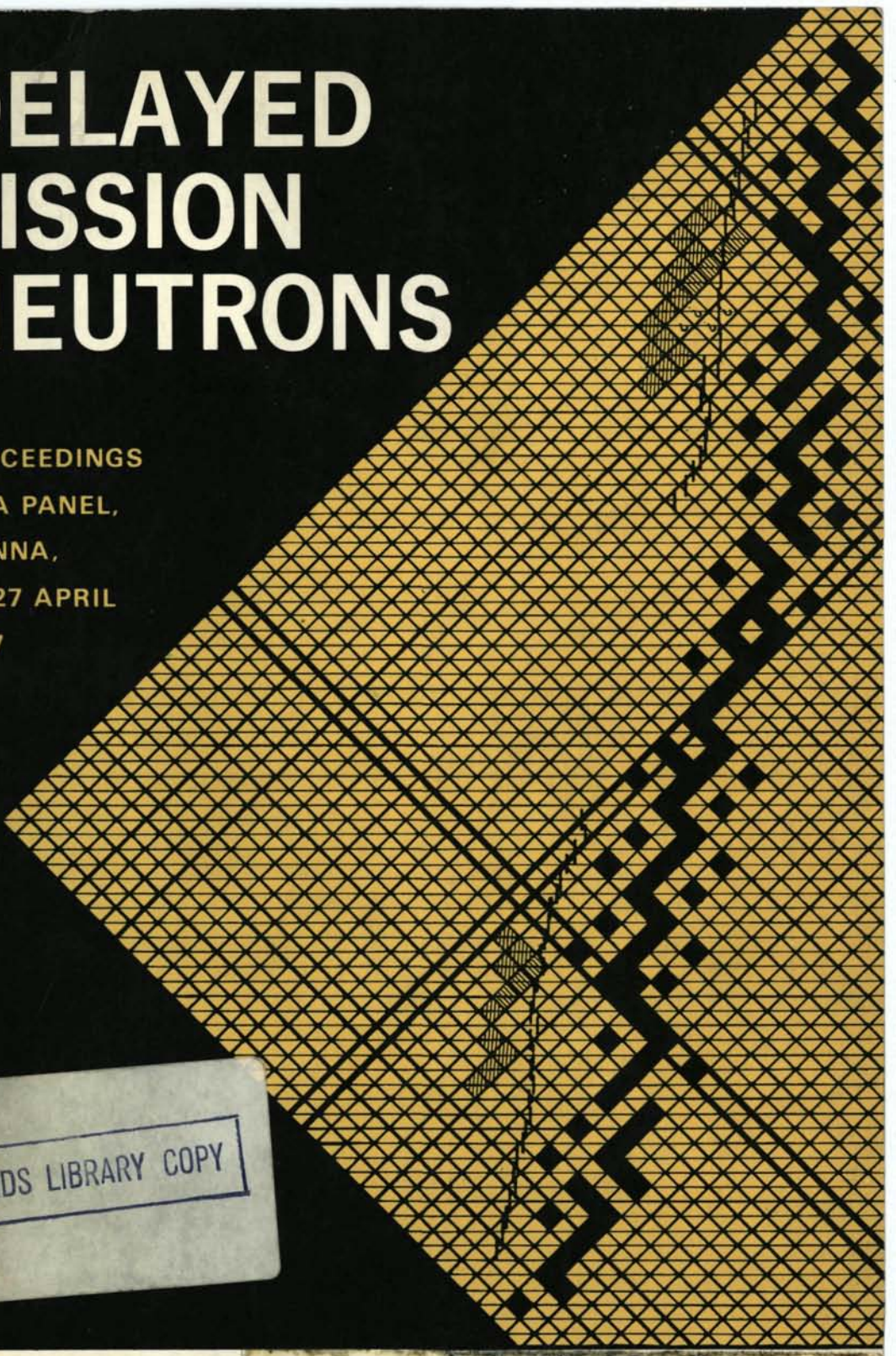

INTERNATIONAL ATOMIC ENERGY AGENCY, VIENNA, 1968

DELAYED FISSION NEUTRONS

The following States are Members of the International Atomic Energy Agency:

AFGHANISTAN
ALBANIA
ALGERIA
ARGENTINA
AUSTRALIA
AUSTRIA
BELGIUM
BOLIVIA
BRAZIL
BULGARIA
BURMA
BYELORUSSIAN SOVIET SOCIALIST REPUBLIC
CAMBODIA
CAMEROON
CANADA
CEYLON
CHILE
CHINA
COLOMBIA
CONGO, DEMOCRATIC REPUBLIC OF
COSTA RICA
CUBA
CYPRUS
CZECHOSLOVAK SOCIALIST REPUBLIC
DENMARK
DOMINICAN REPUBLIC
ECUADOR
EL SALVADOR
ETHIOPIA
FINLAND
FRANCE
GABON
GERMANY, FEDERAL REPUBLIC OF
GHANA
GREECE
GUATEMALA
HAITI
HOLY SEE
HUNGARY
ICELAND
INDIA
INDONESIA
IRAN
IRAQ
ISRAEL
ITALY
IVORY COAST
JAMAICA
JAPAN
JORDAN
KENYA
KOREA, REPUBLIC OF
KUWAIT
LEBANON
LIBERIA
LIBYA
LUXEMBOURG
MADAGASCAR
MALI
MEXICO
MONACO
MOROCCO
NETHERLANDS
NEW ZEALAND
NICARAGUA
NIGERIA
NORWAY
PAKISTAN
PANAMA
PARAGUAY
PERU
PHILIPPINES
POLAND
PORTUGAL
ROMANIA
SAUDI ARABIA
SENEGAL
SIERRA LEONE
SINGAPORE
SOUTH AFRICA
SPAIN
SUDAN
SWEDEN
SWITZERLAND
SYRIAN ARAB REPUBLIC
THAILAND
TUNISIA
TURKEY
UGANDA
UKRAINIAN SOVIET SOCIALIST REPUBLIC
UNION OF SOVIET SOCIALIST REPUBLICS
UNITED ARAB REPUBLIC
UNITED KINGDOM OF GREAT BRITAIN AND NORTHERN IRELAND
UNITED STATES OF AMERICA
URUGUAY
VENEZUELA
VIET-NAM
YUGOSLAVIA

The Agency's Statute was approved on 23 October 1956 by the Conference on the Statute of the IAEA held at United Nations Headquarters, New York; it entered into force on 29 July 1957. The Headquarters of the Agency are situated in Vienna. Its principal objective is "to accelerate and enlarge the contribution of atomic energy to peace, health and prosperity throughout the world".

Printed by the IAEA in Austria
June 1968

PANEL PROCEEDINGS SERIES

DELAYED FISSION NEUTRONS

PROCEEDINGS OF A PANEL
HELD IN VIENNA, 24-27 APRIL 1967

INTERNATIONAL ATOMIC ENERGY AGENCY,
VIENNA, 1968

DELAYED FISSION NEUTRONS
(Panel Proceedings Series)

ABSTRACT. Proceedings of a panel organized by the IAEA and held in Vienna, 24-27 April 1967. The increasing sophistication in reactor design and, in particular, the advent of fast reactors have shown that delayed fission neutrons play a major role in considerations of operational stability and safety. Fourteen leading scientists from nine Member States made vital new data available and defined areas of investigation for future experimental and theoretical work. The data are summarized in an Annex at the end of the Proceedings.

The contents include papers on the importance of delayed neutron data in reactor design, on which fission products should be considered as precursors, and on experimental methods for separating and determining the precursors.

Each paper is in its original language (11 English, 1 French, 2 Russian) and is preceded by an abstract in English with a second one in the original language if this is not English. The summarized discussions, summary and Annex are in English.

(249 pp., 16 x 24 cm, paper-bound, 93 figures) Price: US $5.00; £ 2.1.8
(1968)

DELAYED FISSION NEUTRONS
IAEA, VIENNA, 1968
STI/PUB/176

FOREWORD

Information about delayed fission neutrons and their precursors plays an important role in the study of reactor dynamics and fission mechanisms, and can contribute substantially to the understanding of nuclear structure.

The early data on delayed neutron groups were adequate to satisfy the modest requirements for the design of thermal reactors. But with greater sophistication of reactor design, and particularly with increased interest in fast reactors, there is a growing demand for more precise determinations of half-lives, relative abundances of individual groups, delayed neutron yields as a function of energy, and energy spectra of emitted neutrons. Detailed studies of precursors and delayed neutrons using new detectors and improved experimental equipment can contribute to the solution of open problems in nuclear structure and fission processes, and stimulate new interest for theoretical studies.

In view of these facts, it was felt timely for the International Atomic Energy Agency to convene a Panel of Experts to consider developments in this field as it enters a new phase, which could yield important and immediately applicable results. The Panel summarized, reviewed and analysed the available data on delayed fission neutrons and outlined the future directions of research. The Panel met in Vienna from 24 to 27 April 1967; the papers and summaries of the discussions are included in this publication.

The cover design shows part of a Chart of Nuclides indicating delayed neutron precursors, 1962.

CONTENTS

INTRODUCTION

Shortly after the discovery of nuclear fission, R. Roberts, R. Meyer and P. Wang observed, early in 1939, the delayed emission of neutrons in fission [1]. This phenomenon was soon interpreted by N. Bohr and J. A. Wheeler as being the result of nuclear excitation following the beta-decay of nuclear fission fragments [2]. The importance of delayed neutrons in controlling the rate of a fission chain reaction was first noted in the literature by Ya. B. Zeldovich and Yu. B. Khariton in an early prognosis of the prospects of nuclear energy published in 1940 – more than two years before the first self-sustaining chain reaction was achieved [31].

Since then numerous investigations have been performed on the characteristics of delayed fission neutrons, half-lives, yields and energies, as a function of composition and excitation energy of the fissioning nucleus. Individual delayed neutron precursors were identified and characterized by radiochemical techniques.

The basic mechanism of delayed neutron emission is now reasonably well understood. Beyond a certain displacement from the nuclear stability line, the beta-decay of a nuclide can populate excited states lying above the neutron binding energy of the daughter nuclide. These states may then de-excite promptly through the emission of a neutron. Thus the neutron emission appears to be delayed, its rate following the half-life for β-decay of the precursor nuclide. This process is most likely to occur in nuclides having a few neutrons in excess of a closed neutron shell because of the unusually low neutron binding energy in such nuclides.

The fundamental role of delayed neutrons in the kinetic behaviour, control and safety of nuclear reactors is well known today, being a matter of practical experience in hundreds of installations around the world. The available information on number and energy distribution of delayed fission neutrons is, however, no longer adequate for the design of the coming generation of high power, fast breeder reactors, characterized by large quantities of fertile material (^{238}U or ^{232}Th) in the breeder/blanket reflector. Under high burn-up conditions, relatively large quantities of ^{239}Pu, ^{240}Pu and higher mass plutonium isotopes may also be present. Precise evaluations of the neutron kinetics and control characteristics of such systems require, among other basic data, accurate and complete total delayed neutron spectra for all the main fissionning species. So far, these spectra are known only for the fission of ^{235}U by thermal neutrons. Even the chemical properties of individual delayed-neutron precursors are of importance in the design of certain advanced systems. As examples, one may cite reactors operated at very high temperatures, or reactors with continuous fuel reprocessing, reactors with circulating fuel, in all of which considerable fractions of the precursor nuclides may escape from the core leading to lower margins of reactor control, with obvious implications for reactor kinetics and safety.

Fortunately, this need for a better knowledge of delayed-neutron emission in fission comes at a time of increasing activity in this field due to the growing interest in studies of nuclides far from the stability line. Novel physical and chemical techniques are being developed and applied in order to investigate the properties of very short-lived species

1

among the various fission products. Studies of delayed-neutron emission can give important information on nuclear structure, as for example, the matrix elements in beta-decay, level densities at medium excitation energy, the competition between neutron and gamma emission, and through the decay energies involved on the shape of the nuclear energy surface. In addition, delayed neutrons can serve as a tool for studying the fission process, yielding information on the fission fragment mass and charge distributions of various nuclei for different excitation energies.

In order to review the present status and future trends in delayed neutron research, the International Atomic Energy Agency sponsored a panel meeting of experts representing all aspects of the field. The panel met in Vienna from 24 to 27 April 1967. All participants agreed that it was a very timely meeting, arranged at the beginning of a renewed period of activity in this field. The most urgent needs for delayed-neutron data in fast kinetics and design have not been fully realized by nuclear and fission physicists and chemists. Thus the meeting should not only accelerate the future development of delayed-neutron research but should also encourage fission experimentalists to extend the scope of their work. The informal discussions were very extensive, and accordingly are presented here in condensed form, arranged in groups following the set of contributions making up the individual sections. A summary is given at the end of the proceedings.

REFERENCES

[1] ROBERTS, R., MEYER, R.C., WANG, P., Phys. Rev. 55 (1939) 510.
[2] BOHR, N., WHEELER, J.A., Phys. Rev. 56 (1939) 426.
[3] ZELDOVICH, Ya.B., KHARITON, Yu.B., Zh. eksp. teor. Fiz. 10 (1940) 477.

DELAYED FISSION NEUTRON DATA IN REACTOR PHYSICS AND DESIGN

G.R. KEEPIN
LOS ALAMOS SCIENTIFIC LABORATORY,
UNIVERSITY OF CALIFORNIA,
LOS ALAMOS, NEW MEXICO,
UNITED STATES OF AMERICA

Abstract

DELAYED FISSION NEUTRON DATA IN REACTOR PHYSICS AND DESIGN. The basic input data required for all reactor physics and design calculations include: (1) fundamental nuclear cross-sections; (2) physical properties of materials; and (3) fission parameters, including yields and energy distributions of the delayed and prompt fission neutrons. Although prompt-neutron data are now reasonably well determined, more precise and more extensive data are becoming increasingly necessary in certain, expanding areas of nuclear technology. In this paper we consider some of the basic problems in fast reactor physics and design which require further knowledge of the yields and energy spectra of delayed neutrons. The sensitivity of reactor physics parameters to variations in delayed- and prompt-neutron data are examined quantitatively, and specific areas in which further measurements are required are delineated. The role of delayed- and prompt-neutrons in detailed calculations of neutron importance and effective delayed-neutron fraction is developed and illustrated by specific examples. Such detailed studies are shown to be of particular importance in the field of fast reactor kinetics and control which is basic to the large power breeder reactor development programme now underway in the USA, USSR and Western Europe.

The accuracy of all reactor physics and design calculations is ultimately limited by three main sources of error: (1) uncertainties in calculational methods; (2) uncertainties in physical composition, masses, dimensions, etc. of the system; and (3) uncertainties in the general input data, including basic cross-section, fission parameters, physical characteristics, etc. Of major importance among the fission parameters are the number and energy distributions of the prompt and delayed fission neutrons. This is especially true in the case of the large fast power-breeder reactors at present under development in the United States, the USSR and Western Europe.

Most of the present high power [order of 10^3 MW(e)] fast breeder designs incorporate rather large cores with relatively dilute fissile fuel in the form of ceramic compounds such as mixed plutonium-uranium oxide or carbide. Such cores are characterized by a degraded fission neutron spectrum ($\sim\frac{1}{4}$ to $\frac{1}{2}$ of all fissions produced by neutrons below 100 keV). Table I lists core materials and physics properties for the major fast breeder designs and also for prototype or experimental fast reactors now under construction that have neutron spectra characteristic of the coming generation of 1000 MW(e) dilute fast power reactors. [References cited in Table I include several papers in the ANS Topical Meeting on Fast Reactors just concluded in San Francisco (April 10-14, 1967).]

Here attention will be confined to prototype reactors and fast critical assemblies (idealized systems) as these are of fundamental concern in the conception and design phase of fast reactors, and comparisons between

TABLE I. CORE MATERIALS AND PHYSICS PROPERTIES OF DEGRADED-SPECTRUM FAST REACTORS

Power Reactors	Geometry	Core material				Fissions below 100 keV (%)	Fissile mass (kg)	Total breeding ratio	Doppler coefficient (Tdk/dT)	$\left[\frac{\Delta k}{K}\right]_{co}$
		Fuel	Coolant	Cladding	Control & other					
General Electric Co. [1-3]	Thin Cyl	PuO_2UO_2	Na	SS	B, Be	45	2800	1.26	- 0.01	- 0.07
Allis Chalmers Co. [4]	Annular	PuO_2UO_2	Na	SS	B	< 40	2910	1.32	- 0.003	
Westinghouse Electric Corp. [5,6]	Modular	PuC-UC	Na	SS	B	< 40	3700	≈ 1.4	- 0.008	- 0.0015
Combustion Engineering Inc. [7]	Thin Cyl	PuC-UC	Na	SS	B	< 40	1800	1.4	- 0.003	0
General Atomic [8-10]	Cylinder	PuO_2UO_2	He	SS	-	-	1670	1.5	-	-
Karlsruhe [11-16]	Thin Cyl	PuO_2UO_2	Na	Incoloy	-	-	2015	1.38	- 0.012	+ 0.01 (max.)
Cadarache [13-16]	Cylinder	PuO_2UO_2	Na	SS	-	-	2980	1.36	- 0.0082	
Babcock & Wilcox Steam Cooled [17-19]	Annular	PuO_2UO_2	Steam	Inconel	-	> 50	2530	≈ 1.1	-	≈ 0
Space Reactor [20]	Cylinder	U, Pu	K, Na, Li	W, Ni, Ta, Mo	Eu, BeO	< 25	-	-	-	-
USSR BR-250 [a] [21]	Cylinder	U-Oxide	Na	SS	B, Fuel	-	850	1.5	≈ - 0.008	-
SEFOR [a] [22-24]	Cylinder	PuO_2UO_2	Na	SS	Be	50	300	-	- 0.0084	- 0.008

[a] BR-250 and SEFOR are prototype and experimental reactors respectively which are now under construction and have neutron spectra and other physics properties characteristic of 1000 MWe dilute fast power reactors.

calculation and experiment are more direct and certainly more readily interpretable. Some of the major fast reactor physics and design parameters which can be calculated and checked via measurements on critical assemblies are k_{eff} (via critical mass determination), fission ratios, prompt and delayed neutron importance, material worths (via replacement measurements), effective delay fraction, prompt neutron lifetime, neutron spectra or spectral indices, and Doppler effect (generally very small).

Since both prompt and delayed neutrons contribute significantly to most reactor physics parameters, it is necessary to evaluate effects due to both; as a matter of fact prompt and delayed neutron effects are so closely coupled as to essentially preclude the detailed consideration of one without the other. I shall consider first the variations in reactor physics parameters due to uncertainties in prompt neutron numbers, $\bar{\nu}$, and energy spectra, χ. Later in this paper I shall examine the variations due to delayed neutron yield and spectral uncertainties. Based on the available fission data, representative maximum uncertainties in $\bar{\nu}(E_n)$ for ^{239}Pu can be assumed to be as follows:

$$\bar{\nu} = 2.85 \pm 0.05 + (0.145 \pm 0.02)E_n$$

The average value, $\bar{\nu} = 2.85$, is slightly lower than the figure of 2.87 for ^{239}Pu thermal fission recommended by Keepin [25] and also by Westcott [26]. The average linear slope of 0.145 is essentially the same as the value, 0.148, obtained in Ref. [25] for the range $0 < E_n < 1$ MeV, but somewhat greater than the value of 0.138 indicated [25] for $0 < E_n < 14$ MeV, and considerably greater than the slope indicated by Mather et al. [27] for $0 < E_n < 4$ MeV. The lower extreme of $\bar{\nu}$-thermal (2.80) is near Colvin and Sowerby's [28] value of 2.82, and the upper extreme lies above the data of Hopkins and Diven [29]. Maximum uncertainties in the slope (0.125 to 0.165) were conservatively estimated from all available data up to 14 MeV [30].

Uncertainties in the ^{239}Pu fission neutron spectrum were obtained by assuming different nuclear temperatures, T, in a Maxwellian energy distribution,

$$N(E_n) \approx E_n^{\frac{1}{2}} \exp(-E_n/T)$$

with $T = 1.41 \pm 0.05$, representing a conservatively-estimated 8% spread in nuclear temperatures. Such conservatism is indeed warranted inasmuch as fission neutron spectra are not well described by a Maxwellian or any other simple functional form, and furthermore no precise theoretical justification exists for any of the commonly used functional forms of N(E). The median value for ^{239}Pu, $T = 1.41$, was obtained from recent measurements of Barnard et al. at Harwell [31].

The above variations in $\bar{\nu}$ and χ can be used to study the sensitivity of fast reactor physics and design parameters to these variations. To consider a specific (yet generally representative) example, the ZPR-III Assembly 47 at Argonne National Laboratory (Idaho) is a pre-design critical assembly for the SEFOR experimental fast power reactor [32]. SEFOR (the Southwest Experimental Fast Oxide Reactor) is a ceramic-fuelled, sodium-cooled, ~20 MW(th) experimental fast flux reactor intended to provide data in support of a test programme to demonstrate that

TABLE II. PHYSICS CHARACTERISTICS OF SEFOR CRITICAL ASSEMBLY
(ZPR III Assembly 47)

Pu critical mass	314 kg
Core radius (H/D ~ 1)	44.1 cm
Median fission energy	150 keV
Fissions below 10 keV	22%
Effective delay fraction, $\overline{\gamma}\beta$	0.0032
Prompt neutron lifetime, ℓ	0.66 μsec
Fraction of fissions by isotope:	
^{239}Pu	0.86
^{240}Pu	0.02
^{235}U	0.01
^{238}U	0.11

TABLE III. SENSITIVITY OF FAST REACTOR PHYSICS PARAMETERS TO REPRESENTATIVE UNCERTAINTIES IN $\overline{\nu}(E_n)$, $\chi(E_n)$, AND CROSS-SECTION DATA

Reactor physics parameter	$\overline{\nu}(E_n)$ (~4% var.)	$\chi(E_n)$ (~8% var. in $T(^{239}Pu)$)	$\sigma_f(^{239}Pu)$ (~10% var.)	$\sigma_c(^{238}U)$ (~25% var.)
$\frac{\sigma_f(^{238}U)}{\sigma_f(^{239}Pu)}$	0	+ 2%	- 2%	+ 3%
$\frac{\sigma_c(^{238}U)}{\sigma_f(^{239}Pu)}$	0	< 1%	- 3%	+ 13%
k_{eff}	+ 4%	+ 0.5%	+ 1.8%	- 2.6%
$\overline{\gamma}\beta$	< 1%	+ 4%	< 1%	< 1%
ℓ	< 1%	< 1%	- 5%	- 6%

fast ceramic power reactors can be designed with desirable operating, control and safety characteristics. The SEFOR critical assembly (cf. Table II) has a relatively small PuO_2-UO_2 core to which BeO was added to soften the neutron energy spectrum to that of a typical large fast power reactor. Also $\bar{\gamma}\beta$ and ℓ are typical of a large power reactor, so in general this SEFOR critical assembly provides an excellent representative case for sensitivity comparisons. Some recent sensitivity calculations for the SEFOR critical assembly are summarized in Table III, which has been adapted from extensive fast reactor studies by Greebler and Hutchins [33].

In Table III we see that an increase of about 4% in $\bar{\nu}$ produces the same percentage increase in k_{eff}, since the two quantities are directly proportional to one another. Otherwise, variations in $\bar{\nu}$ are seen to produce only small changes in the reactor physics parameters considered. An increase in the slope of the $\bar{\nu}(E_n)$ function means, of course, relatively more neutron production from higher energy fission, with correspondingly increased importance for higher energy neutrons.

The major effect of hardening the neutron spectrum χ is clearly an increase (2%) in the relative ^{238}U fission rate, causing a relatively-large 4% increase in the effective delayed neutron fraction, $\bar{\gamma}\beta$. (It will be recalled that the absolute delayed neutron yield for ^{238}U fission is nearly an order of magnitude larger than that for ^{239}Pu fission [25].) The influence of the $\chi(E_n)$ spectrum on the other reactor physics parameters listed is small.

For comparison purposes, the $\bar{\nu}$ and χ sensitivity calculations in Table III are compared with similar results for typical variations in basic cross-section data. The indicated $\sim 10\%$ variation in the ^{239}Pu fission cross-section stems from comparison of the recommended values of Davey [34] with the lower σ_f values of White et al. [35] below ~ 100 keV. Similarly the $\sim 25\%$ variation in σ_c (^{238}U) reflects the conflicting data of Moxon and Chaffey [36] as compared to the considerably higher σ_c values of Macklin and Gibbons [37] in the energy range $4 < E_n < 40$ keV.

As may be inferred from the comparison in Table III, fast reactor parameters are generally more sensitive to existing cross-section uncertainties (plus calculational approximations) than to neutron number and spectral uncertainties. However in the case of certain important parameters such as k_{eff} and $\bar{\gamma}\beta$, effects due to $\bar{\nu}$ and χ uncertainties can become dominant, often overshadowing the effect of cross-section and calculational uncertainties. This is of particular significance in fast reactor design since effective delay fraction $\bar{\gamma}\beta$ plays a major role in fast reactor kinetics and control, and hence in reactor safety.

The prompt neutron decay constant at delayed critical $\bar{\gamma}\beta/\ell$ (measurable by Rossi-α, pulsed neutron or cross-correlation noise techniques) [25] may likewise be subject to considerable calculational error due to uncertainties in χ. Similarly, errors arise in the use of measured $\bar{\gamma}\beta/\ell$ and calculated $\bar{\gamma}\beta$ to determine prompt neutron lifetime (which provides a convenient, sensitive low-energy spectral indicator).

In general, critical assembly experiments permit quite accurate and stringent integral checks on important reactor physics parameters; since these integral results represent a composite of many basic fission parameters, cross-section data, etc., there is a never-ending attempt to

TABLE IV. DELAYED NEUTRON FRACTIONS (β) AND PROPAGATED UNCERTAINTIES
(including tabulated delayed neutron yields, n/F, and average total neutron yields per fission, $\bar{\nu}$)

Fission nuclide	Fast fission (E_{eff} ~ fission spectrum)			Thermal neutron induced fission		
	n/F	$\bar{\nu}$	β	n/F	$\bar{\nu}$	β
^{239}Pu	0.0063 ± 0.0003	3.09 ± 0.06	$0.0020_4 \pm 0.0001_1$	0.0061 ± 0.0003	$2.87_4 \pm 0.04$	$0.0021_2 \pm 0.0001_1$
^{233}U	0.0070 ± 0.0004	2.62 ± 0.05	$0.0026_7 \pm 0.0001_6$	0.0066 ± 0.0003	$2.48_2 \pm 0.03$	$0.0026_6 \pm 0.0001_2$
^{240}Pu	0.0088 ± 0.0006	3.3 ± 0.2	$0.0026_6 \pm 0.0002_4$	-	-	-
^{241}Pu	-	-	-	0.0154 ± 0.0015	3.14 ± 0.06	0.0049 ± 0.0005
^{235}U	0.0165 ± 0.0005	2.57 ± 0.04	$0.0064_1 \pm 0.0002_2$	0.0158 ± 0.0005	$2.43_2 \pm 0.02$	$0.0065_0 \pm 0.0002_1$
^{238}U	0.0412 ± 0.0017	2.79 ± 0.10	0.0148 ± 0.0008	-	-	-
^{232}Th	0.0496 ± 0.0020	2.44 ± 0.15	0.0203 ± 0.0015	-	-	-

refine knowledge of as many of the individual input parameters as possible in order to permit of more definitive conclusions about the remaining input parameters and cross-sections. In this sense then, further refinement of delayed and prompt neutron numbers and spectral data will contribute toward more definitive cross-section evaluations from critical experiments and thereby increase the accuracy and reliability of fast power reactor calculations.

Let us now turn to an examination of the sensitivity of reactor physics parameters to variations in delayed neutron yields and energy spectra. Emphasis will be placed on the major parameters involving delayed neutrons directly, namely delayed neutron importance or effectiveness (relative to prompt neutron effectiveness), and the associated variations in effective delayed neutron fraction, $\overline{\gamma}\beta$, which largely determines the kinetic behaviour and control margin of any fission chain reactor. Measured delayed neutron absolute yields, n/F, for the major fission species vary in accuracy from $\sim 3\%$ to $\sim 5\%$ for thermal neutron- and fast (fission spectrum) neutron-induced fission [25]. These uncertainties propagate directly into delayed neutron fraction values, together with additional uncertainties due to prompt neutron number variations (and neutron importance variations, as will be discussed later).

Table IV summarizes recommended "best values" of delayed neutron fractions, $\beta = (n/F)/\overline{\nu}$, together with propagated uncertainties, for fast and thermal fission of all the major fission species. Note that over the incident-neutron-energy range considered ($0 < E_n \lesssim 3$ MeV) delayed neutron yields and fractions are essentially constant, independent of the energy of the neutron inducing fission.

In the region of low-energy fission, reasonably good agreement exists between experimental and calculated delayed neutron yields based upon known fission charge and mass distributions and our limited knowledge of neutron emission probabilities. On the other hand, serious discrepancies persist at the higher neutron energies: most experimental data have indicated a strong increase (roughly a doubling) in delayed neutron yield as one progresses from low energy fission to 14 MeV fission. This is in sharp contrast to long-standing theoretical predictions [38] of a decrease in delayed neutron yield at 14 MeV, based largely on the observed decrease in fission chain lengths with increasing energy of the neutron inducing fission. Some of the papers to be presented at this IAEA panel will undoubtedly shed further light on the energy dependence of delayed neutron yield in high energy fission. It may also be noted here that absolute yield measurements for high energy fission of the major fissioning species are currently in progress at Los Alamos. The delayed neutron fractions in Table IV are appreciably lower than earlier values[1], indicating generally lower margins of reactor control, with consequent implications for reactor kinetics, control and safety [39]. The lower β-values of Table IV have been corroborated by a number of independent kinetics experiments in recent years.

In addition to the rather striking variation (by an order of magnitude) in delayed neutron fractions and yields among the different fission species, the values of "effective" delayed neutron fractions and yields can exhibit

[1] For example, in the case of ^{235}U thermal fission, $\beta = 0.0065$ in Table IV is some 15% lower than the previously widely used value [40] $\beta(^{235}U) = 0.0075$.

still further variation in practical reactors, depending upon spatial and spectral details of individual systems. This is especially true in the case of fast power-breeder reactors, which typically contain large quantities of ^{238}U, ^{232}Th, or ^{240}Pu in the core and/or in the breeder-blanket reflector. In the fast neutron spectra of such reactors a sizeable fraction of total fissions may occur in these threshold-fissioning species. Because of their relatively high delayed-neutron yields, ^{238}U and ^{232}Th can contribute the majority of delayed neutrons in fast breeder reactors and, therefore, might be expected to dominate the kinetic behaviour of such systems. In general this is not the case; to understand why, it is essential to evaluate carefully the effectiveness of the delayed neutrons from fertile materials (such as ^{238}U and ^{232}Th) as compared to the effectiveness of delayed neutrons from the "fuel" (^{235}U, ^{239}Pu, and/or ^{233}U). In addition, one expects markedly different effectiveness for delayed neutrons than for prompt neutrons; viz. delayed neutrons are born with considerably lower energy than prompt neutrons and, hence, exhibit different interaction cross-sections and leakage probabilities than prompt neutrons.

The computation of neutron effectiveness is based on established perturbation methods [41] and is usually carried out by multigroup diffusion or transport theory codes. Effective prompt and delayed neutron yields, and effective delay fractions have been calculated in detail for representative bare and reflected metal critical assemblies at Los Alamos (cf. Table V). Such idealized metal assemblies can provide useful experimental checks on multigroup data and computational methods for calculating the neutronics of fast breeder systems. The simplicity of these metal critical assemblies permits one to focus attention first on the neutron physics involved before introducing numerous perturbations associated with practical engineering problems in actual power-breeder reactors.

TABLE V. SIX BARE AND REFLECTED METAL ASSEMBLIES AT LOS ALAMOS

Assembly	Composition (of idealized assembly)
Bare ^{235}U, (Godiva)	bare Oy (93.8% ^{235}U) sphere, 8.71 cm radius, 51.9 kg mass
Bare ^{239}Pu, (Jezebel)	bare δ-phase Pu sphere, 6.28 cm radius, 16.4 kg mass
Bare ^{233}U, (Skidoo)	bare ~98.1% ^{233}U sphere, 5.96 cm radius, 16.4 kg mass
U-reflected ^{235}U, (Topsy)	~ 8 in. thick natural uranium reflected Oy sphere, 6.05 cm radius, 17.3 kg mass
U-reflected ^{239}Pu, (Popsy)	~ 8 in. natural uranium reflected δ-Pu sphere, 4.44 cm radius, 5.79 kg mass
U-reflected ^{233}U, (23 Flattop)	~ 8 in. natural uranium reflected ^{233}U sphere, 4.17 cm radius, 5.59 kg mass

TABLE VI. COMPARISON OF ^{239}Pu AND ^{235}U FISSION NEUTRON SPECTRA

(Six-group representation)

Energy group, "k"	Energy range (MeV)	^{235}U fission spectrum	^{239}Pu fission spectrum	$\bar{\nu}\sigma_f(^{239}Pu)$
1	0 - 0.1	0.014	0.013	5.863
2	0.1 - 0.4	0.090	0.084	4.810
3	0.4 - 0.9	0.180	0.170	4.981
4	0.9 - 1.4	0.168	0.161	5.472
5	1.4 - 3.0	0.344	0.347	6.026
6	3.0 - ∞	0.204	0.225	6.517

The basic input data required for neutron effectiveness calculations include delayed and prompt neutron energy spectra and absolute yields as well as appropriate cross-section data. For the latter, Hansen's fission-spectrum-averaged six group cross-sections [42, 43] were used, together with modifications of the ^{239}Pu data to take account of the harder fission neutron spectrum of ^{239}Pu compared to that of ^{235}U [44]. The six group ^{239}Pu and ^{235}U fission spectra used are compared in Table VI, which also lists the revised $\bar{\nu}\sigma_f$ (^{239}Pu) data.

Interestingly enough, the energy spectrum of the delayed neutrons is probably the poorest known of all input data required in the calculation of effective delayed neutron yields and fractions. Since the energy of the delayed neutrons largely determines their effectiveness (via neutron leakage and interaction probabilities), it is important to examine the sensitivity of effectiveness calculations to delayed neutron spectral differences. The results of an early attempt to measure individual spectra, χ_i for the first four delay groups, are summarized in Fig. 1. Two composite spectra (for all delayed groups) are shown in Fig. 2; the spectrum labelled 'Batchelor and Bonner' is a composite of the individual group spectra, χ_i, in Fig. 1. The χ_i were weighted according to relative group abundances, ($\chi_D \equiv \sum_i a_i \chi_i$) and an (optimistically) estimated error of ± 10% assigned to the relative neutron intensities. The spectrum labelled 'Burgy et al.' is obtained from independent cloud chamber measurements, normalized to the same area as the Batchelor-Bonner spectrum, and (again optimistically) assigned an overall error of ± 20% on relative yield values.

In lieu of more definitive data, the two crude spectra in Fig. 2 are taken as representative of existing uncertainties in delayed neutron emission spectra. The resulting six-energy-group composite spectra are given in the last two columns of Table VII. Six-energy-group spectral parameters for the first four delay groups are tabulated in columns 3 to 6 of Table VII.

Using the six-group data in multi-region spherical geometry, both actual and effective neutron yields (prompt and delayed) were calculated for all fissioning isotopes present in each of the assemblies listed in

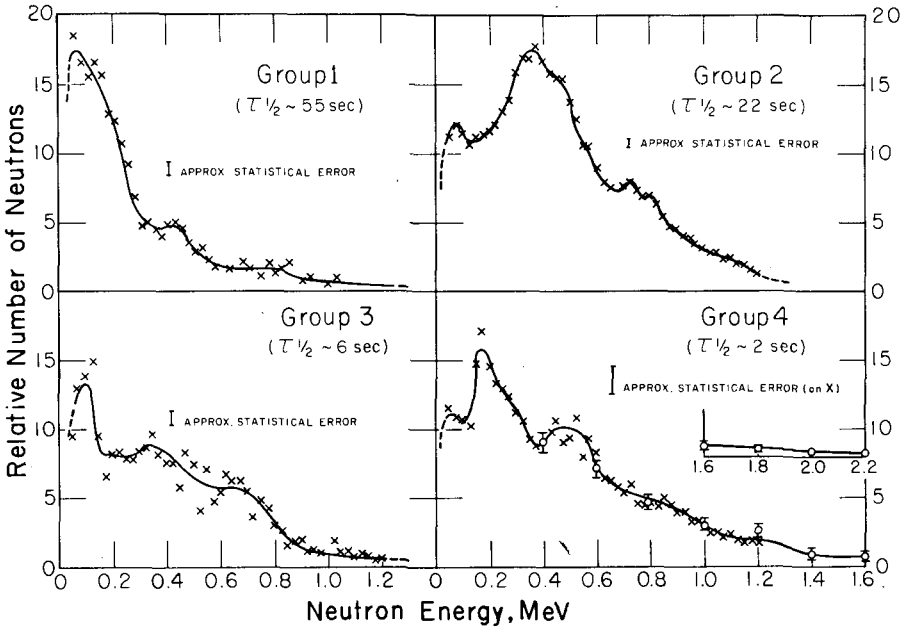

FIG. 1. Measured delayed neutron group spectra. The solid line represents the smooth fit to the data: × ^{3}He spectrometer data of Batchelor and Hyder [45] analysed into individual group spectra using Keepin-Wimett delayed neutron data [46]; Φ cloud chamber data of Bonner, Bame and Evans [47].

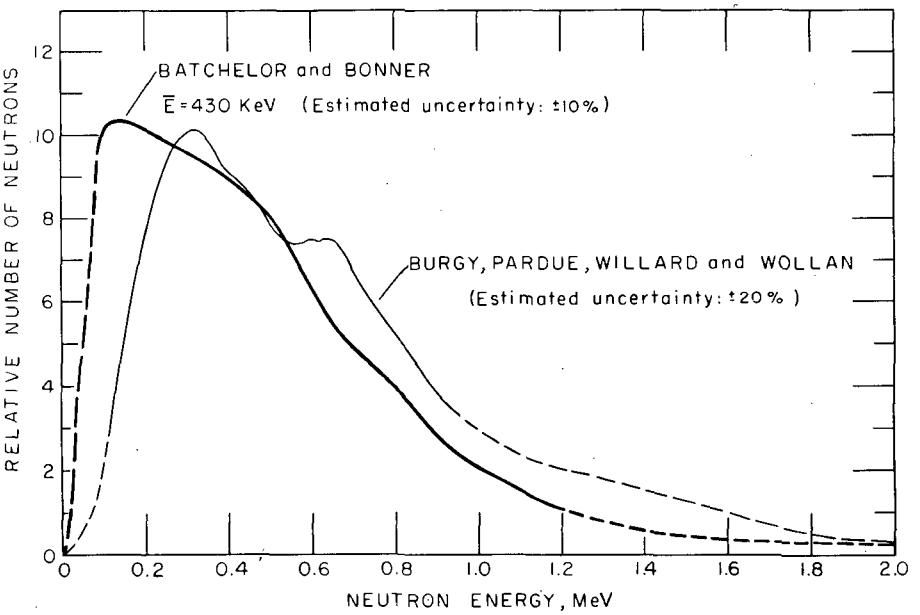

FIG. 2. Composite delayed neutron spectra (yield weighted spectra for all delayed groups, cf. Fig. 1). Thin line is obtained from data by Burgy et al. [48].

Table V. From perturbation theory, the relative importance or "worth" of delayed neutrons from fission of isotope q is calculated by weighting neutron yield with the product of delayed energy spectrum χ_{D_k}, and adjoint flux[2], $\varphi_{0_k}^{+}(r)$:

$$I_D^q \approx \int \sum_k \chi_{D_k} \varphi_{0_k}^{+}(r) \sum_j \nu_j^q \sigma_{f_j}^q N^q(r) \varphi_j(r) \, d\,\mathrm{Vol} \qquad (1)$$

Here the indices j and k denote the six energy groups, χ_D is the composite delayed neutron emission spectrum for all delayed groups and $\sigma_f N(r)$ is the (space-dependent) macroscopic fission cross-section. The indicated volume integration is carried out numerically in spherical geometry with 20 volume regions for bare systems, 34 for reflected systems.

The importance of prompt neutrons from isotope q is evaluated similarly by weighting neutron yield with the prompt spectrum, χ_k and adjoint flux:

$$I_p^q \approx \int \sum_k \chi_k \varphi_{0_k}^{+}(r) \sum_j \nu_j^q \sigma_{f_j}^q N^q(r) \varphi_j(r) \, d\,\mathrm{Vol} \qquad (2)$$

Relative effective yields are then given by the product of importance and neutron fraction; viz: effective delayed neutron yield $E_D^q = I_D^q \beta^q$, and effective prompt neutron yield $E_p^q = I_p^q(1 - \beta^q)$.

Table VIII summarizes the results of these calculations, (by EDF code) giving the relative importance of prompt and delayed neutrons from all fissioning species in each of the six metal systems. Fission ratios and total neutron yield ratios are also tabulated.

The effective delayed neutron fraction for a mixture of fission isotopes is computed from the ratio of effective delayed neutron yield to effective total neutron yield (prompt plus delayed):

$$\overline{\gamma\beta} \equiv \frac{\sum_q E_d^q}{\sum_q (E_p^q + E_d^q)} \qquad (3)$$

where the summation over q includes all fissioning isotopes in the system. Table IX presents calculated effective delayed neutron fractions, $\overline{\gamma\beta}$, together with "experimental" $\overline{\gamma\beta}$ fractions (from surface mass increment measurements [43].) Also included in Table IX are measured "Rossi-α" [50] values (prompt neutron decay constants) at delayed critical, and the resulting prompt neutron lifetime, $\ell = \overline{\gamma\beta}_{calc}/\alpha_{DC}$ for each assembly.

---

[2] The flux and adjoint flux distributions used were computed using the Los Alamos NDSN code [49] in the S_8 transport approximation.

TABLE VII. DELAYED NEUTRON ENERGY SPECTRA, χ_i AND χ_D

(Six-energy-group parameters for the measured energy spectra shown in Figs 1 and 2)

Energy group	Energy interval	Batchelor and Bonner [45, 47]					Burgy [48]
		Group 1	Group 2	Group 3	Group 4	χ_D (all groups)	χ_D (all groups)
1	0 - 0.1	0.17	0.06	0.10	0.06	0.07	0.01
2	0.1 - 0.4	0.53	0.38	0.42	0.41	0.39	0.30
3	0.4 - 0.9	0.22	0.43	0.40	0.39	0.38	0.46
4	0.9 - 1.4	0.06	0.09	0.06	0.09	0.12	0.16
5	1.4 - 3.0	0.02	0.04	0.02	0.05	0.04	0.07
6	3.0 - ∞	0	0	0	0	0	0

TABLE VIII. RELATIVE IMPORTANCE OF INDIVIDUAL FISSION EVENTS IN SIX METAL SYSTEMS

(I_D^q and I_P^q values calculated from Eqs (1) and (2) using S_8 flux and adjoint functions generated by NDSN programme)

Assembly	Fission isotope	Fission ratios	Total neutron yield ratios	Relative importance	
				Prompt neutrons	Delayed neutrons
Bare ^{235}U (Godiva)	^{235}U	1.0	1.0	1.0000	1.0342
	^{238}U	0.0089_4	0.0091_0	0.0090_5	0.0093_6
Bare ^{239}Pu (Jezebel)	^{239}Pu	1.0	1.0	1.0000	0.9459
	^{240}Pu	0.0316	0.0354	0.0354	0.0334
Bare ^{233}U (Skidoo)	^{233}U	1.0	1.0	1.0000	1.0598
U-reflected ^{235}U (Topsy)	^{235}U	1.0	1.0	1.0000	1.0097
	^{238}U	0.2479	0.2540	0.0852	0.0762
U-reflected ^{239}Pu (Popsy)	^{239}Pu	1.0	1.0	1.0000	0.9507
	^{240}Pu	0.0077_4	0.0087_4	0.0088_0	0.0083_7
	^{235}U	0.1032	0.0845	0.0115	0.0095_8
	^{238}U	0.3795	0.3270	0.0803	0.0695
U-reflected ^{233}U (23 Flattop)	^{233}U	1.0	1.0	1.0000	1.0395
	^{238}U	0.3000	0.2962	0.0765	0.0702
	^{235}U	0.0680	0.0639	0.0098_6	0.0086_2

Direct multigroup calculations of prompt neutron lifetimes are in reasonable agreement with the values given in Table IX; unexplained exceptions are the ^{235}U systems (as for example Topsy and Godiva) for which calculated lifetime appears to be several percent low [50].

To examine the dependence of delayed neutron effectiveness on delayed neutron spectra, the calculations of Tables VIII and IX were carried out using the two composite spectra (all delayed groups) in Table VII. The resulting effective delayed fractions are compared in Table X, the higher energy (Burgy) spectrum giving lower effective delay fractions for each of the six assemblies. The relative importance of individual isotopes exhibits nearly the same percentage difference as shown for $\overline{\gamma\beta}$ in Table X.

TABLE IX. EFFECTIVE DELAYED NEUTRON FRACTIONS, ROSSI-α VALUES AND PROMPT NEUTRON LIFETIMES FOR SIX METAL ASSEMBLIES

Assembly	Fission isotopes present	Fraction of total effective delayed neutron yield	Effective delayed neutron fraction, $\overline{\gamma\beta}$	Experimental $\overline{\gamma\beta}$	Measured Rossi-α at delayed critical (per μsec)	Prompt neutron lifetime $= \frac{\overline{\gamma\beta}}{\alpha_{DC}}$ (nsec)
Bare ^{235}U (Godiva)	^{235}U	0.9795	0.0066_4	0.0065_9	- 1.10	6.04
	^{238}U	0.0205				
Bare ^{239}Pu (Jezebel)	^{239}Pu	0.9560	0.0019_5	0.0019_4	- 0.65	3.00
	^{240}Pu	0.0440				
Bare ^{233}U (Skidoo)	^{233}U	1.0000	0.0028_2	0.0029_0	- 1.00	2.82
U-reflected ^{235}U (Topsy)	^{235}U	0.8512	0.0069_4	0.0072	$- 0.38_2$	18.2
	^{238}U	0.1488				
U-reflected ^{239}Pu (Popsy)	^{239}Pu	0.6369	0.0027_7	-	$- 0.22_9$	12.1
	^{240}Pu	0.0073				
	^{235}U	0.0200				
	^{238}U	0.3358				
U-reflected ^{233}U (23 Flattop)	^{233}U	0.7178	0.0035_5	-	$- 0.27_1$	13.1
	^{238}U	0.2680				
	^{235}U	0.0142				

TABLE X. EFFECTIVE DELAYED FRACTIONS COMPUTED USING TWO COMPOSITE DELAYED NEUTRON SPECTRA (from Table VII)

Assembly	Effective delayed fraction		Percent difference
	Batchelor and Bonner spectrum	Burgy spectrum	
Bare ^{235}U (Godiva)	0.0066_4	0.0064_0	3.6
Bare ^{239}Pu (Jezebel)	0.0019_5	0.0019_3	1.0
Bare ^{233}U (Skidoo)	0.0028_2	0.0027_2	3.5
U-reflected ^{235}U (Topsy)	0.0069_4	0.0067_3	3.0
U-reflected ^{239}Pu (Popsy)	0.0027_7	0.0027_4	0
U-reflected ^{233}U (23 Flattop)	0.0035_5	0.0034_3	3.4

In the absence of individual delay group effectiveness values, γ_i, it is customary in reactor calculations to assume all $\gamma_i = \overline{\gamma}$. Using the spectral data of Table VII this approximation can be checked rather closely in the case of the first four delay groups (which constitute some 85% of total delayed neutron yield). For composite systems $\overline{\gamma}$ is computed as the ratio[3] of effective delay fraction, $\overline{\gamma\beta}$, to "actual" delay fraction, $\overline{\beta}$, given by

$$\overline{\beta} \equiv \frac{\sum_q \beta^q \int \sum_j \nu_j^q \, \sigma_{f_j}^q \, N^q(r) \, \varphi_j(r) \, d\,\mathrm{Vol}}{\sum_q \int \sum_j \nu_j^q \, \sigma_{f_j}^q \, N^q(r) \, \varphi_j(r) \, d\,\mathrm{Vol}} \qquad (4)$$

Similarly $\overline{\gamma}_i \equiv \overline{\gamma_i \beta_i} / \overline{\beta}_i$, where $\overline{\gamma_i \beta_i}$ is computed by weighting the i^{th} group delayed neutron yield (cf. Eq. (1)) with the i^{th} group spectrum, χ_i, rather than the composite delayed spectrum χ_D. A comparison of γ_i and $\overline{\gamma}$ values calculated for six metal assemblies is summarized in Table XI. Individual γ_i (excepting γ_1) are seen to differ from $\overline{\gamma}$ by less than 2% for the bare assemblies. (The very low energy spectrum of delay group 1 (relative abundance < 4%) results in larger values for γ_1.) In view of the rather large uncertainties in (^{235}U) delayed neutron spectra the results in Table XI appear to justify the assumption, $\gamma_i \approx \overline{\gamma}$ for bare metal systems (and probably for "slow" systems, which are of course less sensitive to fast

[3] For reflected systems, delayed neutron effectiveness may also be defined as the ratio of effective delay fraction, $\overline{\gamma\beta}$, to actual delay fraction in the core only. This effectiveness value, labelled $\overline{\gamma}_{core}$, is given in Table XI for Topsy, Popsy and 23 Flattop.

TABLE XI. COMPARISON OF DELAYED NEUTRON EFFECTIVENESS VALUES FOR SIX METAL ASSEMBLIES

Assembly	γ_1	γ_2	γ_3	γ_4	$\bar{\gamma}$
Bare ^{235}U (Godiva)	1.096	1.028	1.050	1.033	1.034
Bare ^{239}Pu (Jezebel)	0.963_5	0.942_4	0.947_5	0.944_4	0.945_9
Bare ^{233}U (Skidoo)	1.123	1.055	1.078	1.059	1.060
U-reflected ^{235}U (Topsy)	1.089	0.936_6	0.902_2	0.872_8	0.863_2 ($\bar{\gamma}_{core} = 1.08$)
U-reflected ^{239}Pu (Popsy)	0.739_3	0.668_6	0.585_8	0.498_7	0.530_6 ($\bar{\gamma}_{core} = 1.35$)
U-reflected ^{233}U (23 Flattop)	1.119	0.803_7	0.737_8	0.603_8	0.650_0 ($\bar{\gamma}_{core} = 1.33$)

spectral effects). The three reflected fast assemblies, on the other hand, exhibit disturbingly large differences among individual γ_i values. Thus for reflected fast systems (notably fast breeder reactors) the common assumption $\gamma_i \approx \bar{\gamma}$ must certainly be called into question for precise evaluations of neutron kinetics and control characteristics. The importance or more accurate and complete delayed neutron spectrum measurements for all the main fission species[4] is quite apparent.

Note that, in Table XI, delayed neutron effectiveness – both the γ_i and $\bar{\gamma}$ – exceeds unity for the ^{235}U and ^{233}U bare systems. In these thermal fissioning species, the lower energy of delayed neutrons means higher fission probability (greater Σ_f) and higher non-leakage probability, $\exp(-B^2\tau_D)$, while slowing down. A somewhat anomalous situation occurs in the ^{239}Pu bare assembly: here the γ_i and $\bar{\gamma}$ are actually less than unity due to the dip in the ^{239}Pu fission cross-section in the vicinity of 0.5 MeV. One therefore expects γ_2 to exhibit the smallest effectiveness value for Jezebel, since the second delay group spectrum, χ_2, peaks in the vicinity of 0.5 MeV (cf. Fig. 1).

In reflected systems, a considerable fraction of fissions occur in the ^{238}U of the reflector, giving large relative neutron yields for ^{238}U, as

[4] No delayed neutron spectral data whatsoever exist for other than the case of ^{235}U thermal fission.

shown in column 4 of Table VIII. On the other hand, the importance of neutrons (both prompt and delayed) born in the reflector is much lower than the importance of neutrons born in the core. For example in Popsy (U-reflected ^{239}Pu) some 25% of all fissions occur in the ^{238}U of the reflector, so that over two-thirds of all delayed neutrons in Popsy are from ^{238}U. But the relative importance of these delayed neutrons is sufficiently small that ^{238}U actually contributes only 33% to total effective delayed neutron yield. Similarly in Topsy (U-reflected ^{235}U) over 38% of all delayed neutrons are from ^{238}U, yet these account for less than 15% of the total effective delayed neutron yield, as seen in column 3 of Table IX. The major contribution to $\overline{\gamma\beta}$ clearly comes from the core material in the three reflected systems. Thus despite the large relative neutron yields from ^{238}U in the reflector, overall delay fractions $\overline{\gamma\beta}$ are not radically different from $\overline{\gamma\beta}$ for the corresponding bare assembly.

As noted previously, the accurate determination of delayed neutron spectra, yields and effective delay fractions is particularly important for kinetics and reactivity studies, since $\overline{\gamma\beta}$ provides the bridge between experimental measurement (of ratios: $\overline{\gamma\beta}/\ell$, $\Delta k/k\overline{\gamma\beta}$) and theory (normally in terms of k alone). To illustrate a very practical application of effectiveness calculations in reactor kinetics and control, let us compute the detailed period-reactivity relation in the Popsy (U-reflected ^{239}Pu) and 23 Flattop (U-reflected ^{233}U) assemblies. For a composite system, period versus reactivity is closely approximated by linear interpolation between "pure isotope" curves in direct proportion to the effective delayed neutron yield from each fission isotope present. Thus for a mixture of isotopes q = 1 ... n (having relative delayed neutron abundances $a_i^1 \ldots a_i^n$, and decay constants, $\lambda_i^1 \ldots \lambda_i^n$) we have

$$\$(T) \equiv \frac{\delta k}{k\overline{\gamma\beta}} \approx \sum_{q=1}^{n} \sum_{i=1}^{6} \frac{1}{1+\lambda_i^q T} \left[\frac{E_D^q}{\sum_q E_D^q} \right] a_i^q \qquad (5)$$

where \$(T) represents the reactivity in dollar units, $\overline{\gamma\beta}$ is the effective total delay fraction (cf. Eq.(3)) and E_D^q is the effective delayed neutron yield from isotope q, as calculated above. The resulting period reactivity relations for Popsy and 23 Flattop are shown in Fig. 3. Corresponding relations for the pure isotopes, ^{233}U, ^{239}Pu and ^{238}U are also included for comparison.

SUMMARY

Some of the important reactor physics and design problems have been considered wherein a better knowledge of the yields and energy spectral characteristics of delayed neutrons are of direct concern. In the absence of any spectral data whatsoever for other than the case of ^{235}U thermal fission, there is now a clear need for more accurate and complete delayed neutron energy spectrum measurements, as well as further high-energy delayed neutron yield data, for all of the main fission species. Indeed more complete delayed neutron data are becoming increasingly important

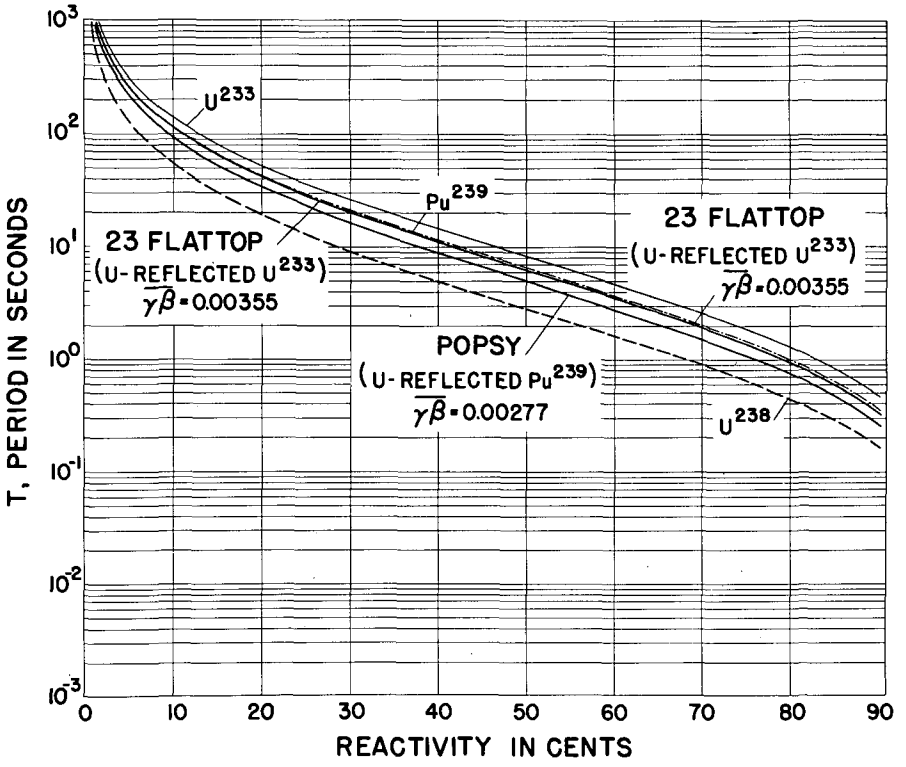

FIG. 3. Computed period versus reactivity relations for uranium-reflected ^{233}U and ^{239}Pu systems (see Table V for composition of systems).

in several expanding areas of nuclear technology, including as has been seen, the field of fast reactor kinetics and control, which is basic to the large power-breeder reactor development programmes now underway in the major nuclear nations.

REFERENCES

[1] McNELLY, M.J., Liquid Metal Fast Breeder Reactor Design Study, USAEC Rep. GEAP-4418 (1964).
[2] WOLFE, B., et al., "General Electric, 300-MW(e) FCR", in ANS National Topical Meeting on Fast Reactors, San Francisco, April 10-14, 1967.
[3] COHEN, K.P., O'NEILL, G.L., Safety and Economic Characteristics of a 1000 MW(e) Fast Sodium-Cooled Reactor Design, ANL-7120 (1966).
[4] Large Fast Reactor Design Study, USAEC Rep. ACNP-64503 (1964).
[5] STECK, R.B., Liquid Metal Fast Breeder Reactor Design Study, USAEC Rep. WCAP-3251-1 (1964).
[6] WRIGHT, J.H., et al., "Westinghouse prototype FCR", in ANS National Topical Meeting on Fast Reactors, San Francisco, April 10-14, 1967.
[7] Liquid Metal Fast Breeder Reactor Design Study, USAEC Rep. CEND-200 (1964).
[8] FORTESCUE, P., SHANSTROM, R.T., FENECH, H., Development of the Gas-Cooled Fast Reactor Concept, ANS-100 (1965).
[9] FORTESCUE, P., et al., "The gas-cooled fast reactor experiment (GAFRE)", in ANS National Topical Meeting on Fast Reactors, San Francisco, April 10-14, 1967.

[10] FORTESCUE, P., et al., "Status of technology of gas cooling for fast reactors", in ANS National Topical Meeting on Fast Reactors, San Francisco, April 10-14, 1967.
[11] HAFELE, W., et al., Karlsruhe Reference Design of a 1000 MW(e) Sodium-Cooled Fast Breeder Reactor, ANL-7120 (1966).
[12] HAFELE, W., et al., "NA-2 design (300-MW(e) German FCR)", in ANS National Topical Meeting on Fast Reactors, San Francisco, April 10-14, 1967.
[13] ZALESKI, C.P., SMIDT, D., Studies of Large Fast Reactors in France and West Germany, ANS-100 (1965).
[14] VENDRYES, G., et al., "The Phenix reactor (French FCR)", in ANS National Topical Meeting on Fast Reactors, San Francisco, April 10-14, 1967.
[15] VENDRYES, G., et al., "Rapsodie development program from design to operation", in ANS National Topical Meeting on Fast Reactors, San Francisco, April 10-14, 1967.
[16] VENDRYES, G., et al., "Main technical problems raised by the construction and testing of Rapsodie", in ANS National Topical Meeting on Fast Reactors, San Francisco, April 10-14, 1967.
[17] EDLUND, M.C., et al., Steam-Cooled Breeder Reactors, ANS-100 (1965).
[18] MURPHY, P., et al., Experimental Steam-Cooled Fast Reactor (ESCR), in ANS National Topical Meeting on Fast Reactors, San Francisco, April 10-14, 1967.
[19] LEITZ, F., RUBINSTEIN, H., "Status of technology for steam-cooled fast reactors", in ANS National Topical Meeting on Fast Reactors, San Francisco, April 10-14, 1967.
[20] OTT, D.C., Space Applications of Fast Reactors, ANS-100 (1965).
[21] LEIPUNSKY, A.I., et al., Nuclear Power Plant BN 350, ANS-100 (1965).
[22] SEFOR Development Program Quarterly Reports, USAEC Rep. GEAP-4594, GEAP-4742, GEAP-4864 (1964 to 1965).
[23] HORST, K., et al., "SEFOR development program", in ANS National Topical Meeting on Fast Reactors, San Francisco, April 10-14, 1967.
[24] BILLURIS, G., et al., "SEFOR plant design", in ANS National Topical Meeting on Fast Reactors, San Francisco, April 10-14, 1967.
[25] KEEPIN, G.R., Chapter 3, Physics of Nuclear Kinetics, Addison Wesley, Reading, Mass. (1965).
[26] WESTCOTT, C.H., EKBERG, K., HANNA, C.C., PATTENDEN, N.J., SANATANI, S., ATTREE, P.M., A survey of values of the 2200 m/s constants for four fissile nuclides, Atomic Energy Rev. 3 2 (1965) 3.
[27] MATHER, D.C., FIELDHOUSE, P., MOAT, A., Nucl. Phys. 66 149 (1965).
[28] COLVIN, D.W., SOWERBY, M.G., "Boron pile $\bar{\nu}$ measurements", Physics and Chemistry of Fission 2, Proc. Symp. Salzburg 1965, IAEA, Vienna (1965).
[29] HOPKINS, J.C., DIVEN, B.C., Nucl. Phys. 48 (1963) 433.
[30] Neutron Cross-Sections, BNL-325, 2nd Edition Supplement 2, Vol.III, TID-4500.
[31] BARNARD, E., FERGUSON, A.T.G., McMURRAY, W.R., van HEERDEN, I.J., Nucl. Phys. 71 (1965) 228.
[32] ANL Reactor Development Program Progress Report, ANL-7122, (1965) 19-21; ANL-7152 (1966) 8-14.
[33] GREEBLER, P., HUTCHINS, B.A., Trans. Am. nucl. Soc. 9 2 (1966) 453; also private communication (1967).
[34] DAVEY, W.G., "A critical evaluation of fast fission cross sections", Conf. on Neutron Cross-Section Technology, Washington, D.C., (March 1966).
[35] WHITE, P.H., HODGKINSON, J.L., WALL, G.J., Physics and Chemistry of Fission (Proc. Symp. Salzburg, 1965) 1, IAEA, Vienna (1965) 219.
[36] MOXON, M.C., CHAFFEY, C.M., see BNL-325, Supplement 2, Vol. III (1965).
[37] MACKLIN, R.L., GIBBONS, J.H., see BNL-325, Supplement 2, Vol. III (1965).
[38] See, for example, KEEPIN, G.R., J. nucl. Energy 7 (1358) 13; also Atomn. Energ. 4 (1958) 250.
[39] THOMPSON, T.J., BECKERLEY, J.G., Eds, The Technology of Nuclear Reactor Safety 1, Reactor Physics and Control, M.I.T. Press, Cambridge, Mass. (1964).
[40] HUGHES, D.J., DABBS, J., CAHN, A., HALL, D., Phys. Rev. 73 (1948) 111.
[41] USSACHOFF, L.N., Int. Conf. peaceful Uses atom. Energy (Proc. Conf. Geneva, 1955) 5, UN, New York (1956) 503; HENRY, A.F., Nucl. Sci. Engng 3 (1958) 52.
[42] HANSEN, G.E., Int. Conf. peaceful Uses atom. Energy (Proc. Conf. Geneva, 1958) 12, UN, New York (1958) 84.
[43] HANSEN, G.E., Physics of Fast and Intermediate Reactors, (Proc. Sem. Vienna 1961) 1, IAEA, Vienna (1962) 445.
[44] GRUNDL, J.A., USNER, A.A., Nucl. Sci. and Engng 8 (1960) 598; see also GRUNDL, J.A., A study of fission-neutron spectra with high-energy activation detectors, Parts I and II, Nucl. Sci. and Engng (1967).

[45] BATCHELOR, R., HYDER, H.R.McK., J. nucl. Energy 3 (1956) 7.
[46] KEEPIN, G.R., WIMETT, T.F., ZEIGLER, R.K., Phys. Rev. 107 (1957) 1044.
[47] BONNER, T.W., BAME, S.J., EVANS, J.E., Phys. Rev. 101 (1956) 1514.
[48] BURGY, PARDUE, WILLARD, WOLLAN, Phys. Rev. 70 (1946) 104.
[49] See, for example, CARLSON, B.G., "Numerical theory of neutron transport", Ch. 1, in Methods in Computational Physics, (ROTENBURG, M., Ed.) Academic Press (1963).
[50] ORNDOFF, J.D., Nucl. Sci. and Engng 2 (1957) 450; see also comprehensive survey of Rossi-α data by BRUNSON, G.S., et al., ANL-6681 (1963).

THE IMPORTANCE OF EXACT DELAYED NEUTRON DATA IN FAST REACTOR DYNAMIC BEHAVIOUR

S. YIFTAH AND D. SAPHIER
DEPARTMENT OF NUCLEAR SCIENCE,
TECHNION, ISRAEL INSTITUTE OF TECHNOLOGY,
HAIFA, ISRAEL

Abstract

THE IMPORTANCE OF EXACT DELAYED NEUTRON DATA IN FAST REACTOR DYNAMIC BEHAVIOUR. The way in which the uncertainties in delayed neutron spectra may affect the dynamic behaviour of fast breeder reactors is discussed. It is shown that an exact knowledge of delayed spectra is a much more important requirement for fast than for thermal reactors. A few cases are given in which changes in delayed neutron effectiveness (γ_i), resulting from uncertainties in delayed spectra, may have serious consequences for the dynamic response and stability. Two simplified calculated examples illustrate this fact. The main cases in which delayed neutron effectiveness may be a crucial factor, and which require further investigation are: 1. Cases where local disturbances may cause serious flux tilting which may be affected by the local γ_i: 2. Cases of marginal stability in which changes in γ_i may shift the reactor into the unstable region (or into a more stable region); 3. Cases where reactor regions are loaded with various fissionable isotopes having different yields of delayed neutrons and different spectra. In these cases it is difficult to predict the effect they may have on the reactor's dynamic performance. It is suggested that to approach solutions to the above problems, one has to solve the time-space and energy dependent Boltzmann equation for the reactor using appropriate approximations. An outline of a programme for the evaluation of the importance of exact delayed neutron data in a fast reactors' dynamic behaviour is given.

AVAILABLE DATA

Three sets of numbers characterize the delayed neutron fraction emitted in a fission process:

β_i the fraction of the delayed neutrons of group i

τ_i the mean half-life of the precursor C_i emitting delayed neutrons into group i

χ_i the energy spectrum in which the delayed neutrons of group i are emitted.

Over the last few years a sufficient amount of information has been accumulated on the first two items. There is however a serious lack of data on the spectrum of delayed neutrons (see Keepin [2]). The reason for this seems to be twofold: first, the complexity of measurement, especially for the groups of small τ; second, in thermal reactor calculations there was little demand for exact delayed neutron spectra. Only recently, with the acceleration of fast breeder programmes, has the need for such data become a matter of greater urgency.

The latest available data on delayed neutrons are collected in Chapters 4 to 6 in Keepin's book [2]: tables for ^{232}Th, ^{233}U, ^{235}U, ^{238}U, ^{239}Pu and ^{240}Pu for fast and slow fission are presented for six groups of delayed neutrons. The data include mainly the delayed fraction and

the precursor's half-life (or disintegration constant). Approximate spectra for four delayed groups are given only for ^{235}U.

INTRODUCTION

For a reactor to behave properly from the dynamic point of view, it should be capable of quickly overcoming, without damage, any reasonable disturbance occurring during its operation; of operating at several power levels, and passing from one level to another without any appreciable overshoots; and the reactor should not display any oscillatory behaviour. These requirements may be achieved by constructing the reactor with a high operational safety margin. Higher safety margins usually mean higher costs, but one cannot avoid this when the basic nuclear and thermal reactor parameters are not exactly known.

This statement is especially true for fast reactors, where operating experience is very limited and many gaps exist in present knowledge. Hence, it would seem necessary to improve and enlarge the basic experimental nuclear data, including the data on delayed neutrons.

The dynamic behaviour of a reactor is dependent on the reactivity coefficient and the delayed neutrons. Apart from certain extreme hypothetical nuclear accidents in which the reactor may attain a prompt critical condition, and where explosion [1] and complete, immediate destruction is considered (these are cases where delayed neutrons may be neglected), it is usually difficult to insert into a fast reactor so much reactivity that prompt critical conditions result. Changes in reactivity accompanying disturbances in fast reactors are smaller than similar disturbances in thermal reactors because of the much smaller cross-sections in the fast region. Since most excursions in fast reactors would be in the vicinity of the delayed critical condition, and the probability of obtaining prompt criticality is very small, availability of exact delayed neutron data is of utmost importance.

The possible influences of the delayed-neutrons data uncertainties on fast reactor stability and on its dynamic behaviour will be considered.

DELAYED NEUTRONS IN FAST AND THERMAL REACTORS

The relative delayed neutron effectiveness in producing fission depends on its position and energy at birth. (Usually, delayed neutrons are born at lower energies than prompt neutrons.) The relative importance of a delayed neutron from isotope k and group i may be obtained by weighting the total neutron yield with the product of the delayed neutron spectrum χ^k_{di} and the adjoint flux ψ^* as in [2].

$$I^k_{di} = \int_R \sum_{g=1}^{G} \chi^{kg}_{di} \, \psi^{g*}(r) \sum_{g'=1}^{G} \nu^{kg'} \, \Sigma^{kg'}_f \, \psi^{g'}(r) \qquad (1)$$

where $\psi^g(r)$ and $\psi^{g*}(r)$ are the flux of groups g at r and its adjoint respectively; ν^{kg} is the total neutron yield of isotope k resulting from fission by a neutron from group g; Σ_f is the fission cross-section; and

I_{di}^k is the relative delayed neutron importance from isotope k and delayed group i. The relative effective yield of the delayed neutrons from group i and isotope k is then given by the product of the importance and the neutron fraction:

$$Y_{di}^k = I_{di}^k \beta_i^k \tag{2}$$

and the effective prompt neutron yield from isotope k is obtained in a similar manner:

$$Y_p^k = I_p^k (1-\beta^k) \tag{3}$$

The effective delayed fraction from a mixture of isotopes is given by:

$$\overline{\gamma\beta} = \frac{\sum_k I_d^k \beta^k}{\sum_k \left(I_p^k (1-\beta^k) + I_d^k \beta^k \right)} \tag{4}$$

It is seen from the above equations that to evaluate the relative importance and/or effectiveness of each delayed group, its spectrum must be known.

In thermal reactors, all neutrons producing fission are slowed down. Delayed neutrons, born at lower energies, have a better chance of becoming thermal and are therefore more effective than prompt neutrons ($\gamma_i > 1$), but the exact energy with which they are born seems to be of no great importance, especially in water-moderated reactors where the mean loss of energy per collision is large.

On the other hand, in fast reactors, most neutron interactions (fission, scattering and absorption) occur in the fast region, the region in which the neutrons are emitted, and therefore an exact knowledge of the energy with which the neutron (prompt or delayed) is born seems to be of paramount importance. This is true especially for reactors where large amounts of ^{238}U, ^{232}Th and ^{240}Pu are present as fertile material in the blanket-reflector. A relatively large amount (up to 25%) of fission reactions may occur in these elements which have high threshold energies for fission.

The delayed neutrons may or may not be able to produce fission in those isotopes, depending on the energy with which they were born. It is obvious that in fast breeders – in distinction to thermal reactors – large variations in the delayed effective fraction may be found in various reactor types on the one hand, and among various delayed neutron groups on the other. This calls for exact evaluation of delayed neutron spectra.

SOME PROBLEMS REQUIRING INVESTIGATION

Keepin (Ref. [2] Table 6-7, p. 182) compares the delayed neutron effectiveness values for six zero power metal assemblies. If we consider one of them, the U-reflected '23-Flattop' for example, we get, for the first four delayed groups, the values 1.119, 0.8303, 0.737 and 0.603, respectively; the total $\overline{\gamma}$ = 0.650 whereas the in-core $\overline{\gamma}$ = 1.33. When

TABLE I. THRESHOLD ENERGIES FOR FISSION IN FERTILE ISOTOPES

U-238 E_{th} = 0.65 MeV	Th-232 E_{th} = 1.1 MeV	Pu-240 $E_{th} \simeq$ 0.25 MeV

looking on the various groups of delayed neutrons as a feedback with a time delay τ_i and an amplitude $\gamma_i \beta_i$, it is clear that the usual acceptance of $\gamma_i = \bar{\gamma}$ may result in predicting erroneously the dynamic behaviour of the reactor. In a simple example calculated by the code "FREDY" [3] which solves the equations of a point kinetic model, it is shown how various γ_i's affect the reactor's response (Fig. 1). A step of reactivity $\delta k = 0.002$ with a duration of 0.4 sec (0.4 sec seems a reasonable time for feedback reactivity effects to reduce reactivity back to zero), and a reactivity ramp of $\delta k = 0.01$/sec for a period of 0.3 sec, is applied to a reactor which has the delayed groups of ^{235}U. Four cases are presented and it is clear that even in this simple case the peak power attained after 0.4 sec varies greatly with the γ chosen. Generally, the smaller the delayed neutron effectiveness the larger the power excursion attained. The results obtained are far from representing what actually goes on in a reactor (see later) but it is clear from the above illustration that the exact evaluation of γ_i for the various isotopes in fast breeders is inevitable.

The two available fertile isotopes ^{232}Th and ^{238}U have a relatively high yield of delayed neutrons (see Table II), and may, therefore, in certain cases dominate the dynamic behaviour of the reactor. If the fissionable and the fertile substances are not homogeneously distributed (which is usually the case) then the dynamic behaviour of different regions in the fast breeder will be characterized by different time scales (i.e. "slow" in regions rich in ^{238}U, ^{232}Th and ^{240}Pu, and "fast" in regions rich in ^{335}U, ^{239}Pu and ^{241}Pu) because of the different β's, λ's and spectra.

It is hard to predict how this effect will influence the dynamic behaviour and the stability of the reactor. Further investigations on this problem are required, but it is reasonable to assume that this fact may, in certain cases, enhance local disturbances. At this point attention should be drawn to the fact that the various feedback effects in fast reactors (i.e. Doppler and sodium reactivity effects) have time delays of the same order of magnitude as the delayed neutrons. Because of the relatively small physical size of fast reactors and the materials used, the heat capacity of a fast reactor is rather small compared to that of a thermal reactor, and hence the temperature rise in a fast reactor due to an excursion would be rapid. As a consequence, a Doppler reactivity effect will appear immediately, together with a somewhat delayed sodium reactivity effect. These two, being the main feedback effects, are dependent on position in the same way as the 'feedback' resulting from delayed neutrons. Interaction between these effects may or may not cause local damage to the reactor (because of flux tilting) and this may be strongly dependent on whether the γ_i of some delayed groups of neutrons are, for instance 1.2 or 0.6; for this case an exact knowledge of the delayed neutron spectra would be of utmost importance.

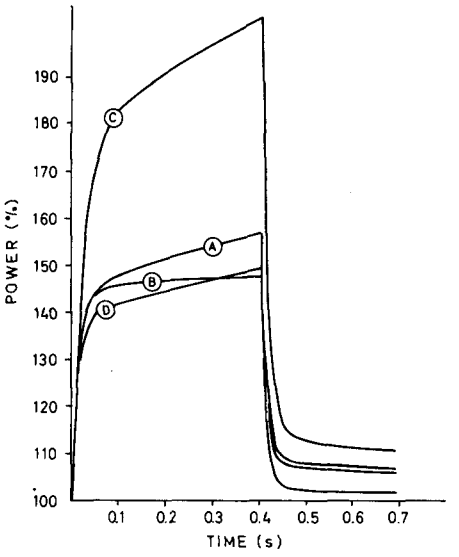

FIG. 1a. Reactor transient response to a step change in reactivity $\delta k/k = 0.002$ for 0.4 sec. The delayed groups are of ^{235}U, and γ_i varies as: A. $\gamma_i = \bar{\gamma} = 1$; B. $\bar{\gamma} = 1$, only one group; C. $\gamma_1 = 1.12$, $\gamma_2 = 0.8$, $\gamma_3 = 0.74$, $\gamma_4 = 0.6$, $\gamma_5 = 0.6$, $\gamma_6 = 0.5$; D. $\gamma_i = \bar{\gamma} = 1.1$.

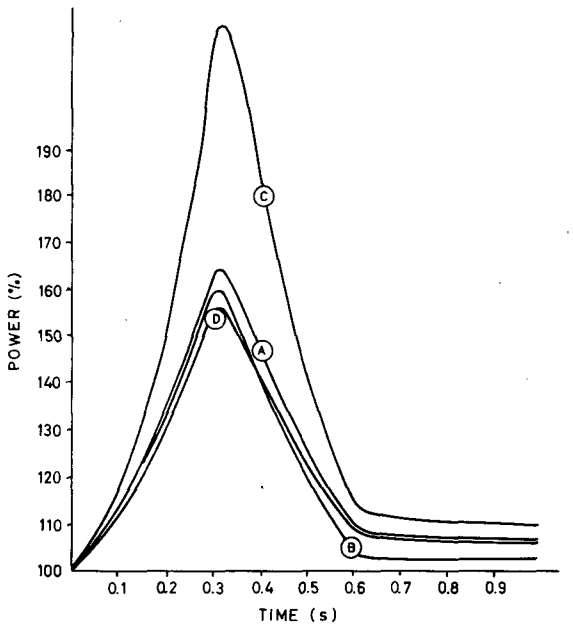

FIG. 1b. Reactor transient response to a ramp change in reactivity increasing at a rate of 0.01 ($\delta k/k$) per second for 0.3 sec, and decreasing at the same rate for 0.3 sec (A, B, C and D defined as in Fig. 1a).

TABLE II. TOTAL DELAYED NEUTRON YIELD AND HALF-LIVES

The various β's are from Keepin [2] as obtained at Los Alamos by irradiating specimens of different isotopes. The "Godiva" central spectrum (which is a slightly degraded fission spectrum) was used as the fast source, whereas thermal fission was achieved within an 8-inch polyethylene block, cadmium shielded, and mounted near "Godiva". $\beta = \sum_i \beta_i$, and $\bar{\tau}$ was calculated from

$$\bar{\tau} = \frac{\sum_i \beta_i \tau_i}{\sum_i \beta_i}$$

	Fast fission			Slow fission			Mean energy (MeV)
	$\bar{\beta}$	relative yield	$\bar{\tau}$ (sec)	$\bar{\beta}$	relative yield	$\bar{\tau}$ (sec)	
Th-232	0.0203	3.17	6.98	___	___	___	0.49
U-233	0.0026	0.406	12.40	0.0026	0.406	12.80	0.39
U-235	0.0064	1.000	8.83	0.0065	1.017	9.02	0.43
U-238	0.0148	2.31	5.32	___	___	___	0.49
Pu-239	0.0020	0.312	10.15	0.0021	0.328	10.71	0.40
Pu-240	0.0026	0.406	9.35	___	___	___	0.42
Pu-241	___	___	___	0.0049	0.765	___	___

In a recent paper [4] by Smets, the author proves that the effect of delayed neutrons on reactor dynamics is not always stabilizing, as generally accepted. Smets shows that, for a point reactor model, complete neglect of delayed neutrons would in certain cases result in a conditionally stable reactor, whereas including delayed neutron effects in the same reactor would show it to be unstable. This fact is clearly proved by the Nyquist plot for the two cases (Fig.2) as was done in Fig.3 of Smets' paper [4].

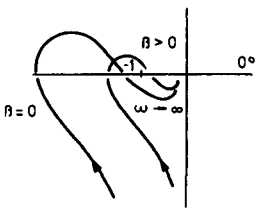

FIG.2. Nyquist plot for $n_0 G(jw) H(jw)$. When $\beta > 0$, the reactor is unstable; when $\beta = 0$, it is conditionally stable.

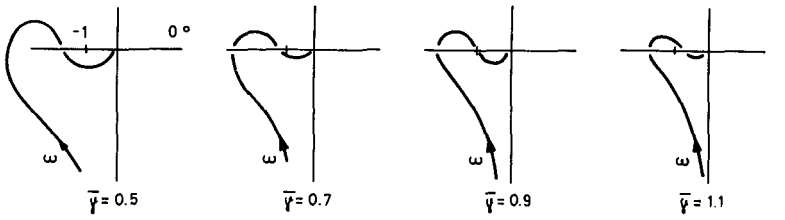

FIG. 3. Nyquist plot for $n_0 G(jw) H(jw)$ with one group of delayed neutrons. In this case it is seen that increasing $\bar{\gamma}$ reduces stability.

$$H(jw) = \frac{Kh(jw + 0.05)(jw + 0.1)}{(jw + 0.001)(jw + 0.01)}$$

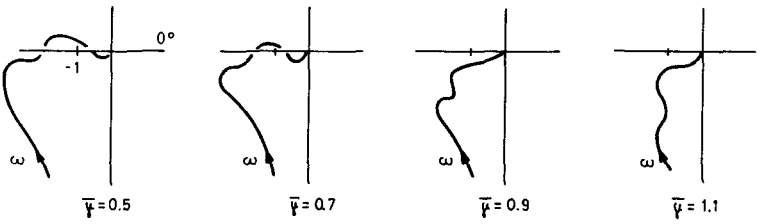

FIG. 4. Nyquist plot for $n_0 G(jw) H(jw)$ with one group of delayed neutrons. In this case it is seen that increasing $\bar{\gamma}$ increases stability.

$$H(jw) = \frac{Kh(jw + 0.001)(jw + 50)(jw + 200)}{(jw + 0.005)(jw + 0.05)(jw + 0.25)}$$

The same argument may be followed when considering the various $\gamma\beta$ or $\gamma_i\beta_i$ resulting from delayed neutron effectiveness calculations. In the examples given below (see Fig. 3) it may be seen that, for certain cases, changes in $\gamma\beta$ resulting from the uncertainties which exist today in the knowledge of delayed neutron spectra may shift the reactor either into the unstable region or to a more stable region, depending on what error is inherent in the calculations of the various γ_i's.

It is evident that for these marginal cases, to state whether a certain reactor configuration is stable or not, and what is the critical power level[1], exact evaluation of γ_i is required and this may be done only if one knows the exact delayed spectra.

The problem becomes even more complicated when one has to deal with space-time behaviour, for example, when calculating the maximum flux tilting due to some local disturbance. In such a case time and space may not be separated, and the point kinetic model used frequently in stability and safety calculations is useless. In a large number of recent papers [5-7] the necessity for space time investigations was treated. Yasinsky and Henry [5] showed that the flux tilting resulting from a local reactivity disturbance, when calculated by an exact method [8], would

[1] Critical power level: the power at which the reactor becomes unstable.

be of an amplitude 10^4 times the peak predicted by a point model kinetic calculation with the same amount of reactivity disturbance.

Hence it is assumed that apart from general stability considerations, the exact time-space problem should be solved as a part of any preliminary safety calculation in order to predict what possible damage a local disturbance could cause, this being true especially in fast breeders where, as mentioned above, regions with different isotopic composition exist. Here again exact knowledge of the effective delayed fraction in each region is required; an error of 20-30% (which is common in present stage of knowledge) may prove serious in certain cases.

It should be added that the plutonium considered for use in fast breeders will be of different "purities", i.e. of different isotopic compositions, depending on the way it was produced [9]. The various isotopic compositions of plutonium will cause different β, λ and χ. (It should be pointed out here that almost nothing is known about the delayed neutrons of ^{241}Pu and ^{242}Pu.)

THE PRESENT PROGRAMME

To study the effect of different delayed neutron concentrations and spectra on a reactor's dynamic performance, a series of research programmes should be initiated.

(a) A set of experimental investigations should be launched in order to evaluate the exact delayed neutron spectral data for the various isotopes and, based on these, theoretical calculations should evaluate the relative effectiveness of delayed neutrons in various configurations of fast breeders.

(b) A set of dynamic calculations should be performed for various reactor configurations to predict by how much the uncertainties in delayed neutron data affect the dynamic behaviour, and the critical cases should be clearly indicated.

In the present programme the solution of the last set of problems is undertaken. From the above discussion, and from Ref. [5], it is clear that a complete solution of the time-space and energy dependent diffusion equation is required. Unfortunately, no computer code is available as yet for adequately solving the complete set of equations, as would be required for the investigation of fast reactor dynamic problems.

From the codes already developed for solving the time-space diffusion equation [1, 8, 10, 11], only "WIGLE II" [8] seems to be applicable, but even this code is written only for two energy groups and one dimension. In "SWANTIME" [10] and "AX-1" [1] the delayed neutrons have been completely neglected. "FREAK" [11] has not yet been completely developed and its successful solution is dependent on the time step chosen.

The main reason that a complete time-space dependent programme has not been produced as yet is the complexity and the long computation time required. To overcome this difficulty a few other approaches are possible:

(a) The best way to solve time dependent dynamic problems is by the use of an analogue computer, but a machine with the precision and

capacity required for such a problem is not available; this may be a task for the new hybrid machines under development.

(b) A good approach which does not require long computation time is to solve the time-space dependent problem by a quasistatic method developed by Henry [12, 13] and treating the delayed neutrons by the method suggested by Ott [7].

(c) To use the inherent capability of analogue computers to solve dynamic problems, and the precision of digital machines (together with low price per solved problem), a new digital differential analyzer (DDA) developed by "Elliott-Computers" [14] may be incorporated for the solution of the problem. By this method the time-space diffusion equation may be simulated by means of a great number of digital integrators (256 or 512) and the solution at any time obtained on an x-y-plotter in the form of space-energy dependent fluxes.

Methods b and c are under development in the present programme and with their help several models of fast reactors with different fuels and isotopic composition will be investigated. By varying the assumed delayed neutron spectra over the limits of uncertainty the transient behaviour exposed by each model would be checked for various disturbances. By comparing the results it will be possible to evaluate to what extent and for what cases exact delayed neutron data are essential.

REFERENCES

[1] OKRENT, D., COOK, J. M., SATKUS, D., LAZARUS, R. B., WELLS, M. B., AX-1, A Computing Program for Coupled Neutronics-Hydrodynamics Calculations, ANL-5977 (1959).

[2] KEEPIN, G. R., Physics of Nuclear Kinetics, Addison-Wesley, New York (1965).

[3] SAPHIER, D., YIFTAH, S., FREDY - A computer program calculating fast reactors' transient response and its transfer function (to be published).

[4] SMETS, H. B., On the effect of delayed neutrons in reactor dynamics, Nucl. Sci. Engng 25 (1966) 236.

[5] YASINSKY, Y. B., HENRY, A. F., Some numerical experiments concerning space time reactor kinetics behaviour, Nucl. Sci. Engng 22 (1965) 171.

[6] JOHNSON, S. O., GYFTOPOULOS, E. P., DODD, M. E., Effect of flux shape changes on power excursion behaviour, Trans. ANS 8 1(June 1965) 221.

[7] OTT, K., MADELL, I. T., Quasistatic treatment of spatial phenomena in reactor dynamics, Nucl. Sci. Engng 26 (1966) 563.

[8] CADWELL, W. R., HENRY, A. F., VIGILOTTI, A. J., "WIGLE - A Program for the Solution of the Two-Group Space-Time Diffusion Equations in Slab Geometry", WAPD-TM-416 (1967).

[9] YIFTAH, S., "Effect of the plutonium isotopic composition on the performance of fast reactors", Physics of Fast and Intermediate reactors (Proc. Sem. Vienna, 1962) IAEA, Vienna (1962) 257.

[10] BRICKSTOCK, A., DAVIES, A. R., SMITH, I. C., SWANTIME - A Time Dependent Multi-Group Diffusion Code for IBM-7030, AWRE 0-3166 (May 1966).

[11] PERKS, M. A., "FREAK", Proc. Conf. Application Computing Methods to Reactor Problems, ANL-7050 (August 1965).

[12] HENRY, A. F., The application of reactor kinetics to the analysis of experiments, Nucl. Sci. Engng 3 (1958) 52.

[13] HENRY, A. F., CURLEE, N. J., Verification of a method for treating neutron space-time problems, Nucl. Sci. Engng 4 (1958) 727.

[14] SHANI, A., "Incremental computers", Proc. 5th Nat. Conv. of Electronics and Control Engineers of Israel, Haifa 1965.

DISCUSSION

On the papers by Keepin, and Yiftah and Saphier

In very high temperature reactors there is a possibility of delayed neutron precursor loss by diffusion. A specific example is the nuclear propulsion reactor – typically a graphite moderated ^{235}U system – with liquid-hydrogen coolant passing rapidly through the core. In such systems the gaseous fission products, including the major bromine and iodine precursors may be lost, losing at the same time the margin of control provided by these delayed neutrons. This phenomenon clearly depends on the diffusion rate of particular precursor elements through the medium in question; for such systems therefore, the identification of precursors and the determination of their diffusion rates will be very important.

The question of precursor diffusion rate out of graphite and other fuel-element materials must be investigated in detail. There are some old data of Cowan et al.[1] which give good estimates up to a maximum temperature of 2400°C (measuring diffusion rates through the graphite at different temperatures). However, better diffusion-rate data are now needed for incorporation in modern high-temperature reactor calculations. Also, more detailed data on the abundances of precursors are desirable – it is not possible to compute high-temperature diffusion effects, etc. if yield data on precursors are insufficient. There are presently big discrepancies in the data on diffusion rates, for example, of krypton and xenon out of uranium dioxide (i.e. the data given by different workers in the field differ by seven orders of magnitude in the diffusion coefficient, and by a factor of two in the activation energy which governs the temperature dependence): better data are required and should be incorporated in calculations. In the near future, 90% of the individual neutron precursors will undoubtedly be known, and by taking all individual data, it should be possible to construct the precursor composition expected in a given situation, and even include fractionation effects at high energies. Also, in circulating fuel reactors (e.g. liquid metal fuel reactors) where the delayed neutron precursors are being transported out of the core and returned in a certain cycle time (delayed neutrons being effectively lost during this process), the control associated with these neutrons is lost. In such practical cases, as just discussed, not only the abundances and periods of delayed neutrons should be known but the identification of the precursors (at least Z, and hopefully also A) may be of considerable importance.

The problem of the high energy tail of the total steady-state delayed neutron spectrum is not explained as yet. Is this tail really due to the delayed neutrons or is there a significant contribution from prompt neutrons, as has been suggested in the literature. Normally the effective maximum energy of delayed neutrons approaches 2 to 3 MeV. But for some short-lived precursors, like ^{93}Br, which may be represented in the sixth delay group, the $Q_\beta - B_n$ value (theoretical maximum neutron energy) is estimated to be about 9 MeV. This would seem to imply that at least a part of the high energy tail in delayed neutron spectra can be attributed to delayed neutrons. Nevertheless, it is quite reasonable to expect that part of the high energy neutrons in the spectrum could be due to prompt neutron

[1] COWAN, C.A., ORTH, C.J., Int. Conf. peaceful Uses atom. Energy (Proc. Conf. Geneva, 1958) 7 UN, New York (1958) 328.

contamination (arising from delayed-neutron-induced fissions in the sample giving rise to prompt fission neutrons, with a known higher-energy spectrum).

It is not yet clear how reliable the spectra of Batchelor et al.[2] are in the low energy region. The measurements, done with a ^{3}He proportional counter, are very sensitive to the contribution of slowed-down neutrons which might be reflected from surrounding materials, and then detected in the counter with a high detection probability. The ^{3}He recoils will cause confusion at low energies, and no quantitative correction was made for this perturbation. Batchelor[2] and Bonner[3] considered these effects to be too small and did not try to estimate them. Therefore, the errors assigned by Batchelor and Bonner (8%) are probably too optimistic. At the time (1956) their measurements were indeed very welcome, being all that was available. The spectra have been measured only for thermal fission of ^{235}U. Today, however, more accurate spectral data are urgently required. These measurements have to be done for other fissionable species and for different energies of incident neutrons.

More extensive delayed neutron yield and spectral data are especially needed in the field of fast reactor kinetics and control that underlies the large power-breeder reactor development programmes presently underway in several countries. For example, the USAEC is evaluating proposals from several US industrial firms for a 1000 MW fast breeder reactor. In the USSR, the BR250, presently under construction, is a second-stage prototype reactor of 240 MW, as a continuation of the Obninsk BR5 reactor (which used plutonium oxide fuel and sodium cooling). The SEFOR reactor has already been mocked-up as a critical assembly, and many low power experiments have been carried out. The construction of such a sodium-cooled fast oxide reactor will start soon. The Karlsruhe fast oxide reactor and the Cadarache reactor are heading toward the actual reactor construction phase. For the future, many fast power-breeder reactor systems are being planned: in such systems the best possible delayed neutron data are required.

With the use of Ge(Li) detectors, prompt analysis of the unseparated fission products can be made, but of course it would be difficult to determine which primary fragment gives rise to a particular gamma ray line. In the case of delayed neutron precursors, more complete information could be obtained with neutron-gamma coincidence. Since it is difficult to use a neutron pulse as the trigger for coincidence measurements, it might be possible to use the recoil nuclei. The recoil energy associated with neutron emission is three orders of magnitude greater than that associated with beta emission, so pulses from neutron recoils could be easily discriminated from beta recoil pulses. Such discrimination methods (as well as range-discrimination and modern pulse-shape discrimination techniques) might be very useful for coincidence work.

---

[2] BATCHELOR, R., HYDER, H.R. McK., J. nucl. Energy 3 (1956) 7.

[3] BONNER, T.W., BAME, S.J., EVANS, J.E., Phys. Rev. 101 (1956) 1514.

DELAYED NEUTRON EMISSION, THEORY AND PRECURSOR SYSTEMATICS

T. JAHNSEN, A.C. PAPPAS AND T. TUNAAL
UNIVERSITY OF OSLO,
BLINDERN, NORWAY

Abstract

DELAYED NEUTRON EMISSION, THEORY AND PRECURSOR SYSTEMATICS. Information on the properties of observed delayed neutron precursors and emitters is reviewed. As far as possible emphasis is laid on charge, mass, half-life, β-energetics, neutron-branching, levels, spin and neutron energy spectra. The theory of delayed neutron emission given by Bohr and Wheeler and later refined is presented and analysed with respect to its potentialities and limitations. Even if the theory gives a good general picture of the process itself, it has not been possible to develop it to such detail as would be necessary for satisfactory delayed neutron precursor systematics. Consequently, the systematics which are available today are based mainly on energetics as criteria, and suggest a wide range (in charge and mass) of precursors, much wider than anticipated, earlier or even now, from those that have already been identified. Nevertheless systematics have their use in a search for precursors and have in recent years resulted in a substantial increase in the member of *known* species. The process is analysed step by step (i.e. matrix element, Fermi function, level density, spin distribution, "the energy and the angular momentum paths", and neutron-to-total width). Improvements are suggested that would give rise to a more realistic treatment, and outlines are given for guiding future work. Emphasis is put onto that experimental and theoretical information which must be obtained before a satisfactory and advanced theoretical treatment can be obtained. Some attempts made along these lines are presented. Their importance in the estimate of P_n values and shapes of neutron spectra are shown and discussed. For the latter the more different factors (i.e. $|M|^2$, $\omega(E,J)$, Γ_n/Γ_{tot}, J, π, levels, etc.) are considered, the more evidence is obtained for a "piling up" of the neutron spectrum towards low energies. Finally the importance is stressed of detailed delayed neutron studies for considering nuclear structure phenomena.

1. INTRODUCTION

In a general study of nuclear decay the complex two-step process of delayed particle emission should provide valuable information on nuclear structure, shape of the nuclear energy surface and applicability of current nuclear mass formula in regions far off the stability line.

Delayed particle emission is known both from neutron-deficient nuclei (alphas and protons) and from neutron-rich nuclei (neutrons). Delayed proton emission was first observed in 1962, whereas the emission of delayed neutrons had been discovered in 1939. It is the latter which will be discussed.

After the discovery of nuclear fission it was considered that newborn fragments having a large excess of neutrons over stable isotopic nuclei would emit prompt neutrons either at the instant of fission or very soon after. However, some serious discussion centred on the idea that a fission fragment may undergo several steps of β-decay and still reach a state where de-excitation by neutron emission is possible.

In fact the emission of delayed neutrons was observed by Roberts, Meyer and Wang [1] early in 1939 before the existence of the prompt neutrons had been proved. Bohr and Wheeler [2] in their paper on the "Mechanism of nuclear fission" analyse the possible origins of neutrons

and conclude "... that the delayed emission of neutrons indeed arise as a result of nuclear excitation following the β-decay of nuclear fragments".

Since then studies of delayed neutron emission have followed two different paths. This is because the process itself and its mechanism is of basic interest in nuclear science, and because the delayed neutrons are of major importance in the control of nuclear reactors. Reactor control cannot be based only on the fast generation time of the prompt fission neutrons, but must depend on the delayed neutrons, also. For the successful construction of advanced reactors, i.e. fast reactors, reactors operating at extremely high temperatures and, perhaps, liquid fuel reactors with continuous reprocessing, the delayed neutrons and their influence on reactor parameters seem to have a crucial influence. Such implications have been discussed by Keepin [3], Cowan and Orth [4], and others, and it seems clear that further knowledge of delayed neutron precursors is necessary for usefully studying the response and stability in the above-mentioned reactors.

The aim of the present paper is to review and analyse the state of delayed neutron emission theory and the precursor systematics based on this, and to stress potentialities and limitations of the available approaches. Due to lack of detailed knowledge concerning the systematics of nuclear structural properties far from the stability line, these studies are today performed in a way which could be termed 'experimental theory'.

2. OUTLINE OF THE MECHANISM OF DELAYED NEUTRON EMISSION

2.1. Identified delayed neutron precursors

Delayed neutron emission is made possible by the fact that the greater the distance from stability, the less the neutron binding energy B^n and the greater the mass difference between adjacent isobars, and hence the total β-decay energy Q^β. Thus at a certain or greater distance from stability $Q^\beta - B^n > 0$, and beta-decay from a nuclide (Z, N) can populate states above the neutron binding energy in the daughter nuclide (Z+1, N-1). This may then promptly emit a neutron giving the nuclide (Z+1, N-2) or de-excite through γ-emission to its ground state (Fig. 1). Thus the neutron emission seems to be delayed and will take place with the half-life of the precursor.

It was believed for a long time that only six precursors existed. That the half-lives were due to mixtures of two or more precursors was first indicated by Pappas [5], with later additional confirmation [6], in an intercomparison of reported abundances and half-lives with estimated individual probabilities for delayed neutron emission.

Since then the number of delayed neutron precursors established in fission has steadily increased and includes today close on twenty species (Tables Ia-c). The caution necessary when giving physical significance to the six delayed neutron groups has further been stressed by Bemis [7] who pointed to the existence of unidentified parents and their influence in gross delayed neutron decay analysis. (See Ref. [8] for comments to the latter item). Thus off-hand comparison of delayed neutron group abundances with precursor yields must be made taking great precaution unless proper

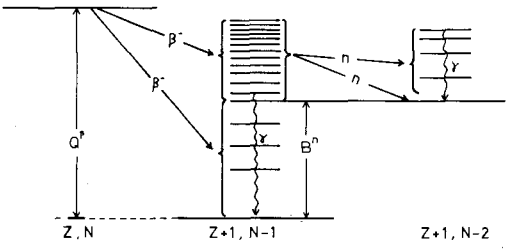

FIG. 1. Schematic representation of delayed neutron emission.

consideration can be given to identified and unidentified precursors and their parents.

The delayed neutron precursors identified today, as found in the literature, are given in Tables Ia, Ib and Ic together with information available on the spin of the precursor and final product, the total beta-decay energy and the neutron binding energy. The mass-differences given are either reported or based on information from Nuclear Data Sheets, that is to say that mass formulae are not used. The measured neutron branchings available are crude and neutron energy spectra are very poorly known. The four spectra reported by Batchelor and Hyder [27] (for groups 1 to 4 out of the 6 groups assumed to be present) for delayed neutrons from fission fragments are old (1956) and thus ipso-facto measured with poor resolution (10% or worse). These are, however, still the best ones available. The spectra are essentially continuous with some pronounced structure, but without any distinct peaks [27, 28] (Fig. 2). The structure may be explained by the fact, shown later, that the various groups in reality are composed of two or more precursors (except group 1 which at present seems to be ^{87}Br only). Inspection of the spectra against this background has led to the assumption that these are composites of essentially continuous single spectra [6].

After delayed proton emission from light nuclei was observed to give typical line spectra [29], and remembering that the light delayed neutron precursors ^{9}Li and ^{17}N do also (Table Ia), the above assumption might be questioned. The known neutron spectra, however, are from nuclei with $N > 50$ or $N > 82$, i.e. with mass numbers in the vicinity of 90 or 140. Comparison with proton spectra may therefore be ill-founded, especially as the latter spectra all show high energies due to the Coulomb barrier effect. Known delayed proton emitters from nuclei with $Z > 50$ are scanty, as only two to three seem to have been identified. These, however, (notably ^{109}Te [30] and ^{111}Te [31]) also show line spectra over the energy range of about 2 to 4 MeV.

Therefore it can be concluded that the delayed neutron spectra hitherto observed in fission fragments should in fact be 'smoothed-out' spectra.

3. SYSTEMATICS OF DELAYED NEUTRON EMISSION

During the early discussion of closed nuclear shells and their implications on nucleonic binding energies, Mayer [32] in 1948 was the first to point out the effects of closed neutron shells in delayed neutron emission.

TABLE Ia. A SURVEY OF DELAYED NEUTRON PRECURSORS REPORTED IN THE LITERATURE

Mass region[a] 8 to 17

Precursor	Emitter	$T_{\frac{1}{2}}$ (sec)	Q^{β} (MeV)	B^{n} (MeV)	$Q^{\beta}-B^{n}$ (MeV)	n-branch (%)	Ground-state spin Precursor	Ground-state spin Final product	Comments	Ref.
$^{8}_{2}He_{6}$	$^{8}_{3}Li_{5}$	0.122	11.4 [1] 10.1 [2]	2.0	9.5 [1] 8.1 [2]	12 ± 1	0	3/2		[9,10]
$^{9}_{3}Li_{6}$	$^{9}_{4}Be_{5}$	0.176	13.5	1.7	11.8	75 ± 15	3/2	0	n-energies: 0.7 MeV (90-95%) 3-4.5 MeV (5-10%)	[11, 12]
$^{12}_{4}Be_{8}$	$^{12}_{5}B_{7}$	0.011	~11.7	3.4	~8		0		Open to question, may be ^{11}Li.	[13, 14]
$^{16}_{6}C_{10}$	$^{16}_{7}N_{9}$	0.74	8.0	2.5	5.5		0	1/2		[11, 15]
$^{17}_{7}N_{10}$	$^{17}_{8}O_{9}$	4.16	8.7	4.1	4.6	95 ± 1	(1/2)	0	n-energies: 0.40 MeV (47%) 1.22 MeV (47%) 1.79 MeV (6%)	[16 - 18]

[a] All data for this mass region are taken from the given references.

TABLE 1b. A SURVEY OF DELAYED NEUTRON PRECURSORS REPORTED IN THE LITERATURE

Mass region 85 to 96

Precursor	Emitter	$T_{\frac{1}{2}}$ (sec)	Q^{β} (MeV)	B^{n} (MeV)	$Q^{\beta}-B^{n}$ (MeV)	n-branch (%)	Ground-state spin: Precursor	Ground-state spin: Final product	Comments	Ref.
$^{85}_{33}As_{52}$	$^{85}_{34}Se_{51}$	2.15	~8	~5	~3	11±3		0	n-branch based on fission yield calculations	[19, 20]
$^{87}_{35}Br_{52}$	$^{87}_{36}Kr_{51}$	55.4	8.0	5.5	2.5	3±1	3/2, 5/2	0		[21-24]
$^{88}_{35}Br_{53}$	$^{88}_{36}Kr_{52}$	16.3	10	7.4	2.6	6±2		7/2		[22, 24]
$^{89}_{35}Br_{54}$	$^{89}_{36}Kr_{53}$	4.4	9	5	4	10±3		0		[22, 24]
$^{90}_{35}Br_{55}$	$^{90}_{36}Kr_{54}$	1.6	10.5	6.5	4	15±4				[22, 24]
$^{92,93}_{36}Kr$	$^{92,93}_{37}Rb$	~1.4								[25]
$^{94}_{36}Kr_{58}$	$^{94}_{37}Rb_{57}$	~1.4								[25]
$^{93}_{37}Rb_{56}$	$^{93}_{38}Sr_{55}$	5.9	7	5	2			0		[25, 26]
$^{94}_{37}Rb_{57}$	$^{94}_{38}Sr_{56}$	2.7	8.5	6.3	2.2					[26]
$^{95}_{37}Rb_{58}$	$^{95}_{38}Sr_{57}$	0.36	7	5.2	1.8			0		[26]
$^{96}_{37}Rb_{59}$	$^{96}_{38}Sr_{58}$	0.23								[26]

TABLE Ic. A SURVEY OF DELAYED NEUTRON PRECURSORS REPORTED IN THE LITERATURE

Mass region 135 to 145 and mass 210

Precursor	Emitter	$T_{\frac{1}{2}}$ (sec)	Q^{β} (MeV)	B^{n} (MeV)	Q^{β}-B^{n} (MeV)	n-branch (%)	Ground-state spin Precursor	Ground-state spin Final product	Comments	Ref.
$^{135}_{51}Sb_{84}$	$^{135}_{52}Te_{83}$	2	7	3.5	3.5	~1	7/2 ?	0		[19,20]
$^{137}_{53}I_{84}$	$^{137}_{54}Xe_{83}$	24.4	5.5	3.1	2.4	3±1	7/2 ?	0	n-branch based on fission yield calculations	[22,24]
$^{138}_{53}I_{85}$	$^{138}_{54}Xe_{84}$	6.3	7.8	6.1	1.7	2±1	2 ?	3/2		[22,24]
$^{139}_{53}I_{86}$	$^{139}_{54}Xe_{85}$	2	7	3	4	5±2		0		[22,24]
$^{142}_{55}Cs_{87}$	$^{142}_{56}Ba_{86}$	2.3	~8						A feeble neutron activity	[26]
$^{143}_{55}Cs_{88}$	$^{143}_{56}Ba_{87}$	1.6	~7						A feeble neutron activity	[26]
$^{210}_{81}Tl_{129}$	$^{210}_{82}Pb_{128}$	~80	5.5	5.2	0.3				Might be due to photoneutrons	

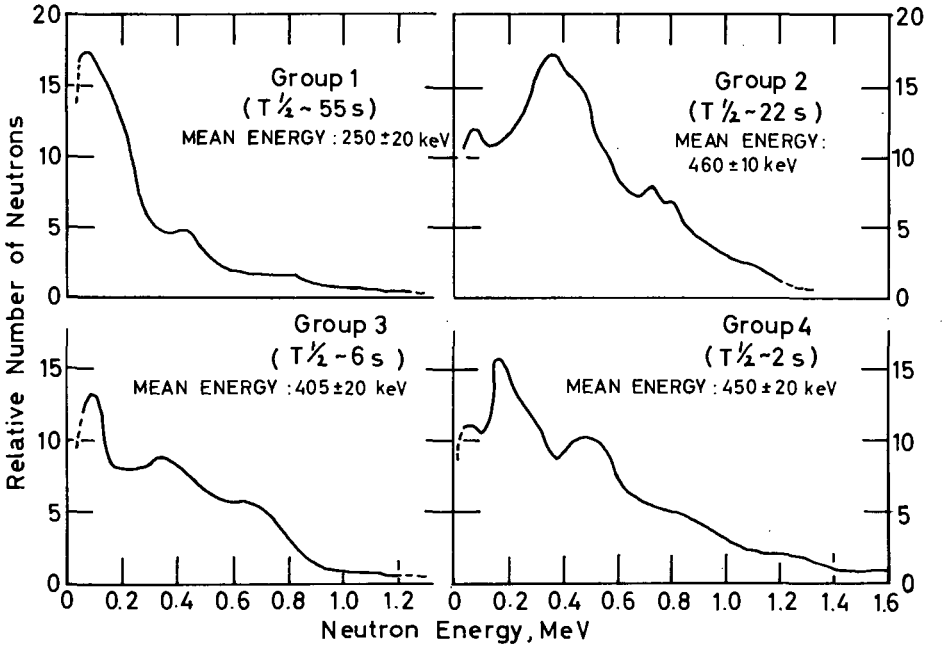

FIG. 2. Delayed neutron spectra from fission products (from [27]).

Further considerations along this line were made by Glendenin, Coryell and Edwards [33], and by Pappas [5]. A more fundamental treatment of the probability for delayed neutron emission is given by Pappas [6] and by Keepin [34].

These authors refine and extend the Bohr-Wheeler theory [2] to account for nuclear shell effects and use the results to predict fission products contributing to the delayed neutron groups. The prediction by Pappas [6] points towards fifty or so prospective precursors while Keepin [34] after reducing predicted precursors to fit the six group periods and yields, arrives at about a total of thirty main precursors and contributors.

More recently Pappas and Rudstam [35] have developed an extended systematics covering the whole Table of Nuclides (Fig. 3). This systematics is mainly based on energetics and suggests that delayed neutron precursors might frequently occur also in regions far from closed neutron shells. These prospective emitters are, however, located at distances rather far from stability. Using as a measure for the threshold for delayed neutron emission $(Z_{N-1} - Z_\beta)$ introduced[1] by Pappas [5], the average minimum threshold predicted is far from stability and for odd Z precursors it increases from about 3 charge units for light nuclei to about 8 charge units for heavy nuclei. For even-Z precursors these distances are about two units longer. Just beyond closed neutron shell regions the

[1] Z_{N-1} is the most stable charge corresponding to the neutron number of the delayed neutron emitter and is given by the crossing of the isotone line N-1 with the line of maximum β-stability Z_A. Z_β is the charge of the delayed neutron precursor (in the present paper $Z_\beta \equiv Z$).

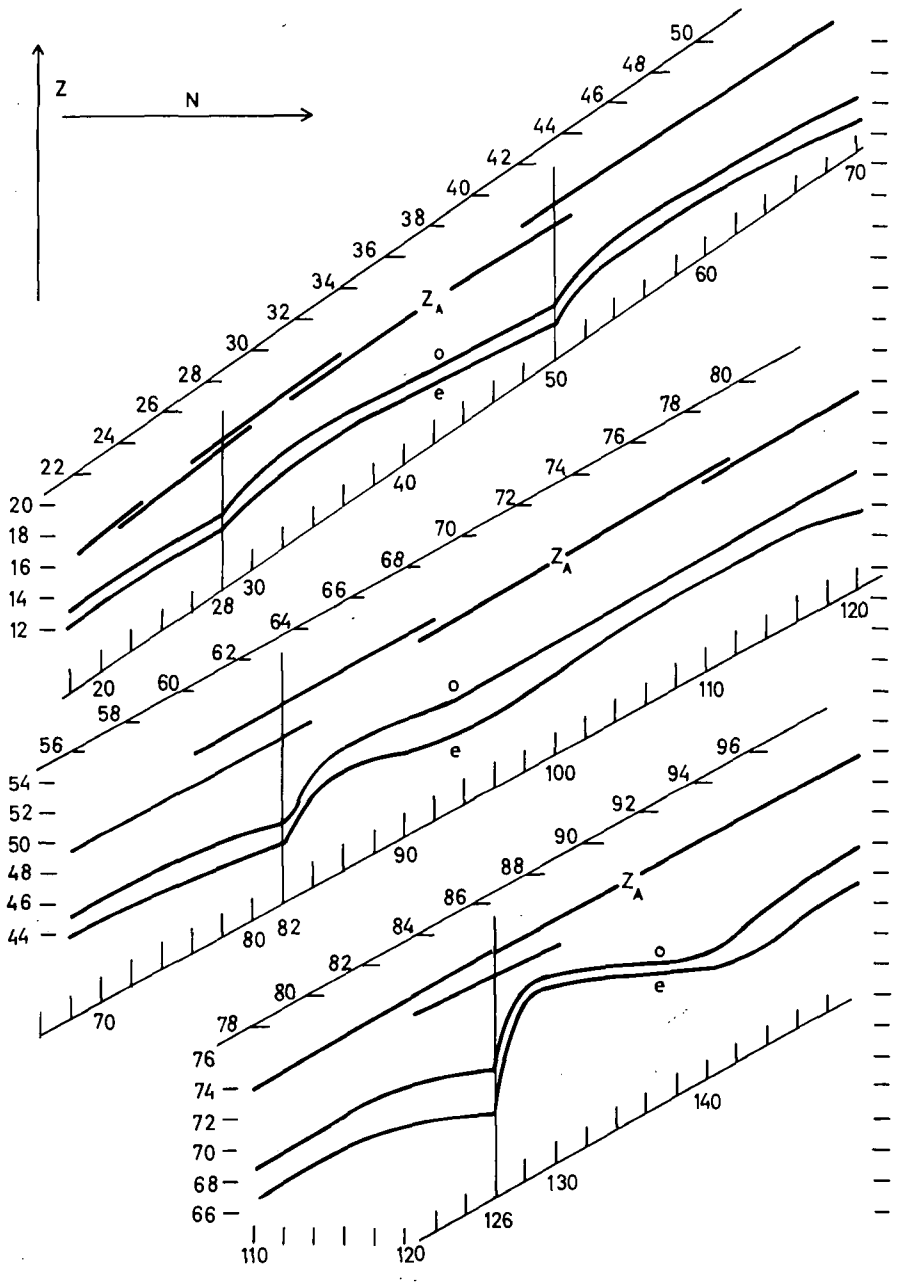

FIG. 3. Systematics of delayed neutron precursors and the influence of closed neutron shells on these systematics. Z_A: β stability. Curves o and e: upper limits (in Z) for odd Z and even Z precursors, respectively, expected to show characteristics of delayed neutron precursors (from [34]).

thresholds are moved towards stability with about 1, 2, 3 and 5 charge units at the 28, 50, 82 and 126 neutron shell, respectively [35].

The expectations from these systematics in regions far from closed neutron shells seem at present not to be borne out by experimental information. This may be due to either too optimistic views in the systematics not accounting for spin and parity effects, or experimental difficulties in reaching such species. Rudstam, Svanheden and Pappas [36] may have indications for the latter view, but Dostrovsky et al. [37] have not been able to verify this.

4. SEMI-THEORETICAL APPROACH TO DELAYED NEUTRON EMISSION

The probability for delayed neutron emission P_n (also called the neutron branch) is defined [5, 6, 34] as the fraction of β-decays from the precursor leading to neutron emitting states in the emitter. The value of P_n for a given nuclide is expected to be independent of its origin. Where fission products are concerned, this probability is often regarded as identical with the observed ratio of delayed neutron yield to cumulative fission yield of the delayed neutron precursor, i.e. $y_n / Y_{Z,N}$. This is so unless the delayed neutron precursor is formed in excited states (isomers) which through β-decays give the delayed neutron emitter. Just beyond regions of closed shells, however, conditions of isomerism are ruled out both on the basis of nuclear shell theory and on experimental evidence and $P_n \equiv y_n / Y_{Z,N}$. But isomerism is frequently present away from closed shells and P_n may not always be identical to $y_n / Y_{Z,N}$ in these regions.

According to the simple model of delayed neutron emission already briefly outlined, it should in principle be possible to estimate the emission probability as well as the form of the neutron spectrum. Earlier general attempts along these lines are made by Pappas [5, 6] and by Keepin [34] for probabilities. The results from different approaches used to estimate Q_β and B_n values are reviewed by Pappas and Rudstam [35]. An attempt to estimate the neutron spectrum (for group one) has been made by Batchelor and Hyder [27], but with a result in marked disagreement with that observed. For some specific cases the present authors have tried to make more precise calculations of P_n values and shapes of neutron spectra.

We shall therefore in the following suggest lines of improvements to existing approaches, and we shall try to use some of these on a few fission product precursors in order to get a feeling for potentialities and limitations, as well as a background for further investigations. In doing so we have to proceed step by step in the process of delayed neutron emission. The "trial nuclides" selected are ^{85}As, ^{87}Br and ^{137}I.

From the Fermi theory the probability of β-decay is governed by the energy release $(Q_Z^\beta - E)$, where Z is the atomic number of the precursor (see Fig. 1), in the transition and the degree of overlapping of the wave functions of the initial and final states. The latter is expressed by the square of the nuclear matrix element M for the transition involved. If $\omega(E)$ is the level density in the emitter nuclide at the excitation energy E, then the probability of reaching a state within the energy interval E to E + dE is given by:

$$W(E)\,dE = \text{const.} \times |M|^2 \, f(Z+1, Q_Z^\beta - E)\, \omega_{Z+1}(E)\,dE \qquad (1)$$

4.1. The matrix element

The actual probability will depend on the comparative values of the matrix element for the β-transitions to the various states in the emitter. In all previous treatments the simple assumption has been made that the matrix elements concerned do not show a systematic variation with energy of the final state in the β-decay. Further, as β-decay presumably proceeds via a high multiplicity of branches (see later), it is most likely to be characterized by the statistics of the distribution of final allowed states. Since $|M|^2$ is on the average, a factor of 10^2 or more greater for allowed than for forbidden transitions, the neutrons are assumed predominantly to follow allowed transition modes. For these transitions M is known to be nearly independent of the excitation energy in the daughter nucleus and $|M|^2$ has therefore been regarded as insensitive to E and replaced by a constant (average) value.

It could, however, be argued that instead of using a constant $|M|^2$, a constant value per energy interval might be closer to the truth; there are indications that the matrix element for β-transitions probably has a tendency to decrease with increasing level density in the daughter [38]. This tendency would result in a depression of the population of a higher lying state as compared to a lower lying state. This idea is not made use of in the present work.

4.2. The Fermi function

The Fermi function $f(Z+1, Q_Z^\beta - E)$ is a non-analytic integral taken over the β-spectrum. In most treatments this function has been replaced by the fifth power dependence of the energy released [2, 5, 6] see Ref.[2][9]. In one case, however, [34], the true Fermi function has been used, which lead essentially to the same results concerning P_n values, other factors being equal [35].

The observation by Bonner, Bame and Evans [28] that the neutron spectrum for one of the delayed neutron groups with the highest yield varies approximately with the fifth power of $(Q_Z^\beta - E)$ has not been found for two other groups [27]. This discrepancy might, however, be due to relatively large contributions from unresolved activities in the latter two groups, and more knowledge of delayed neutron spectra is needed.

In the present paper the fifth power dependence will be used. This will slightly favour the decay to the highest states as the ratio of $f(0, Q_Z^\beta - E)/(Q_Z^\beta - E)^5$ for $Q_Z^\beta - E \approx 0.5$ MeV is about one third of that for $Q_Z^\beta - E \approx 2$ MeV and above [39]. The overall difference, however, is small (see 4.3) in the final result using the present approach.

4.3. Level density

The average level density in a nuclide depends on its excitation energy, even-odd character, its level spin, and the proximity to closed shells. The level density is at its greatest in a nuclide half-way between shells and lowest in a closed shell nuclide.

---

[2] In Ref.[27] a fourth power dependence is used.

On the basis of the statistical model Blatt and Weisskopf [40] give the overall trend of the level density as function of energy:

$$\omega(E) = C \exp 2(aE)^{\frac{1}{2}} \quad (2)$$

where the constants a and C depend on the nuclide in question. This formula has been used in Refs [5, 6, 27] while in Ref. [34] the Hurwitz-Bethe proposal [41] to measure the energy from a characteristic level free from even-odd and shell effects is used. Even if the influence of the energy parameters Q^{β} and B^{n} is the overriding one in the final results, corrections along the line suggested by Hurwitz and Bethe should be included in Eq. (2). It should, however, be kept in mind that at present very little is known about the real shape of the nuclear energy surface in the regions of interest. Thus one can argue as to which form of correction should be used. In the present work a level density formula of the following type is assumed to be appropriate until more is known for the regions of interest.

$$\omega(E) = C \exp \{2a^{\frac{1}{2}}[E - P(Z) - P(N)]^{\frac{1}{2}}\} \quad (3)$$

where the pairing energies P(Z) and P(N) for protons and neutrons, respectively, are taken from Cameron [42] and the values for the mass dependent parameters C and a from Ref. [40][3].

The densities obtained as function of excitation energy in the two main mass regions of interest, A = 85 - 95 and A = 135 - 145, are given in Figs 4 and 5. These curves show a high density of levels in the neutron emitter above the neutron binding energy and support the assumption of high multiplicity of β-branches mentioned under point 4.1 above.

4.4. P_n and spectra via "the energy path"

The probability for population of levels in the neutron emitter as function of energy, i.e. $(Q_Z^{\beta} - E)^5 \omega_{Z+1}(E)$, is given in Figs 6 and 7 for the precursors[4] ^{87}Br and ^{137}I.

If the levels above the neutron binding energy B^{n} should all decay by neutron emission to the ground state of the final product, the neutron emission probability P_n would be given through the ratio of populated levels above B^{n} to all populated levels, which would result in values that are too high. Similarly, Figs 6 and 7 should also indicate the shape of the energy spectrum of neutrons emitted in the decay of ^{87}Br and ^{137}I, respectively. The spectrum for ^{87}Br would already from "zero energy" start to decrease very slowly and continuously with increasing neutron energy, while that for ^{137}I would show a peak at about 400 keV and thereafter would follow the same trend. Both spectra would be in severe disagreement with the observed ones (Fig. 2, group 1 and 2).

---

[3] Arguments could be given for using values for the parameter a as given by other authors. In most cases these values are higher than the Blatt-Weisskopf ones, by a factor of about 1.5 and about 2 in the mass number regions to be discussed. The use, however, of lower values compensates for the use of the fifth power law instead of the true Fermi function above (see 4.2).

[4] In Figs 6 and 7, E_{β} - and E_{ex} denote Q_Z^{β} -E and E, respectively.

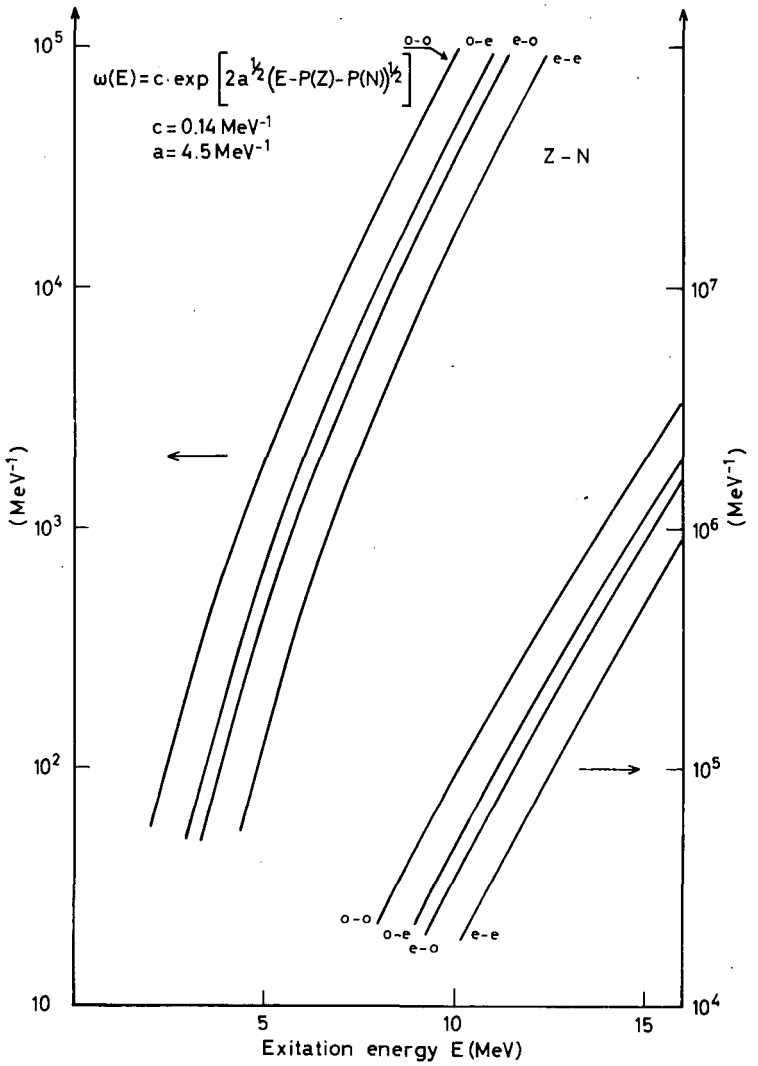

FIG. 4. Level densities in the mass region 85-95.

It is, however, obvious that where estimates of general trends of delayed neutron emission probabilities are concerned these are feasible only when angular momentum and parity effects are smoothed out to crude averages in the β-decay, and are also considered to cause no severe restriction in the neutron emitting step [6, 7, 34]. But as shown above this approach cannot be used successfully for single nuclides for which more exact data are wanted. Therefore, it should be kept in mind that even if energetically possible, neutron emission might very well be made improbable by the requirements of conservation of angular momentum and parity.

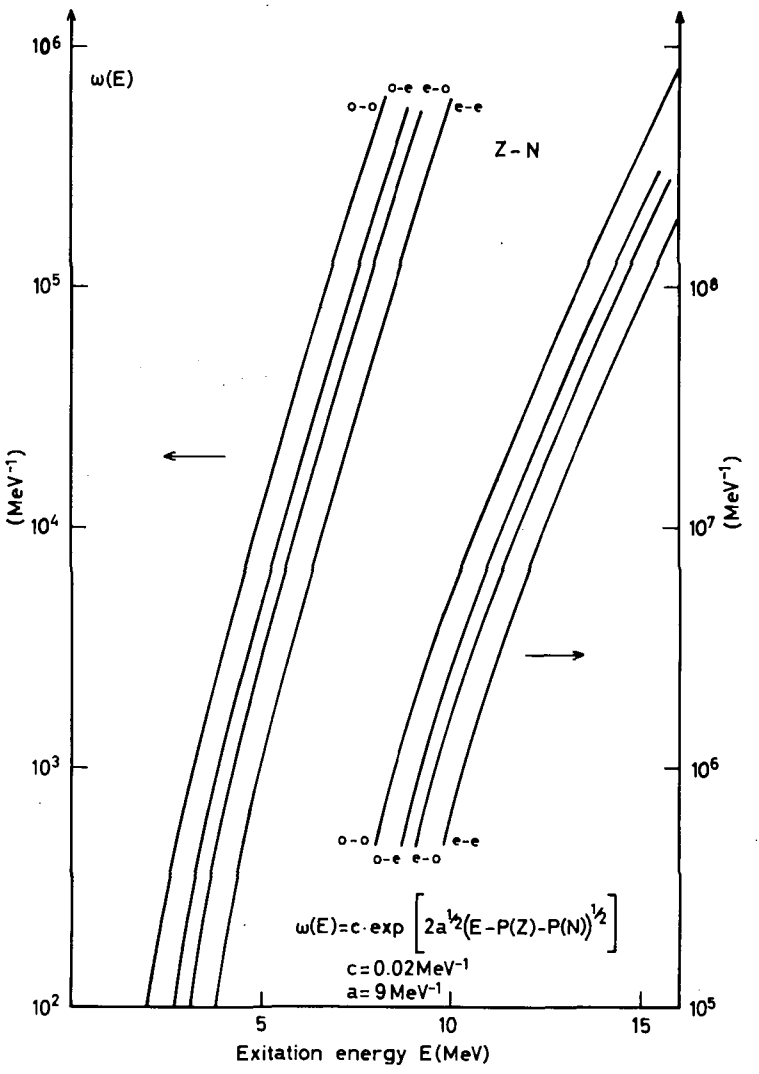

FIG. 5. Level densities in the mass region 135-145.

4.5. Spin considerations

While the necessity for introducing spin and parities in these studies had been realized for some time the first serious attempt along "the angular momentum path" was made by Sugihara [43] during his stay in Oslo in 1961 - 62. His approach is also of necessity based on certain assumptions. These lead to emission of s- and p-wave neutrons only, and to the severe restriction that the neutron emission populates the final nuclide (Z + 1, N - 2) in its ground state only. He leaves energy considerations and level densities out of the picture and works from the final product towards the emitter. In this way, he is able to assign relative values

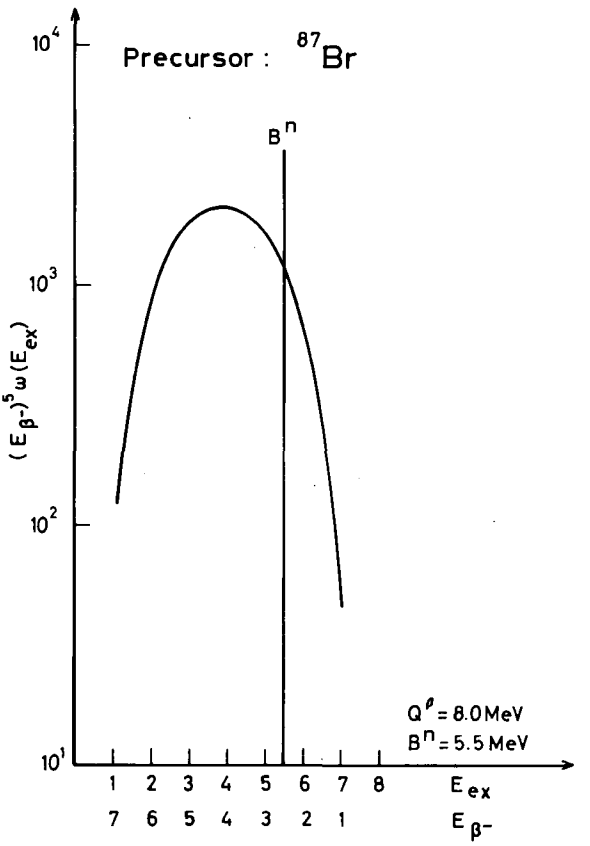

FIG. 6. Population probabilities in ^{87}Kr.

In Figs 6 and 7, E_{β^-} and E_{ex} denote Q^B_Z -E and E, respectively.

to each step and to obtain a crude estimate of the order of magnitude of the relative probability that an odd Z nuclide (giving a final product with zero spin) is a delayed neutron precursor.

Thus while the systematics along "the energy path" given by Pappas and Rudstam [35] predict mass number 133 to be the lowest limit for the antimony isotopes which may be delayed neutron precursors, Sugihara's treatment concludes that ^{133}Sb is (relatively) unlikely to be a precursor when compared with some other prospective species. This is ascribed to large forbiddenness in β-decay to neutron emitting levels in ^{133}Te.

Thus if it could be possible to extend Sugihara's treatment in a more general way it would, together with the systematics in Ref.[35], be a valuable help in selecting nuclides of interest (this as "the energy path" in Ref.[35] is to be regarded as the "optimistic" one, while the "angular momentum path" in Ref.[43] is the "pessimistic" one).

In the present work angular momentum effects are introduced in a way quite different to that of Sugihara, as the aim is also to be able to estimate absolute delayed neutron emission probabilities and shape of neutron

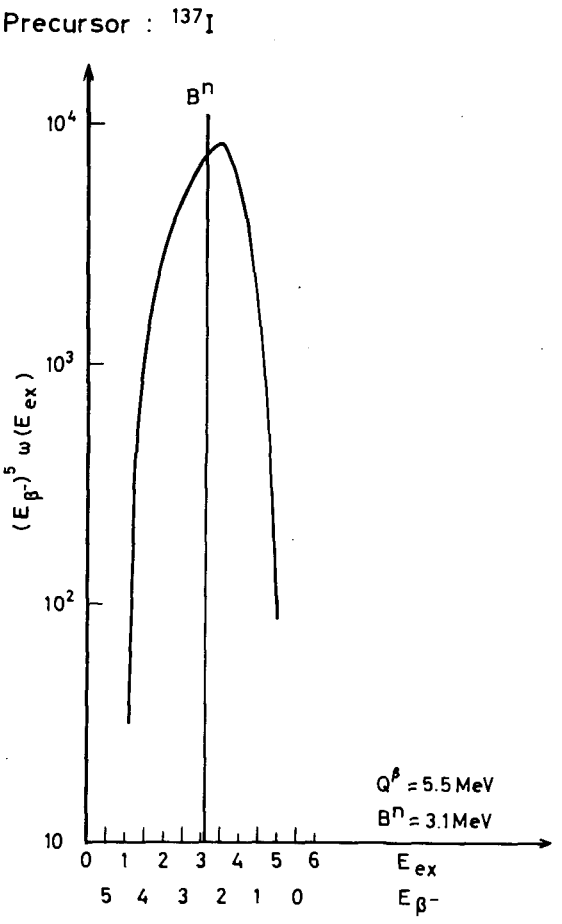

FIG. 7. Population probabilities in ^{137}Xe.

spectra. It would be extremely valuable to gain information on nuclear structure properties in the region of delayed neutron precursors.

Thus we replace $\omega(E)$ in Eq. (1) by some $\omega(E, J)$ and introduce the density of levels with spin J as given by the Huizenga-Vandenbosch model [44, 45]:

$$\omega(E, J) = \omega(0)\,(2J+1)\,\exp\left[\frac{-J(J+1)}{2\sigma^2}\right] \qquad (4)$$

where $\omega(0)$ is the density of levels with zero spin, and is equal to $\omega(E)$ used earlier (Figs 4 and 5). The spin cut-off factor σ is taken to be 4 as this seems to give the best fit to experimental data [45].

4.6. Competition between neutron and γ emission

In previous work the only competition considered has been γ-emission with s- or p-wave neutron emission. The probability for emission of a

neutron is given by $\Gamma_n/(\Gamma_n+\Gamma_\gamma)$. This ratio has for s- and p-wave neutrons been taken to increase from zero to unity when the excitation energy goes from B^n to (B^n+50) keV [6, 9, 34].

In order to better evaluate the competition between emission of γ-rays and l-wave neutrons in general the present authors have calculated neutron emission probabilities using the following expression for the neutron width, Γ_n (Ch. 9, 2A of Ref. [40]):

$$\frac{\Gamma_n}{D^*} = \frac{4k}{K}\,\frac{1}{2\pi}\,v(l) \tag{5}$$

Here D* is expected to be of the order of the actual energy separation between levels of same angular momentum J and parity. The neutron wave number outside the nucleus is given by $k = (2ME)^{\frac{1}{2}}/\hbar$ and inside the nucleus by K. The latter is approximately 10^{13} cm^{-1}. The barrier penetration factor v(l) is calculated from equations given in Ch. 8, 5. of Ref. [40]. By inserting appropriate values we obtain

$$\frac{\Gamma_n}{D^*} = 1.4\times 10^{-4}\ E^{\frac{1}{2}}\ v(l) \tag{5a}$$

where E is in electron-volts.

In Fig. 8 are given the results for s, p, d and f-wave neutrons in the mass number regions of interest.

In calculating the competition between emission of a given neutron wave and the emission of γ-rays, the width for γ emission Γ_γ is taken to be about 0.1 eV. This value is considered to be a good average of recent experimental results, which also shows that Γ_γ is nearly independent of

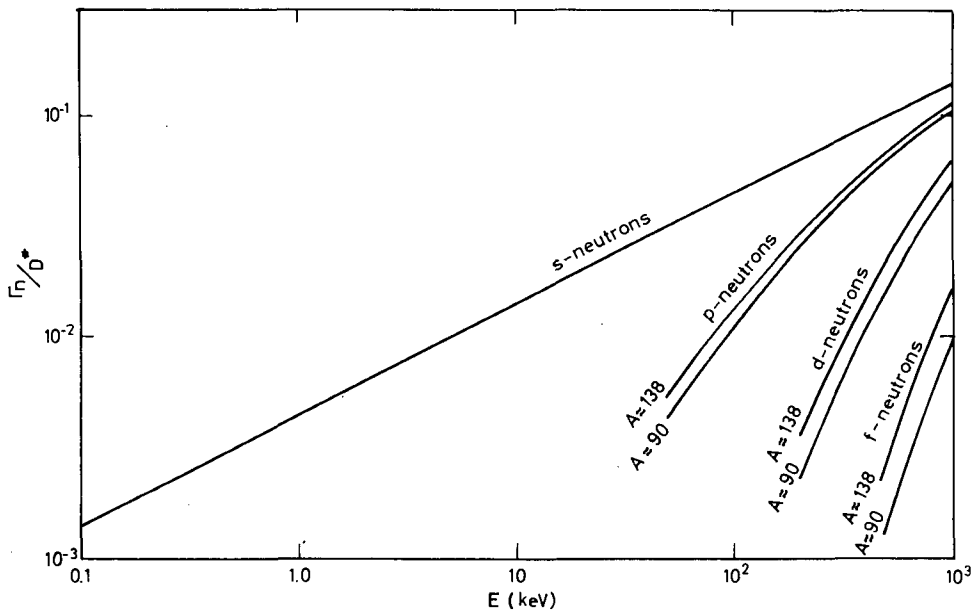

FIG. 8. Γ_n/D^* for different types of neutrons.

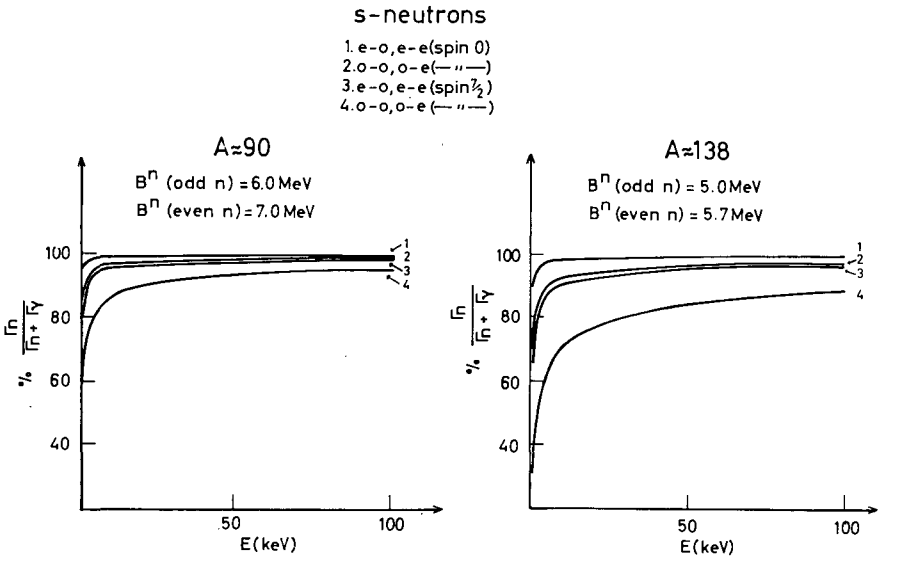

FIG. 9. Competition between s-wave neutron and γ-emission.

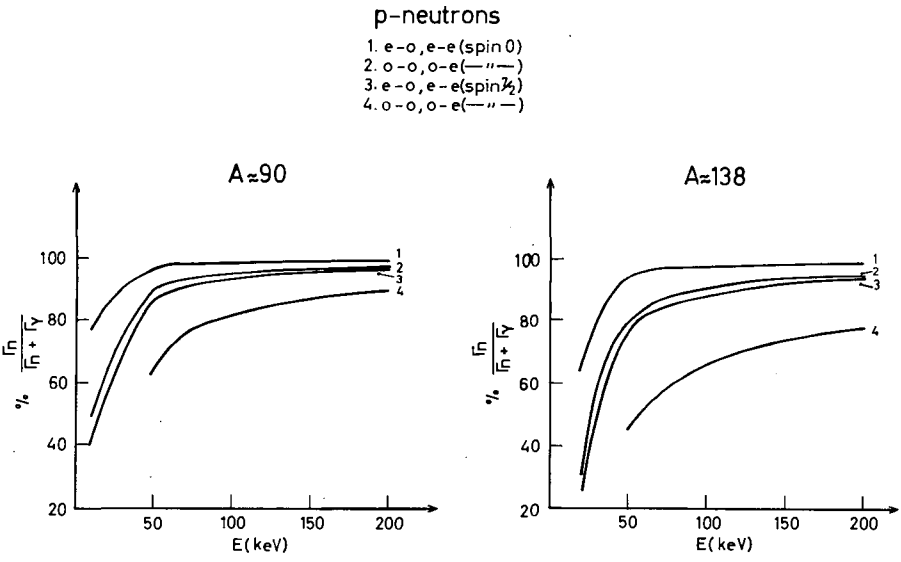

FIG. 10. Competition between p-wave neutron and γ-emission.

mass number when this is larger than 90 [46]. The resulting $\Gamma_n/(\Gamma_n+\Gamma_\gamma)$ values and their energy dependence for neutron waves of increasing angular momentum are given in Figs 9, 10, 11 and 12. Various proton and neutron characteristics in the emitter are considered; in addition two extreme values are chosen for the spins of the excited levels in the emitter, i.e. 0 and 7/2, the latter representing the peak of the spin distribution, Eq. (4).

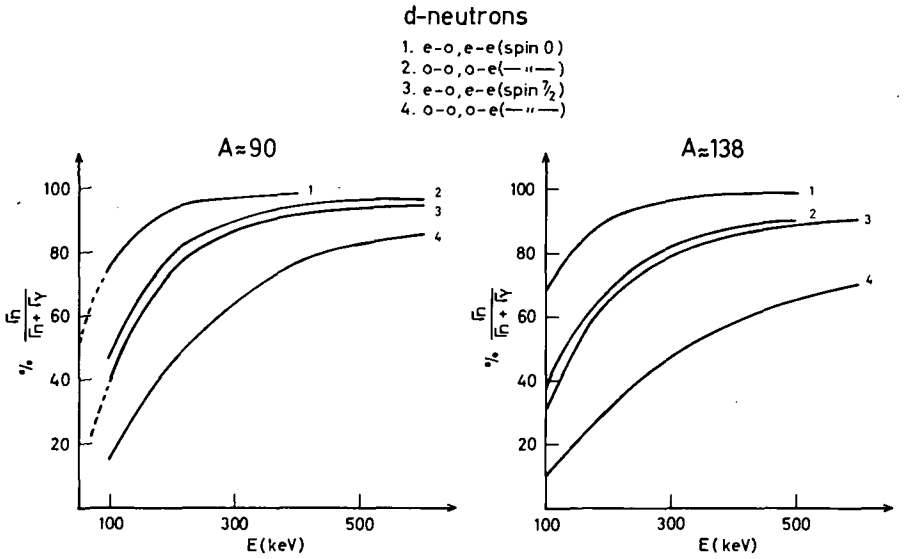

FIG. 11. Competition between d-wave neutron and γ-emission.

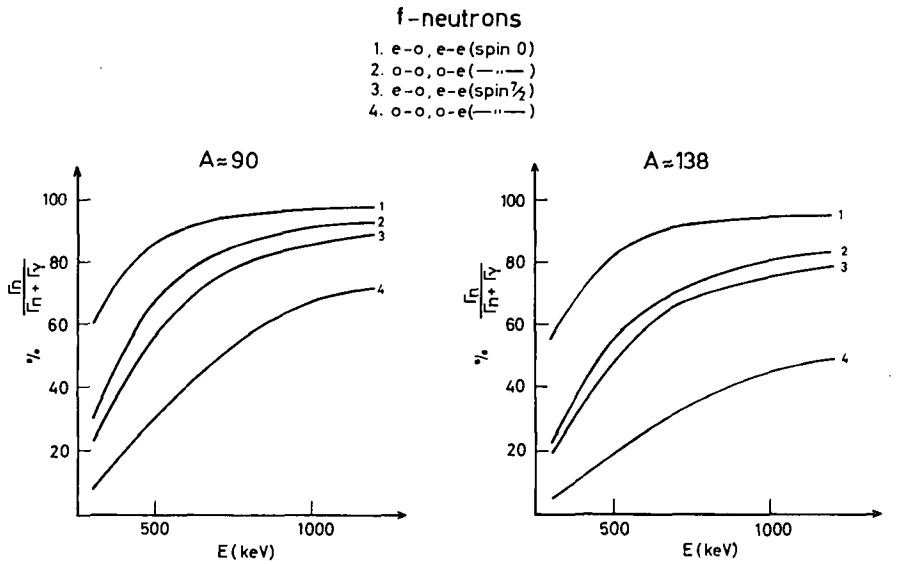

FIG. 12. Competition between f-wave neutron and γ-emission.

As these curves are certainly not correct at low energies in the rising phase, where one should expect a larger tendency towards a step function, neutron emission is taken to be predominant when $\Gamma_n / (\Gamma_n + \Gamma_\gamma)$ reaches a value of 95%. Below the corresponding energy the levels are assumed to de-excite by γ-emission only.

5. EVALUATION OF NEUTRON EMISSION PROBABILITIES

In order to follow up the ideas and results obtained in previous sections it was found appropriate to carry through estimates of delayed neutron emission probabilities for some precursors for which neutron branches are reported in the literature (cf. Tables Ia, b and c). We selected ^{85}As, ^{87}Br and ^{137}I.

Referring to previous discussions, the matrix element is assumed to be independent of energy. It decreases by a factor of 10 from one order of forbiddenness to another in β-transitions, i.e. $|M|^2$ changes by a factor of 10^{-2}. Therefore allowed β-transitions are the most interesting. On the basis of Gamow-Teller selection rules we then have $\Delta I = 0$ or 1 with no parity change for allowed transitions, and with parity change for first forbidden transitions.

In these calculations the 95% neutron emission limits (cf. 4.6) are taken from appropriate curves in Figs 9 to 12. The amounts of s, p, d and f-wave neutrons emitted are proportional to the relative population of levels in the emitter nuclide, i.e. ^{85}Se, ^{87}Kr or ^{137}Xe. These are obtained from Figs 6 and 7, and from Eq.(4).

The amount of s, p, d and f-wave neutrons emitted are then determined by the fraction of the area under the curve (in Fig.6 for ^{85}As and ^{87}Br, and Fig.7 for ^{137}I) above the corresponding $B^n + 95\%$ limits (neutron fraction) multiplied by the fraction of the corresponding populated levels. These data and results are given in Tables II to IV for the nuclides concerned.

The results in Tables II to IV are compared in Table V with expectations from previous approaches - the latter are all based on the 'energy path' approach only.

This comparison makes it quite clear that in general the 'energy path' alone is too crude, giving results that are either too high or too low, depending on how Q^β and B^n are estimated. Using 'measured' values of these parameters the results are of course too high. When coupled with the 'angular momentum path' including both spin and parity considerations the results obtained seem to be within the limits of experimental uncertainties. Additional estimates are, however, necessary before final arguments can be given. It would be possible to obtain P_n values for an additional 6 delayed neutron precursors (cf. Tables Ib and Ic), and such estimates are underway.

6. EVALUATION OF DELAYED NEUTRON SPECTRA

As the estimates of delayed neutron emission probabilities in the previous section give encouraging results it would be of interest to 'stretch' the ideas outlined earlier in this paper to include also estimates of the delayed neutron spectra. In doing so one must be aware that important details in the neutron emission step will not be accounted for in the first approach, but will be stressed later. Here ^{87}Br is selected, for three reasons:

(a) This is the delayed neutron precursor in the fission product region which seems to have the best known neutron energy spectrum. That this has not been measured with good resolution might in this case be an advantage. The result of the summations or integrations performed would

TABLE II. DELAYED NEUTRON EMISSION PROBABILITY P_n FOR ^{87}Br

$Q^{\beta} = 8.0$ MeV, $B^n(^{87}Kr) = 5.5$ MeV

The ground state spin of ^{87}Br is most likely 3/2 as the possible 5/2 level is known to be filled in pairs. If the former is assumed we have the following chain on the basis of "spin only":

$$^{87}_{35}Br_{52}\,(3/2) \xrightarrow[\Delta I = 0 \text{ or } 1]{\beta} {}^{87}_{36}Kr_{51}\begin{bmatrix}5/2\\3/2\\1/2\end{bmatrix}\begin{matrix}d\\p\\s\end{matrix} \xrightarrow{n} {}^{86}_{36}Kr_{50}\,(0)$$

Properties of ^{87}Kr (excited)

Spin	Relative population of levels	Type of neutrons emitted	95% limit	Neutron fraction
1/2	20%	s	B^n + 10 keV	13.0%
3/2	35%	p	B^n + 80 keV	12.6%
5/2	45%	d	B^n + 500 keV	4.1%

Taking into consideration parity restrictions, and remembering that precursor and final product have opposite parity only, odd neutron waves can follow allowed β-transitions and even neutron waves must follow first forbidden β-transitions. The latter is assumed to have a probability factor about 100 lower than the allowed. The result obtained for a 3/2 spin assigned to ^{87}Br is

$$P_{n\,calc.} \sim 7\%, \qquad P_{n\,exp.} = (3 \pm 1)\,\%$$

Using a spin of 5/2 instead of 3/2 for ^{87}Br should reduce the calculated P_n.

surely correspond to a very bad resolution as the level distance in the excited emitter nuclide is of the order of 10^2 eV or so. Furthermore there seem to be indications that in the mass number regions around 55 and around 155, neutron waves of even parity have much larger transmission coefficients than those of nearby odd parity, while in the mass number region 100 the opposite seems to be true [47]. If so, such local effects will seriously influence the spin argument and might be very difficult to account for. The nuclide ^{87}Br is outside the two mentioned regions and should, to our knowledge, not be influenced by such effects.

(b) The ground state spin of ^{87}Br is in this case taken to be 3/2 with odd parity and the spectrum is in accordance with the decay scheme in Table II expected to be a composite of many neutron waves, i.e. s, p, d and f, if allowed, and first forbidden β-transitions are accounted for.

(c) On the basis of similar calculations to those outlined in previous sections the relative amounts of neutrons emitted with increasing kinetic

TABLE III. DELAYED NEUTRON EMISSION PROBABILITY P_n FOR ^{85}As

$Q^{\beta} \approx 8$ MeV, $B^n(^{85}Se) \approx 5$ MeV (both are uncertain)

The ground state spin of ^{85}As is assumed to be 3/2 for the same reason as for ^{87}Br. We thus have the following chain for "spin only":

$$^{85}_{33}As_{52}(3/2) \xrightarrow[\Delta I = 0 \text{ or } 1]{\beta} {}^{85}_{34}Se_{51}\begin{bmatrix}5/2\\3/2\\1/2\end{bmatrix}\begin{matrix}d\\p\\s\end{matrix} \xrightarrow{n} {}^{84}_{34}Se_{50}(0)$$

Properties of ^{85}Se (excited)

Spin	Relative population of levels	Type of neutrons emitted	95% limit	Neutron fraction
1/2	20%	s	B^n + 10 keV	24.0%
3/2	35%	p	B^n + 80 keV	21.7%
5/2	45%	d	B^n + 500 keV	13.0%

Taking into consideration here also parity restrictions (see Table II) the situation is the same as for ^{87}Br and hence:

$$P_{n\,calc.} \sim 12\%, \qquad P_{n\,exp.} = (11 \pm 3)\ \%$$

TABLE IV. DELAYED NEUTRON EMISSION PROBABILITY P_n FOR ^{137}I

$Q^{\beta} = 5.5$ MeV, $B^n(^{137}Xe) = 3.1$ MeV

The ground state spin of ^{137}I is assumed to be 7/2, by analogy with ^{135}I, as opposed to a possible 5/2. For 7/2 the following chain is found:

$$^{137}_{53}I_{84}(7/2) \xrightarrow[\Delta I = 0 \text{ or } 1]{\beta} {}^{137}_{54}Xe_{83}\begin{bmatrix}9/2\\7/2\\5/2\end{bmatrix} d \xrightarrow{n} {}^{136}_{54}Xe_{82}(0)$$

Here only d-wave neutrons can be involved as precursor and final products have the same parity. Parity restrictions are therefore already taken care of above. The "95% limit" is rather uncertain, but taken to be at B^n + 1000 keV. This result is:

$$P_{n\,calc.} = 2.5\%, \qquad P_{n\,exp.} = (3 \pm 1)\ \%$$

The f-wave neutrons as result of first forbidden β-transitions can be neglected.

TABLE V. COMPARISON OF P_n VALUES AS OBTAINED THROUGH DIFFERENT APPROACHES

Path		Nuclide ^{85}As	^{87}Br	^{137}I	Reference
MOMENTUM		12	7	2.5	Present work
ENERGY	extrapolated energy	18	2	7	[5]
	systematics	38	1	10	[16]
	Cameron masses	5	1	5	[6]
	Measured	11±3	3±1	3±1	Tables Ib and c

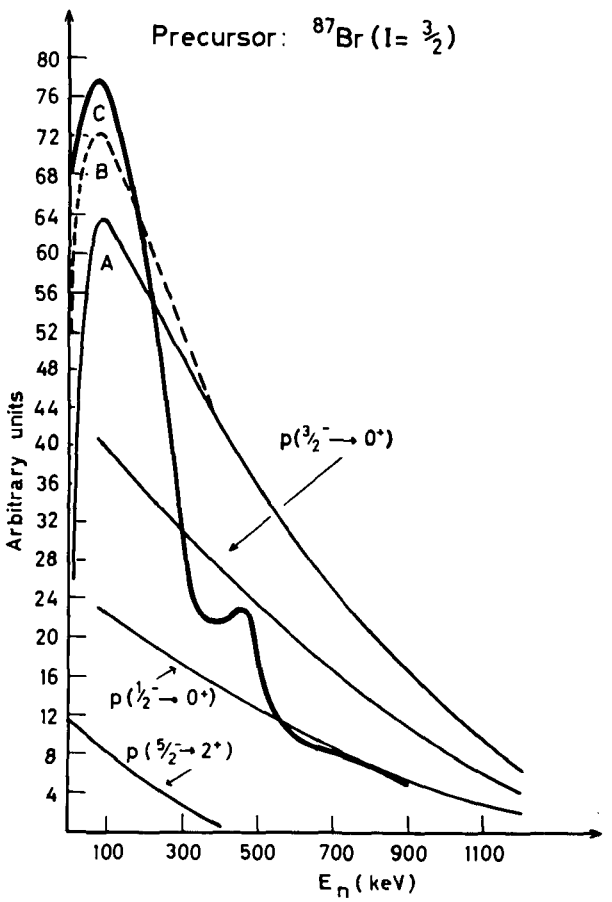

FIG. 13. Estimated trend of spectrum for delayed neutrons from ^{87}Br when neutron emission leads to: A. The ground state of ^{86}Kr, and B. Both to the ground state and to a 2+ (about 1 MeV) excited level in ^{86}Kr; C. "Group 1" spectrum.

energies are obtained. Use is made of the curve in Fig. 6, corrected for spin distribution, stressing the 95% neutron emission limits and adding statistical weights. The spectrum so obtained is sketched in Fig. 13 and compared with the spectrum reported by Batchelor and Hyder [27] for "group 1". This is known to consist predominantly of neutrons from ^{87}Br. The peak at about 80 keV in the calculated spectrum fits nicely into the observed one. The 500 keV "peak", however, which in the observed spectrum is very low, does of course not show up. Furthermore the calculated spectrum does not fall off as fast as the experimental one.

Besides the explanation that the whole approach is very simplified, a possible further explanation to the discrepancy in the shape is conceivable, namely that the neutron emission branches leading to the ground state in the final product also populate low-lying states which in turn decay by γ-emission (see Fig. 1).

$^{86}_{36}Kr_{50}$ having a closed neutron shell and 36 protons will probably not show many low-lying states. The possible ones would, however, be the result of promotion of a proton from the p 3/2 level to the close lying f 5/2 level, resulting in excited levels in the nucleus having spins 2 and 4, both with even parity. The mere existence of such levels would favour p-wave neutrons from the 5/2 level in ^{87}Kr if these levels are at energies above the spin 2 and 4 levels[5] in ^{86}Kr. Assuming that at least the 2+ is in the vicinity of 1 MeV an increase in the contribution from p-waves with low energies will be the result pressing the whole spectrum towards lower energies as observed. (It should be pointed out that including decay to excited states in the calculation of P_n would raise the value given in Table II to about 8.5%).

From this it can be concluded that the delayed neutron emission (at least for ^{87}Br) besides populating the ground state may also populate low lying excited levels in the final product (^{86}Kr). Thus measurements of neutron-γ-coincidences are urged as being of major interest and a necessary requirement before further profitable development in this field can be made.

Angular momentum effects can according to Grover [48] and to Grover and Gilat[6] [49] alter the competition between neutron emission and γ-emission in such a way that de-excitation through γ-rays may be compatible with neutron emission even at 1 to 2 MeV above the neutron binding energy. As the upper excitation limit which can be reached in ^{87}Kr through β-decay from ^{87}Br is about 2.4 MeV above the neutron binding energy the possible existence of severe γ-competition should be taken into consideration. This can be done in a very crude way by assuming that neutron widths corresponding to high angular momenta and parity restrictions add to the γ width. If, in addition, neutron emission to excited levels in the final product (in case of ^{86}Kr mainly the 2+ level) is also taken into account, a relative increase of the low energy part of the spectrum will result. This is due to a greater contribution from low energy p-waves over that from the f-waves with higher energy.

Thus the more the details of the "decay" are taken into consideration, the more the spectrum is moved (piled up) towards lower energies.

---

[5] There is maximum 2.4 MeV ($Q^{\beta} - B^{n} - 80$ keV).

[6] The authors would like to thank Dr. E. Hagebø, CERN, for kindly placing to our disposal copies of reprints of the works of Drs Grover and Gilat.

It should be mentioned that enhanced γ-emission will lower the P_n value and bring it in closer agreement with the experimental one.

7. STATUS AND SUGGESTIONS

Perhaps the most striking fact which comes out of this report is the, rather primitive and incomplete state of experimental and theoretical evidence of factors which can help further developments in this field. It is therefore at present only possible to consolidate the treatment and then await further improvements in the theory when results from some crucial experiments are known. These would be studies of neutron branchings, n-γ-coincidences, if possible β-n-γ-coincidences. But, first of all, knowledge is required on the detailed shapes of the delayed neutron spectra, and a decision as to whether these are line spectra (as they most likely will be) or continuous spectra. Second, it is of interest to know if there are local regions "preferring" even parity neutron emission while other local regions prefer odd parity neutron emission, and the importance of levels at angular momenta which can be obtained in β-decay processes far from stability and which are followed by neutron emission.

The further studies outlined should result in information not only of major interest for the delayed neutron problem itself, but might also throw some light on parameters of importance for our understanding of nuclear structural properties (i.e. $|M|^2$, $\omega(E, J)$, Γ_n / Γ_{tot}, Q^β and B^n, and spin and parities involved in the neutron emitting step), and should of course be of importance in the practical aspects of delayed neutron emission.

The authors would like to conclude this paper by quoting E. Rutherford (1905)

> "The value of any working theory depends upon the number of experimental facts it serves to correlate and upon the power of suggesting new lines of work".

hoping that the importance of this interplay of theory and experiment has become clear in this report.

ACKNOWLEDGEMENTS

The authors are glad to express their sincere appreciation and thanks to Mrs. Andrea Birch Aune and Mr. Arne Melbye for excellent assistance in preparing the manuscript. Their never failing interest and help over a long period of time have contributed in no small measure to the rapid preparation of the final copy.

REFERENCES

[1] ROBERTS, R., MEYER, R.C., WANG, P., Phys. Rev. 55 (1939) 510.
[2] BOHR, N., WHEELER, J.A., Phys. Rev. 56 (1939) 426.
[3] KEEPIN, G.R., Proc. Conf. on Reactor Kinetics and Control, Tucson, Arizona (1963).
[4] COWAN, C.A., ORTH, C.J., Int. Conf. peaceful Uses atom. Energy (Proc. Conf. Geneva, 1958) 7, UN, New York (1958) 328.
[5] PAPPAS, A.C., Rep. LNS-MIT-63, AECU-2806 (1953) Part IV.

[6] PAPPAS, A.C., Int. Conf. peaceful Uses atom. Energy (Proc. Conf. Geneva, 1958) 15, UN, New York (1958) 373.
[7] BEMIS, C., Discussion in Physics and Chemistry of Fission (Proc. Symp. Salzburg, 1965) 2, IAEA, Vienna (1965) 221.
[8] KEEPIN, G.R., Discussion in Physics and Chemistry of Fission (Proc. Symp. Salzburg, 1965) 2, IAEA, Vienna (1965) 222.
[9] POSKANZER, A.M., ESTERLUND, R.A., McPHERSON, R., Phys. Rev. Letters 15 (1965) 1030.
[10] DETRAZ, C., CERNY, J., PEHL, R.H., Phys. Rev. Letters 14 (1965) 708.
[11] DOSTROVSKY, I., DAVIS, R., Jr., POSKANZER, A.M., REEDER, P.L., Phys. Rev. 139 (1965) B1513.
[12] ALBURGER, D.E., Phys. Rev. 132 (1963) 328.
[13] POSKANZER, A.M., REEDER, P.L., DOSTROVSKY, I., Phys. Rev. 138 (1965) B18.
[14] POSKANZER, A.M., COSPER, S.W., HYDE, E.K., CERNY, J., Phys. Rev. Letters 17 (1966) 1271.
[15] HINDS, S., MIDDLETON, R., LITHERLAND, A.E., PULLEN, D.J., Phys. Rev. Letters 6 (1961) 113.
[16] PERLOW, G.J., RAMLER, W.J., STEHNEY, A.F., YNTEMA, J.L., Phys. Rev. 122 (1961) 899.
[17] GILAT, J., O'KELLEY, G.D., EICHLER, E., Rpt. ORNL-3488 (1963).
[18] SILBERT, M.G., HOPKINS, J.G., Phys. Rev. 134 (1964) B16.
[19] DEL MARMOL, P., NEVE DE MEVERGNIS, M., J. Inorg. Nucl. Chem. 29 (1967) 273.
[20] TOMLINSON, L., J. Inorg. Nucl. Chem. 28 (1966) 287.
[21] STEHNEY, A.F., SUGARMAN, N., Phys. Rev. 89 (1953) 194.
[22] PERLOW, G.J., STEHNEY, A.F., Phys. Rev. 113 (1959) 1269.
[23] CORYELL, C.D., WILLIAMS, E.T., Nucl. Appl. 2 (1966) 256.
[24] ARON, P.M., KOSTOCHKIN, O.I., PETRZHAK, K.A., SHPAKOV, V.L., Atomnaja Energija 16 (1964) 368.
[25] STEHNEY, A.F., PERLOW, G.I., Bull. Amer. Phys. Soc. 6 (1961) 62.
[26] AMAREL, I., BERNAS, R., FOUCHER, R., JASTRZEBSKI, J., JOHNSON, A., TEILLAC, J., GAUVIN, H., To be published in Physics Letters.
[27] BATCHELOR, R., HYDER, H.R.McK., J. nucl. Energy 3 (1956) 7.
[28] BONNER, T.W., BAME, S.J., EVANS, J.E., Phys. Rev. 101 (1956) 1514.
[29] GOLDANSKY, V.I., A. Rev. nucl. Sci. 16 (1966) 1.
[30] KARNAUKHOV, V.A., TER-AKOPYAN, G.M., VERTOGRADOV, L.S., PETROV, L.A., Nucl. Phys. A90 (1967) 23.
[31] BOGDANOV, D.D., DAROSZY, S., KARNAUKHOV, V.A., Preprint from Joint Establishment for Nuclear Research, Dubna, 1967.
[32] MAYER, M.G.M., Phys. Rev. 74 (1948) 235.
[33] GLENDENIN, L.E., CORYELL, C.D., EDWARDS, R.R., National Nuclear Energy Series, Div. IV, 9, McGraw-Hill, New York (1951) Paper 52.
[34] KEEPIN, G.R., J. nucl. Energy 7 (1958) 13; see also KEEPIN, G.R., Ch.4, Physics of Nuclear Kinetics, Addison-Wesley, (1965).
[35] PAPPAS, A.C., RUDSTAM, G., Nucl. Phys. 21 (1960) 353.
[36] RUDSTAM, G., SVANHEDEN, Å., PAPPAS, A.C., Nature, Lond. 188 (1960) 1178.
[37] DOSTROVSKI, I., Personal communication to A.C. Pappas, Sept. 1963.
[38] MOTTELSON, B., personal communication to A.C. Pappas, Apr. 1967.
[39] EVANS, R.D., Ch.17, §3, The Atomic Nucleus, McGraw-Hill, New York, (1955)
[40] BLATT, J.M., WEISSKOPF, V.F., Ch.8, 6A, Theoretical Nuclear Physics, John Wiley, New York (1952).
[41] HURWITZ, H., Jr., BETHE, H.A., Phys. Rev. 81 (1951) 898.
[42] CAMERON, A.G.W., Can. Rep. PD-292 (1957), Can. J. Phys. 36 (1958) 1040.
[43] SUGIHARA, T.T., A. Prog. Rep. Clark Univ. 6 (1962) 49.
[44] HUIZENGA, J.R., VANDENBOSCH, R., Phys. Rev. 120 (1960) 1305.
[45] VANDENBOSCH, R., HUIZENGA, J.R., Phys. Rev. 120 (1960) 1313.
[46] HUGHES, D.J., ZIMMERMAN, R.L., Ch. 8, 4, Nuclear Reactions I (Endt, P.M., Demeur, M. Eds), North-Holland, Amsterdam (1959); see also: Stolovy, A., Harvey, J.A., Phys. Rev. 108 (1957) 353.
[47] SUGIHARA, T.T., personal communication to A.C. Pappas, after a visit to Chalk River, Nov. 1962.
[48] GROVER, J.R., Phys. Rev. 127 (1962) 2142.
[49] GROVER, J.R., GILAT, J., Rep. BNL-10427, and Phys. Rev. (in press, 1967).

WHICH FISSION PRODUCT ISOTOPES ARE DELAYED NEUTRON PRECURSORS?

L. TOMLINSON
ATOMIC ENERGY RESEARCH ESTABLISHMENT,
HARWELL, BERKS., UNITED KINGDOM

Abstract

WHICH FISSION PRODUCT ISOTOPES ARE DELAYED NEUTRON PRECURSORS? Since the first detailed predictions of delayed neutron precursors were made some 7 to 10 years ago, new theoretical and experimental data has become available. Using the latest data, new predictions are made of delayed neutron precursors in fission together with their P_n values and half-lives. In this paper, the predictions are limited to the thermal neutron fission of ^{235}U but the method could be applied to any fissile nuclide for which fission yields can be calculated. One notable difference between the present predictions and those given earlier is the far larger range of elements included in the light peak region. Elements such as strontium, yttrium and niobium should all have isotopes with detectable neutron emission. The predictions are compared with the presently known delayed neutron precursors and areas for future work are defined. Finally, physical and chemical techniques capable of extending our knowledge in this field are briefly reviewed.

1. INTRODUCTION

Detailed predictions of delayed neutron precursors amongst the fission products have been published by Pappas [1] and Keepin [2]. Pappas and Rudstam [3] have also made a general theoretical study of delayed neutron emission for nuclear charge (Z) values from 11 to 100 and predicted minimum mass numbers (A) above which delayed neutron emission is possible.

The predictions of these authors for fission product isotopes differ markedly. Pappas in his early paper [1], considers that about 50 delayed neutron precursors from fourteen different elements should be present amongst the fission products, whilst Keepin [2] believes that almost all the delayed neutrons come from eleven iodine and bromine isotopes with possible smaller contributions from a very limited number of other elements. In the later study by Pappas and Rudstam [3], the possible number of delayed neutron precursors amongst the fission products has been greatly increased above the 50 predicted earlier [1]. However the range of isotopes seems to be too large, as several high-yield, fission product nuclides are included which have half-lives greater than 55 seconds (^{91}Rb (72 s), ^{96}Y(2.3 m), ^{133}Sb(2.6 m) and ^{140}Cs (66s)). In searches for long-lived delayed neutron groups amongst the fission products, no conclusive evidence has ever been presented for the existence of genuine delayed neutron groups with half-lives greater than 55 seconds [4].

There is also a large divergence between the authors [1-3] in their predictions of the neutron emission probability (P_n) from any individual isotope, one giving values up to 5 times larger than the other. Since these predictions were made, two new mass equations have been published [5, 6] which claim to be more accurate in their predictions of nuclear masses than previous equations. Tables of beta decay energies (Q_β) and neutron binding energies (B_n) calculated from these equations are available [7, 8]. The latter have been utilized in the present paper to redefine

the minimum A values above which delayed neutron emission can occur amongst the fission products. In view of the widely divergent P_n values predicted previously, the strictly theoretical approach has been abandoned in favour of a semi-empirical method based on experimentally measured values of P_n.

Largely for reasons of experimental convenience, most of the work carried out on separating individual delayed neutron precursors has so far been concerned with fission products from the thermal neutron fission of ^{235}U. The predictions given in the present paper have therefore been restricted to this single fission reaction, but the same general technique can be applied to any other fission reactions for which fission yields are calculable.

The predictions are finally compared with present experimental findings and areas for future work are defined. Physical and chemical techniques which are thought capable of extending our knowledge in this field are also briefly listed and discussed.

2. THEORY

The method adopted follows broadly the pattern set out by Pappas [1] but with several differences. The aim throughout has been to provide a guide for the experimenter rather than a complete theoretical treatment, and to indicate which isotopes are worthy of experimental investigation.

The first selection criterion applied for delayed neutron emission was simply that $Q_\beta - B_n > 0$, Q_β referring to the delayed neutron precursor and B_n to the delayed neutron emitter. Values for $Q_\beta - B_n$ were calculated from the tables of Wing and Varley [7], and Hillman [8]. Neither method alone predicted all the known delayed neutron precursors. This is perhaps not surprising in view of the accuracy of these equations in predicting the masses of stable and near stable nuclides ($\pm$ 0.4 MeV). The errors for nuclides considered in this paper – well removed from stability – will almost certainly be greater than this. In order that no delayed neutron precursors be missed out at this first selection stage, the minimum A values calculated by either method, at a given Z, were used as a starting point before applying other selection criteria. These minimum A values, listed in Table I, are on average, 1 mass unit larger than those given by Pappas and Rudstam [3].

The second criterion applied was that the neutron emission should be experimentally detectable. Again, following the method of Pappas [1], the product $Y \cdot P_n$ was used as a measure of neutron emission from individual isotopes (where Y is the cumulative fission yield). If both Y and P_n are quoted in per cent, then the limit for detection by present methods was set at $Y \cdot P_n \geq 0.1$. Fission yields for the thermal neutron fission of ^{235}U were taken from the compilation of Weaver, Strom and Killeen [9], only isotopes with $Y > 0.01\%$ being considered. In view of the wide divergence of theoretical P_n values, recent experimental values have been used to construct curves which define the variation of P_n with the charge displacement of the neutron emitter ($Z_{N-1} - Z$). Values of Z_{N-1} were estimated from Fig. 4 in Ref. [1]. A list of all known delayed neutron

TABLE I. MINIMUM A VALUES FOR DELAYED NEUTRON PRECURSORS AMONGST THE FISSION PRODUCTS

Light-peak elements			Heavy-peak elements		
element	Z	A	element	Z	A
Ge	32	84	Sn	50	133
As	33	84	Sb	51	134
Se	34	87	Te	52	136
Br	35	87	I	53	137
Kr	36	92	Xe	54	142
Rb	37	92	Cs	55	140
Sr	38	98	Ba	56	146
Y	39	98	La	57	146
Zr	40	103			
Nb	41	102			
Mo	42	> 109			
Tc	43	108			

precursors produced in fission together with their P_n values are listed in Table II and the derived curves are shown in Fig. 1.

Differences between even- and odd-N nuclides have been ignored, as these are small compared with the general uncertainties. As experimental values are only available for odd Z precursors, curves for even Z precursors were constructed as follows. Inspection of the theoretical curves [1] for the variation of P_n with $(Z_{N-1} - Z)$, showed that those for even Z were of approximately the same shape as those for odd Z, but displayed by about 1.5 units to higher $(Z_{N-1} - Z)$ values. "Experimental" curves for even Z precursors were therefore constructed simply by displacing those for odd Z precursors by a similar amount.

According to Sugihara [10]: "P_n ought to include factors that depend on angular momentum as well as energy. Those factors will in general decrease P_n." Because angular momentum effects and differences between even- and odd-N nuclides have been ignored in the present treatment, the predicted P_n values cannot be very accurate but should be regarded more as approximate upper-limits values. Perhaps future theories will include some quantitative estimates of angular momentum hindrance on P_n values for individual nuclides.

The third criterion applied was that the half-life should be > 0.5 seconds, as this was thought to be the limit of present day experimental techniques. Unknown half-lives were estimated by the method described by Bolles and Ballou [21]. These authors have shown that there is a rough correlation

TABLE II. KNOWN DELAYED NEUTRON PRECURSORS AMONGST THE FISSION PRODUCTS

Element	A	Half-life (sec)	Experimental P_n (%)	Reference
As	85	2.0	11 ± 3	[11, 12]
Br	87	55	2.9 ± 0.6	[13 - 15] - correction is required for the P_n value for ^{87}Br given in this reference, because of the presence of ^{86}Br [16-18]
	88	16	5.9 ± 1.6	
	89	4.4	9.5 ± 3	
	90	1.6	15 ± 4	
Kr	92	1.9		[19]
	93	1.2		
Rb	92	5.3		[12, 19]
	93	5.6		
Sb	134	11	~ 0.1	[12, 20]
	135	1.6	~ 4	
I	137	24	3.0 ± 0.5	[13 - 16, 18]
	138	6	2.1 ± 0.5	
	139	2.0	4.5 ± 1.5	

between the half-lives of short-lived nuclides and their displacement from the most stable nuclear charge (Z_A - Z). A plot of half-life against (Z_A - Z) was made using recent half-life values down to 1 second. In general, this agreed well with the curve of Bolles and Ballou, although the half-lives of Sb, I and Xe were higher than the average, perhaps because of the stabilizing influence of the 50 proton shell. The final results are given in Tables III and IV.

One notable difference between the predictions in Tables III and IV and those given earlier [1, 2], is the far larger range of elements now included in the light-peak region. Elements such as strontium, yttrium, and niobium are all predicted to have isotopes with half-lives up to 40 seconds and measurable neutron yields. Delayed neutrons from these elements might help to explain the hitherto rather puzzling results obtained for the spontaneous fission of ^{252}Cf [25]. Previously it had been assumed that

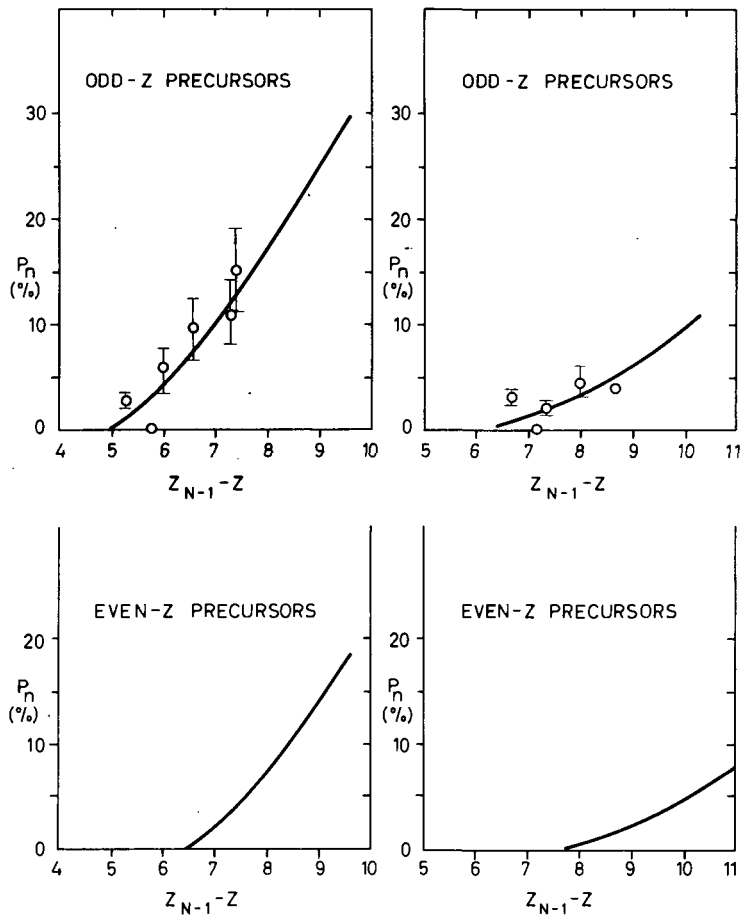

FIG. 1. Delayed neutron emission probabilities.

Z_{N-1} = most stable nuclear charge corresponding to the neutron number (N - 1) of the delayed neutron emitter [1]: Z = nuclear charge of the delayed neutron precursor: P_n = delayed neutron emission probability: (In addition to the data from Table II, a point has been included for ^{84}As for which P_n appears to be 0[11,12,20].

all the delayed neutron precursors in this fission reaction came from the heavy-peak, but no distinct 6 second group (^{138}I) was detected. If however, delayed neutrons are also coming from Sr, Y and Nb, then the relative contribution of ^{138}I would be smaller and possibly not resolvable in the gross delayed neutron decay curve.

3. AREAS FOR FUTURE WORK

Comparison of Table II with Tables III and IV indicates the gaps in our knowledge. The possible contributions of unknown delayed neutron

TABLE III. PREDICTED DELAYED NEUTRON PRECURSORS IN THE LIGHT-PEAK REGION (^{235}U thermal neutron fission)
Known delayed neutron precursors are included for comparison, experimental P_n values being indicated by "e". Estimated half-lives are shown in brackets. Measured half-lives were taken from [22] except for ^{85}As [11, 12], and ^{87}Se [20].

Element	A	Half-life (sec)	P_n (%)	Y (%)	Y·P_n
Ge	84	(1.2)	9	0.26	2
	85	(0.9)	14	0.06	0.8
As	84	(3)	< 0.1e	0.74	< 0.07
	85	2.0	11e	0.44	4.9
	86	(1.4)	17	0.34	6
	87	(1.0)	22	0.19	4
	88	(0.5)	29	0.08	2
Se	87	6	2	1.09	2
	88	(1.7)	5	0.91	5
	89	(1.1)	10	0.58	6
	90	(0.7)	14	0.30	4
Br	87	55	2.9e	2.16	6.3
	88	16	5.9e	2.61	15
	89	4.4	9.5e	2.58	24
	90	1.6	15e	2.10	31
	91	(1.1)	17	1.15	20
	92	(0.8)	21	0.54	11
Kr	92	1.9	2	2.84	6
	93	1.2	5	1.88	9
	94	(1.0)	9	0.90	8
	95	(0.7)	14	0.40	6
Rb	92	5.3	1	5.30	5
	93	5.6	4	4.92	20
	94	2.9	8	3.19	25
	95	(2.0)	12	2.52	30
	96	(1.2)	17	1.38	24
	97	(0.8)	21	0.61	13
Sr	98	(1.4)	5	1.41	7
	99	(1.0)	9	0.50	5
Y	98	(8)	4	4.15	17
	99	(2.5)	8	2.79	22
	100	(1.8)	12	1.24	15
	101	(1.2)	16	0.32	5
	102	(0.9)	21	0.06	1
Zr	103	(1.5)	5	0.40	2
	104	(1.1)	9	0.08	0.7
	105	(0.8)	12	0.03	0.4
Nb	102	(40)	0.7	2.87	2
	103	(10)	3	1.68	5
	104	(4.5)	7	0.61	4
	105	(2.2)	12	0.27	3
	106	(1.4)	15	0.10	2
	107	(0.9)	19	0.04	0.8
Tc	108	(10)	3	0.06	0.2
	109	(5)	6	0.02	0.1
	110	(1.8)	11	0.01	0.1

precursors to the various gross delayed neutron groups are listed in Table V.

4. EXPERIMENTAL TECHNIQUES

Because of the very short half-lives involved, the method used must be fully automatic. The techniques available at present can be broadly divided into physical and chemical; the physical systems generally only separating mass numbers (A) and the chemical systems separating only elements (Z).

4.1. Physical methods

The basic tool is the mass separator or mass spectrometer applied in various ways. Some typical systems are listed below:

(a) Fission Fragment Mass Spectrometer: Ewald, and others [26, 27]. Recoiling fission fragments, still retaining their initial ionic charges of +18 to +25, are fed directly into a mass spectrometer. A system of this nature would be ideal for a general survey of all masses if sufficient activity of these short-lived nuclides could be obtained.

(b) The ISOLDE project at CERN: Rudstam, Hagebø, and others [27]. This is an on-line system with the mass separator attached to the high-energy accelerator. A hot target is used to allow all the fission products to diffuse away quickly.

(c) Rare gas systems: Holm et al. [27] and Talbert et al. [27]. Several systems are operating in which the fission product rare gases are pumped from a cold uranium oxide or stearate target into a mass separator.

(d) Orsay system: Bernas, Lefort, Gauvin, and others [27]. Thin uranium foils covered with graphite are used in the ion-source of an on-line mass spectrometer. Only caesium and rubidium fission products diffuse through the graphite and ionize. This powerful technique should enable the short-lived caesium and rubidium delayed neutron precursors to be studied thoroughly.

(e) Livermore system. Stevenson, and others [27]. Recoiling fission fragments are stopped in mixtures of noble gases. By varying the composition of the noble gas mixture it should be possible to vary the ionic charges of the stopped fragments depending on the element involved. Some initial element separation should therefore be obtained before feeding into the mass separator.

(f) Soreq system. Amiel, and others [27]. A novel system, not using a mass separator, in which the daughters of the delayed neutron emitters are separated from the general fission product β-emitters by means of their far greater recoil energies.

4.2. Chemical methods

The first problem to be overcome in chemical separation methods is that of rapid removal of the irradiated material or separated element from the irradiation source. This problem can be solved in three basic ways:

(a) By using a high speed 'rabbit', containing the fissile material dissolved in solution. After returning from the reactor, one end of the rabbit containing a thin diaphragm is pierced by a hypodermic needle and the fission products rapidly removed by suction [28].

TABLE IV. PREDICTED DELAYED NEUTRON PRECURSORS IN THE HEAVY-PEAK REGION
(^{235}U thermal neutron fission)
Known delayed neutron precursors are included for comparison, experimental P_n values being indicated by "e". Estimated half-lives are shown in brackets. Measured half-lives were taken from [22] except for ^{133}Sn [23], ^{134}Sb [24] and ^{135}Sb [12, 20].

Element	A	Half-life (sec)	P_n (%)	Y (%)	$Y \cdot P_n$
Sn	133	55	0.7	0.66	0.5
	134	(20)	4	0.10	0.4
Sb	134	11	0.1e	1.80	0.2
	135	1.6	4e	0.44	1.8
	136	(0.4)	7	0.03	0.2
Te	137	(1.0)	1	0.46	0.5
	138	(0.5)	2	0.13	0.3
I	137	24	3.0e	2.66	8.0
	138	6	2.1e	1.46	3.1
	139	2.0	4.5e	0.79	3.6
	140	(0.9)	5	0.29	1
	141	(0.5)	6	0.04	0.2
Xe	142	1.17	0.7	0.54	0.4
	143	0.96	1	0.19	0.2
Cs	142	2.3	0.7	2.85	2
	143	2.0	1	1.70	2
	144	(1.3)	2	0.78	2
	145	(1.0)	4	0.26	1
	146	(0.6)	5	0.03	0.2
La	147	(6)	0.1	1.22	0.1
	148	(2.0)	1	0.56	0.6
	149	(1.6)	2	0.17	0.3

TABLE V. POSSIBLE CONTRIBUTIONS OF UNKNOWN DELAYED NEUTRON PRECURSORS TO THE GROSS DELAYED NEUTRON GROUPS

Gross delayed neutron group (sec)	Unknown delayed neutron precursors	
	Half-life range (sec)	Nuclides contributing to each group (in decreasing order of importance)
55	> 40	Nb-102, Sn-133 (Y for this nuclide has recently been shown to be < 0.015% [22]).
22	10 to 40	Nb-102 to Nb-103, Sn-134, Tc-108.
6	4 to 10	Y-98, Nb-103 to Nb-104, Se-87, La-147, Tc-109.
2	1 to 4	Rb-94 to Rb-96, Y-99 to Y-101, Br-91, Sr-98 to Sr-99, Se-88 to Se-89, As-86 to As-87, Kr-94, Cs-142 to Cs-145, Nb-105 to Nb-106, Zr-103 to Zr-104, Ge-84, La-148 to La-149, Te-137, Xe-142, Tc-110.
0.5	< 1	Rb-97, Br-92, Kr-95, Se-90, As-88, I-140 to I-141, Y-102, Ge-85, Nb-107, Zr-105, Te-138, Sb-136, Xe-143, Cs-146.

(b) By using a gas flow system in which the element of interest is converted to a gas or gaseous compound inside the reactor and transported to the counter by gas sweeping.

(c) By working in a neutron beam (from a reactor or accelerator) which can be rapidly shut-off.

The second problem is the development of rapid and specific chemical methods which can be completely automated. Several methods which have been used and show further potential in this field are as follows:

(i) Conversion of the element in question to a gaseous form, Kr and Xe[29, 30, 31], Br and I[17]; or conversion to a gaseous hydride, Sb, As, Ge and Sn [32, 12, 20, 33, 11] and Se[20].

(ii) Exchange in solution of the fission product element with a freshly formed precipitate of the same element, Se[34]; or with some compound of the element, e.g. Br, I, Cs[35, 18], Ba, Sr, Sn [36]. This method could no doubt be applied to most elements.

(iii) Automated precipitation procedures. Techniques requiring only a few seconds have been developed for Sn and Te [23]. This is a general method which could be developed for most elements.

(iv) Recoil techniques in which the recoiling fission fragment reacts chemically with a gaseous compound, e.g. the halogens react with methane to form methyliodide [37] and methylbromide [38]; fission product zirconium reacts with chlorine to form gaseous $ZrCl_4$ [39].

ACKNOWLEDGEMENTS

I am indebted to Drs P.O. Strom, A.A. Delucchi and A.E. Greendale for permission to quote their recent measurement of the half-life of ^{134}Sb, and to Mr. G.N. Walton for helpful discussion and for correcting this script. The two mass equations used in this work were suggested by Mr. I.F. Croall.

REFERENCES

[1] PAPPAS, A.C., Int. Conf. peaceful Uses atom. Energy (Proc. Conf. Geneva, 1958) 15, UN, New York (1958) 373.
[2] KEEPIN, G.R., J. nucl. Energy 7 (1958) 13.
[3] PAPPAS, A.C., RUDSTAM, G., Nucl. Phys. 21 (1960) 353.
[4] KEEPIN, G.R., Prog. nucl. Energy, Ser.1, Phys. Math. 1, Pergamon Press, London (1956).
[5] WING, J., FONG, P., Phys. Rev. 136 (1964) B 923.
[6] HILLMAN, M., Proc. 2nd Int. Conf. Nuclidic Masses (Johnson, W.H., Ed.) (Proc. Conf. Vienna, July 1963), Springer (1964).
[7] WING, J., VARLEY, J.D., Rep. ANL-6886 (1964).
[8] HILLMAN, M., Rep. BNL-846 (T-333) (1964).
[9] WEAVER, L.E., STROM, P.O., KILLEEN, P.A., Rep. USNRDL-TR-633 (1963).
[10] SUGIHARA, T.T., A Prog. Rep. Clark Univ. 6 (TID-15020) (1962) 49.
[11] DEL MARMOL, P., NEVE DE MEVERGNIES, M., J. inorg. nucl. Chem. 29 (1967) 273.
[12] TOMLINSON, L., J. inorg. nucl. Chem. 28 (1966) 287.
[13] SNELL, A.H. et al., Phys. Rev. 72 (1947) 545.
[14] SUGARMAN, N., J. chem. Phys. 15 (1947) 544; 17 (1949) 11.
[15] STEHNEY, A.F., SUGARMAN, N., Phys. Rev. 89 (1953) 194.
[16] ARON, P.M. et al., Soviet Atomic Energy 16 (1964) 447 (translated from Atomnaja Energija).
[17] PERLOW, G.J., STEHNEY, A.F., Phys. Rev. 107 (1957) 776; 113 (1959) 1269.
[18] HERRMANN, G. et al., Physics and Chemistry of Fission (Proc. Conf. Salzburg, 1965) 2, IAEA, Vienna (1965) 197.
[19] STEHNEY, A.F., PERLOW, G.J., Bull. Am. phys. Soc. 6 II (1961) 62.
[20] TOMLINSON, L., HURDUS, M.H., to be published.
[21] BOLLES, R.C., BALLOU, N.E., Nucl. Sci. Engng 5 (1959) 156.
[22] HERRMANN, G., Radiochim. Acta 3 (1964) 169 (English translation, AERE-Trans 1036 (1965)).
[23] STROM, P.O. et al., Phys. Rev. 144 (1966) 984.
[24] STROM, P.O., DELUCCHI, A.A., GREENDALE, A.E., to be published.
[25] COX, S. et al., Phys. Rev. 112 (1958) 960.
[26] INTERNATIONAL ATOMIC ENERGY AGENCY, Physics and Chemistry of Fission (Proc. Conf. Salzburg, 1965) 2 vols, IAEA, Vienna (1965).
[27] Why and How Should We Investigate Nuclides Far Off the Stability Line? (Proc. Symp., Aug. 1966), to be published in Ark. Fys.
[28] GREENDALE, A.E., LOVE, D.L., Nucl. Inst. Meth. 23 (1963) 209.
[29] WAHL, A.C., DANIELS, W.R., J. inorg. nucl. Chem. 6 (1958) 278.
[30] WAKLGREN, M.A., MEINKE, W.W., J. inorg. nucl. Chem. 24 (1962) 1527.
[31] OCKENDEN, D.W., TOMLINSON, R.H., Can. J. Chem. 40 (1962) 1594.

[32] TOMLINSON, L., Analyt. chim. acta 31 (1964) 545; 32 (1965) 157.
[33] GREENDALE, A.E., LOVE, D.L., Analyt. Chem. 35 (1963) 632; 35 (1963) 1712.
[34] SATTIZAHN, J.E., KNIGHT, J.D., KAHN, M., J. inorg. nucl. Chem. 12 (1960) 206.
[35] FIEDLER, J. et al., Angew. Chem. 75 (1963) 1130.
[36] RAI, R.S., NETHAWAY, D.R., WAHL, A.C., Radiochim. acta 5 (1966) 30.
[37] DENSCHLAG, H.O., HENZEL, N., HERRMANN, G., Radiochim. acta 1 (1963) 172.
[38] SILBERT, M.D., TOMLINSON, R.H., Radiochim. acta 5 (1966) 217; 5 (1966) 223.
[39] ZVARA, I. et al., Dokl. Akad. Nauk. SSSR 148 (1963) 555.

DISCUSSION

On the papers by Jahnsen et al., and Tomlinson

Theoretical considerations, such as the detailed investigation of the application of Fermi beta-decay theory to delayed neutron emission, indicate a very small contribution of high energy neutrons in delayed neutron spectra. It is probable that prompt neutron contamination spoiled the results of the delayed neutron spectra measurements. This important question should be solved by new detailed investigations of delayed neutron spectra, preferably from single precursors and it is expected that the high energy tail will be weaker than shown in the spectra obtained by Batchelor's measurements[1]. Early data on delayed neutron spectra, including those of Batchelor, have probably been influenced by sample self-multiplication and back-scattering into the sample during the process of spectrum measurements. All the refinements of the theory and detailed calculations seem to push or "pile up" the spectra toward the low energy end. Even if there is some contribution due to high energy delayed neutrons, it must be low since such neutrons would in general appear in highly forbidden transitions in major precursors. The refined measurements of spectra will be of crucial importance in this question.

An open question is if there are any cases among fission products where double neutron emission could be found. To reach such a case, one would have to go far from the stability line where the region of prompt neutron emission is approached. Trusting the mass formulas a region could be reached where the total Q_β approaches 20 MeV and there would be enough energy to allow the emission of two neutrons. But the half-lives involved would probably be so short that they would fall outside the limits given by the beta-decay theory, and a prompt neutron will be emitted.

The problem of the growth-decay relationships of delayed neutron precursors was already mentioned at the IAEA Symposium on Physics and Chemistry of Fission (Salzburg, 1965). Some aspects of this problem were discussed at the Panel. The question was stated as follows:

"Is there any delayed neutron precursor which has an intrinsic die-out characteristic where the time scale would be important in reactor kinetics?" This would be a precursor formed during irradiation and decaying with a defined half-life (similar to the xenon problem in reactor behaviour).

The observed gross delayed neutron decay data could not be fitted properly by a superposition of six negative exponentials, corresponding to the six groups, if a positive growth term was included. From the least-square's fit of this artificial approach it can be seen that growth-decay characteristics do not seem to introduce an appreciable effect, from the practical point of vew. This question could be of importance with photo-neutrons where the growth-decay effects must be taken into account.

From the point of view of reactor kinetics, it is therefore sufficient to consider only the decay processes and ignore the growth-decay phenomena.

However, some individual delayed neutron precursors do show a growth-decay effect. For example, in chain 93, the build-up of ^{93}Rb can be observed since it is longer-lived than its parent (1.2 sec half-life for

[1] BATCHELOR, R., HYDER, H. R. Mc. K., J. nucl. Energy 3 (1956) 7.

^{93}Kr and 5.6 sec for ^{93}Rb). The same is true in the 94 chain (0.4 sec half-life for ^{94}Kr and 2.7 sec for ^{94}Rb).

Another case was described by Tomlinson. The half-life of ^{87}Se has been determined and found to be 6 sec. ^{87}Se undergoes beta decay forming the delayed neutron precursor, ^{87}Br. The cumulative fission yields of ^{87}Se and ^{87}Br in the thermal neutron fission of ^{235}U are calculated to be 1.09 and 2.16%, respectively. Approximately half the ^{87}Br is therefore formed from ^{87}Se. Using the normal method of back-extrapolation of the 55 second group in a burst-type irradiation, one estimates a value for the ^{87}Br activity at time zero which is twice the true value. In the case of a 'saturation' type of irradiation, this effect would be much smaller.

Because the mathematical analysis of gross delayed neutron curves ignores these growth-decay effects, the contributions of the shorter-lived groups are increasingly underestimated. One should therefore not expect to get exact agreement between the sums of the contributions of individual precursors and the delayed neutron group abundances.

In evaluations of delayed neutron precursors, often only the fission of ^{235}U is considered. In future, different cases of fission should be included (fast, thermal, 14 MeV of different species) where the mass yield curves and charge distribution change substantially. In predictions of delayed neutron precursors, observed yields, fission yields, and neutron emission probability, data are not complete if the results are not confirmed for all different species. The most obvious example is californium. Good measurements with this element are needed. For example, the problem of whether or not ^{138}I is a precursor could be clarified.

RADIOCHEMICAL MEANS OF INVESTIGATING DELAYED NEUTRON PRECURSORS

P. del MARMOL
C. E. N.
MOL, BELGIUM

Abstract

RADIOCHEMICAL MEANS OF INVESTIGATING DELAYED NEUTRON PRECURSORS. Fast radiochemical methods used now for the determination of delayed neutron precursors are classified and reviewed: precipitations, solvent extractions, range experiments, milking, gas sweeping, isotopic and ion exchange, hot-atom reactions and diffusion loss. Advantages and limitations of irradiation systems with respect to fast separations are discussed: external beams which allow faster separations only have low neutron fluxes, internal beams which are mostly fit for gaseous reactions; and rabbits for solution irradiations. Future prospects of radiochemical procedures are presented; among these, studies should be mostly oriented towards gaseous reactions which offer possibilities of isolating very short-lived delayed neutron precursors. Chemical procedures for delayed neutron precursor detection are compared with mass spectrometric and isotope-separator techniques; it is concluded that the methods are complementary.

1. INTRODUCTION

So far most indentifications of delayed neutron precursors have been made by means of radiochemical separations. With the introduction of mass spectrometers and of on-line isotope separators it seems worthwhile to review the analytical methods that have been used in the past and to discuss whether chemical methods should be considered obsolete for future work in delayed neutron precursor half-life and yield determination.

For the sake of clarity the chemical methods that have been used are classified roughly by function of the main separation step, although there is often considerable overlapping between typical procedures. Once the gross delayed neutron activities were observed in fission and broken down into groups following their half-lives [1] it was natural that historically the longer-lived ones were the first to be investigated as they required less sophisticated separations than the shorter-lived ones. If not otherwise specified, irradiations were made with thermal neutrons on uranium (natural or enriched in ^{235}U).

2. CHEMICAL SEPARATIONS

2.1. Precipitation

Snell et al. [2] tried some group precipitations about 30 to 60 sec after the end of irradiation; $BaSO_4$ and $BaCl_2$ precipitations yielded no noticeable neutron activity while mixed silver halide precipitations carried down both the 23 sec and the 56 sec neutron activities. This gave evidence that these half-lives could be associated with halogen delayed neutron precursors.

2.2. Solvent extraction

The same authors carried out an ether extraction 40 sec after the irradiation of a solution of uranyl nitrate in water; most of the neutron activity was observed in the organic phase.

However one of the best methods for effecting halogen separation from fission products is their extraction in CCl_4 as Br_2 and I_2. By using suitable oxidation-reduction steps one can extract either I_2 keeping Br^- in the aqueous phase, or Br_2 leaving IO_3^- in the aqueous phase. This method was that one generally applied by investigators of halogen delayed neutron precursors.

By using this method they observed a 23.8 sec half-life in the iodine extraction and a 54 sec half-life in the bromine extraction; shorter half-lives which were present in the latter separation (probably 15.5 sec ^{88}Br) were believed to belong to iodine contaminants. The minimum separation time between the end of irradiation and beginning of counting was about 30 sec. These half-lives were tentatively attributed respectively to ^{137}I and ^{87}Br, of which the half-lives were already roughly known [3, 4, 5] (30 ± 6 sec for ^{137}I, and 50 ± 10 sec for ^{87}Br).

The results of Br^- and I^- extractions in triphenyl-tin hydroxide [6] to measure residual neutron activities in the water phase will be treated in sub-section 2.6.

2.3. Range measurement

Sugarman [7] used a recoil technique based on range measurements of fission fragments in aluminium to compare masses of delayed neutron emitters with those of known fission fragments. A fast rabbit containing an uranium target, an aluminium absorber and a bakelite recoil catcher were used. The neutron activity of the catcher was measured for different absorber thicknesses by eight boron counters and the decay was followed on the moving tape of an electro-cardiograph from as little as 1 sec after the end of irradiation. The 4.51 sec neutron half-life was observed to follow the 55.6 sec bromine half-life with possible mass assignments from 86 to 90, and the 1.52 sec followed the 22.0 sec iodine with possible mass assignments from 129 to 135. The chemical separation of bromine by CCl_4 extraction showed that the 4.51 sec half-life belonged to this element. Chemistry on the 1.52 sec half-life was not attempted.

2.4. Milking

This technique was not used directly for delayed neutron measurements but to clarify half-life assignments of prospective bromine and iodine delayed neutron precursors. Sugarman [8] measured with good precision the half-lives of ^{87}Br (56.1 ± 0.7 sec) and ^{88}Br (15.5 ± 0.3 sec) by milking known ^{87}Kr and ^{88}Rb descendants from AgBr precipitates, and the half-lives of ^{137}I (19.3 ± 0.5 sec), ^{138}I (5.9 ± 0.4 sec) and ^{139}I (2.7 ± 0.1 sec) by milking ^{137}Xe, ^{138}Cs and ^{139}Ba, respectively, from AgI precipitates. Precipitation times as short as 7 sec after the end of irradiation were attained. Owing to the parent-daughter half-life relationships, isotopes of higher masses could not be detected for either element.

2.5. Gas sweeping

Stehney and Sugarman [9] applied a method used by Strassman and Hahn [3] to study the ^{87}Br decay characteristics. Carrier bromine was added as Br^- and BrO_3^- (BrO_3^- oxidizes I^- to IO_3^- and Br^- to Br_2) to an acid solution of the uranium target and Br_2 was swept with air into a 1N HNO_3 solution containing Ag^+, where bromine precipitated as AgBr. They measured the thermal fission yield of ^{87}Br as 3.1% using ^{139}Ba as standard. The irradiations were performed using a 'rabbit'.

Perlow and Stehney [10] shortened the separation time of bromine by working in an external neutron beam, i.e. in an opening of the thermal column of the CP-5 Argonne research reactor; the Br_2 carried in an air stream was absorbed in a CCl_4 solution and the delayed neutrons, counted by two BF_3 counters, led to the discovery of a 15.5 sec bromine activity which was assigned to ^{88}Br on the grounds of Sugarman's [8] half-life determinations. This activity was previously believed to be caused by iodine contamination [2]; however any iodine activity in this experiment was trapped in a solution containing $KBrO_3$. A shorter lived activity of bromine was not inconsistent with a 4.5 sec half-life. Both equilibrium and non-equilibrium runs were performed, the irradiation times being controlled by the use of a fast shutter. Perlow and Stehney [11] further refined their technique so as to shorten the gas burst to 1.2 sec. Bromine and iodine delayed neutron precursors were both studied. The solution containing the uranium to be irradiated contained suitable oxidation-reduction reagents so as to investigate one or the other halogen which was also carried in its inert form in the burst of air. This study resulted in making the following half-life and mass assignments: 54.5 sec ^{87}Br, 16.3 sec ^{88}Br, 4.4 sec ^{89}Br and 1.6 sec ^{90}Br, the relative yields of their neutron activities being 0.37/1.0/1.9/1.5; and 24.4 sec ^{137}I, 6.3 sec ^{138}I and 2.0 sec ^{139}I with relative neutron yields of 1.0/0.47/0.38. It is worthwhile noting that the bromine and iodine yields were assumed to be directly correlated but were not measured relative to each other. The two shorter lived iodine delayed neutron precursors have half-life and mass assignments compatible with isotopes with half-lives and masses previously determined by Sugarman [8]. The two shorter lived bromine isotopes were assigned masses 89 and 90 on the grounds of similarities in half-life decrease of iodine and bromine isotopes having the same number of neutrons above shell closure.

Using a similar chemical procedure, but in the case of 14 MeV neutron fission of ^{235}U, Aron et al. [12] measured by neutron and β-counting the neutron emission probabilities of the three longer lived bromine and of the two longer lived iodine delayed neutron precursors. The recording apparatus, located 20 m from the target was reached 7 sec after irradiation.

Stehney and Perlow [13] applied the sweeping technique to rare gases, using suitable precautions to prevent contamination from halogen delayed neutron precursors. The disruption of the burst of the helium carrier gas on the irradiated solution was attenuated by glass beads, and the rare gases were counted in an evacuated bottle surrounded by nine BF_3 counters embedded in paraffin. From a 2 sec Kr parent they observed a 1.5 sec Kr delayed neutron precursor and a 6 sec Rb precursor of a sevenfold lower

neutron yield; (these precursors were assigned respectively to ^{92}Kr, ^{93}Kr or ^{94}Kr, and to ^{92}Rb or ^{93}Rb on the ground of known half-lives. Their total neutron activities amounted only to 0.5% of the total delayed neutron yield of ^{235}U. No detectable amounts of xenon delayed neutron precursor were observed.

Another set of gas sweeping experiments was carried out to search for delayed neutron precursors among elements having the properties of forming volatile hydrides. Tomlinson [14] used an electrolytic cell containing uranium and suitable carriers in an HCl solution placed in the horizontal hole close to the core of the Harwell swimming-pool reactor, Lido. The irradiation conditions were set by the start-up and the shut-down of the reactor core. Using helium as carrier the hydrides of antimony, arsenic, tin and germanium were decomposed after passing them through a heated silica tube and counted 6.5 sec later; varying the furnace temperature between 350 and 950°C permitted of preferential deposition of one or the other element. This effect suggested a neutron group half-life of 2 sec, contributing 4% to the total delayed neutrons: 1% to ^{135}Sb, which was previously radiochemically determined as having a 1.9 sec half-life [15], and 3% to ^{85}As, ^{86}As or ^{87}As.

Hydrides of antimony, arsenic and germanium were also investigated by del Marmol and Nève de Mévergnies [16]. An H_2SO_4 solution containing uranium and suitable tracers and carriers was irradiated in the external beam of the BR-2 reactor at Mol. After irradiation the solution was drawn by vacuum over pre-heated zinc particles, and the hydrides, carried by nitrogen, were decomposed by passing them through a heated furnace, the neutrons being counted 2 to 7 sec later. Electronic timers permitted all operations to proceed automatically. A 2.15 sec half-life neutron activity was observed. Its yield was measured using tracers and was compared to the ^{87}Br delayed neutron activity. It also showed a 4% contribution to total delayed neutrons; this activity was assigned to ^{85}As on the grounds of fine structure of the fission mass-yield curve, ^{87}As being excluded as its half-life is ≤ 1.5 sec. An upper limit to any contribution of an antimony delayed nitrogen precursor to this activity was set as 25%, compatible with the value observed by Tomlinson.

Both experiments showed the presence of a 10 to 14 sec half-life neutron activity; del Marmol and Nève de Mévergnies showed that this activity could not be attributed to arsenic, antimony or germanium.

2.6. Isotopic and ion exchange

Hermann et al. [6] used both solvent extraction of Br^- and I^-, as mentioned earlier, and heterogeneous exchange of halogens with preformed AgCl to measure the residual neutron activities in thermal neutron fission of ^{235}U and 14 MeV neutron fission of ^{232}Th and ^{238}U. The results showed evidence that in thermal fission about 2%, 8% and 20% of the 55, 22 and 6 sec half-lives were issued by non-halogen delayed neutron precursors; by using a technique proposed by Ziegler and Gieseler [17] they observed similar activity ratios by exchange with CdS on cellulose. Shorter neutron half-lives were not observed, the counting time after irradiation being of the order of 15 sec. This technique was further improved [18] to separate bromine and iodine by exchange with silver halides and caesium, barium and thallium compounds. A fast rabbit system carried the glass vial

containing the solution from the accelerator to a filter. The vial was broken before hitting this preformed precipitate. This technique made it possible to count the sample 2 seconds after irradiation.

2.7. Hot-atom reactions

A separation based on the facility with which recoiling halogen fission fragments form organic halides was applied by Silbert and Tomlinson [19] to measure the relative primary yields of delayed neutron precursor bromine isotopes of 55 sec, 16 sec and 4.4 sec half-lives. The target consisted of ^{235}U or ^{233}U layers which were irradiated inside the beam tube of the McMaster nuclear reactor. Methane gas carried the fission recoil bromine following the reaction:

$$Br^* + CH_4 \rightarrow CH_3Br + H^\cdot$$

Iodine was removed by passage of the gas through a $AgNO_3$ trap and bromine was retained in a trap containing Pyrex tubing filled with Molecular Seive 13X. The relative primary yield results coupled with the neutron emission probabilities given by Aron et al. [12] are in good agreement with the independent yields of ^{87}Br, ^{88}Br and ^{89}Br calculated by using Wahl's [20] smooth Z_p function. This gives further evidence for the assignment of the 4.4 sec half-life to ^{89}Br.

2.8. Diffusion loss

Cowan and Orth [21] studied diffusion losses at high temperatures (1600 to 2600°C) of various fission products fission products from graphite and magnesium oxide. Among these the delayed neutron activities were measured after diffusion. The delayed neutron precursors diffuse out of graphite at rates consistent with those measured for iodine and bromine. Gas-trapping experiments showed no significant contribution of rare gas precursors or daughter products.

A method based both on hot-atom and diffusion loss reactions was applied is the study of the 122 msec ^{8}He delayed neutron precursor by Poskanzer et al. [22]. It was produced by spallation on the carbon or oxygen of thin plastic foils or absorbent cotton fibres irradiated in the 2.2 GeV external proton beam of the Brookhaven cyclotron. The recoil nucleus, after coming to the end of its range, diffuses out of the last foil or fibre. Inert helium then carries the helium activity to the traps and counters.

3. IRRADIATION FACILITIES

One of the basic points for isolation of very short-lived fission products is their usefulness for recuperating the fissile target as quickly as possible after irradiation in a form suitable to start the chemical operations.

Irradiations in external beams offer the easiest way to attain this aim as the transit time between the irradiation cell and the reagent products can be reduced to a minimum. However reactor external neutron fluxes

are usually low (10^8 to 10^{10} $n \cdot cm^{-2} \cdot sec^{-1}$) which leads to large expenditure of often costly fissile products (for instance gram quantities of ^{235}U).

Introducing the target in the beam holes close to the reactor core leads to increasing fluxes but necessitates an often complicated and cramped apparatus which is usually away for repair during reactor running time! However this system varies strongly with the different types of reactors and beam tubes, and is often suitable for gas-sweeping and diffusion experiments.

The use of a pneumatic rabbit permits one to reach the highest pile neutron fluxes and hence only small amounts of fissile material are needed. Transit times can be reduced to a few tenths of a second. Fast opening of the sample holders, however, is often a delicate problem. Although crushing the sample holder has been tried [18], one of the handiest methods for fast recuperation was described by Greendale and Love [23]: a nylon or a Teflon rabbit containing 1 to 2 ml of solution is impaled at the end of its run on two hypodermic needles; through one of these the solution is drawn out of the container and air or a rinsing solution is introduced through the second one to flush the system. Chemical separations can be started within 3 sec after the irradiation. Other rabbit systems based on the same principle are in use elsewhere [24, 25]. Similar irradiation devices can be used with accelerator irradiations.

4. DISCUSSION

By using a fast rabbit of the model just described in conjunction with simple chemical processing, such as precipitation, isotopic exchange or solvent extraction in which the reagents are drawn by vacuum through the different chemical steps until the final counting form is obtained, it is possible to detect delayed neutron activities of half-lives of down to 1 or 2 sec, depending on the procedures involved.

The different stages of the chemical reactions are regulated by means of electronic timers opening or closing electromagnetic valves. Our laboratory has plans to study the delayed neutron precursors of selenium and tellurium by this technique.

The advantage of these "classical" chemical separations is that using tracers or carriers the chemical yield of the final product is easily measured; moreover the delayed neutron yields can be obtained by comparison with the unseparated 56 sec delayed neutron activity of a known amount of uranium (or other fissile material) irradiated under the same conditions and measured with the same geometry. As evidence indicates that the 56 sec activity belongs only to ^{87}Br [26], these experiments, connected with the fission yield measurement or calculation of the isotope under study, can lead finally to the determination of its neutron emission probability (P_n). Of course great care should be taken to ensure that both the neutrons of the unknown and the standard are well thermalized before counting. Other possibilities involving rabbits are group co-precipitations (as sulphide precipitations) followed by neutron counting. Positive or even negative results can orient further investigations towards definite elements.

Nevertheless for the study of half-lives of the order of, or shorter than, 1 to 2 sec, gaseous phases have to be used. Distillation and gas-

sweeping methods depend mainly on the availability of volatile compounds of the element of interest, while the mechanisms involved in diffusion-loss methods are much more complex. Bryant et al. [27] in their study of loss rates of fission products from uranium-graphite fuels showed that many parameters appear to be involved, such as melting and boiling points, tendency to form compounds with the diffusion medium, atomic radii, etc.

Recoil losses of carbon atoms diffusing out of stacked plastic foils irradiated by high energy protons were observed by Cumming et al. [28]. Analyses of the liberated gas showed that it was composed of hydrogenated compounds of carbon. A broad field of gaseous separations remains to be explored where atoms of various organic materials can form volatile compounds with fission products. For instance volatile hydrides and possibly chlorides could diffuse out of organic materials containing hydrogen or chlorine and be rapidly swept away in suitable gas carriers.

Separation by volatilization of elements or their compounds followed by fractional condensation in a column along which a temperature gradient was established has been successfully applied by Merinis and Buissières [29]. They isolated in this way mercury, platinum, indium, osmium and rhenium spallation products from a gold target. A systematic study of such separation possibilities for various gas carriers should probably be rewarding for fast fission product separations.

It is not the purpose of this paper to discuss the advantages or limitations of various mass spectrometers or radioisotope separators. These have been reviewed by Bruninx [30] while more recent developments have been presented by various investigators at the Lysekil symposium in August 1966 [31]. Evidently purely chemical separations offer the possibility of determining the charge of the delayed neutron precursor, then the mass has to be found by indirect means (such as milking). Since mass separators have been applied to the field of fission product separation, one has the possibility of directly isolating a given mass, allied, in the case of on-line instruments, to the advantage of reaching half-lives often too short to be determined by chemical means.

However, mass spectrometers are limited by their resolving power and, for a given set of isobars, the activities of those with high primary yields (and their daughter products) can hide activities of nuclides of lower yields; often these yield determinations require the knowledge of the individual decay schemes or complementary measurements of γ-ray intensities. Thus the problem encountered for the mass determination of a delayed neutron precursor of a given charge (in a chemical separation) is now the problem of determining the charge of a delayed neutron precursor of a given mass (mass spectrometry). So the methods are complementary.

Isotope separation allies both techniques: an initial element separation is followed by mass isolation. A fine example is in the work of Amarel et al. [32] who diffused rubidium and caesium fission products through hot graphite and determined the half-lives of separated masses by β-counting, while neutron counting showed the existence of 4 rubidium and 2 caesium delayed neutron precursors with well defined mass assignments. The shorter delayed neutron precursor half-life they observed was 0.23 sec; among these isotopes they showed that the 6 sec rubidium activity found by Stehney and Perlow [13] belonged to mass 93.

Thus it does not seem that radiochemical methods are doomed; they should be used in conjunction with mass separators, one technique acting as a cross-check for the other.

REFERENCES

[1] For a general discussion on the subject see KEEPIN, G.R., Ch. 4, Physics of Nuclear Kinetics, Addison Wesley, Reading, Mass.(1965).

[2] SNELL, A.H., LEVINGER, J.S., MEINERS, E.P. Jr., SAMPSON, M.B., WILKINSON, R.G., Phys. Rev. 72 (1947) 545.

[3] STRASSMANN, F., HAHN, O., Naturwiss. 28 (1940) 817.

[4] BORN, H.J., SEELMANN-EGGEBERT, W., Naturwissenschaften 31 (1943) 59.

[5] BORN, H.J., SEELMANN-EGGEBERT, W., Naturwissenschaften 31 (1943) 86.

[6] HERMANN, G., FIEDLER, J., BENEDICT, G., ECKHARDT, W., LUTHARDT, G., PATZELT, P., SCHÜSSLER, H.D., Physics and Chemistry of Fission (Proc. Symp. Salzburg, 1965) 2 IAEA, Vienna (1965) 197.

[7] SUGARMAN, N., J. chem. Phys. 15 (1947) 544.

[8] SUGARMAN, N., J. chem. Phys. 17 (1949) 11.

[9] STEHNEY, A.F., SUGARMAN, N., Phys. Rev. 89 (1953) 194.

[10] PERLOW, G.J., STEHNEY, A.F., Phys. Rev. 107 (1957) 776.

[11] PERLOW, G.J., STEHNEY, A.F., Phys. Rev. 113 (1959) 1269.

[12] ARON, I.M., KOSTOCHKIN, O.I., PETRZHAK, K.A., SHPAKOV, V.J., Atomn. Energ. 16 (1964) 368.

[13] STEHNEY, A.F., PERLOW, G.J., Bull. Am. phys. Soc. II, 6 (1961) 62.

[14] TOMLINSON, L., J. inorg. nucl. Chem. 28 (1966) 287.

[15] BEMIS, C.E., GORDON, G.E., CORYELL, C.D., J. inorg. nucl. Chem. 26 (1964) 213.

[16] del MARMOL, P., NEVE de MEVERGNIES, M., J. inorg. nucl. Chem. 29 (1967) 273.

[17] ZIEGLER, M., GIESELER, M., Z. analyt. Chem. 191 (1962) 122.

[18] ECKHARDT, W., HERMANN, G., SCHÜSSLER, H.D., Z. analyt. Chem. 226 (1967) 71.

[19] SILBERT, M.D., TOMLINSON, R.H., Radiochim. Acta 5 (1966) 217; 5 (1966) 223.

[20] WAHL, A.C., FERGUSON, R.L., NETHAWAY, D.R., TROUTNER, D.E., WOLFSBERG, K., Phys. Rev. 126 (1962) 112.

[21] COWAN, G.A., ORTH, C.J., Int. Conf. peaceful Uses atom. Energy (Proc. Conf. Geneva, 1958) 7 UN, New York (1958) 328.

[22] POSKANZER, A.M., ESTERLUND, R.A., Mc PHERSON, R., Phys. Rev. Lett. 15 (1965) 1030.

[23] GREENDALE, A.E., LOVE, D.L., Nucl. Instrum. Meth. 23 (1963) 209.

[24] JOHSON, N.R., EICHLER, E., O'KELLEY, G.D., Nuclear Chemistry, Ch. 4, Coll. Technique of Inorganic Chemistry 2, Interscience, New York (1968).

[25] DENSCHLAG, H.O., GORDUS, A.A., Z. analyt. Chem. 226 (1967) 62.

[26] WILLIAMS, E.T., CORYELL, C.D., Nucl. Appl. 2 (1966) 256.

[27] BRYANT, E.A., COWAN, G.A., SATTIZAHN, J.E., WOLFSBERG, K., Nucl. Sci. Engng 15 (1963) 288.

[28] CUMMING, J.B., POSKANZER, A.M., HUDIS, J., Phys. Rev. Lett. 6 (1961) 484.

[29] MERINIS, J., BOUISSIERES, G., Analytica chim. Acta 25 (1961) 498.

[30] BRUNINX, E., Atomic Energy Rev. IAEA, Vienna 4 1(1966) 107.

[31] Why and How Should We Investigate Nuclides Far Off The Stability Line? (Proc. Symp. Lysekil, Aug. 1966), proceedings to be published in Ark. Fys.

[32] AMAREL, I., BERNAS, R., FOUCHER, R., JASTRZEBSKI, J., JOHNSON, A., TEILLAC, J., GAUVIN, H., Phys. Lett. 24B (1967) 402.

DISCUSSION

On the paper by del Marmol

The internal comparison with bromines or iodines would be very useful and can be done in many experiments. Such a measurement was performed by the Mainz group. The Soreq group measured P_n values experimentally for krypton and rubidium isotopes, using the gas sweeping technique. At the collector side, whatever element is extracted from the target, the longer-lived nuclei at the end of the chain are counted in the case mentioned, i.e. rubidium-91, -92 and -93. These can be measured independently of their precursor krypton because of the long half-lives and thus be used for comparison with bromine. A reference standard must be used in such work and the best is obviously ^{87}Br. The decay scheme of this isotope should therefore be studied in detail even if such a study is very complicated due to contamination from ^{88}Br which has the same half-life. But the P_n value for ^{87}Br should be known better if this isotope is to be used as a standard. The P_n value of ^{87}Br can be obtained with a 2% accuracy by comparing yields of the 55 sec period in several fission reactions with calculated accumulative yields of ^{87}Br which for low energy reactions are very close to the chain yield. The advantage of the established chemistry is that the contributions of various precursors to period yield can be compared. As long as one is studying the delayed neutrons from fission, the investigation based on changes of fission fragment yields and ranges proved to be valuable, and is a very good method. When delayed neutrons from spallation are studied, the range measurements are rather difficult, as ranges of products formed in the spallation processes are very small compared to the ranges of fission products. Also, in range measurements, the high-yield emitters hide the low-yield ones.

MEASUREMENT OF DELAYED NEUTRON MASS- AND TIME-DEPENDENCE BY AN ON-LINE MASS SEPARATOR OF THE COHEN TYPE

E. ROECKL, J. EIDENS AND P. ARMBRUSTER
INSTITUT FÜR FESTKÖRPER UND NEUTRONENPHYSIK,
KERNFORSCHUNGSANLAGE JÜLICH,
FEDERAL REPUBLIC OF GERMANY

Abstract

MEASUREMENT OF DELAYED NEUTRON MASS- AND TIME-DEPENDENCE BY AN ON-LINE MASS SEPARATOR OF THE COHEN TYPE. A helium-filled or Cohen type mass separator for fission products has been installed at the FRJ-2 reactor. A source of ^{235}U is exposed to a thermal neutron flux of 10^{14} n cm^{-2} sec^{-1} and yields 2.5×10^{12} fission events per second. The fission products coming from the beam hole collimator pass through a helium-filled focusing magnetic deflection system, travelling on a constant radius path of radius ρ under field B and are separated such that the $B\rho$-value is proportional to $A^{2/3}$. For a helium pressure of 7 mmHg an optimum resolving power of $A/\Delta A = 16$ has been obtained. The separation time ($\sim 1\,\mu$sec) is the flight time in the separator. For high yield fission products, beams of 10^4 n cm^{-2} sec^{-1} have been measured in the focus of the separator. To determine absolute yields of delayed neutron emitters an activity build-up technique has been used, with a neutron detection system at the focus of the separator. For activity decay measurements the detection system is situated 25 cm above the focus. A discontinuously operating transport tape collects the fission products and transfers the irradiated target rapidly to the detector position. The delayed neutron detection system used is an assembly of ^3He-counters embedded in polyethylene and a β-proportional counter; they operate in coincidence. With optimized coincidence resolution time the signal-to-background ratio is increased by up to two orders of magnitude. The n-β-coincidence method is discussed. Delayed neutron activities have been measured in the mass region of light fission products. Their variation both with the mass of the fission products and with time has been investigated. The measurements are compared with published data. Evidence is given for neutron activities with half-lives smaller than a few seconds and masses larger than 90.

1. INTRODUCTION

Fast radiochemical techniques [1-4] have been used to identify delayed neutron emitters and to determine their yields. The moderate speed of separation, the identification of elements with similar behaviour, and the mass determination of isotopes of a specific element are difficulties inherent in the radiochemical techniques. The advantages in applying on-line mass separator techniques for delayed neutron experiments are obvious. The separation time of 1 μsec enables short-lived emitters to be investigated. The mass identification is unambiguous. The new on-line separation techniques will, supplemented by radiochemical techniques, answer many of the still open questions in the identification of delayed neutron emitters.

The usefulness of a helium-filled mass separator in delayed neutron experiments was pointed out by Cohen and Fulmer in 1958 [5]. The performance of the helium-filled on-line mass separator at the research reactor FRJ-2 and the specific experimental techniques used in work on delayed neutrons are reported. The first experimental results of the

time- and mass-distribution of delayed neutron emitters in the light fission product group are given.

2. EXPERIMENTAL TECHNIQUES

2.1. The on-line mass separator

A helium-filled mass separator, similar to those built by Cohen and Fulmer [5] in 1958 at Oak Ridge National Laboratory and Armbruster [6] in 1961 at München, has been operated since 1966 at the research reactor FRJ-2 [7], Fig. 1.

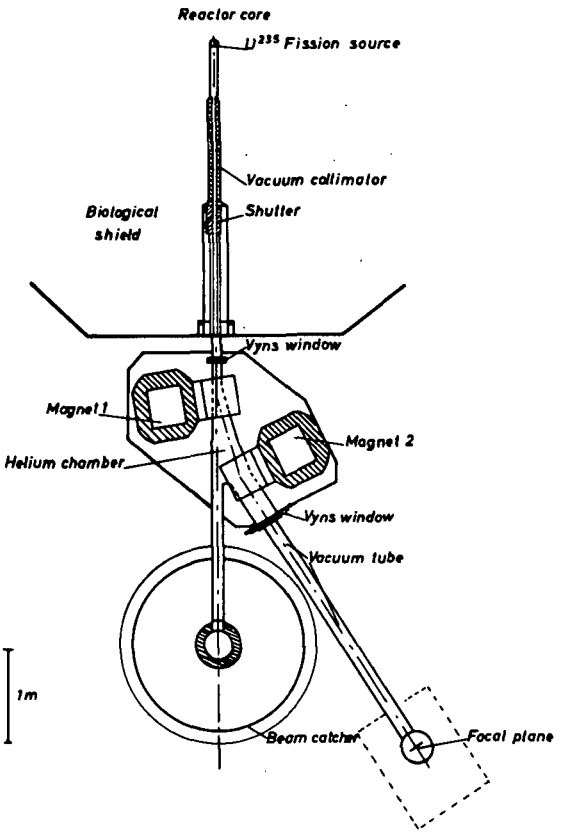

FIG. 1. The on-line mass separator.

A fission source of ^{235}U is deposited in a thermal flux of 10^{14} n cm^{-2} sec^{-1} at the end of an evacuated beam tube. In a layer, 1 mg/cm^2 thick, 2.5×10^{12} fission events/sec are induced. Having passed through a collimator, which defines an aperture of 1.4×10^{-6}, the fission products enter a stigmatically focusing magnetic deflection system. They are separated from the strong neutron and γ-beam, which is stopped in a beam catcher. A beam of fission products of selected mass leaves the deflection system with a time-of-flight from the source to the focus position of ~ 1 μsec.

For high yield fission products, beams of 10^4 n cm^{-2} sec^{-1} have been obtained in the focus of the deflection system.

The deflection of charged particles in a magnetic field B is given by:

$$B\rho \propto \frac{A\,v}{e} \tag{1}$$

where ρ is the radius of curvature of the ion in the magnetic field, A is its mass number, v its velocity, e its ionic charge and Z its nuclear charge. As postulated by Bohr [8] and experimentally verified by Fulmer and Cohen [9] for helium at low pressure, the average charge of fission products is proportional to the velocity of the fragment. This is given by

$$\bar{e} \propto v\, Z^{1/3} \tag{2}$$

Equations (1) and (2) give

$$B\rho \propto \frac{A}{Z^{1/3}} \propto A^{2/3} \tag{3}$$

The nuclear charge is proportional to the mass number of fission products after neutron evaporation to within a few percent, over the whole fission product mass region. The deflection in the magnetic field depends neither on the velocity of the fission product nor its ionic charge state. Rather thick fissionable layers which have a velocity spread large in comparison to the velocity spread produced in the fission process ($\Delta v/v = 6.5\%$) may be used as sources. The thick source and the independence of the deflection on the specific ionic charge yield the great beam intensities, the most important advantage of the helium-filled mass separator technique.

Equation (2) holds for the average charge of the fission products. In spite of the wide distribution of charge states ($\Delta e/e = 23\%$) a separation with moderate resolution becomes possible when the beam passes within the deflection system through a region filled with helium at low pressure. The fission products interact with the gas atoms. Their ionic charge states are changed in collisions, their directions of flight are changed by multiple nuclear scattering, and their energies are degraded by electronic stopping. The deflection in the magnetic field is proportional to the average of all charge values a fission product takes during its passage through the gas-filled part of the deflection system. The width of the distribution of these average charge values decreases with increasing number of charge changing collisions, i.e. the resolving power should grow with increasing helium pressure. On the other hand the angular spread of the beam caused by multiple nuclear scattering increases with increasing number of collisions and decreasing energy of the fission products, i.e. the resolving power decreases with increasing pressure. The best value of the resolving power at full-width-half-maximum amounts to $A/\Delta A = 16$ and is obtained with a helium pressure of 7 mmHg.

Known long-lived fission products have been used to calibrate the mass separator. They are identified by the energy of pronounced γ-lines and their known half-lives. The calibration procedure is similar to the technique described later in this paper for decay measurements of delayed

neutron emitters. Figure 2 gives the result of the mass calibration for light fission products on a log-log scale plot. The deviations from the proportionality between $B\rho$ and $A^{2/3}$ are about 1%. If a pronounced γ-line exists and is resolved in the γ-energy spectrum it is possible to determine the mass of an unknown fission product despite the moderate resolving power. The dependence of the γ-line intensity on the magnetic field gives a distribution the maximum of which unambiguously determines the mass of the emitting nuclide.

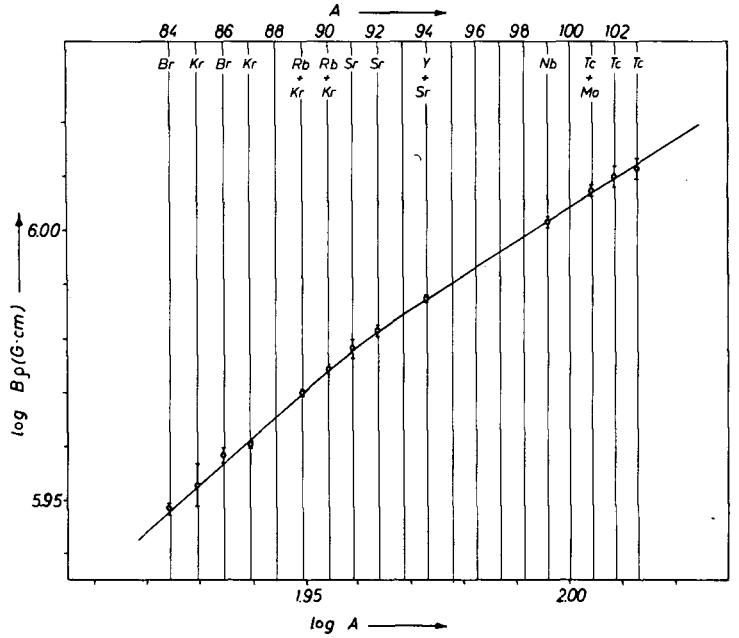

FIG. 2. Calibration curve of the mass separator.

2.2. Yield determination by activity build-up measurements

For yield determinations the continuously working separation procedure and the separation time short compared to all β-decay half-lives make possible the application of an activity build-up technique [10, 11]. The time characteristic of a specific emitter which depends on all the decays of its mostly unknown precursors does not affect the yield determination. The build-up technique has been successfully used for β-chain length measurements of fission products, and is advantageously applied for the measurement of the yield distribution of delayed neutron emitters over the mass region of fission products.

A target is irradiated by a beam of fission products of constant beam intensity S_0. The fission products are stopped in the target which is placed in front of a neutron detector, Fig. 3. The irradiation time chosen has to be long compared to the half-lives of the delayed neutron precursors. The saturation value n of the neutron activity will then be proportional to the

absolute yield of the delayed neutron emitters. The measurement of n gives directly the absolute yield $P_n \cdot Y_n$ of delayed neutron emitters folded with the resolution function of the mass separator.

$$n(A) = \frac{\epsilon \cdot S_0}{\sqrt{\pi} \cdot \Delta A} \sum_{A_i} Y_n(A_i)\, P_n(A_i) \exp\left[-\left(\frac{A - A_i}{\Delta A}\right)^2\right] \qquad (4)$$

ϵ = detection probability for delayed neutrons, ΔA = width of the intensity distribution of a nucleus of mass A_i given by the resolving power of the mass separator.

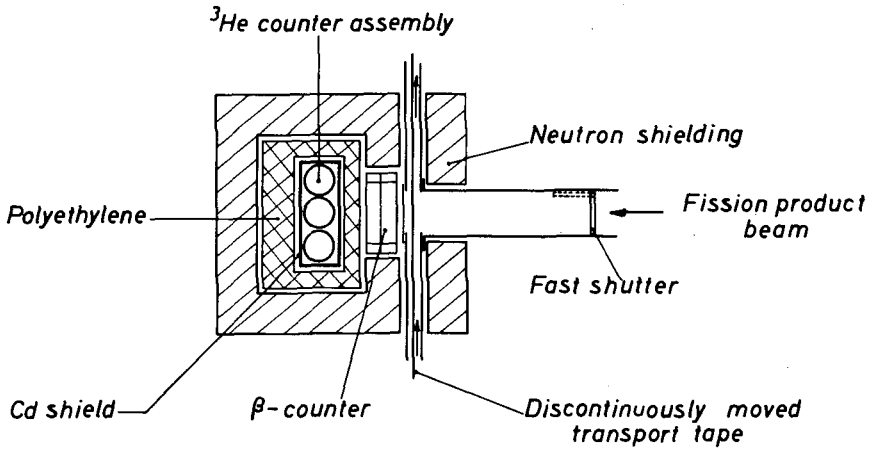

FIG. 3. Detector arrangement for build-up measurements.

The time-dependence of the activity build-up is given by:

$$n(A, T) = n(A) \int_0^T \nu(t, A)\, dt \qquad (5)$$

where the integral approaches a value of 1 for values of T long compared to the half-lives and $\nu(t, A)$ is a function describing the time- and mass-dependent release of delayed neutrons.

2.3. Study of the time characteristics of delayed neutron emitters

For the study of the decay of a specific nucleus the irradiation position of the target has been spatially separated from its counting position [12], see Fig. 4. Having been irradiated for a preselected time the target is moved by an intermittently operating fast transport system to a counting position. The transport time is small compared to the irradiation time, being 0.1 sec. While the decays in the target are analysed a new target is irradiated in the irradiation position. The target is a small area (6 cm^2) of a 500 m long nylon tape, which is used for activity transport. The

irradiation-counting cycle is repeated for constant magnetic field on the deflector until counting-statistics criteria are satisfied. By suitably changing the magnetic field the whole mass range of fission products may be investigated.

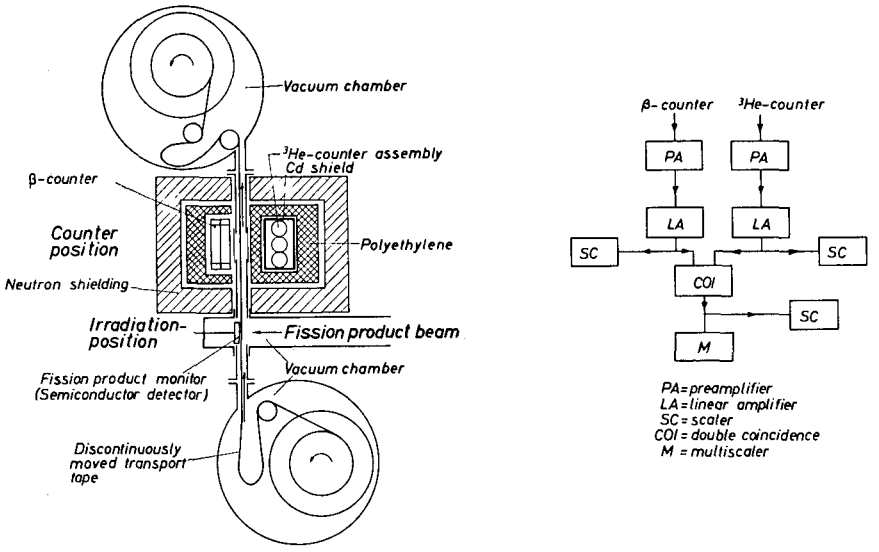

FIG. 4. Detector arrangement for decay measurements, transport system, and block diagram of electronics.

For the same distance between irradiation and counting positions the intermittently moving transport system shows an intensity gain by a factor of four over that of a continuously moving system.

The irradiation time may be adjusted to suit the half-life to be investigated. With optimum adjustment 40% of the activity collected in the irradiation position decays in the counting position. Fig. 5 gives the fraction of the collected activity decaying in the counting position as a function of the ratio between half-life and irradiation time. The time resolution of the transport system is poor, as may be seen from Fig. 5, but a first guide as to the time dependence of an unknown activity will be obtained.

2.4. Neutron detection

The delayed neutrons, having energies larger than a few 100 keV, are slowed down in polyethylene slabs, and are detected in an assembly of ^{3}He proportional counters. The detection efficiency of the counter assembly is 5%. Pulse height discrimination makes the detector insensitive to pulses from γ-quanta and electrons. The detection efficiency for γ-quanta has been checked with a strong ^{60}Co source. A discriminator setting has been found where the counters are not sensitive to γ-quanta. The good discrimination properties are vital for all delayed neutron measurements, as the number of β-decays with subsequent γ-emission is much higher than the number of β-decays with subsequent emission of a neutron.

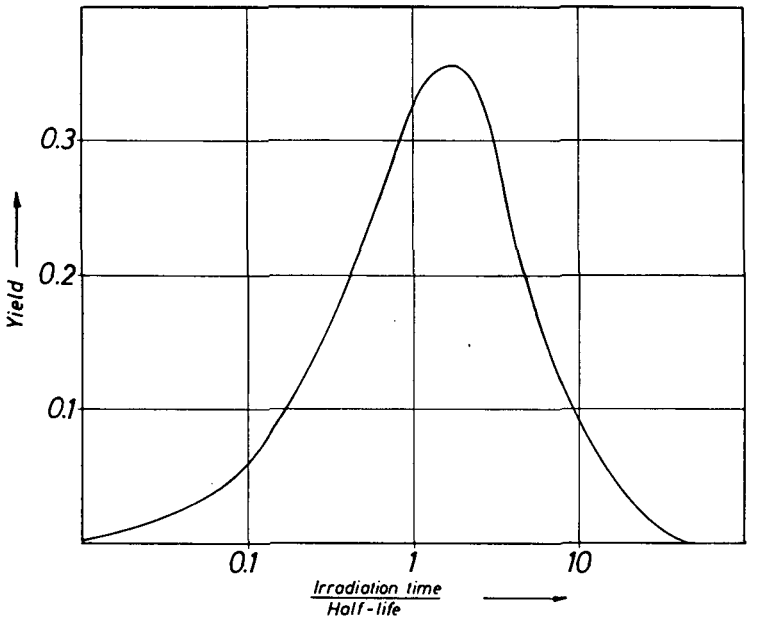

FIG. 5. Yield function of the discontinuously moved transport tape.

Every delayed neutron is preceded by the β-decay of its precursor. All neutrons are emitted in coincidence with β-particles. This fact is used to improve the signal-to-noise ratio in the measurement. Using a good geometry β-counter restricts the loss in counting rate by the coincidence condition to a factor of 2 to 3, a disadvantage largely offset by the great improvement in the background conditions. In our measurements a methane-flow proportional counter has been used as β-detector. The counter assembly may be seen from Figs 3 and 4.

To determine the optimum time resolution of the coincidence circuit, time spectra of neutrons were taken for different arrangements of moderator and cadmium shielding. The time spectra were recorded by a time-of-flight unit of the multichannel analyser. β-pulses started and the subsequent n-pulses stopped the time-of-flight measurement. Electron collection times in the proportional counters and the moderation times of neutrons are taken into account by this method of determining the coincidence time resolution. For the detector arrangements shown in Figs 3 and 4, values of $2\tau = 16.5$ μsec and $2\tau = 8.3$ μsec, respectively, have been found.

The number of random coincidences is determined by the single rates R_β and R_n in the two counters. These rates derive from different contributions. The time- and mass-dependence of the release of β-particles from fission products mainly determines the rate R_β [11]. The neutron rate R_n is made up from the constant background near the reactor (2/sec) and two time- and mass-dependent rates, one coming from delayed neutrons emitted by fission products in the irradiation position of the target and another coming from delayed neutrons emitted in the counting position. Only this last contribution gives rise to true coincidences, all the others have to be

considered only in the correction for random coincidences. The large number of β-particles emitted from fission products in the target not followed by a neutron emission and the long coincidence-resolution time make a consideration of random coincidences necessary. The highest value obtained for the signal-to-noise ratio is about 100 and is in favourable cases more than two orders of magnitude better than without the coincidence condition.

In Fig. 4 a block diagram is given of the electronics used in the build-up and decay measurements. The n-β-coincidence pulses are registered by a multiscaler which is started by an external electronic clock. This clock controls all functions in the irradiation-counting cycle. Additional multiscaler spectra have been taken for the single rates R_β and R_n to correct for random coincidences. Moreover, all rates, singles and coincidences, are recorded and read out every few minutes.

2.5. Energy determination of delayed neutrons

^{3}He-proportional counters have been used as neutron energy spectrometers (see Ref. [13]). The energy resolution of a ^{3}He-proportional counter for 400 keV neutrons is about 25% and its detection probability even in good geometry is smaller than 3×10^{-4}. The high detection probability for all low energy neutrons and the poor resolution makes pulse height discrimination for these background pulses of doubtful value. On the other hand time discrimination for keV-neutrons is impossible, as the electron collection times in the proportional counter are about 0.5 μsec. Energy spectra of delayed neutrons obtained with ^{3}He-proportional counters are all heavily distorted at the low energy end of the spectra.

These difficulties are overcome applying fast time-of-flight techniques. In a fast (β, n)-time-of-flight spectrometer plastic scintillators are used for the detection of neutrons and β-particles. Neutrons of energies larger than 200 keV are detected by the energy from the proton recoil reaction in a plastic scintillator. This makes the detector insensitive to neutrons of lower energies. γ-quanta detected in the neutron detector give rise either to a continuous background of random coincidences in the time-of-flight spectrum or to a definite peak in the time-of-flight spectrum, if the pulse originates from a (β, γ)-coincidence.

Using a thick scintillator for neutron detection, a good geometry thin scintillator for β-detection, fast large-area photomultipliers, a flight path between 20 and 40 cm, and nanosecond electronics, a time-of-flight spectrometer of energy resolution equal to the ^{3}He proportional counter will have a detection probability 10 times higher than the ^{3}He proportional counter. The energy resolution can be improved to values of a few per cent, if a loss in detection probability may be tolerated. A time-of-flight spectrometer of equal detection probability as an optimum ^{3}He-proportional counter spectrometer has in addition to its better discrimination properties a better energy resolution, 10% instead of 25%. Delayed neutron energy spectra will be measured using a time-of-flight spectrometer in the counting position of the on-line separator.

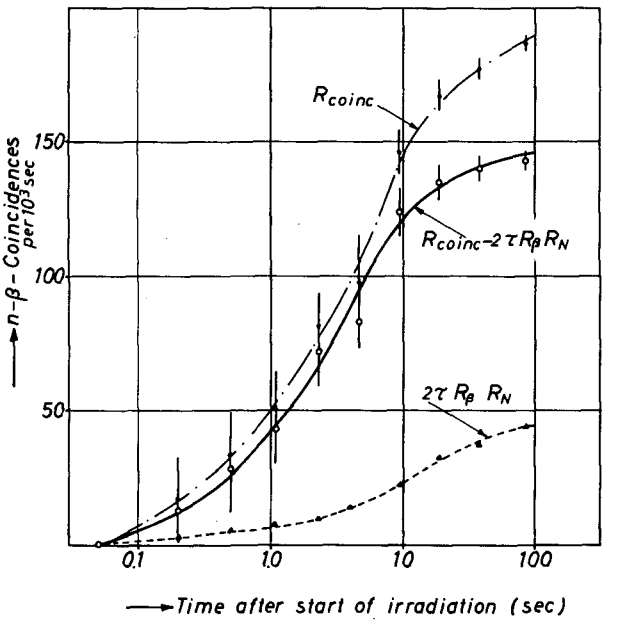

FIG. 6. Typical activity, build-up curve for 300 cycles. R_{COINC} = measured coincidence rate, $2\tau R_\beta R_N$ = calculated random coincidence rate.

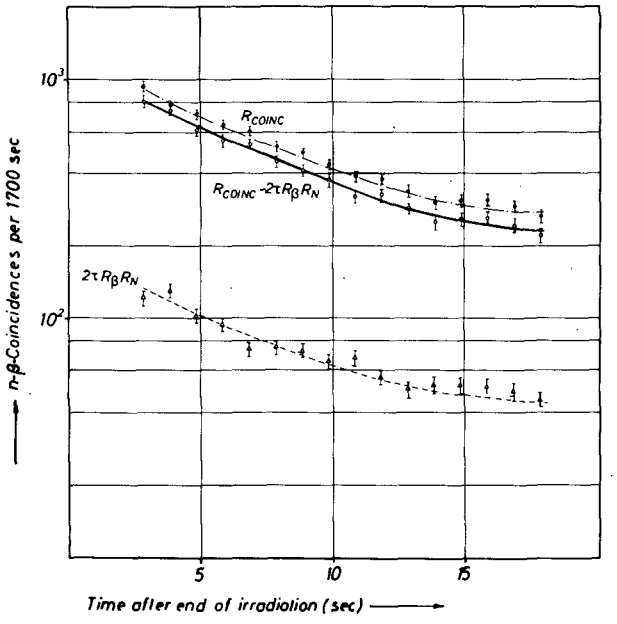

FIG. 7. Typical activity decay curve for 1700 irradiation-counting cycles: R_{COINC} = measured coincidence rate, $2\tau R_\beta R_N$ = calculated random coincidence rate.

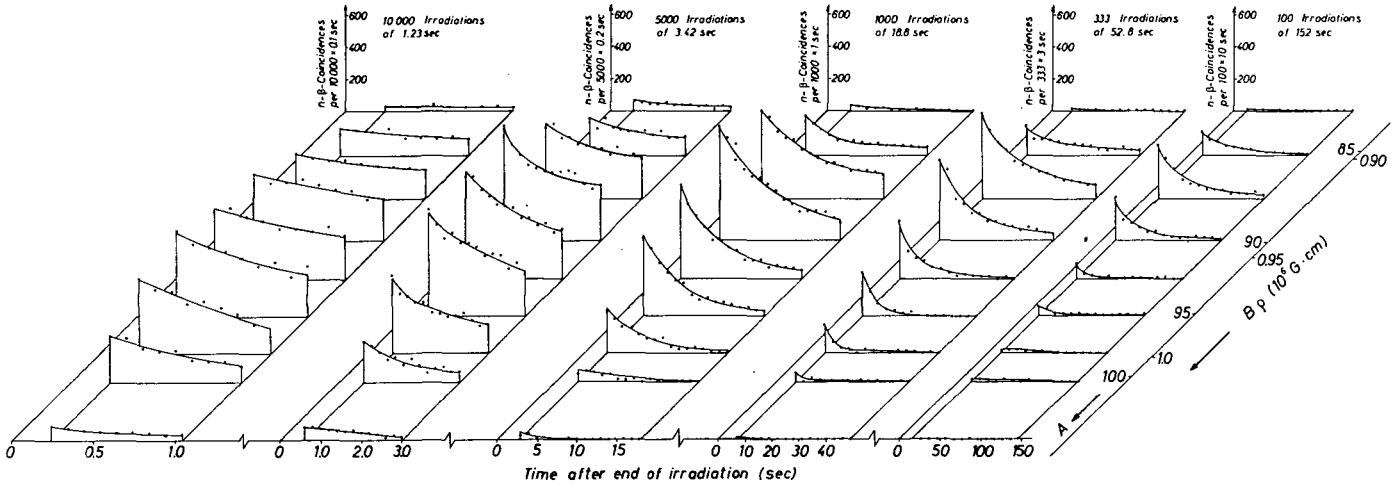

FIG. 8. Activity curves as a function of fission product mass for different cycle times.

3. MEASUREMENTS

As a mass calibration of the heavy fission product group has not yet been completed, all investigations performed have been restricted to the light fission product group. Apart from the lack of calibration, all measurements could have been done as well in the heavy group.

3.1. Build-up measurements

A build-up experiment using the experimental arrangement shown in Fig. 3 was performed to determine the distribution of neutron yields over the light fission product group. Zero time was defined by the opening of a fission product beam shutter, the switching time of which is less than 0.1 sec. For 10 different $B\rho$-values the growth of activity has been measured up to 100 sec. At this time all emitters except the most long-lived ones, as ^{87}Br and ^{88}Br, have reached the saturation activity. At the end of each cycle the transport system replaces the target by a new one. Fig. 6 gives as an example the build-up near mass 92. The time of measurement for this curve amounted to 10 h. The contribution of random coincidences has been calculated from build-up measurements of the single rates, and may be seen from the figure. The signal-to-noise ratio is time- and mass-dependent and is about 4.

3.2. Decay measurements

With the experimental set-up shown in Fig. 4 the time- and mass-dependence of delayed neutron activities in the light fission product group was investigated. The activities after end of irradiation were measured for various irradiation and counting times. Data have been taken for 9 values of $B\rho$ and the irradiation-times 152 sec, 52.8 sec, 18.8 sec, 3.42 sec, and 1.23 sec. The total data collection time amounted to 14 days. Fig. 7 gives a typical decay curve for 1700 cycles of 18.8 sec near mass 88. The contribution of random coincidences has been calculated from decay measurements of the single rates and may be seen in the figure. The number of cycles necessary for the measurement of the single rates is determined by the signal-to-noise ratio and the statistics wanted. It varies considerably for different times and $B\rho$-values. Fig. 8 is a summary of all measured decay curves. The coincidence rates are corrected for random coincidences and for the burn-up of the fission source, which is not negligible over the time of measurement. The rates are all normalized to a time of 10^3 sec for each point of measurement.

4. RESULTS OF THE MEASUREMENTS

In the build-up technique the activity at a certain time T after start of irradiation is proportional to the release of delayed neutrons up to the time T after fission (cf. Eqs (4) and (5)). Figure 9 represents the mass-dependence of the neutron yields for different times after fission. It is obtained from the activity values at 0.1 sec, 1 sec, 10 sec, and 100 sec after start of irradiation. All yields are given as coincidence rates

normalized to 10^3 sec. The total neutron activity, integrated over the light fission product range, may be seen for the different times after fission from Table I. In addition the activities released over different time intervals are given.

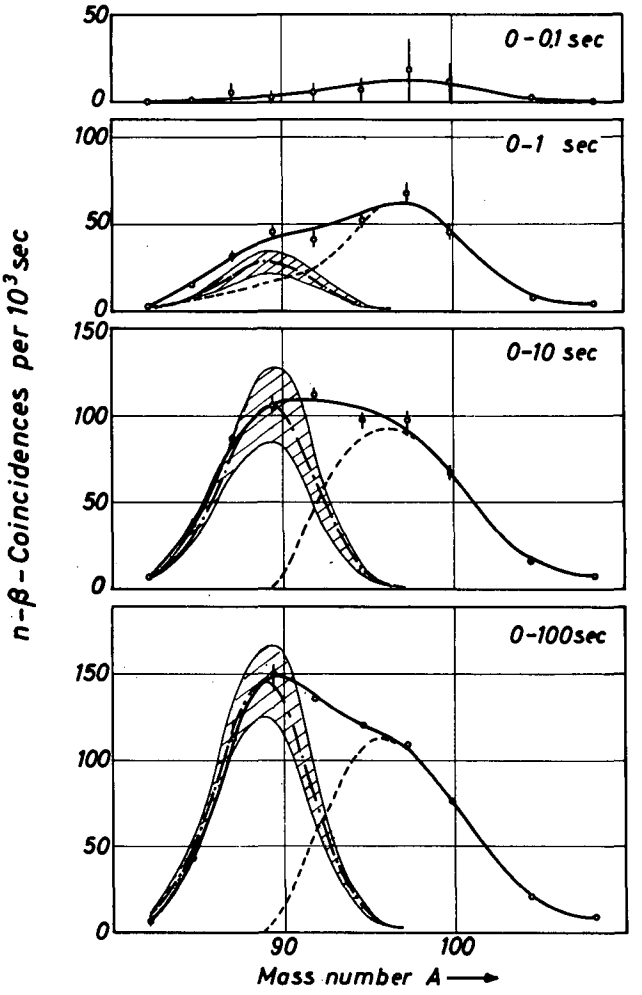

FIG. 9. Mass dependence of delayed neutron yields for different times after fission: —○— measured; ////// calculated contribution of identified precursors; - - - - - unidentified part.

The decay measurements have been preliminarily evaluated neglecting the information present in the time dependence of the coincidence rates during the cycle time, as represented in Fig. 8. The rates have been integrated over the cycle times, and the integrated rates obtained have been normalized to a time of 10^4 sec. The time information still present is given by the time resolving characteristic of the transport system,

TABLE I. MEASURED DELAYED NEUTRON YIELDS, AND UNIDENTIFIED PERCENTAGE FOR DIFFERENT TIMES AFTER FISSION IN THE LIGHT FISSION PRODUCT GROUP

Time after fission (sec)	0.1	1	10	100			
Time interval (sec)					0.1 to 1	1 to 10	10 to 100
Part of total yield (%)	≈5	40	80	98	35	40	18
Thereof not identified (%)		75	55	50	75	35	35

Fig. 5. Each cycle time corresponds to a favoured half-life, the values of which are given in Table II. Fig. 10 gives the mass dependence of the integral coincidence rates for the different cycle times.

The measurements are compared to the yields and the time dependence of the identified delayed neutron emitters. Table III gives the data used for the comparison. The absolute yield of ^{85}As has been taken from the measurements of Tomlinson [3] and del Marmol et al. [4]. The absolute yields of the bromine isotopes have been calculated from the emission probabilities P_n determined by Aron et al. [2] and the cumulative yields Y_n calculated by Amiel [14]. Another set of yields for the bromine isotopes has been obtained from the relative yields measured by Perlow and Stehney [1]. The absolute yields are determined if the yield of the 55 sec-group of the total neutron activity, as measured by Keepin [15], is assumed to be due to ^{87}Br, an assumption verified by measurements of Williams and Coryell [16].

The average value of the absolute yields have been folded with the mass resolution of the separator and with time functions corresponding to the build-up and the decay techniques. In the mass region A = 85 - 90 the calculated identified activity was fitted for the build-up measurement to the activity increase between 10-100 sec and for the decay measurement to the integrated activity of the 152 sec cycle.

From Figs 9 and 10 the mass dependence of the contribution of identified emitters may be seen. The shaded regions give the uncertainty of the calculated contributions due to errors of the absolute yield measurements. Further, the difference between the identified and the measured activity is shown.

In Tables I and II the values integrated over the light fission product range are given for the two measurements and are compared to the corresponding values calculated from the yields of the identified emitters.

5. CONCLUSIONS

The following conclusions have to be drawn from the presented measurements.

1. Among the light fission products, there are, beside the identified emitters, new and as yet unidentified emitters.

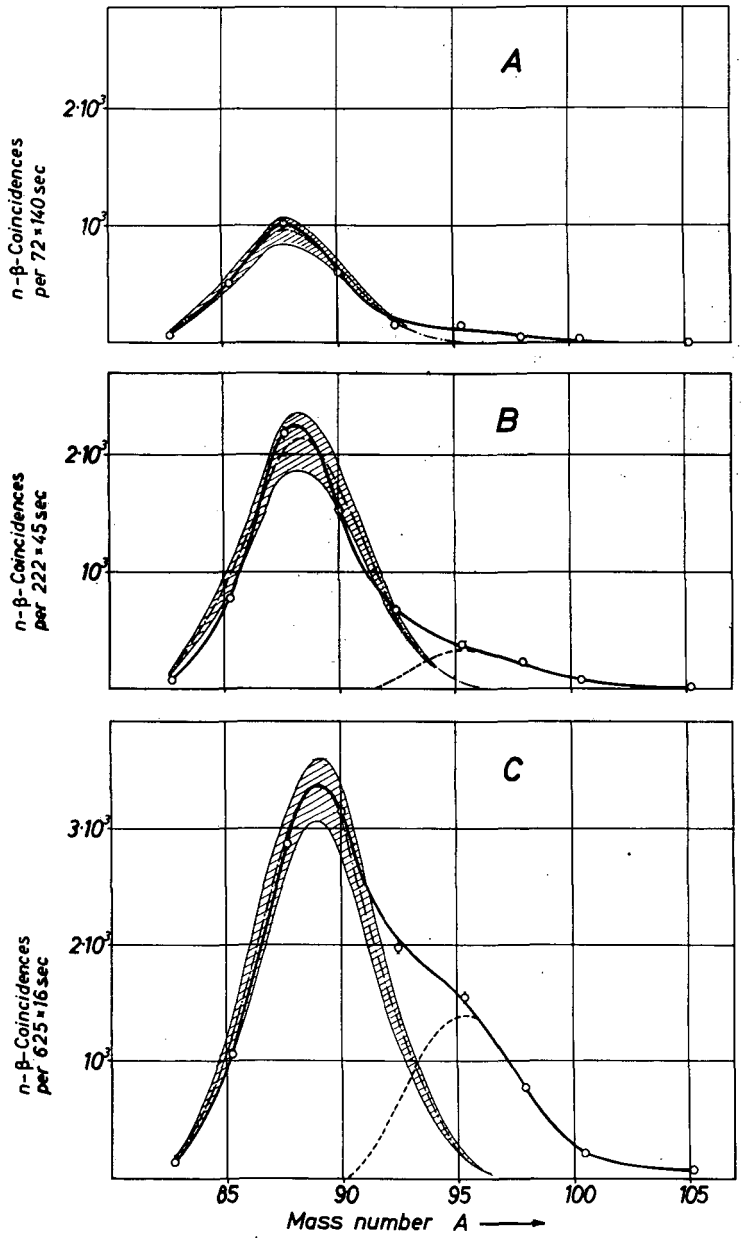

FIG. 10. Mass dependence of integral delayed neutron activity for different cycle times. For time programme for measurements A to E see Table II: —○— measured; /////// calculated contribution of identified precursors; – – – – – – unidentified part.

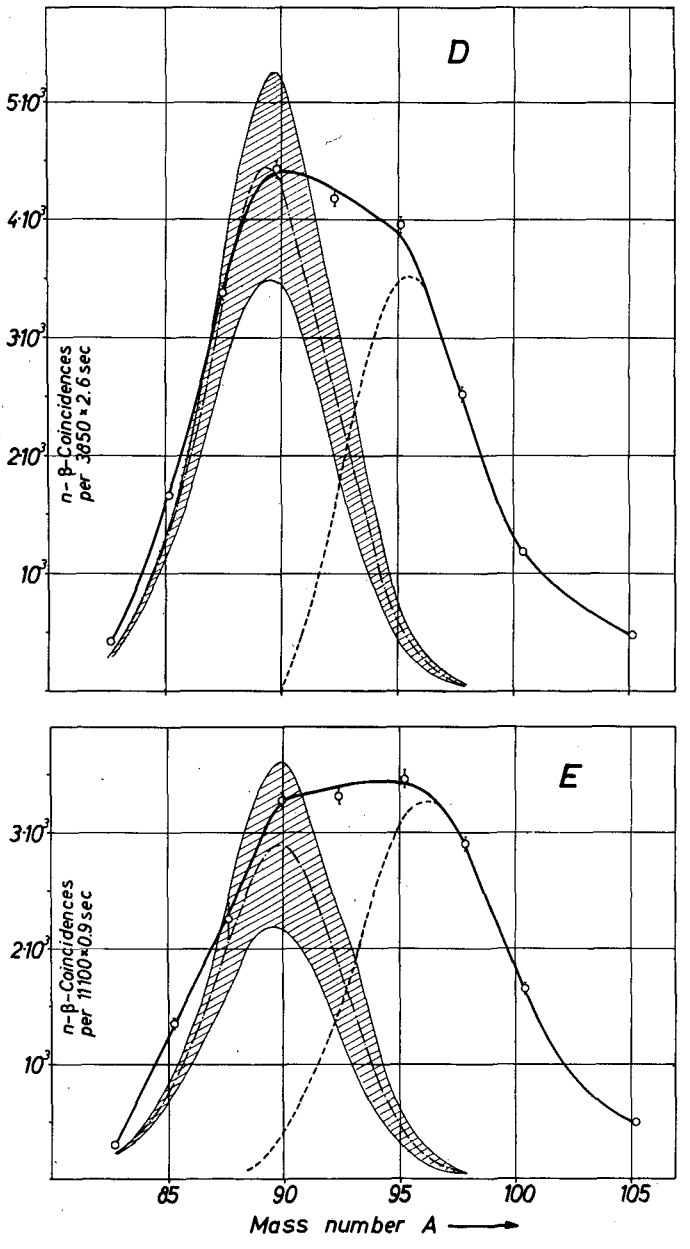
D
5·10³
4·10³
3·10³
2·10³
10³
n-β-Coincidences per 3850±2.6 sec
E
3·10³
2·10³
10³
n-β-Coincidences per 11100±0.9 sec
85
90
95
100
105
Mass number A

TABLE II. UNIDENTIFIED PERCENTAGE OF DELAYED NEUTRON ACTIVITY FOR THE DECAY MEASUREMENTS A TO E IN THE LIGHT FISSION PRODUCT GROUP

Measurement	A	B	C	D	E
Number of irradiation counting cycles	72	222	625	3850	11 100
Irradiation time (sec)	152	52.8	18.8	3.42	1.23
Counting time after end of irradiation (sec)	11.2 to 151.2	5.2 to 50.2	2.3 to 18.3	0.48 to 3.08	0.19 to 1.09
Favoured half-life (sec)	90	30	10	2.1	0.8
Unidentified part (%)	5	10	25	45	60

TABLE III. IDENTIFIED DELAYED NEUTRON PRECURSORS, USED FOR COMPARISON WITH THE EXPERIMENTAL DATA

Precursor	$T_{\frac{1}{2}}$ (sec)	P_n (10^{-2})	Y_n (10^{-2})	$P_n \cdot Y_n$ (10^{-4})	Relative yield [1]	$P_n \cdot Y_n$ [15] (10^{-4})	$P_n \cdot Y_n$ (10^{-4})	$\overline{P_n \cdot Y_n}$ (10^{-4})
As-85	2.2 [3,4]	11 ± 3 [4]	0.54 [4]	5.9 + 1.6 4.8+1.2 [3]				5.5 ± 1.0
Br-87	54.5 [1]	3.1 + 6 [2]	2.37 [14]	7.3 + 1.4	0.37 ± 0.08	5.8	5.8 ± 1.3	6.5 ± 1.0
Br-88	16 [1]	6 ± 1.6 [2]	2.98 [14]	17.9 ± 4.8	1.00		15.7 ± 3.1	17.0 ± 3.0
Br-89	4.5 [1]	7 ± 2 [2]	2.63 [14]	18.4 ± 5.2	1.9 ± 0.4		29.8 ± 6.3	24.0 ± 4.0
Br-90	1.6 [1]				1.5 ± 0.6		23.7 ± 9.5	23.5 ± 9.5

2. The contribution of the unknown emitters amounts to about 50% of the total delayed neutron activity in the light fission product group.
3. The unidentified emitters are mostly short-lived, their contribution increases with decreasing half-life. Half-lives of less than 0.1 sec do not contribute importantly to the delayed neutron activity.
4. For all times investigated the centre of gravity of masses of the unidentified delayed neutron activity is near A = 96. With decreasing half-lives the mean mass of the total delayed neutron activity in the light fission product group shifts to higher mass values. The main contribution to the unidentified activity will be found in the mass region A > 92, in agreement with a prediction of Hermann et al. [17].

Further identification of the emitters seems possible if the decay characteristics for the different cycle times (Fig. 8) and the resolving of the measured curves with the mass separator are included in the analysis. If each neutron emitter is characterized by a well-defined neutron energy and if these energies are separated by about 10% for different emitters, then the time-of-flight technique will be a promising additional tool in identification procedures. The measurements will be extended to the heavy fission product group.

REFERENCES

[1] PERLOW, G.J., STEHNEY, A.E., Phys. Rev. 113 (1959) 1269.
[2] ARON, P.M., KOSTOCHKIN, O.I., PETRZHAK, K.A., SHAPKOV, V.I., Atomn. Energ. 16 (1964) 368.
[3] TOMLINSON, L., J. inorg. nucl. Chem. 28 (1966) 287.
[4] Del MARMOL, P., NEVE DE MEVERGNIES, M., J. inorg. nucl. Chem. 29 (1967) 273.
[5] COHEN, B.L., FULMER, C.B., Nucl. Phys. 6 (1958) 547.
[6] ARMBRUSTER, P., Nukleonik 3 (1961) 188.
[7] ARMBRUSTER, P., EIDENS, J., ROECKL, E., in Why and How Should We Investigate Nuclides Far Off the Stability Line? (Proc. Symp. Lysekil, Aug.1966), proceedings to be published in Ark. Fys.
[8] BOHR, N., Mat. Fys. Medd. Dan. Vid. Selsk. 18 8 (1948).
[9] FULMER, C.B., COHEN, B.L., Phys. Rev. 109 (1958) 94.
[10] ALZMANN, G., Nukleonik 3 (1961) 7.
[11] ARMBRUSTER, P., MEISTER, H., Z. Phys. 170 (1962) 274.
[12] HOVESTADT, D., ARMBRUSTER, P., Nukleonik (in press, 1967).
[13] BATCHELOR, R., HYDER, McK. H.R., J. nucl. Energy 3 (1956) 7.
[14] AMIEL, S., Physics and Chemistry of Fission (Proc. Symp. Salzburg, 1965) 2, IAEA, Vienna (1965) 171.
[15] KEEPIN, G.R., Ch.4, Physcis of Nuclear Kinetics, Addison-Wesley (1965).
[16] WILLIAMS, E.T., CORYELL, C.D., Nucl. Applic., 2 (1966) 256.
[17] HERMANN, G., et al., Physics and Chemistry of Fission (Proc. Symp. Salzburg, 1965) 2, IAEA, Vienna (1965) 197.

PRELIMINARY STUDIES OF DELAYED NEUTRON EMISSION FROM SEPARATED ISOTOPES OF GASEOUS FISSION PRODUCTS

G.M. DAY, A.B. TUCKER AND W.L. TALBERT, Jr.
IOWA STATE UNIVERSITY
OF SCIENCE AND TECHNOLOGY,
AMES, IOWA, UNITED STATES OF AMERICA

Abstract

PRELIMINARY STUDIES OF DELAYED NEUTRON EMISSION FROM SEPARATED ISOTOPES OF GASEOUS FISSION PRODUCTS. An on-line isotope separator system is described that was designed for use in studies of short-lived activities produced at a reactor. A detailed description is presented for the use of this system in the study of radioactive decay and delayed neutron emission for gaseous fission products formed in fission of uranium-235. Experiences with sample configuration and characteristic limitations of the system (such as half-life) are discussed. Preliminary results are presented regarding the assignment of delayed neutron precursors to mass number (by neutron counting) and element (by half-life determination). At present, definite assignments have been made for ^{91}Kr, ^{92}Kr, ^{93}Rb, and ^{93}Kr. Indications of delayed neutron emission for masses 141 and 142 are discussed. Future plans for delayed neutron studies are discussed and nuclear structure studies in progress are outlined.

1. INTRODUCTION

A system designed to study short-lived activities produced at the Ames Laboratory Research Reactor became operational in November, 1966. Preliminary descriptions of the system have been reported [1, 2]. The system incorporates an isotope separator operated on-line to the reactor and provides isotopically pure samples for decay studies using detectors appropriate to the radiation of interest. The entire system is called "TRISTAN".

Figure 1 shows the layout of TRISTAN, in which the component parts are indicated. In its present configuration, TRISTAN is set up to analyse gaseous fission products formed in the fission of ^{235}U; in principle, modifications to the sample chamber and transport line leading to the ion source of the isotope separator would enable the study of non-gaseous activities produced either by fission or by neutron capture at the sample.

Krypton and xenon fission products are transported to the separator ion source by molecular flow through a line of 1.27 cm diameter and approximately 5.5 m long. For molecular flow conditions, the transit time through the line is distributed, with a most probable value of about 10 sec for krypton; however, a significant portion of the gas produced at the sample experiences a shorter transit. Evidence of the shorter transit stems from the observation of ^{93}Kr and ^{142}Xe as provided by the separator (both have half-lives less than 2 sec). The transport line is brought out of the reactor through a horizontal beam tube plug. Figure 2 shows the plug before insertion into the reactor, with the sample chamber at the left end of the plug.

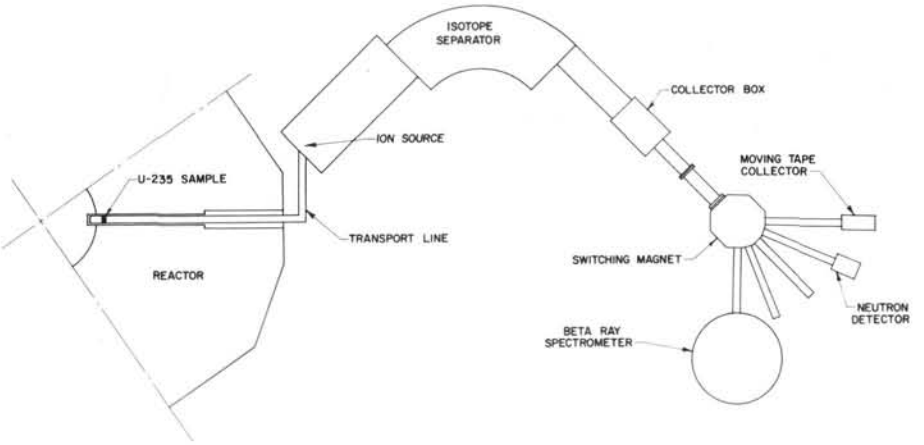

FIG. 1. Layout of TRISTAN on-line isotope separator system.

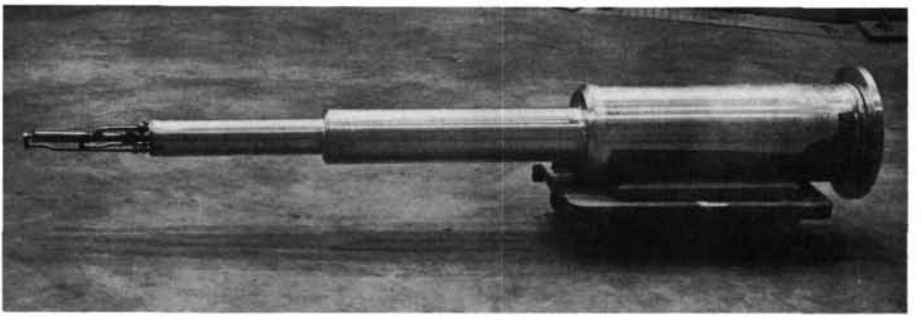

FIG. 2. Reactor beam tube plug prior to insertion.

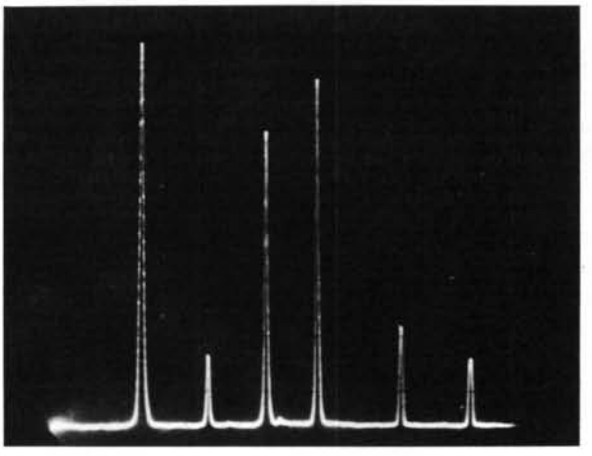

FIG. 3. Xenon spectrum scan at 250 μA.

Since the transport line out of the reactor is held at ground potential and the ion source operates at about 60 kV, an insulator has been developed which allows the voltage gradient to be impressed on the transport line and at the same time suppresses gaseous electrical discharge. With this insulator, it is possible to operate the system with transport line pressures encountered for molecular flow in the transport line (of the order of 10 μmHg).

The isotope separator is of the standard Scandinavian design, with an analysing stage of a 90° sector magnet. It has exhibited excellent resolution for currents up to 250 μA, as illustrated in Fig. 3.

At the collector plane of the separator, a plate with a slit in it allows the mass of interest to proceed into the switching magnet system while collecting all neighbouring masses. The switch magnet then steers the selected ion beam to the proper experimental arrangement, providing not only the benefit of separation of the activity of interest from interfering neighbours (which are left behind), but also enhancing the separation by further discrimination of contaminants in the selected ion beam. Furthermore, it is possible to provide a refocused beam at the collector station either by sector magnetic field focusing for 45° deflection or by crossed electric and magnetic field sector focusing at the 0° and 22.5° ports. At present, the crossed-field focusing is still under study to improve the quality of focus, but it is suitable for the neutron studies, which do not require an exact reformation of the beam image.

At the collector, then, TRISTAN provides a continuous current of a selected activity which replenishes decaying activity previously deposited under a steady-state condition. Three distinct experimental arrangements have been set up to collect activities: a high-resolution beta-ray spectrometer, a neutron counting facility, and a moving tape collector. The neutron counting facility utilizes a simple collecting plate upon which the ion beam is deposited and which is viewed by a long-counter arrangement or by a ^{3}He detector. With this collector studies on delayed neutron emission have been carried out, to be described below.

The moving tape collector employs a Kapton-base tape with a deposited conducting layer which can be driven at variable speeds or stepped. At the point of deposit, two detectors can view the activity while two more detectors are located in positions to view the tape at different times after deposit. The detectors view the tape-deposited activity through lead collimators to enhance the discrimination of activities when the tape is moved. Figure 4 shows a view of the tape collector with one side panel removed. The ion beam enters the collector from the right of the picture and embeds in the tape near the right edge of the collector box. The tape moves clockwise around the periphery of the box from the supply reel to the take-up reel. The tape motion is governed by use of a stepping motor which can be commanded to move the tape continuously with variable speed or in steps of selected tape length. At present, gamma-ray detectors (NaI(Tl) or Ge(Li)) can be used at all viewing ports, and one of the ports viewing the point of deposit can be made to accommodate a beta-ray counter (plastic scintillator or Si(Li) detector).

Use of the moving tape collector allows the experimenter to carry out successive multiscaling measurements without building up long-lived activities (the tape is stepped for such measurements) or to enhance the observation of parent decays (at the point of deposit) or daughter decays

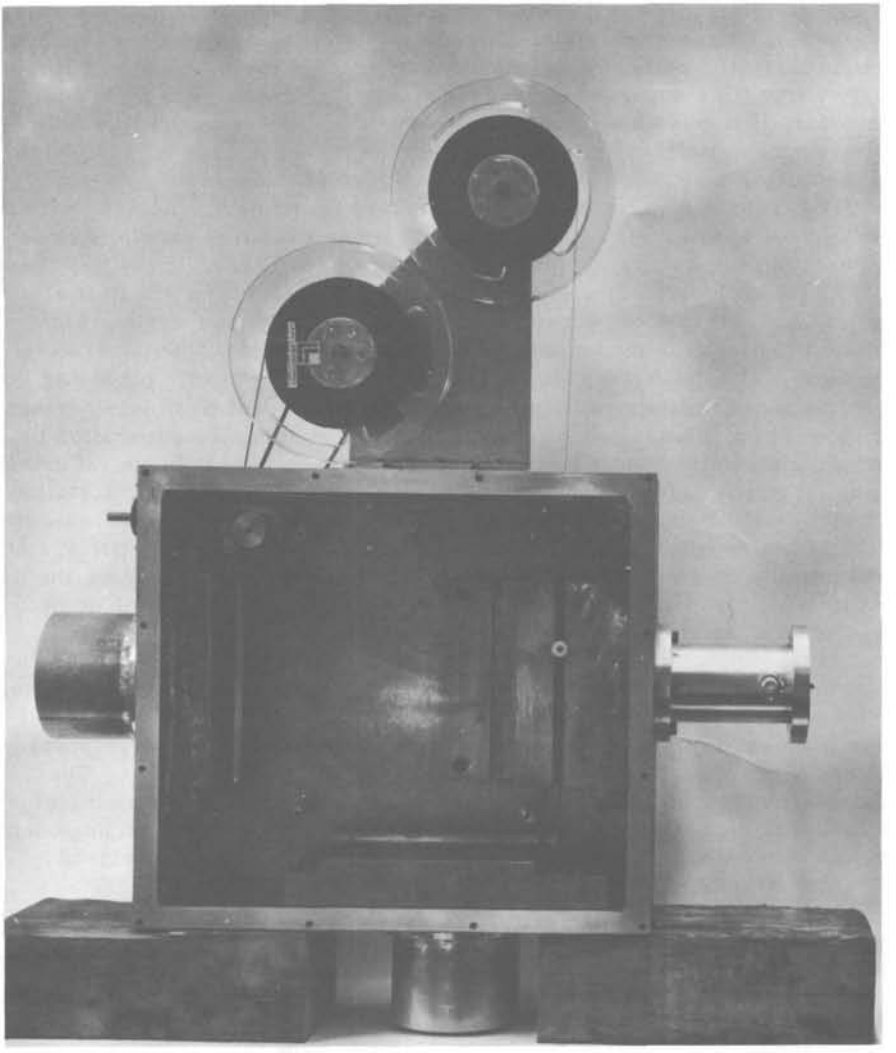

FIG. 4. View of moving tape collector.

(downstream) by moving the tape continuously. The moving tape collector is located at a 45° port of the switching magnet because of the rather rigid focusing requirements for depositing the entire activity on the 6 mm wide tape.

In terms of the studies of the activities made available by TRISTAN, it is important to realize that, in the present system, the activity deposited at the collector is that of a gaseous fission product. Thus, the isobaric decay chain resulting from the deposited activity has a definitely known starting point, krypton or xenon.

2. FISSION PRODUCT SAMPLE

The form of ^{235}U used in the sample has been changed to investigate, empirically, the optimum form for emanation of gaseous fission products in the high radiation level environment existing near the core of the reactor. Initially, the sample was made up of a mixture of UO_2 powder and powdered graphite, with sufficient graphite used to immerse each UO_2 grain in an environment of carbon. It was felt that, for the temperatures encountered in the sample, gaseous fission products which recoil into the graphite would diffuse readily out of the sample and proceed into transit to the isotope separator with a minimum of delay. Two other samples were prepared in the same manner, and it was found that the activity available from samples with this form diminished with a period of several hours but that the activity would be returned to essentially the starting level by simply removing the sample from the high neutron flux and allowing it to cool. The explanation for this behaviour is not yet clear.

Following the suggestions of Patzelt and Herrmann [3], another sample was prepared in which uranyl ions were deposited on a substrate of hydrous zirconium oxide. This form of sample possesses good emanation properties for gaseous fission products, when used at low flux levels. This sample was found to be a prolific source of fission product activity; however, it was temperature sensitive and was difficult to tolerate in the vacuum system. The most unsuitable feature of this sample was its effect on the operation of the ion source; it became necessary to clean out the exit hole of the ion source regularly due to a deposit which would build up after only a few hours of operation. This deposit was found throughout the interior of the discharge chamber and was exceedingly radioactive. The vacuum and ion source difficulties did not appear for any other form of sample used.

The third form of sample which has been used is a pure UO_2 powder sample. Preliminarily, no advantage is apparent in the use of the other forms of sample over this one. Furthermore, the decrease of activity apparent with a UO_2-C mixture has not appeared to be as pronounced with a pure UO_2 sample, and the transport line achieves suitable vacuum in a significantly shorter time with the simpler form. It appears as though future studies with gaseous fission products using the TRISTAN system are most easily approached using this form of sample.

The present sample being used consists of 80 mg of ^{235}U in the form of UO_2 and is contained in a stainless steel chamber, capped with a sintered stainless steel disc with pore size of about 5 μm. The stainless steel chamber is pushed against a water-cooled seat when the system is in operation; when not in operation, the sample can be withdrawn to about one metre from the high neutron flux. The temperature of the outer stainless surface is measured to be about 600°C when in operation. With this sample, the transport line leading to the isotope separator ion source exhibits a radiation level of about 2 R/h; hence, a lead wall surrounds the entire source region of the separator. Similar radiation levels are experienced at the focal plane of the isotope separator, and shielding has been installed at this region as well.

Plans for the future use of TRISTAN include continuing studies on the decays of gaseous fission products and daughters, adaptation of the sample

chamber and transport line to include non-gaseous activities, and, in collaboration with A. F. Stehney of the Argonne National Laboratory, development of a sample and transport system for the study of halogen fission products. It is anticipated that the halogen system will be in operation by late 1967.

3. EXPERIMENTAL STUDIES

Studies on the gamma-ray spectra of gaseous fission products (^{139}Xe to ^{142}Xe and ^{90}Kr to ^{93}Kr) and their daughters are in progress. Due to the complexity of the spectra, decay scheme determinations will require more study. No work has been done on the beta-ray spectra at all. The only significant results obtained thus far are those in which delayed neutron emission has been studied.

In the study of delayed neutron emitters among the gaseous fission products, four basic experiments have been performed using separated isotopes: neutron counting and multiscaling, neutron spectra measurements, collection of mass number A on a plate with subsequent gamma-ray counting of longer-lived activities to determine the presence of (A-1) activities, and determination of half-lives by gamma-ray spectrum multiscaling and beta-ray multiscaling to confirm the neutron multiscaling results.

The collection plate for the neutron counting experiments is simply a copper-clad segment of a glass epoxy printed circuit board. The ion beam, which is focused to an area of about 25 mm by 10 mm, is collected and the beam current (of the order of nA) monitored to maximize the deposit of activity. Most of the beam current is presumed to be due to some natural stable contaminant in the separator system, and it is generally found that maximum beam current yields maximum neutron activity. A count rate meter is also monitored to give an independent indication of activity. Neutrons from the activity being collected are detected by five BF_3-filled proportional counters embedded in a block of paraffin which surrounds the collection plate. Shielding from room neutrons is accomplished by a 5 cm layer of boron-loaded paraffin on all sides of the detector array, plus cadmium and boron-loaded paraffin bricks where needed. Room background is within acceptable limits (about $\frac{1}{2}$ count/sec) but has been sensitive to the operation of other experiments in the room involving neutron diffraction. For this reason, low counting rate experiments have been performed with the neutron diffractometer experiments shut down. Simple scaling of neutrons has been used to indicate the presence, if any, of neutron emitters in all of the mass numbers available.

The same experimental arrangement has been used for the multiscaling of neutrons in order to identify the half-life of the neutron precursor. In multiscaling, the ion beam is deflected during the counting period and is deposited in the collector box of the isotope separator, far removed from the neutron counters and shielded from them by the massive switch magnet. Multiscaling and deflection are controlled by an automatic cycling device. During the beam-on phase of the cycle, the short-lived krypton and rubidium activities come to equilibrium; during the beam-off phase, the decay of the neutron activity is observed in a multichannel analyser operated in the multiscaling mode and using the output of the detector array.

Neutron spectra have been recorded for the high-yield neutron activities. A ^{3}He spectrometer was used, and the spectra obtained analysed for neutron groups. This measurement was taken at the same time a sample was collected for gamma-ray measurements of activity from mass (A-1). After a long collection of a particular mass number (to yield a reasonable gamma-ray counting rate for longer-lived activities in the decay chains), the collection plate was removed and counted periodically with a Ge(Li) spectrometer. Gamma-ray peaks characteristic of the longer-lived activities of the mass A decay chain and the mass (A-1) decay chain were followed as a function of time to verify neutron emission. The relative counting rates can be converted to neutron emission branching ratio. This technique is not easily applied to some mass numbers; it is planned to use the moving tape collector to study cases where suitable long-lived activities are not present.

As a check on the assignment of delayed neutron precursors by half-life, the moving tape collector has been used to determine half-lives by following the decay of emitted gamma-rays and by multiscaling the integrated beta-ray spectrum. In the cases where delayed neutron precursor assignments have been made, the neutron half-life has been verified by these independent measurements. Final analysis of the data obtained has not been completed.

4. RESULTS

The results which can be reported at this time are as follows: Delayed neutron precursors have been identified for the krypton isotopes ^{91}Kr, ^{92}Kr, and ^{93}Kr. ^{93}Rb has also been seen to be a delayed neutron precursor, verifying the results of Amarel et al. [4]. Figures 5 and 6 show neutron multiscaling plots for mass numbers 92 and 93. It is clear from Fig. 5 that the neutron activity at mass 92 is from the decay of Kr; the measured half-life of 2.0 ± 0.1 sec is in agreement with the ^{92}Kr half-life of 1.92 ± 0.07 sec reported by Patzelt and Herrmann [5]. The half-life reported by Amarel et al. [4] for ^{92}Rb of 4.43 ± 0.05 sec is sufficiently different from that for krypton to eliminate the possibility of neutron emission from ^{92}Rb. The assignments with respect to rubidium isotopes agree with the data reported by the Orsay group [4].

In Fig. 6, the solid curve is the sum of the two dashed curves which represent contributions from ^{93}Kr and ^{93}Rb individually. The longer-lived component has a half-life of 5.63 ± 0.05 sec, which lies between the 5.1 ± 0.3 sec value published by Wahl et al. [6] and the value of 5.89 ± 0.04 sec reported by Amarel et al. [4] for ^{93}Rb. Hence, this component is assigned to the decay of ^{93}Rb. The shorter-lived component was analysed using the half-life value of 1.17 ± 0.04 sec given by Patzelt and Herrmann [5]. It is to be noted that if both the krypton and rubidium activities are delayed neutron precursors, the decay curve obtained by multiscaling is not a simple combination of exponential decays, due to the build up of daughter activity during the first portion of the time interval.

Similar neutron multiscaling studies have been made for the decays of mass number 91, with the definite indication of a component with 8 sec half-life. Due to the small neutron yield for this activity, it was not possible to get a precise value of neutron half-life. No indication of a 7.2 sec

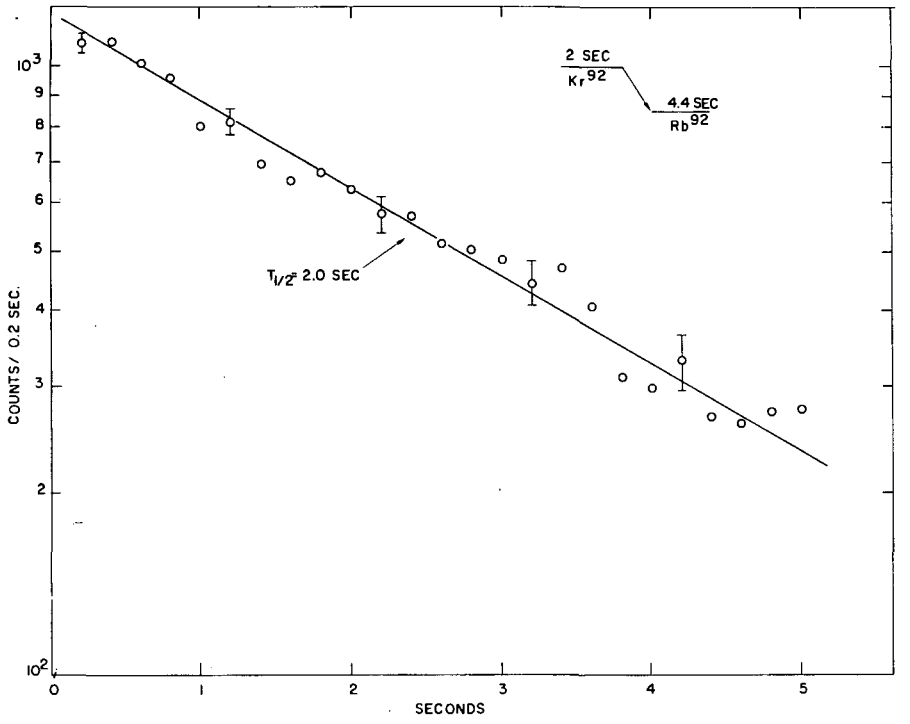

FIG. 5. Neutron multiscaling for mass 92.

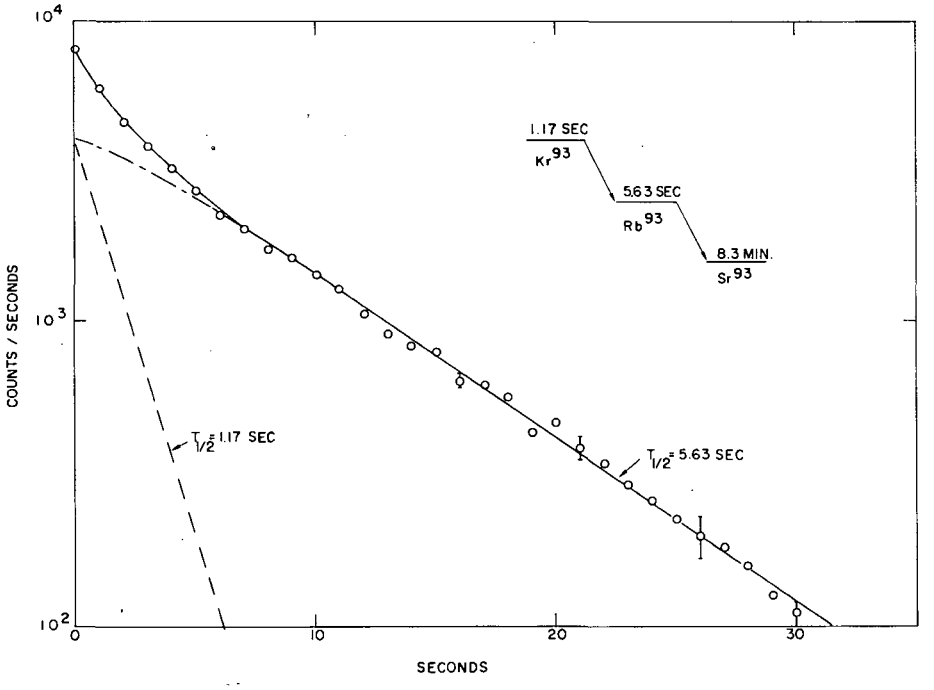

FIG. 6. Neutron multiscaling for mass 93.

activity was observed so the neutron activity found at mass 91 has been assigned to the decay of ^{91}Kr.

Neutron emission has been verified by studying the residual gamma activity on the beam collector plates. After long periods of collection, the plates were removed and gamma-ray activities of long-lived daughters observed with a Ge(Li) detector to identify decays of neughbouring mass chains. Figure 7 shows the gamma-ray spectrum of a mass 93 collector plate, observed at two times after removal from the switch magnet port. The 0.27 MeV and 0.94 MeV lines appear in the decay of 10 h ^{93}Y and can be compared to the 1.38 MeV and 0.23 MeV lines from 2.7 h ^{92}Sr. The presence of the ^{92}Sr lines confirms neutron emission in the decay chain of mass 93. For the collection of mass 92, the 1.03 MeV gamma ray from 9.7 h ^{91}Sr was used to confirm neutron emission in the decay chain of mass 92. Similarly, observation of the gamma-ray activities from the collector plate for mass 91 confirms the neutron scaling data.

Neutron scaling at masses 141 and 142 indicated weak neutron emission in the decay chains of these masses. The neutron precursor at mass 141 is tentatively assigned to ^{141}Xe, subject to verification by neutron multiscaling, since ^{141}Cs has been reported not to be a neutron precursor [4]. The weak neutron emission indicated for mass 142 is in agreement with the results of the Orsay group [4], in which ^{142}Cs appeared to be a delayed neutron precursor. Thus, a tentative assignment to ^{142}Cs can be made subject to verification by neutron multiscaling. ^{142}Xe should not be ruled out as a neutron precursor until multiscaling data have been analysed.

As a check of cross-contamination in the separated isotope beams, a collector plate for mass 88 was analysed for gamma-ray activity from the mass 87 decay chain; none was observed. This last check served also to verify that halogen activities are excluded from introduction into the separator.

Neutron spectra are difficult to obtain with the low-efficiency counter used, combined with the low neutron yield of most of the activities under study. For the neutron activity present in the decay of mass 93, peaks

TABLE I. DELAYED NEUTRON PRECURSORS IN THE DECAYS OF GASEOUS FISSION PRODUCTS

Mass number	Neutron multiscaling half-life (sec)	Delayed neutron precursor assignment
91	8	^{91}Kr
92	2.0 ± 0.1	^{92}Kr
93	5.63 ± 0.05	^{93}Rb
	1.17 (see Ref.[5])	^{93}Kr
141	-	Probably ^{141}Xe
142	-	^{142}Cs, and possibly ^{142}Xe

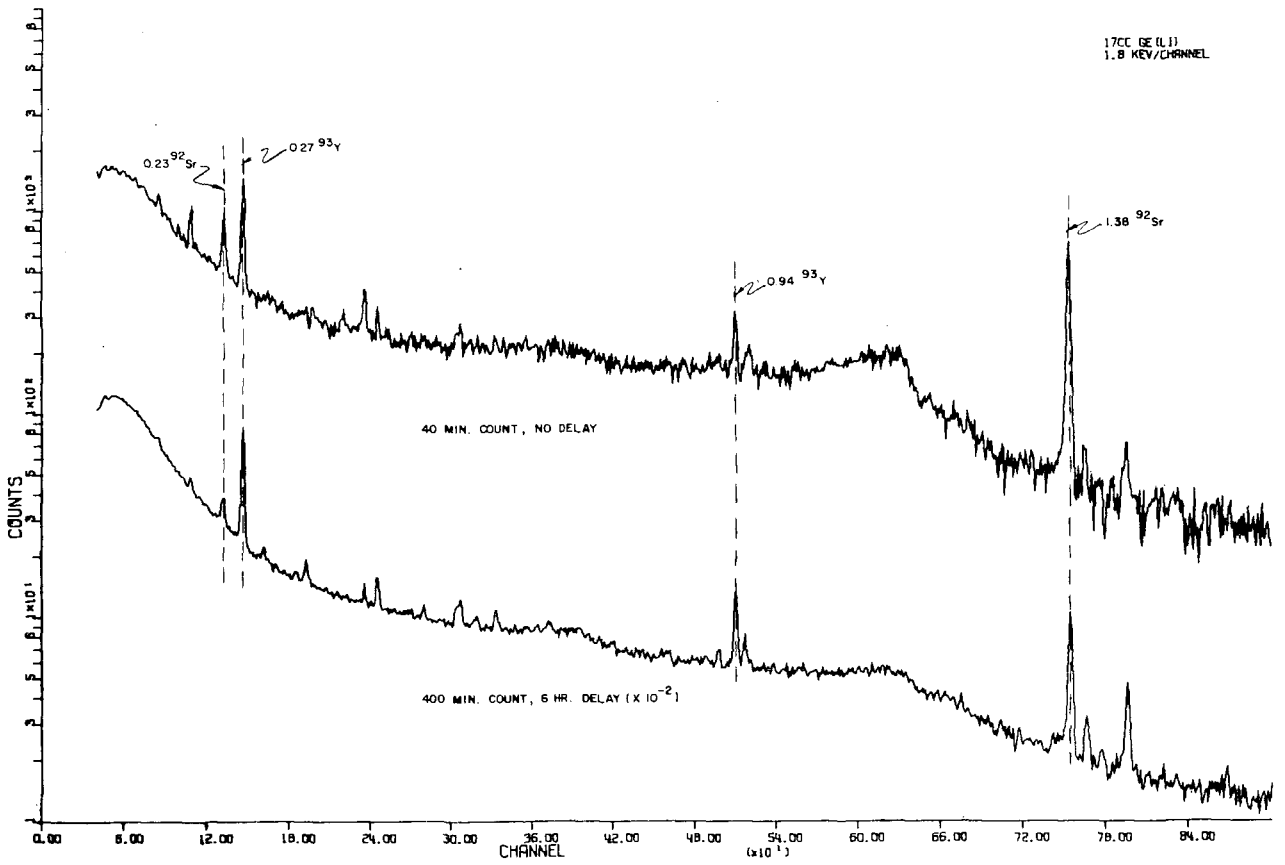

FIG. 7. Long-lived gamma-ray spectra for mass 93 collection.

were observed in the neutron spectrum at energies of 80 keV and 300 keV, with no indication of neutrons at higher energies. These measurements are rather marginal with the low yields of other mass numbers and will be made where feasible.

Table I summarizes the results obtained to date in these studies. At this point, there will be no discussion of the results compared to theoretical implications, except that it is to be noted that neutron activities have not been previously predicted for the decays of ^{91}Kr and ^{92}Kr [7, 8].

ACKNOWLEDGEMENTS

The authors would like to thank the following people for their contributions to this work: J. Cook and K. Malaby for their assistance in the preparation of samples of ^{235}U in the various forms and configurations; R. Struss and R. Michaud for their efforts in the design of the sample and collector systems; and especially J. McConnell and J. Eitter for the long hours spent in operation of TRISTAN during the accumulation of data.

REFERENCES

[1] THOMAS, D., TALBERT, W.L., Jr., Nucl. Instr. Methods 38 (1965) 306.
[2] McCONNELL, J.R., TALBERT, W.L., Jr., Ark. Fys. (in press).
[3] PATZELT, P., HERRMANN, G., private communication.
[4] AMAREL, I., BERNAS, R., FOUCHER, R., JASTRZEBSKI, J., JOHNSON, A., TEILLAC, J., GAUVIN, H., unidentified preprint, private communication from BERNAS, R.
[5] PATZELT, P., HERRMANN, G., Physics and Chemistry of Fission, Vol. II, p. 243, IAEA, Vienna, 1965.
[6] WAHL, A.C., FERGUSON, R.L., NETHAWAY, D.R., TROUTNER, D.E., WOLFSBERG, Z.K., Phys. Rev. 126 (1962) 112.
[7] PAPPAS, A.C., Int. Conf. Peaceful Uses of Atomic Energy 15 (1958) 373.
[8] KEEPIN, G.R., J. nucl. Energy 7 (1958) 13.

A PROGRAMME FOR A SYSTEMATIC EXPERIMENTAL STUDY OF DELAYED NEUTRON EMISSION IN FISSION

S. AMIEL, J. GILAT, A. NOTEA AND E. YELLIN
SOREQ NUCLEAR RESEARCH CENTRE,
YAVNE, ISRAEL

Abstract

A PROGRAMME FOR A SYSTEMATIC EXPERIMENTAL STUDY OF DELAYED NEUTRON EMISSION IN FISSION. The programme of the Soreq-On-Line Isotope Separator (SOLIS) aimed at the study of very short-lived nuclides produced in thermal and 14 MeV neutron-induced fission is outlined. The use of appropriate chemical separation methods in conjunction with the isotopic separation facilitates the observation, at steady state conditions, of individual rapidly decaying nuclides. This system will be used for a systematic investigation of delayed neutron emission, viz. identification and characterization of precursors followed by a detailed study of nuclear structure and independent yields. At present, techniques for the rapid separation of rare gas and halogen fission products, suitable for on-line isotopic separation, are being developed. For rare gas studies, a uranium-barium stearate emanation source swept by a stream of nitrogen gas is being used. The decontamination factor with respect to halogen is $\approx 10^5$, and higher for other activities. Separation time of ~2 seconds is routine. With this system (without isotopic separation), it was possible to establish delayed neutron emission from both ^{93}Kr ($T_{\frac{1}{2}}$ = 1.19 t 0.05 sec, P_n = 3.9%) and ^{93}Rb ($T_{\frac{1}{2}}$ = 5.60 ± 0.05 sec, P_n = 2.6%). The half-life of ^{94}Kr is estimated as 0.4 ± 0.1 sec. For bromine and iodine, selective recoil labelling is used (for extraction of independently produced species while the same nuclides produced by beta decay are discriminated against) followed by fast gas chromatography. Using empirical P_n-values and fission yields for 14 known precursors, good fits to experimental total delayed neutron yields of groups 1-4 were obtained for a series of fission reactions. Systematic deviations indicate unidentified precursors. The inconsistencies between expected and reported results on delayed neutron yield variations with the energy of the fission-inducing neutrons are being checked by high resolution γ-ray spectrometry in conjunction with neutron counting, with the aim of determining these relations with neutrons of various energies (thermal, fission and 14 MeV). A technique for obtaining data on the masses and half-lives of delayed neutron precursors, based on selective collection, through a bias potential, of recoils from neutron emission, is being studied. The energies of delayed neutrons from gross and separated elements produced in fission are being studied with an improved ^{3}He spectrometer and time-of-flight techniques.

1. INTRODUCTION

Although delayed neutron emission after fission was observed and interpreted in as early as 1939, the numerous investigations to date have not yielded a clear picture of this subject. Most studies were concerned either with analyses of gross decay properties, such as group half-lives, group abundances and mean group neutron energies, or with radiochemical separations of selected elements, with subsequent neutron counting and resolution of the decay curves into their exponential components. Identification and characterization of the individual delayed neutron precursors, clarification of their nuclear properties and structure, and information on their abundance in fission are still a problem, the solution of which lies in the future. Figure 1 shows the distribution of the known delayed neutron precursors among the fission products.

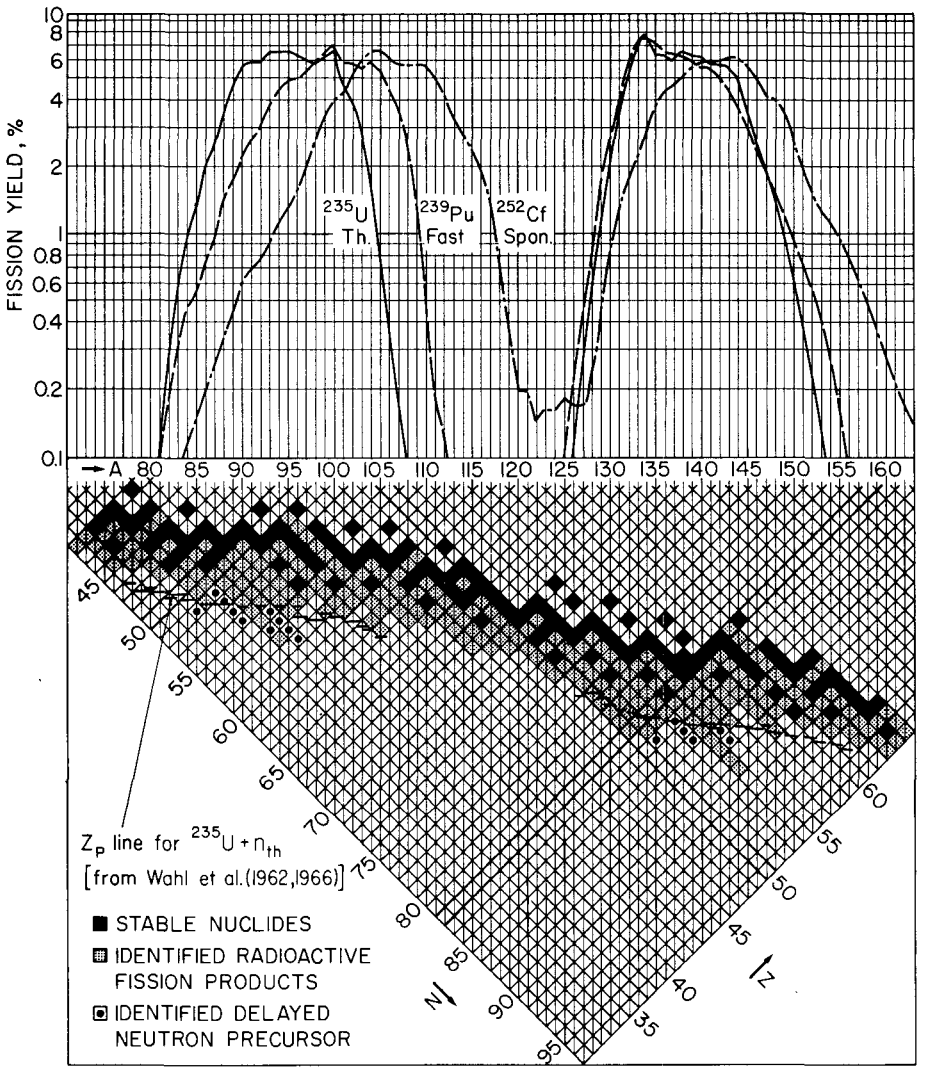

FIG. 1. Delayed neutron precursors among the fission products. Upper: Mass distribution in fission; Lower: Identified delayed neutron precursors among the fission products and most probable charge Z_p in ^{235}U thermal fission.

The state of information on delayed neutrons from fission has recently been reviewed and analysed by Keepin [1], Amiel [2], and Pappas and Tunaal [3]. Several attempts to account for the observed gross delayed neutron decay properties and yields based on a systematic analysis of data from different fission reactions were reported [2, 4-6].

The major difficulty in investigating delayed neutron emission arises from the very short half-lives of the delayed neutron precursors and hence the need to perform the separation and the measurements in extremely

short times. Another difficulty is that chemical separations yield mixtures of isotopes of a selected element and their corresponding decay products, all produced in fission and in the subsequent decay – a composite, for which an analysis into individual species poses a major technical problem when detailed nuclear data are sought.

The introduction of electromagnetic analysis, whether in the form of mass spectrometers [7,8] or mass separators [9] in conjunction ('on-line') with very fast (or 'instantaneous') chemical separation of nuclear reaction products, facilitates the formation of non-decaying sources (at equilibrium), of individually separated, short-lived isotopes.

Such a programme is being carried out at Soreq. This project – SOLIS – is aimed at the setting up of an electromagnetic isotope separator on-line with a fission source at the IRR-1 reactor, with the option of using a 14 MeV neutron generator. The layout is given in Fig. 2 and other details are described elsewhere [10]. This system will be used for various fission studies, among them a systematic investigation of delayed neutron emission, viz. identification and characterization of precursors and measurement of their distributions in various fission reactions. Figure 3 gives an idea of the radioactivities expected from such an experimental assembly.

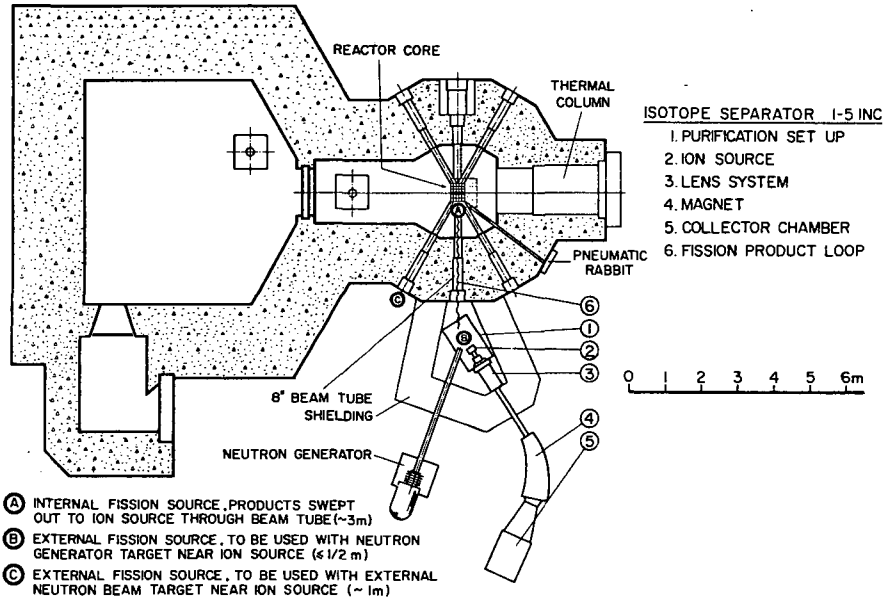

FIG. 2. Schematic layout of the Soreq On-Line Isotope Separator.

2. SEPARATION PROCEDURES

Chemical separations suitable for on-line operation with an electromagnetic isotope separator have to meet several requirements; some of these are listed in Fig. 4. Separation under dynamic conditions, viz. during rapid flow is of major importance.

ESTIMATE OF FISSION PRODUCT ACTIVITIES EXPECTED WITH AN ON-LINE ISOTOPE SEPARATION SYSTEM

$$\left(\frac{dN}{dt}\right)_{coll} = \underbrace{N\phi_n\sigma_f}_{fiss/sec}\,[IFY][EE][CY][IE][T][Y_c][D]$$

N = NUMBER OF FISSIONABLE ATOMS
Ø = NEUTRON FLUX
σ = FISSION CROSS SECTION

10 mg U^{235} AT A THERMAL NEUTRON FLUX OF 10^{13} N/cm²·sec YIELDS ~10^{11} fiss/sec

[IFY]	INDEPENDENT FISSION YIELD	(10^{-5} - 10^{-2})
[EE]	EXTRACTION EFFICIENCY	(0.01 - 1)
[CY]	CHEMICAL YIELD	(0.01 - 1)
[IE]	IONIZATION EFFICIENCY	(0.005 - 0.2)
[T]	TRANSMISSION	(1)
[Yc]	COLLECTION YIELD	(0.5 - 1)
[D]	DECAY LOSSES	(0.1 - 1)

$$\left(\frac{dN}{dt}\right)_{coll} = 10^{11} \times 10^{-5} = 10^{6}\ dps$$

ESTIMATED OVERALL EFFICIENCY FOR AN AVERAGE CASE: ~10^{-5}

FIG. 3. Expected fission product activity yields for an on-line isotope separator.

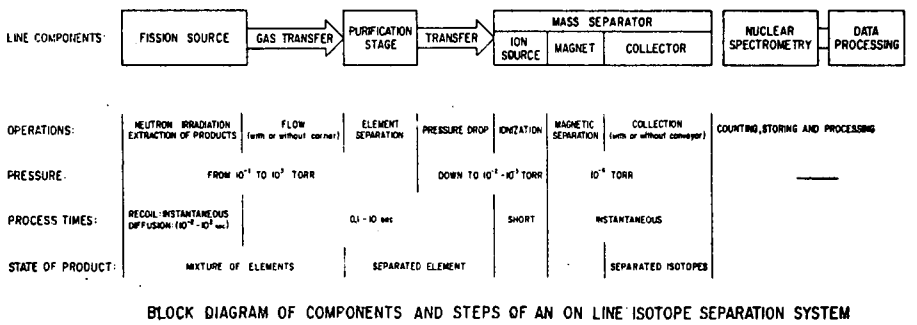

FIG. 4. Flow diagram of an on-line isotope separation system.

Gas flow through long tubes is much faster at atmospheric pressure than at pressures that are below a few centimetres of mercury [11]. Chemical processing and other manipulations are also conveniently performed at atmospheric pressures. Since the ion source of an electromagnetic separator operates only at pressures below 10^{-2} mmHg, one encounters the problem of efficient transfer of the separated species over a pressure drop of several orders of magnitude. One method of solving this problem is aerodynamic separation with differential pumping, a method being studied at present in our laboratory. Other methods may involve intermittent operation of cycles composed of – deposition of activity – carrier removal (evacuation) – evaporation of activity.

These points, as well as outlines of promising procedures were recently reviewed [12-15].

At present two main radiochemical separation techniques are being investigated by our group. The first technique concerns halogens formed in fission and employs selective recoil labelling of primary products in a mixture of methyl-iodide and helium, and the second, rare gas isotopes and their decay products, using an emanation source.

Selective recoil labelling is based on high energy chemical displacement reactions in the gaseous phase, the reaction thresholds being above the kinetic energy available to beta decay products. "Primary" fragments (after the prompt de-excitation processes) cause such a displacement, while "secondaries", essentially the same atoms formed by precursor decay, are discriminated against [16]. The reaction $CH_3I + I^* \rightarrow CH_3I^*$ was studied in detail with fission iodine [17]. It was found that the labelling efficiency for independently produced iodines is high (30-50%), and that under appropriate conditions the isotopic ratio of the iodine represents the primary distributions of iodine isotopes in fission [18]. This method, when coupled with fast gas chromatography, was found to permit isolation, in a very short time, of iodine and bromine. Figure 5 represents a layout of the experimental set-up used with a fission source placed in the thermal column of the IRR-1 [19]. Figure 6 represents a typical separation curve obtained with the system.

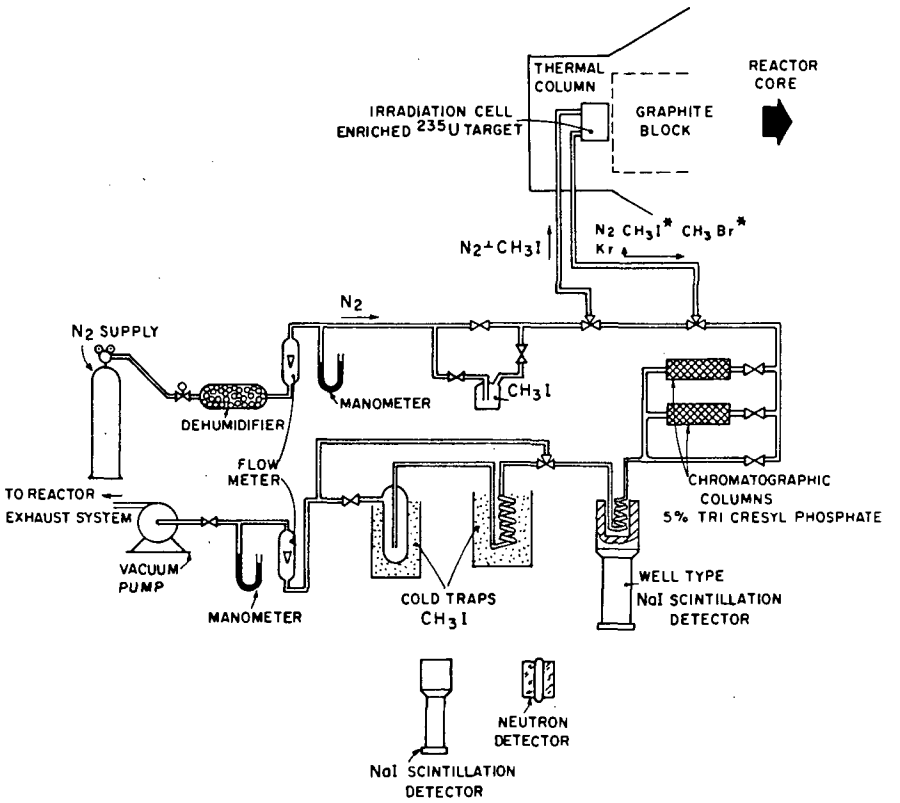

FIG. 5. System for fast separation of bromine and iodine activities by selective recoil labelling.

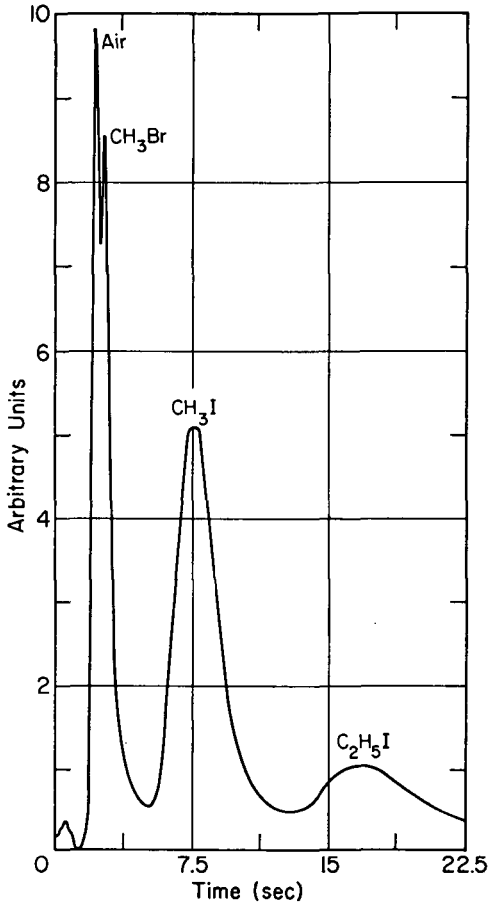

FIG. 6. Chromatographic separation of labelled CH_3Br and CH_3I (5% Tri-cresyl-phosphate column, 1.2 cm i.d., 15 cm long, helium carrier).

In addition to its general use for the study of halogen fission products, in conjunction with an on-line isotope separator, this technique will be used for a thorough investigation of the bromine and iodine delayed neutron precursors. Recently published results [20] on the relative delayed neutron yields from ^{87}Br, ^{88}Br and ^{89}Br do not agree with the widely accepted values of Perlow and Stehney [21]. Since bromine and iodine isotopes contribute a substantial fraction of the total delayed neutrons emitted, exact data on their yields are essential for any systematic analysis of delayed neutron emission.

The system used for the study of short-lived rare gas isotopes and their decay products is shown schematically in Fig. 7. It is essentially similar to the system described in Ref. [11], with the following modifications: (a) The target chamber was modified to fit deeper into the beam tube, in the reactor wall, i.e. into a region of higher flux (up to 2×10^9 n cm^{-2}sec^{-1}). Its design is shown in Fig. 8; (b) The target itself was prepared by coating finely powdered U_3O_8 uniformly with barium stearate.

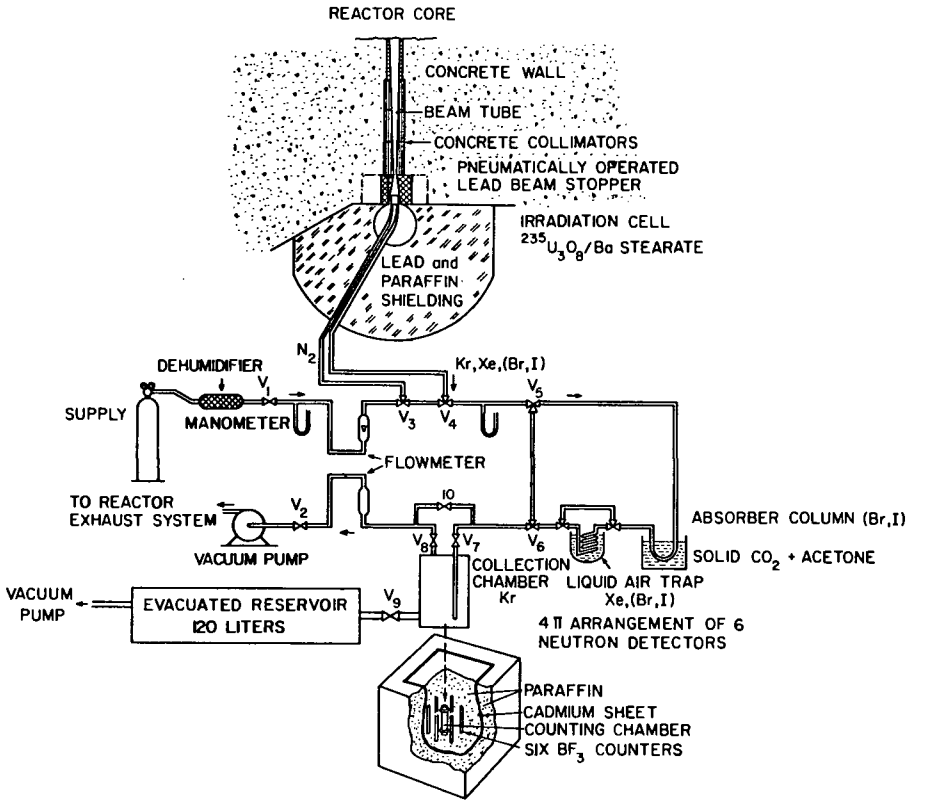

FIG. 7. System for the study of short-lived rare gas delayed neutron precursors.

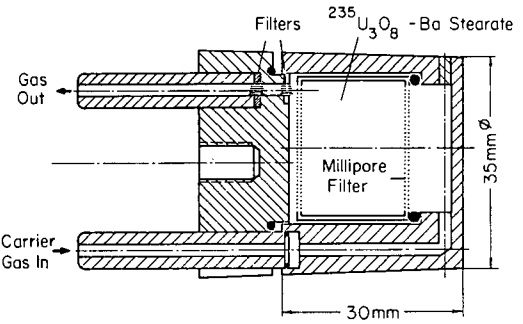

FIG. 8. Emanation target chamber.

This was carried out by evaporating a suspension of 250 mg of U_3O_8 (93% ^{235}U) in a benzene solution of 10 g of barium stearate, with constant stirring. The emanation power of this target did not deteriorate in the course of many hours of irradiation; (c) Good separation of rare gases from halogens was obtained by cooling a tri-cresyl-phosphate (TCP) coated powdered firebrick column to about - 80°C; (d) For rapid evacuation of all gaseous activities in the counting chamber, the latter was connected via a solenoid valve (V_9) to a large (120 litre) reservoir kept continuously under vacuum.

Several schemes for transferring the activity from the target to the counting chamber were tried. For fastest transit, the following sequence was found to give the best results. With valve V_4 closed and V_3 open, 1 to 2 atm pressure of nitrogen was introduced into the target side, while the rest of the system was held under vacuum. Valve V_8 was then closed and the beam stopper opened for a preset time (usually a few seconds), to allow activity to accumulate in the target chamber. Immediately after turning off the beam, valve V_4 was opened, sending a pulse of gas into the counting chamber and, simultaneously, counting was commenced. A number of seconds later the counting chamber was sealed off by closing valve V_7, and the decay of the collected activity was followed. While counting was in progress, fresh nitrogen was blown through the column via the bypass valve V_{10} to remove all absorbed halogen activities. The entire sequence was then repeated, until adequate counting statistics were obtained. Transfer times were 1.5 to 3 seconds, depending on the nitrogen pressure and the nature and size of the purifying devices inserted into the line.

Since the delayed neutron yield from rare gas precursors is, as reported by Stehney and Perlow [22], only a minute fraction of that from halogens, high decontamination factors from the latter are essential. By the same token, delayed neutron measurements provide a very sensitive test of halogen contamination. In our experimental arrangement, initial decontamination of about 50 - 100 is obtained by the preferential emanation of the rare gases from the target. The second stage consists of gas chromatographic separation of halogens from the rare gases by the cooled TCP column. The effect of this column is to delay the flow of halogens with respect to the rare gases. Typical separation patterns are shown in Fig. 9. In this experiment the neutron beam was turned on for 60 seconds to emphasize the long-lived halogen activities. Gas was then transferred into the counting cell as described previously. Curve A shows a delayed neutron decay curve obtained from the barium stearate target, without any further purification. Long-lived activities are evident. Curve B shows a similar decay curve obtained with the TCP column. Here the counting cell was sealed off 10 sec after flow started. Two distinct activity peaks, corresponding to the arrival of krypton (in about 2 sec) and bromine ($\sim$ 8 sec later) are seen. The data of curve C were obtained by introducing another purification stage consisting of a coil of copper tubing cooled to liquid air temperature. The pattern is similar to that of curve B, but the relative amount of bromine is reduced by a factor of about 3. In curve D, the flow was stopped after 3 seconds. Under these conditions only short-lived activities are present, with no detectable traces of 16 sec ^{88}Br or 56 sec ^{87}Br. The decontamination factor between curves A and D can be estimated as $\geq$ 500. The total decontamination factor of the rare gases from bromine fission products is therefore estimated to be $> 5 \times 10^4$. Decontamination from other products, including iodine, is even larger.

This excellent decontamination is due mainly to the delaying effect of the TCP column on the bromine activity. The technique is, therefore, not suitable for continuous flow conditions, i.e. for the production of steady state "non-decaying" sources (highly desirable for detailed decay scheme studies of short-lived nuclides, delayed neutron spectroscopy, etc.). This difficulty may be overcome by connecting a number of columns

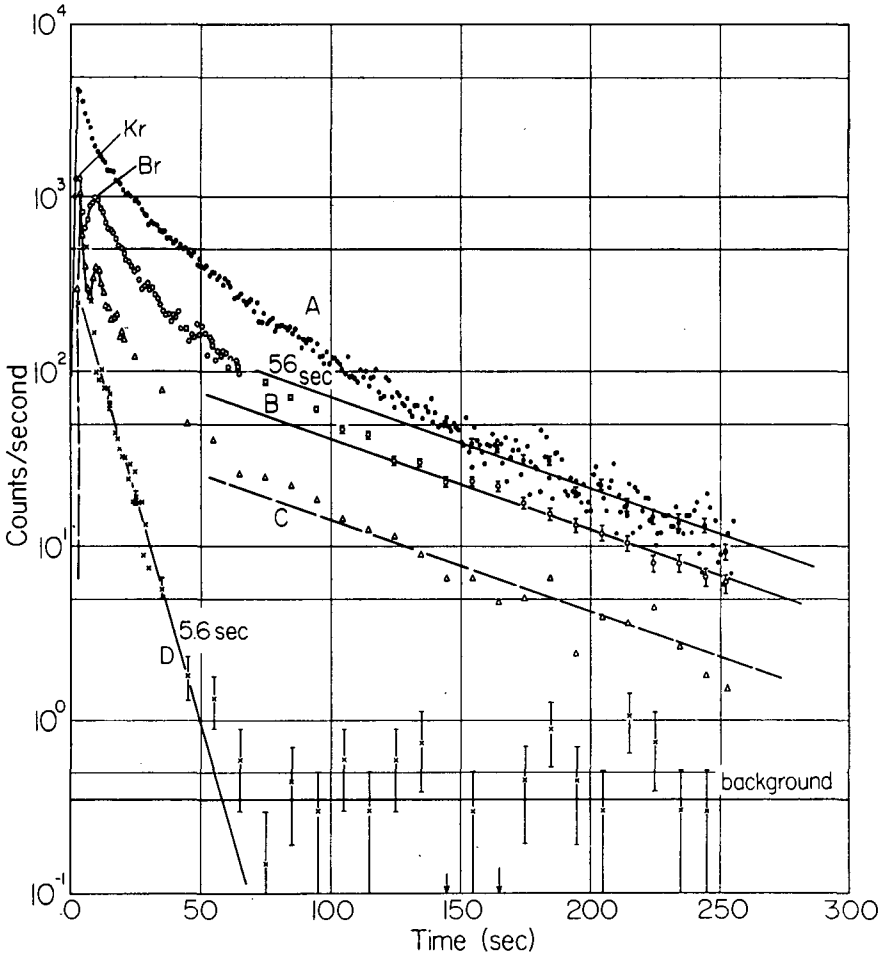

FIG. 9. Separation of krypton and bromine activities.

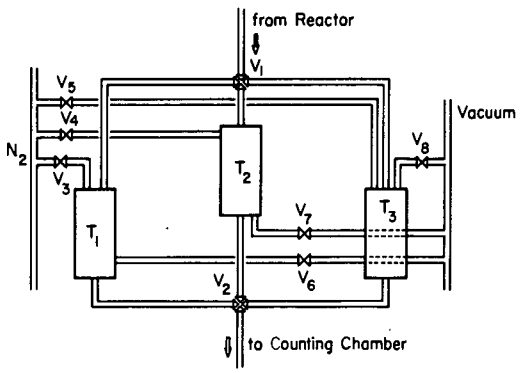

FIG. 10. System for continuous production of non-decaying sources of purified rare gas fission products (Kr - Xe).

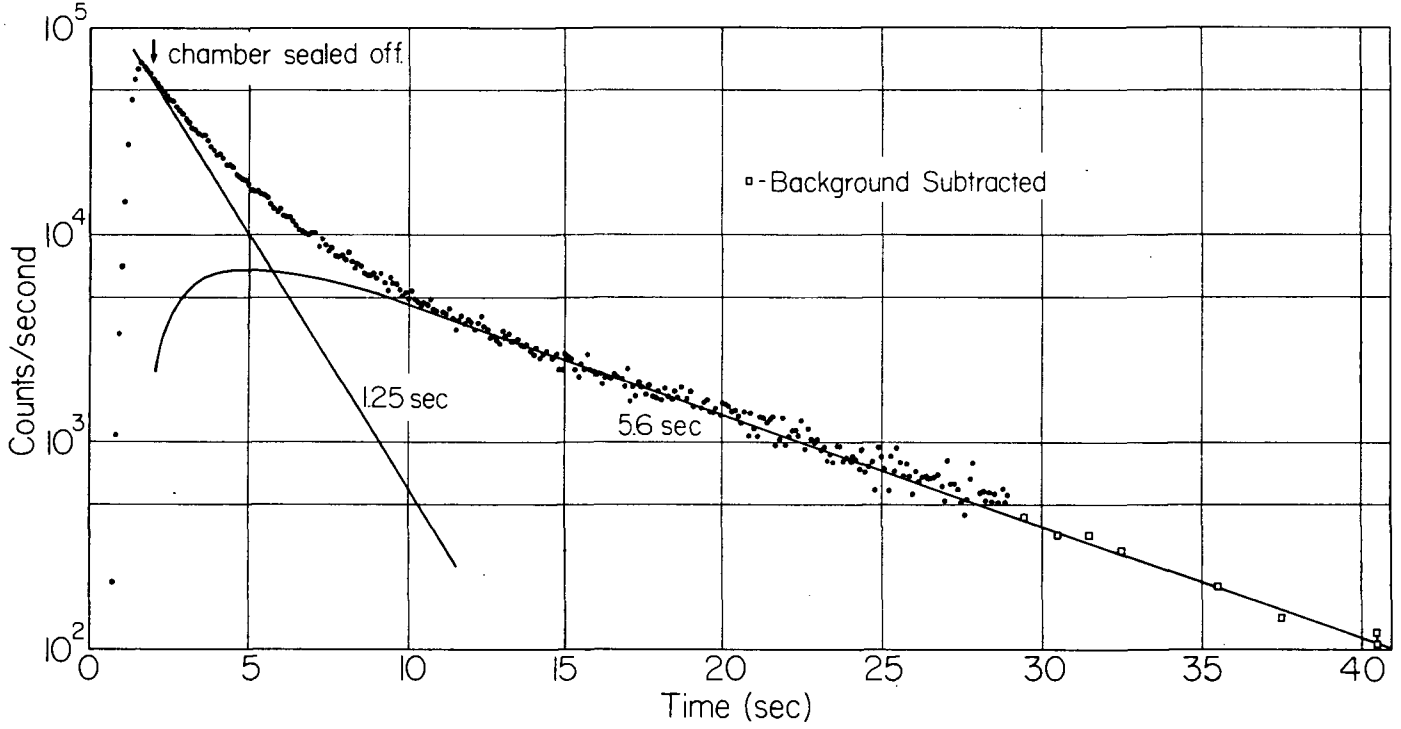

FIG. 11. Gross decay curve of krypton and rubidium delayed neutron activity (5 sec irradiation, 2 sec transfer, repeated 75 times).

(T_1, T_2, T_3) in parallel, as shown in Fig. 10. The flow of active gases from the target to the counting chamber is first directed through column T_1. After a few seconds, the flow is transferred to column T_2, while T_1 is connected to a source of pure nitrogen to purge it of all absorbed activities. A few seconds later, the active flow is switched from T_2 to T_3 and T_2 is purged. This procedure is continued until the last column is reached. The sequence is then repeated starting from the regenerated column T_1.

3. RESULTS ON DELAYED NEUTRON PRECURSORS FROM AN EMANATION SOURCE

3.1. Rubidium-93

A typical counting rate versus time curve for the delayed neutron activity of halogen-free rare gas fission products is shown in Fig. 11. The origin of the time scale coincides with the end of the 5 sec irradiation period and the simultaneous start of gas flow from the pressurized target into the evacuated counting chamber. Activity first reaches the chamber after ~ 0.8 seconds, rises rapidly (~ 3 orders of magnitude in 0.7 seconds) to a peak at ~ 1.5 seconds, and proceeds to decay. The counting chamber was sealed off at 2 seconds, and from then on the curve represents radioactive decay unperturbed by gas flow. Two main components can be seen, corresponding to the 1.5 and 6 sec components reported by Stehney and Perlow [22] and assigned, on the basis of half-lives, to ^{92}Kr, ^{93}Kr or ^{94}Kr, and ^{92}Rb or ^{93}Rb respectively. In our experiments the insertion of a liquid-nitrogen-cooled trap, which eliminates xenon activities [11], did not alter the shape of the decay curve, proving that indeed both delayed neutron activities should be ascribed to krypton and daughters. In order to distinguish between krypton and rubidium, we used the rapid evacuation step described earlier. After the end of irradiation the active gases were transferred into the counting chamber and allowed to decay for a preset period of time, following which all residual gaseous activity was rapidly removed from the chamber. In this procedure all rare gases are eliminated and only their decay products are left behind. The counting chamber was filled with glass wool to provide a large surface area for deposition of the decay products.

A series of typical plots of activity versus time, obtained by varying the delay period between closing of the counting chamber and evacuation of residual gaseous activities, is shown in Fig. 12. The initial pattern is similar to that of Fig. 11, except that in this case transfer is somewhat slower and the activity peak is reached in ~ 2.5 rather than in 1.5 seconds. For curves A-D, the counting chamber was sealed off at 3 seconds, and rapidly re-evacuated τ seconds later, with τ = 0, 1, 3 and 5 seconds for curves A, B, C and D, respectively. For curve E, the gas flow was stopped at 2 seconds (i.e., before the activity reached its peak), and the counting chamber evacuated immediately. The 'full-width-half-maximum' of the resulting activity peak is only 0.4 seconds. After evacuation, the activity exhibits a single component decay, with a half-life of 5.6 seconds. (An exception is curve E, where some indications of a weak shorter-lived activity can be seen. This is discussed in a later section.) The amount

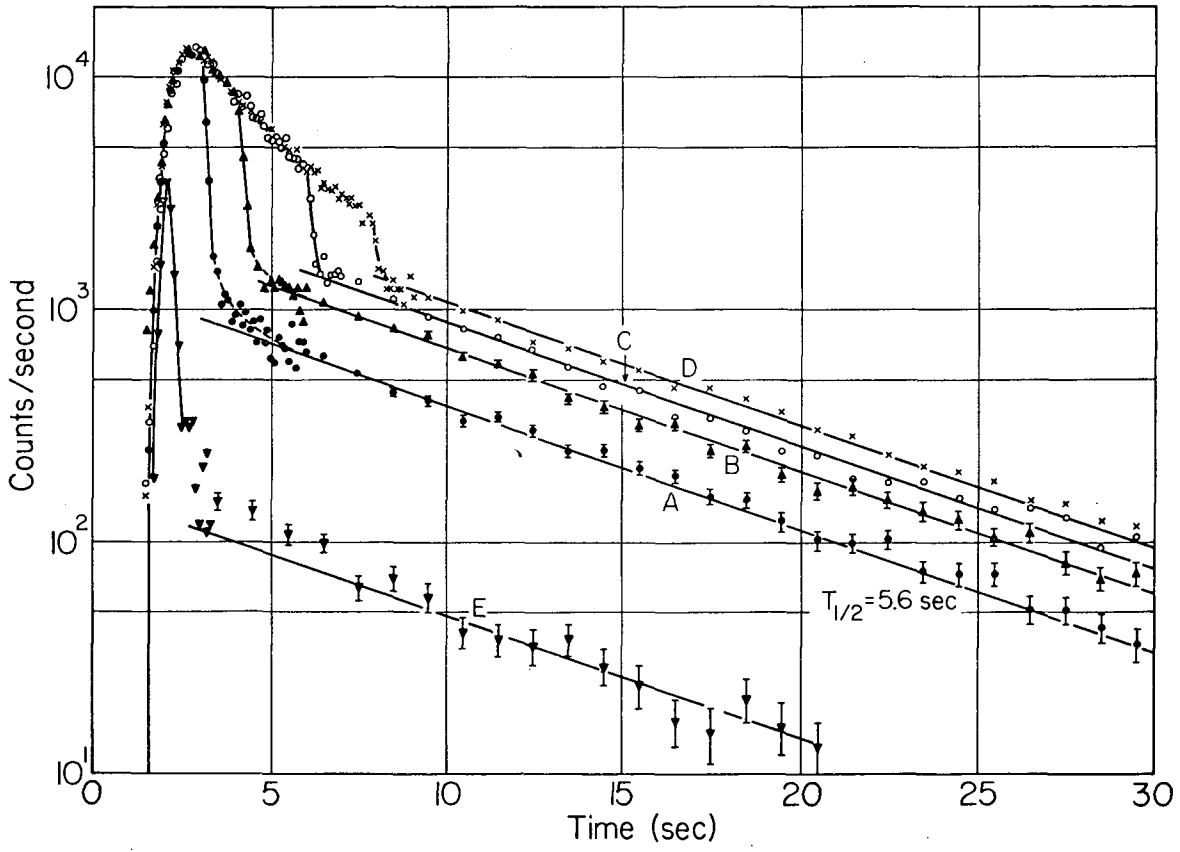

FIG. 12. Growth of ^{93}Rb.

of activity increases as a function of the delay period τ. On this basis it can be definitely assigned to a krypton daughter, and since all strontium isotopes in this region of masses are long-lived, it must be an isotope of rubidium. The half-life of the parent krypton can be obtained from an analysis of the growth of the rubidium daughter as a function of τ. In Fig. 13 we plot, as a function of τ, the quantity

$$W = (1 - Q) \exp(-\lambda_R \tau)$$

where Q is the ratio of the 5.6 second rubidium activity obtained after a

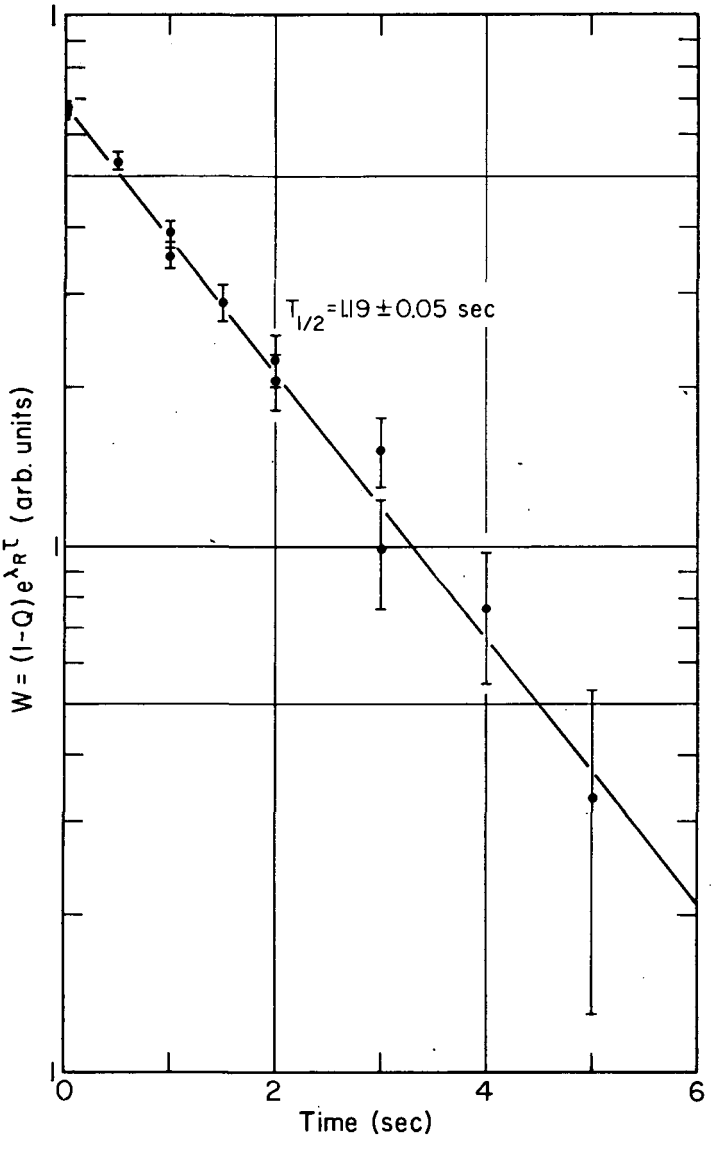

FIG. 13. Half-life of ^{93}Kr.

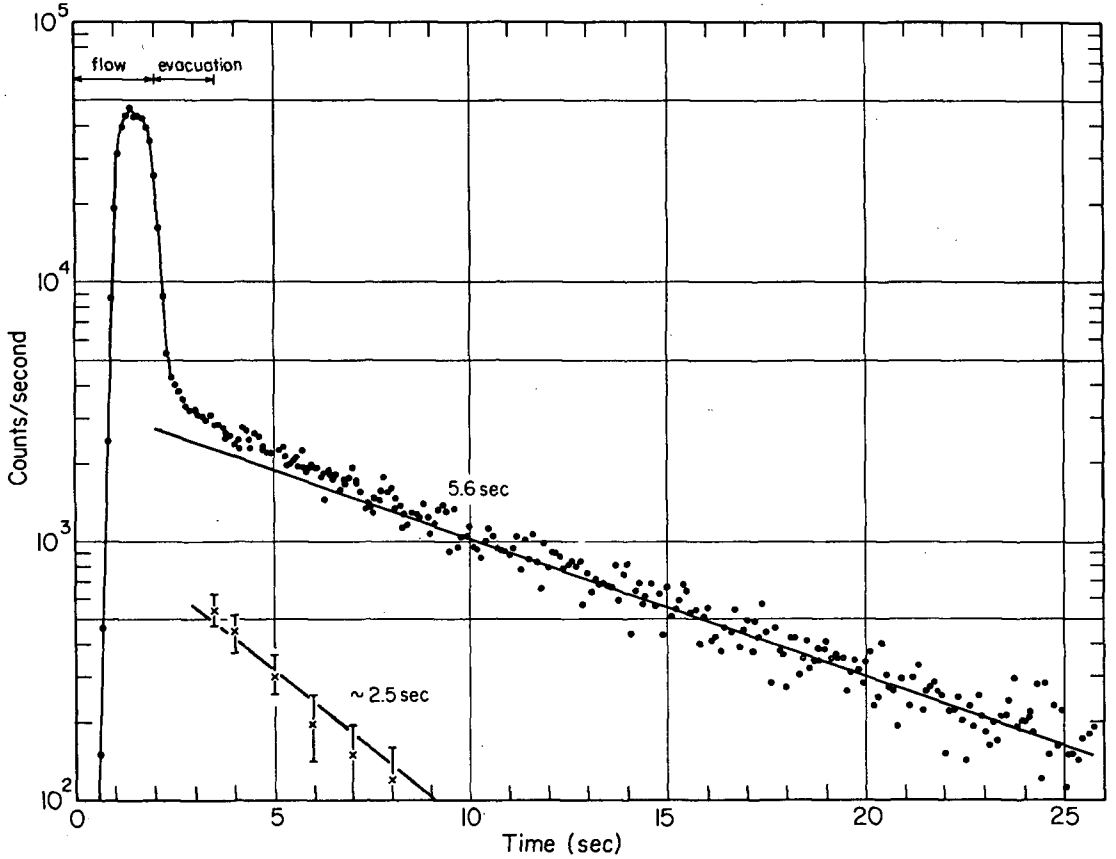

FIG. 14. Decay of ^{93}Rb and ^{94}Rb (5 sec irradiation, 2 sec transfer, immediate evacuation, repeated 50 times).

growth period of τ seconds to that obtained after a longer period τ' (= 8 sec), corrected to equal time after fission, and λ_R = (ln 2/5.6) is the decay constant of the rubidium activity. The straight line is a least-squares fit to the data. A half-life of 1.19 ± 0.05 seconds is obtained, in excellent agreement with the ^{93}Kr half-life of 1.17 ± 0.04 sec reported by Patzelt and Herrmann [23], and shows that the 5.6 second activity belongs to ^{93}Rb. This assignment agrees with recent measurements by Amarel, Bernas et al. [8] who studied the decay of mass-separated rubidium fission products from 150 MeV proton induced fission of uranium, and reported delayed neutron emission from 2.7 sec ^{94}Rb, and 5.9 sec ^{93}Rb, but no delayed neutrons from 4.4 sec ^{92}Rb.

The half-life of ^{93}Rb has been variously reported as 5.6 ± 0.5 [24], 5.1 ± 0.3 [25] and 5.89 ± 0.04 [8] sec. The last value is based on the beta decay of mass separated ^{93}Rb; the other two are derived from radiochemical studies of the ^{93}Sr-^{93}Y daughter growth. In measurements similar to those shown in Figs. 12 and 14, we were able to follow the decay of essentially pure ^{93}Rb (other activities present do not interfere with the neutron counting), over at least 5 half-lives, with background not exceeding a fraction of a percent of the initial activity. The results of several independent determinations, least-squares analysed using the QMBLSQ programme [26] for the Philco-2000 computer, are given in Table I.

TABLE I. HALF-LIFE OF ^{93}Rb

	1	2	3	Average
$T_{\frac{1}{2}}$ (sec)	5.64 ± 0.08	5.55 ± 0.05	5.60 ± 0.06	5.60 ± 0.05

3.2. Krypton-93 and other precursors

The pronounced effect of the evacuation step on the shorter-lived components of the delayed neutron activity (see Figs. 11 and 12) proves that this activity is due to krypton precursors. Analysis of complex decay curves of the type shown in Fig. 11, taking into account the growth of the 5.6 sec ^{93}Rb activity established in the preceding section, indicates the presence of essentially one component, with a half-life of 1.2 ± 0.1 seconds. This rules out 1.9 sec ^{92}Kr [23] as the precursor. Moreover, the excess of the beta decay energy of ^{92}Kr over the neutron binding energy in ^{92}Rb, as calculated from semi-empirical mass formulae [27] is only ~ 0.5 MeV, i.e. considerably lower than that of all known delayed neutron precursors. For ^{93}Kr and ^{94}Kr this energy excess is 1.92 MeV and 2.36 MeV respectively, i.e. both should be delayed neutron precursors. Only an upper limit of 1 sec has been reported for the half-life of ^{94}Kr [23]. If, however, the half-life of this isotope were as long as 1 sec, we should be able to observe large amounts of 2.7 sec ^{94}Rb, which is reported by Amarel, Bernas et al. [8] to emit delayed neutrons with branching ratio ten times higher than that of

^{93}Rb. This high branching ratio should more than compensate for the lower yield of ^{94}Kr in fission [28]. In order to observe the 2.7 sec ^{94}Rb activity, the conditions were optimized so that a transfer time of 1.5 seconds was followed by evacuation at 2 seconds. Results are shown in Fig. 14. A weak 2.7 sec component can be resolved. From its magnitude we can estimate the half-life of ^{94}Kr as 0.4 ± 0.1 seconds. Thus, the only possible assignment of the 1.2 second delayed neutron activity is ^{93}Kr.

3.3. Delayed neutron yields of krypton and rubidium precursors

In the preceding section we established a parent-daughter relationship between the two delayed neutron emitters in the mass 93 chain which we observe. Analysis of the composite curve into the relative neutron counting rates should give directly the ratio of their delayed neutron emission probabilities (P_n-values). This is true, provided that: (a) No rubidium activities are swept along the line into the counting chamber. This assumption is reasonable in the light of the high decontamination obtained from the more volatile halogen activities, and also in view of the results obtained with very short flow and decay times, as shown in Fig. 12; (b) The efficiency of the counting system is the same for both parent and daughter activities. This assumption also seems reasonable since the average energies of delayed neutrons from fission products do not exceed ~ 500 keV and do not vary by more than a few hundred keV [1]. For such possible energy variations the counting efficiency of our system should not differ by more than a few percent.

From our data, we obtain the ratio:

$$\frac{P_n(^{93}\mathrm{Kr})}{P_n(^{93}\mathrm{Rb})} = 1.5 \pm 0.1$$

In order to determine the absolute neutron yields of ^{93}Kr and ^{93}Rb the counting efficiency of our system was measured. This was done by measuring under identical geometry the neutron activity of 56 sec ^{87}Br and that of an irradiated uranium sample calibrated through the yield of ^{140}Ba. The absolute neutron yield of ^{87}Br in the thermal fission of ^{235}U was taken as 0.06% which is the accepted experimental value obtained in a number of laboratories [1].

The fraction of chain 93 collected in the counting chamber as ^{93}Kr was determined by measuring, in the very same sample, the fraction of chains 91 and 92 collected as ^{91}Kr and ^{92}Kr. Chains 91 and 92 were determined quantitatively by measuring the γ-rays from ^{91m}Y and ^{92}Sr with a 3 in × 3 in NaI crystal. From the determination of the collection efficiency for each of these chains it was possible to calculate the collection efficiency for ^{93}Kr. Mass yields were taken from the compilation by Katcoff [29], and Z_p (most probable change) and fractional yield values from the formula given by Wahl et al. [28]. Abundances of the various γ's were taken from the Nuclear Data Sheets using latest results. Half-lives of ^{91}Kr and ^{92}Kr were taken from Ref. [23]. Table II summarizes the yields obtained in these measurements.

TABLE II. P_n VALUES OF ^{93}Kr AND ^{93}Rb

	$T_{\frac{1}{2}}$ (sec)	P_n		P_n (Average)
		Using chain 91 for calibration	Using chain 92 for calibration	
^{93}Kr	1.19 ± 0.05	0.042 ± 0.006	0.036 ± 0.005	0.039 ± 0.006
^{93}Rb	5.60 ± 0.05	0.028 ± 0.004	0.024 ± 0.004	0.026 ± 0.004

Although Stehney and Perlow [22] reported delayed neutron activity from ^{93}Rb a few years ago, it attracted very little interest since in their estimate it contributed only about 0.1% to the total delayed neutron emission from the fission of ^{235}U. However, keeping in mind that they observed the rubidium activity by extracting krypton, thereby losing all the independently formed ^{93}Rb, one can correct their result (using Wahl's Z_p) to obtain a total neutron yield from ^{93}Rb of about 1%. Its relative contribution to Group 3 is therefore so large that it must be considered a major contributor. Our measured P_n-value for ^{93}Rb (0.026) emphasizes its significance even further. As can be seen from Table III its contribution to the total delayed neutron yield in the thermal fission of ^{235}U is about 7%. Its contribution to group 3 is over 30%, being of much greater importance than ^{138}I. Our value for the contribution of ^{93}Kr to the total in ^{235}U is about 1.2% as compared with the previously reported 0.5% [22].

4. SYSTEMATICS OF DELAYED NEUTRON EMISSION DATA AND INDICATIONS OF NEW PRECURSORS

The constantly growing body of data on delayed neutron precursors makes it clear that the resolution of the gross delayed neutron decay curve into six (or nine) exponentials [1] is no more than a mathematical result, that despite its great utility in reactor kinetics certainly does not provide accurate information about the true composition. At present, we can point with confidence to 14 identified precursors, with half-lives not necessarily associated with any specific group period. Moreover, the variations in yield of each known or unknown precursor may be different in each case (i.e. different fissile nuclides and fission energies), and hence may affect the group half-life and yield to various extents.

If we compare the various known group delayed neutron yields with known fission data (i.e. fission yields, Z_p and isobaric dispersions) we should expect a systematic fit, if the data taken are accurate and the precursors listed are indeed the ones responsible for the neutron emission observed. Conversely, any clear discrepancies should permit prediction of precursors not taken into account, and indicate their relative importance and even their probable location on the chart of nuclides. As an illustration, let us consider the fission of uranium isotopes, ^{233}U, ^{235}U and ^{238}U, with

TABLE III. COMPARISON BETWEEN CALCULATED AND EXPERIMENTAL DELAYED NEUTRON YIELDS

GROUP NUMBER	1	2			3			4							
D.N. PRECURSOR	$^{87}_{35}Br$	$^{88}_{35}Br$	$^{137}_{53}I$	($^{136}_{52}Te$) [a]	$^{89}_{35}Br$	$^{93}_{37}Rb$ [b]	$^{138}_{53}I$	$^{85}_{33}As$ [c]	$^{90}_{35}Br$	$^{93}_{36}Kr$ [b]	$^{94}_{37}Rb$ [d]	$^{135}_{51}Sb$ [c]	$^{139}_{53}I$	$^{142}_{55}Cs$ [d]	$^{143}_{55}Cs$ [d]
$T_{\frac{1}{2}}$ (sec)	55	16	24	?	4.5	5.6	6.3	2.1	1.6	1.2	2.7	1.9	2.0	2.3	1.6
P_n (%)	2.5 [e]	4.8 [e]	2.4 [e]	(4)	5.7 [e]	2.6 [b]	1.6 [e]	9.5	13.5 [f]	3.9	(~10)	4.4	2.3 [f]	(~1)	(~2)
THORIUM-232 fast fission (fission neutrons)															
CY(%) [g]	6.2	6.4	6.7	5.6	6.6	6.4	7.0	3.8	6.9	6.4	6.3	5.5	7.3	7.5	7.7
Z_p [h]	34.00	34.39	52.74	52.06	34.90	36.77	52.93	33.16	35.32	36.77	37.19	51.88	53.38	54.84	55.40
FCY [i]	1.00	0.97	0.90	0.78	0.85	0.90	0.84	0.72	0.62	0.33	0.71	0.26	0.58	0.87	0.57
DNY(calc.)	0.154	0.299	0.145	0.157	0.320	0.150	0.094	0.260	0.578	0.080	0.450	0.063	0.097	0.065	0.088
Group DNY (calc.)	0.154		0.601			0.564					1.681				
Group DNY (exp.) [j]	0.169		0.744			0.769					2.212				
THORIUM-232 fast fission (14 MeV neutrons)															
CY (%) [k]	5.1	5.4	5.2	5.0	5.6	5.9	5.4	3.4	5.5	5.9	6.2	4.6	5.6	5.8	5.7
Z_p [h]	34.43	34.82	53.17	52.49	35.33	37.20	53.36	33.59	35.75	37.20	37.62	52.31	53.81	55.27	55.82
FCY [i]	0.97	0.88	0.71	0.50	0.61	0.70	0.53	0.43	0.33	0.12	0.42	0.08	0.29	0.65	0.28
DNY (calc.)	0.123	0.228	0.089	0.090	0.194	0.107	0.051	0.139	0.245	0.027	0.262	0.169	0.037	0.038	0.032
Group DNY (calc.)	0.123		0.407			0.353					0.949				
Group DNY (exp.) [l]	0.13		0.39			0.42					~0.9				
Group DNY (exp.) [m]	0.34		1.19			1.31					3.31				

URANIUM-233 thermal fission															
CY ($)[n]	4.56	5.37	6.58	6.63	5.86	6.98	6.50	2.51	6.43	6.98	6.68	6.03	6.45	6.83	5.99
Z_p[h]	34.92	35.31	53.76	53.21	35.86	37.67	53.95	34.08	36.25	37.67	38.11	52.96	54.54	55.88	56.38
FCY[i]	0.85	0.64	0.32	0.11	0.26	0.38	0.21	0.15	0.095	0.023	0.14	0.005	0.035	0.25	0.06
DNY (calc.)	0.097	0.170	0.050	0.029	0.087	0.067	0.022	0.036	0.082	0.006	0.093	0.001	0.005	0.017	0.007
Group DNY (calc.)	0.097		0.249			0.176					0.247				
Group DNY (exp.)[j]	0.057		0.197			0.166					0.184				
URANIUM-235 thermal fission															
CY ($)[o]	2.50	3.58	6.17	6.47	4.73	6.51	6.68	1.30	5.77	6.51	6.55	6.45	6.42	5.80	5.71
Z_p[h]	34.52	34.91	53.26	52.58	35.42	37.29	53.45	33.68	35.84	37.29	37.71	52.40	53.90	55.36	55.92
FCY[i]	0.96	0.85	0.66	0.45	0.56	0.65	0.53	0.38	0.28	0.075	0.36	0.055	0.25	0.60	0.23
DNY (calc.)	0.060	0.145	0.097	0.117	0.152	0.110	0.057	0.047	0.217	0.019	0.236	0.016	0.037	0.035	0.026
Group DNY (calc.)	0.060		0.359			0.319					0.633				
Group DNY (exp.)[p]	0.058		0.346			0.310					0.624				
URANIUM-238 fast fission (fission spectrum neutrons)															
CY ($)[q]	2.1	2.4	6.0	6.0	2.8	4.6	6.0	1.3	3.4	4.6	4.7	6.0	6.0	5.1	4.8
Z_p[h]	33.97	34.36	52.71	52.03	34.87	36.74	52.90	33.13	35.29	36.74	37.16	51.85	53.27	54.81	55.37
FCY[i]	1.0	0.98	0.92	0.83	0.87	0.91	0.86	0.75	0.65	0.32	0.73	0.27	0.66	0.89	0.60
DNY (calc.)	0.053	0.115	0.144	0.200	0.132	0.110	0.083	0.093	0.296	0.057	0.340	0.071	0.092	0.045	0.058
Group DNY (calc.)	0.053		0.459			0.325					1.052				
Group DNY (exp.)[j]	0.054		0.564			0.667					1.599				

TABLE III (cont.)

URANIUM-238 fast fission (14 MeV) neutrons)														
CY (%) [r]	1.9	2.3	5.2	5.3	2.7	4.5	4.9	1.3	2.9	4.5	5.0	5.5	4.6	3.6	3.4
Z_p [h]	34.39	34.78	53.13	52.45	35.29	37.16	53.40	33.55	35.71	37.08	37.58	52.27	53.98	55.23	55.79
FCY [i]	0.98	0.90	0.75	0.54	0.65	0.73	0.56	0.47	0.36	0.16	0.45	0.09	0.20	0.69	0.31
DNY (calc.)	0.047	0.099	0.098	0.114	0.100	0.084	0.044	0.058	0.140	0.027	0.225	0.022	0.021	0.025	0.021
Group DNY (calc.)	0.047		0.311			0.228					0.539				
Group DNY (exp.) [k]	0.050		0.370			0.420					~0.6				
Group DNY (exp.) [m]	0.150		1.139			1.165					2.808				
PLUTONIUM-239 thermal fission														
CY (%) [s]	0.92	1.42	6.63	6.63	1.71	3.97	6.31	0.54	2.25	3.93	4.48	7.17	5.87	5.01	4.57
Z_p [h]	34.95	35.34	53.68	53.13	35.87	37.70	53.89	34.11	36.29	37.70	38.14	52.83	54.43	55.76	56.15
FCY [i]	0.83	0.61	0.38	0.13	0.26	0.34	0.25	0.14	0.08	0.02	0.13	0.01	0.05	0.32	0.13
DNY (calc.)	0.019	0.042	0.060	0.034	0.025	0.035	0.025	0.008	0.024	0.003	0.058	0.003	0.007	0.016	0.012
Group DNY (calc.)	0.019		0.136			0.085					0.131				
Group DNY (exp.) [j]	0.021		0.182			0.129					0.199				
CALIFORNIUM-252 spontaneous fission														
CY (%) [t]	0.26	0.34	4.57	4.24	0.44	0.87	5.05	0.16	0.62	0.87	1.10	3.60	4.58	5.89	6.02
Z_p [h]	34.74	35.12	53.31	52.88	35.58	37.57	53.71	33.89	36.02	37.57	38.06	52.45	54.17	55.64	56.11
FCY [i]	0.90	0.75	0.63	0.26	0.44	0.45	0.36	0.26	0.18	0.03	0.17	0.05	0.13	0.40	0.15
DNY (calc.)	0.006	0.012	0.069	0.044	0.011	0.010	0.029	0.004	0.015	0.001	0.019	0.008	0.014	0.024	0.018
Group DNY (calc.)	0.006		0.125			0.050					0.103				
Group DNY (exp.) [u]	~0		0.220			~0					0.290				

a Inserted as a likely candidate for the missing precursor in group 2.

b From this work.

c From references 31 and 33 . Delayed neutron emission probability, P_n , derived from the quoted total delayed neutron yields, assuming a 3:1 ratio between the ^{85}As and ^{135}Sb contributions in ^{235}U thermal fission.

d From reference 8. P_n for ^{94}Rb estimated as explained in text. P_n's for $^{142,143}Cs$ are estimates based on decay energy systematics.

e Experimental values of ref.34, reduced systematically by 20% to normalize the ^{87}Br yield in ^{235}U fission.

f P_n calculated from $^{90}Br/^{88}Br$ and $^{139}I/^{137}I$ yield ratios of ref.21. It should be noted that these values are open to doubt in view of the discrepancy between the $^{89}Br/^{88}Br$ ratio reported in the same reference and that of ref.20. The latter was found to be in much better agreement with the $^{89}Br/^{88}Br$ ratio calculated on the basis of ref.34.

g Chain yield, from ref.44.

h Z_p (most probable charge) values for ^{235}U based on empirical (and calculated) results of ref.28 and 36. For other fission reactions empirical values of ref.37 and estimates based on the formula $Z_p - Z_p(^{235}U) = 0.5\Delta Z_f - 0.19\,\Delta A_f + 0.19\,\Delta\nu$ [38]. Empirical values are underlined.

i Fractional cumulative yield. A universal charge dispersion curve of $\sigma = 0.59$ ($c = 0.86$) [36] was used to calculate the fractional cumulative yields. In view of recent indications of systematic variation of charge-dispersion with mass number [39], this treatment should be carefully examined, especially for isobars of low mass yield.

j Keepin's 6 period analysis, see ref.1.

k From ref.41.

l From ref.5.

m From ref.32.

n From ref.35.

o From ref.40.

p Same as j , except for the yield of group 1, which was adjusted to 0.058, in accordance with the more recent 9 period analysis [1].

q From refs.29 and 41.

r From ref.41.

s From ref.29.

t From ref.42.

u From ref.43.

neutrons in two different energy ranges – low (thermal and fission spectrum) and high (14-15 MeV). At low energy the total delayed neutron yield was observed to decrease with decreasing mass number A of the uranium isotope (see Table III). This is interpreted as being due to the shortening of the chains (i.e. Z_p values moving toward stability, $Z_p \rightarrow Z_A$). The competing effect of the shift of the light mass fission product peak to lighter masses, where delayed neutron precursors such as ^{85}As [31, 33] are likely to be present, is apparently of lesser importance since this would tend to raise the yield, and we conclude that no unexpected precursors of importance are present. Comparison of the delayed neutron yields at 14 MeV with those at low energy (for constant A), is less conclusive since conflicting experimental results have been reported [5, 32]. The Z_p values shift to about the same extent as in the previous case. Thus if neutron yields decrease at 14 MeV [5] the shortening of the chains must again be the dominant effect. However, if the yields increase [32], we may conclude that precursors which did not contribute significantly at low energies become prominent at 14 MeV and their effect masks the decrease due to shortening of the chains. These precursors would be located in regions where fission yields increase substantially at 14 MeV, i.e. at the valley and wings of the mass distribution curve.

The validity of possible conclusions should be examined in the light of the entire bulk of data from all different fissionable nuclides and energies, where delayed neutron emission, fission yields and charge distribution values are available.

An attempt to examine the agreement between the calculated and measured yields in groups 1 to 4 is given in Table III. The overall agreement is quite gratifying. In group 1, the only real discrepancy is the high calculated delayed neutron yield in the thermal fission of ^{233}U. It is conceivable that the fractional yields of mass 87 in ^{233}U fission are affected by the 50 neutron shell, so that the yield of ^{87}Br is lower than expected on the basis of charge distribution systematics. Generally, the calculated results for ^{233}U and ^{239}Pu should be the most sensitive to uncertainties in the fractional chain yields.

In groups 2 - 4 the main difference between the present compilation and previous similar attempts [2, 3, 6] is the reduced relative contribution of iodine precursors, which now account, on the average, for less than 25% of the total group yields. This is brought about mainly by the introduction of the high fission yield ^{93}Rb and ^{94}Rb precursors into groups 3 and 4, respectively, and to a lesser degree by other, less prominent species. The long-standing discrepancy between the high neutron branching ratios for the iodines inferred from total group yields [5, 6] and the low values derived from direct experimental measurements [34] is thus removed. The puzzling very low yield of group 3 activities in the spontaneous fission of ^{252}Cf [43] is also resolved.

The reduction in the iodine contribution calls for at least one, as yet unidentified, major contributor to group 2. In view of the ^{252}Cf results, the mass of this precursor should be close to the heavy mass peak or in the mass region of 105-110. ^{136}Te was included in the table as a likely candidate, but closed proton shell ^{134}Sn and other nuclides should also be considered. The 10-14 sec activity observed by a number of investigators [49, 31, 33] may be due to one of these isotopes. Inclusion of ^{136}Te may be sufficient to account for the ^{235}U and ^{233}U results, but additional

delayed neutron precursors will have to be discovered in order to account for the entire yield in ^{238}U and ^{252}Cf.

In group 4, the major new precursor is 2.7 sec ^{94}Rb. According to Ref. [8], its P_n-value should be about 10 times that of ^{93}Rb, i.e. ~ 25%. Such a high value is inconsistent with the total delayed neutron yield of ^{235}U. Also, P_n-values in excess of 20% should cause pronounced fine structure fluctuations in the mass yield curve. There is no evidence of fluctuations in the 93-94 mass region [40]. The value of $P_n \approx 0.1$ adopted here is more consistent with the data. The other major contributor to this group is ^{90}Br. Its calculated yield is based on the $^{90}Br/^{88}Br$ delayed neutron yield ratio of Ref. [21]. However, the disagreement noted in Table III (see footnote f) between the $^{89}Br/^{88}Br$ yield ratio from this reference and recently published results [20] throws some doubt also on the adopted $^{90}Br/^{88}Br$ value. In any case, the large number of quite poorly characterized precursors in this group precludes an unambiguous fit of the data at this stage.

In fast fission of ^{238}U and to a lesser degree of ^{232}Th, our calculated yields fall short of the experimental values, especially for groups 3 and 4. For these two cases one expects the longest decay chains, i.e. relatively high fission yields of species even further removed from stability than the known delayed neutron precursors. Therefore, one may attribute the excess of the observed delayed neutron yield in the fission of ^{238}U and ^{232}Th, over that calculated in Table III, to unidentified neutron precursors. As mentioned above, increasing the energy of the bombarding neutrons causes shortening of the average chain length and should therefore reduce the contribution of these unidentified precursors. At 14 MeV, our calculated values agree with those measured by Patzelt et al. [6], but disagree, by a factor of 3-4, with the results reported by Maksyutenko et al. [32].

In view of the disagreement in many of the delayed neutron emission values further experimental work is necessary. At Soreq this problem is being tackled in two ways, in addition to the detailed on-line isotopic separation studies.

4.1. Assessment of total and group delayed neutron yields per fission by using a flat-response neutron detector and high resolution γ-ray spectrometry

With the advent of lithium-drifted germanium detectors it has become possible to determine simultaneously a considerable number of fission products in an untreated fission sample [46-48]. This can facilitate accurate determination of the number of fissions taking place in a sample, as well as the relative yield variations of individual products and chains, from the known γ-ray peaks corresponding to nuclides scattered over a broad range of masses. This technique is superior to standard radiochemical techniques which involve errors and corrections. The use of the same unopened sample irradiated at different energies, both for γ-ray spectrometry and neutron counting (with the latter count subsequently resolved by a computer into the accepted group half-lives) should yield accurate data which, when displayed as in Table III, may elucidate the question of missing precursors, at least in groups 2 and 3, and maybe 4.

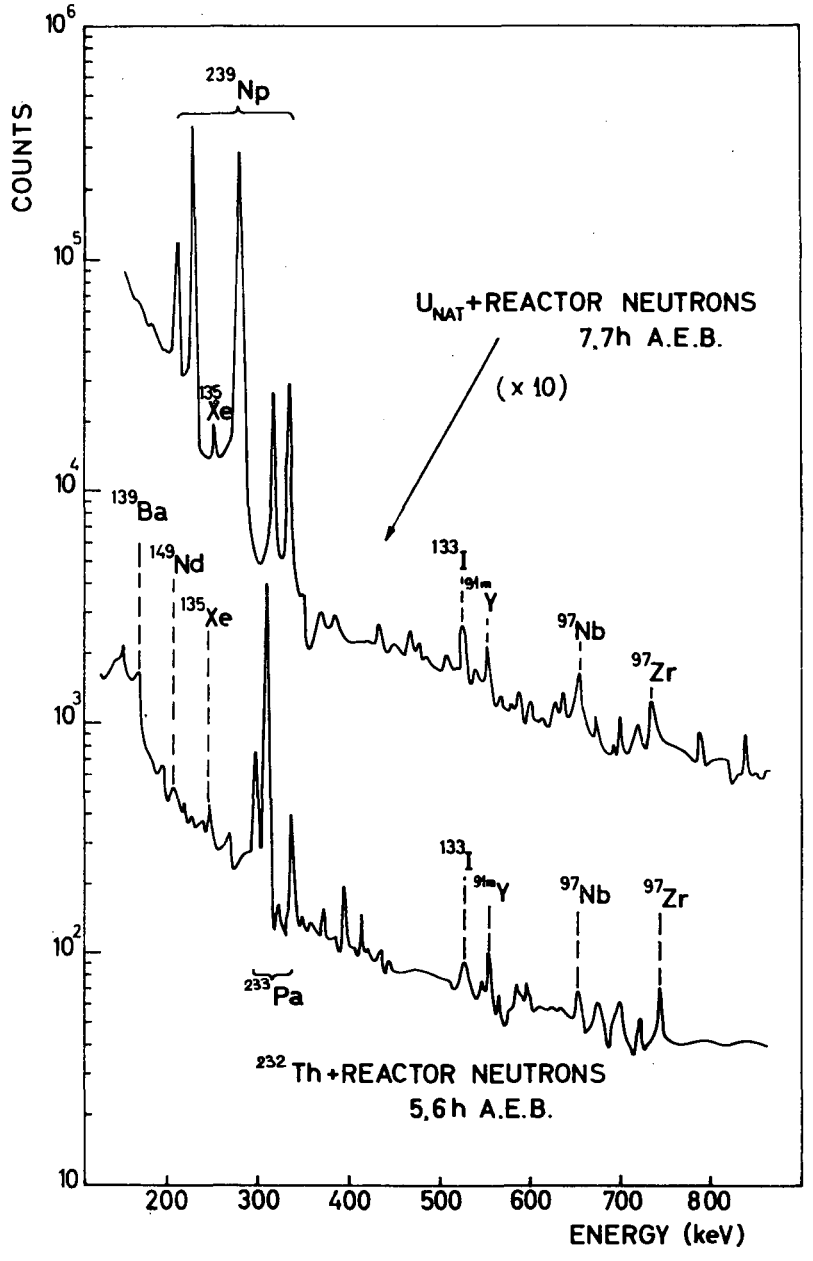
COUNTS
10^6
10^5
10^4
10^3
10^2
10
^{239}Np
^{135}Xe
^{139}Ba
^{149}Nd
^{135}Xe
^{133}I
^{91m}Y
^{97}Nb
^{97}Zr
U_{NAT}+REACTOR NEUTRONS
7,7h A.E.B.
(x 10)
^{133}I
^{91m}Y
^{97}Nb
^{97}Zr
^{233}Pa
^{232}Th+REACTOR NEUTRONS
5,6h A.E.B.
200
300
400
500
600
700
800
ENERGY (keV)

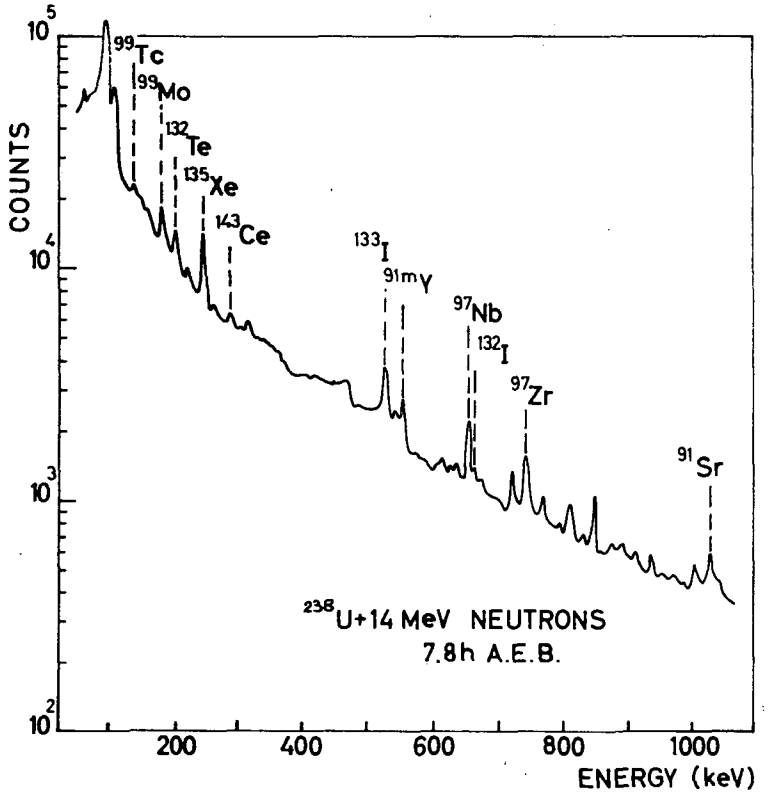

FIG. 15. Gamma ray spectra from irradiated uranium and thorium.

Gamma ray spectra obtained in preliminary experiments with natural uranium and thorium irradiated at the reactor and at the 14 MeV neutron generator, in both cases with the aid of a fast automatic pneumatic system ("shuttle rabbit"), are displayed in Fig. 15. The γ-rays used for evaluating the method are indicated in the figure. The peaks were assigned to known fission products on the basis of their energies and half-lives. The results so far are inconclusive and in view of the conflicting published data [5, 32] require careful analysis and many repetitions.

4.2. A method for obtaining data on the mass numbers and half-lives of delayed neutron precursors

A combination of entrainment of fission fragments in a flowing gas, differential pumping deposition on a catcher and collection through a bias potential, is being studied as a method for using the recoil of delayed neutron emission products to isolate them from other fission products. The apparatus is depicted in Fig. 16. Fission fragments are stopped in helium at atmospheric pressure and are then pumped through a narrow nozzle into an evacuated chamber in which they are deposited on a controlled-velocity circulating conveyor. On a secondary catcher, delayed neutron emission products are collected through a retarding electrostatic field, which stops beta decay recoils ($E_r \leq 10$ eV) but allows the passage of the energetic neutron-decay recoil products ($E_r \approx 10$ keV). Through the longer-lived daughters growing from the nuclides collected on the secondary catcher, mass assignments and half-life values of the corresponding delayed neutron precursors may be determined.

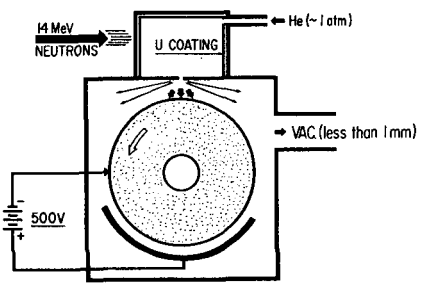

FIG. 16. System for double recoil study of delayed neutron precursors.

5. ENERGIES OF DELAYED NEUTRONS

The state of knowledge on the energies of the delayed neutrons emitted from fission products in even less satisfactory than that on yields. Only gross spectra in unseparated irradiated samples at various times after fission, emphasizing the relative contribution of the different group periods, have been reported [1, 50]. Such measurements provide useful data for reactor kinetics, but their interpretation in terms of

nuclear properties of the individual precursors is difficult, if not impossible. On the other hand, many nuclear parameters can be extracted from delayed neutron spectra of separated precursors. The endpoint of such spectra is related to the difference $Q_\beta - B_n$ between the beta decay energy of the precursor and the neutron binding energy of its decay product, and can be used as a test of semi-empirical mass formulae. The shape of the spectrum in general, and of its low energy part in particular, yields information on level densities above the neutron binding energy; pronounced peaks in the spectra should be related to the spins of the levels involved, etc. Moreover, neutron spectra can be used as a sensitive test of the assumptions involved in theoretical calculations of P_n-values from the statistical model.

The measurement of delayed neutron spectra poses a number of experimental problems in addition to precursor separation itself:

(a) The efficiency of most neutron spectrometers is typically about 10^{-5} or less.
(b) The lower energy limit for most spectrometers is 100 to 200 keV.
(c) Large amounts of beta and gamma radiation are present even in separated precursors. This interference sets an upper limit on the intensity of sources that can be used. Massive shields can reduce the gamma ray background, but impair the efficiency and resolution.

We have examined two techniques for the measurement of delayed neutron energies, namely: time-of-flight and ^{3}He proportional spectrometry. The time-of-flight investigations involved either the associated particles, i.e. beta for ^{17}N [51] and gamma for the ^{9}Be$(\alpha, n\gamma)$ [52] and ^{18}O$(\alpha, n\gamma)$ [53] reactions, or neutron-proton scattering with time-of-flight measurement of the scattered neutron at a known angle [54]. It was concluded that due to excessive intensity of betas in unseparated fission samples the time-of-flight technique is much more suitable for separated nuclides, and will be used when the SOLIS mentioned earlier is in operation. Improvements in the performance of the spectrometer at low neutron energies (100-500 keV) are also essential since a major portion of the delayed neutrons is in this energy range.

Preliminary spectra obtained with a commercial ^{3}He spectrometer of $\sim$ 75 keV resolution, for gross and partly separated delayed neutrons from ^{235}U fission, are shown in Fig. 17. The two gross spectra were obtained by repeated irradiations of a uranium sample in a fast, automatic, pneumatically operated irradiation facility ("shuttle rabbit") installed in a radial beam port of the IRR-1 [55]. Transfer time is $\sim$ 0.1 sec. The unit includes a flexible programmer, which permits selection of any desired set of irradiation, delay, counting and cooling times. The third spectrum represents a mixture of ^{93}Kr and ^{93}Rb, with some bromine contamination. All the spectra are similar to those obtained in Ref. [50], and clear evidence of structure can be seen.

A large high pressure ^{3}He counter was constructed in order to improve the efficiency and resolution of the present detector. The improved resolution, resulting in a narrower epithermal peak, will permit extension of the measurements to energies lower than 200 keV. This spectrometer will be used to complement the time-of-flight measurements on separated precursors.

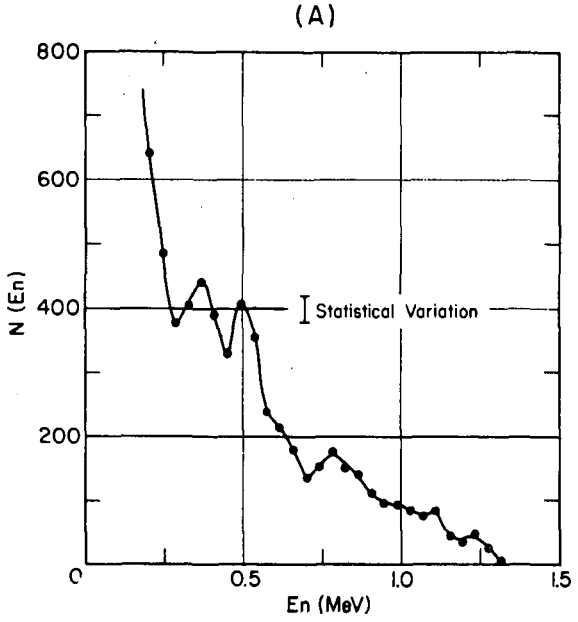
(A)
800
600
400
200
0
N (En)
Statistical Variation
0.5
1.0
1.5
En (MeV)

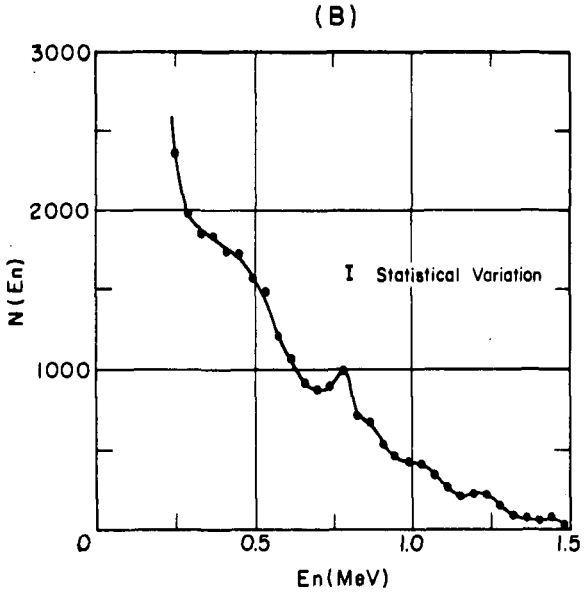
(B)
3000
2000
1000
0
N(En)
I Statistical Variation
0.5
1.0
1.5
En(MeV)

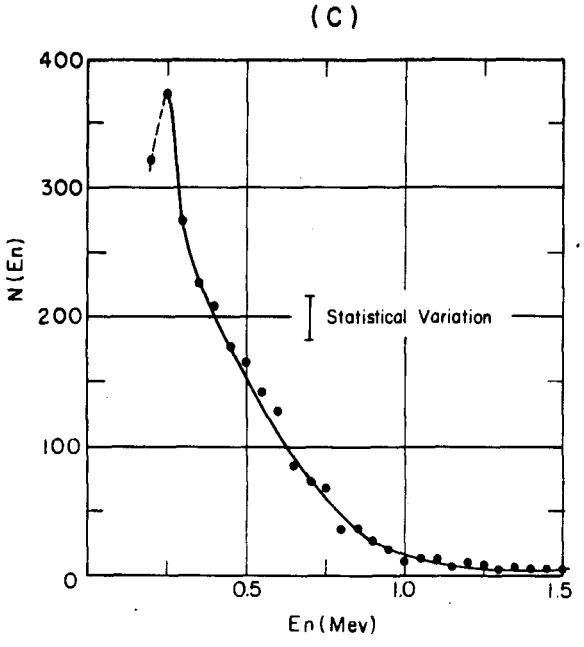

FIG. 17. Delayed neutron spectra obtained with a ^{3}He spectrometer: A. unseparated sample, groups 1 and 2; B. unseparated sample, mainly group 2; C. ^{93}Kr (~60%), ^{93}Rb (~30%), ^{87}Br to ^{89}Br (~10%).

ACKNOWLEDGEMENTS

We gratefully acknowledge the assistance of Mr. Z. Segal, for his help with the experiments; Mr. M. Baer helped with the computer data processing. The work on ^{3}He spectrometry is part of a M. Sc. Thesis by Mr. J.M. Cuttler. Dr. E. Bruninx of CERN (at present with Philips Research Laboratories, Eindhoven) actively participated in the early stages of the work with the emanation source. The paper includes parts of a study carried out by A. Notea in partial fulfillment of the requirements for a Ph. D. degree of the Hebrew University, Jerusalem.

REFERENCES

[1] KEEPIN, G.R., Ch.4, Physics of Nuclear Kinetics, Addison-Wesley, Mass. (1965).
[2] AMIEL, S., Physics and Chemistry of Fission (Proc. Symp. Salzburg, 1965) 2, IAEA, Vienna (1965) 171.
[3] PAPPAS, A.C., TUNAAL, T., Why and How Should We Investigate Nuclides Far Off the Stability Line (Proc. Symp. Lysekil 1966) proceedings to be published in Ark. Fys.
[4] BEMIS, C.E., Ph.D. thesis, MIT (1964).
[5] HERRMANN, G., FIEDLER, J., BENEDICT, G., ECKHARDT, W., LUTHARDT, G., PATZELT, P., SCHÜSSLER, H.D., Physics and Chemistry of Fission (Proc. Symp. Salzburg, 1965) 2 IAEA, Vienna (1965) 197.
[6] PATZELT, P., SCHÜSSLER, H.D., HERRMANN, G., Why and How Should We Investigate Nuclides Far Off the Stability Line (Proc. Symp. Lysekil 1966), proceedings to be published in Ark. Fys.

[7] AMAREL, I., BERNAS, R., CHAUMONT, J., FOUCHER, R., JASTRZEBSKI, J., JOHNSON, A., KLAPISCH, R., TEILLAC, J., Why and How Should We Investigate Nuclides Far Off the Stability Line (Proc. Symp. Lysekil 1966), proceedings to be published in Ark. Fys.
[8] AMAREL, I., BERNAS, R., FOUCHER, R., JASTRZEBSKI, J., JOHNSON, A., TEILLAC, J., GAUVIN, H., preprint (submitted to Phys. Lett., Feb. 1967).
[9] ANDERSSON, G., Why and How Should We Investigate Nuclides Far Off the Stability Line (Proc. Symp. Lysekil 1966), proceedings to be published in Ark. Fys.
[10] AMIEL, S., Why and How Should We Investigate Nuclides Far Off the Stability Line (Proc. Symp. Lysekil 1966), proceedings to be published in Ark. Fys.
[11] AMIEL, S., GILAT, J., NOTEA, A., YELLIN, E., Why and How Should We Investigate Nuclides Far Off the Stability Line (Proc. Symp. Lysekil 1966), proceedings to be published in Ark. Fys.
[12] ZVARA, I., ZVAROVA, T.S., KRZHIVANEK, M., CHUBURKOV, Yu.T., Radiokhimiya 8 (1966) 77.
[13] HERRMANN, G., Why and How Should We Investigate Nuclides Far Off the Stability Line (Proc. Symp. Lysekil 1966), proceedings to be published in Ark. Fys.
[14] AMIEL, S., Nuclear Chemistry (YAFFE, L., Ed.), Academic Press New York (1967).
[15] RUDSTRAM, G., ANDERSSON, G., unpublished reports (CERN); BERGSTROM, I., Lectures at the Yugoslavian Summer School, Herzeg-Novi, 1965 (unpublished).
[16] PAISS, Y., AMIEL, S., J. Am. chem. Soc. 86 (1964) 2332; AMIEL, S., PAISS, Y., Radiochim. Acta 4 (1965) 157.
[17] AMIEL, S., PAISS, Y., Israel AEC Report IA-1096 (1966).
[18] AMIEL, S., PAISS, Y., YOSHIDA, H., Israel AEC Report IA-1100 (in print).
[19] BRAUN, C., PAISS, Y., AMIEL, S., Israel AEC 1966 Annual Report, IA-1128.
[20] SILBERT, M.D., TOMLINSON, R.H., Radiochim. Acta 5 (1966) 223.
[21] PERLOW, G.J., STEHNEY, A.F., Phys. Rev. 113 (1959) 1269.
[22] STEHNEY, A.F., PERLOW, G.J., Bull. Am. phys. Soc. II, 6 (1961) 62.
[23] PATZELT, P., HERRMANN, G., Physics and Chemistry of Fission (Proc. Symp. Salzburg, 1965) 2 IAEA, Vienna (1965) 243.
[24] FRITZE, K., KENNETT, T.J., Can. J. Phys. 38 (1960) 1614.
[25] WAHL, A.C., NORRIS, A.E., FERGUSON, R.L., Phys. Rev. 146 (1966) 931.
[26] BAER, M., Israel AEC Report IA-1047 (1965).
[27] ZELDES, N., GRONAU, M., LEV, A., Nucl. Phys. 63 (1965) 1; and private communication.
[28] WAHL, A.C., FERGUSON, R.L., NATHAWAY, D.R., TROUTNER, D.E., WOLFSBERG, K., Phys. Rev. 126 (1962) 1112.
[29] KATCOFF, S., Nucleonics 18 (1960) 201.
[30] WILLIAMS, E.T., CORYELL, C.D., Nuclear Applications 2 (1966) 256.
[31] DEL MARMOL, P., NÈVE de MÉVERGNIES, M., J. inorg. nucl. Chem. 29 (1967) 273.
[32] MAKSYUTENKO, B.P., Atomn. Energ. 7 (1959) 474; and 15 (1963) 321; SHPAKOV, V.I., PETRZHAK, K.A., BAK, M.A., KOVALENKO, S.S., KOSTOCHKIN, O.I., Atomn. Energ. 11 (1961) 539.
[33] TOMLINSON, L., J. inorg. nucl. Chem. 28 (1966) 287.
[34] ARON, P.M., KOSTOCHKIN, O.I., PETRZHAK, K.A., SHPAKOV, V.I., Atomn. Energ. 16 (1964) 368.
[35] BUNNEY, L.R., SCADDEN, E.M., Rep. USNRDL-TR-769 (1964).
[36] NORRIS, A.E., WAHL, A.C., Phys. Rev. 146 (1966) 326.
[37] WOLFSBERG, K., Phys. Rev. 137B (1965) 929.
[38] CORYELL, C.D., KAPLAN, M., FINK, R.D., Can. J. Chem. 39 (1961) 646.
[39] STROM, P.O., LOVE, D.L., GREENDALE, A.E., DELUCCHI, A.A., SAM, D., BALLOU, N.E., Phys. Rev. 144 (1966) 984.
[40] FARRAR, H., FICKEL, H.R., TOMLINSON, R.H., Can. J. Phys. 40 (1962) 1017.
[41] WALKER, W.H., (Atomic Energy of Canada, Ltd.) Rep. AECL-2111 (1964).
[42] FRASER, J.S., MILTON, J.C.D., BOWMAN, H.R., THOMPSON, S.G., Can. J. Phys. 41 (1963) 2080.
[43] COX, S., FIELDS, P., FRIEDMAN, A., SJOBLOM, R., SMITH, A., Phys. Rev. 112 (1958) 960.
[44] ZYSIN, YR. A., LBOV, A.A., SELCHENKOV, L.I., Fission Products Yields and Their Mass Distribution, Consultants Bureau, New York (1964).
[45] GANAPATHY, R., KURODA, P.K., J. inorg. nucl. Chem. 28 (1966) 2071.
[46] GORDON, G.E., HARVEY, W.J., NAKAHARA, H., Nucleonics 24 12 (1966) 62.
[47] TAKAYANAGI, S., NOBORN, O.I., KOBYASHI, T., SUGITA, T., J. nucl. Sci. Tech. 3 (1966) 200.

[48] BANHAM, N.F., FIDGE, A., HOWES, J.H., Analyst 91 (1966) 180.
[49] YELLIN, E., SONNINO, T., AMIEL, S., unpublished results, see Ref.[2].
[50] BATCHELOR, R., HYDER, H.R.M. J. Nucl. Energy 3 (1956) 7.
[51] GILAT, J., O'KELLEY, G.D., EICHLER, E., USAEC Rep. ORNL-3488 (1963) p.4.
[52] SADEH, D., CATZ, A.L., AMIEL, S., Nucl. Phys. 52 (1964) 25.
[53] CATZ, A.L., Ph.D. thesis, Israel AEC Report IA-1122 (1967); AMIEL, S., CATZ, A.L., SADEH, D., Israel AEC Semi-Annual Report 1964, IA-984, p.107.
[54] NOTEA, A., M.Sc. thesis, Israel AEC Report IA-1025 (1965); NOTEA, A., CATZ, A.L., AMIEL, S., Israel AEC Semi-Annual Report 1964, IA-1021, p.96.
[55] CUTTLER, J.M., M.Sc. thesis, Israel AEC Report (in print).

RECENT WORK ON DELAYED FISSION NEUTRONS AT THE UNIVERSITY OF MAINZ*

G. HERRMANN,
INSTITUT FÜR ANORGANISCHE CHEMIE
UND KERNCHEMIE,
MAINZ UNIVERSITY,
FEDERAL REPUBLIC OF GERMANY

Abstract

RECENT WORK ON DELAYED FISSION NEUTRONS AT THE UNIVERSITY OF MAINZ. The Mainz group is investigating the following aspects of delayed neutron emission in low-energy fission: (1) Delayed neutron yields reported for various fission reactions are compared with calculated cumulative fission yields of known and predicted precursor nuclides to show whether the delayed neutron yields can be explained by known precursors or whether improvements result if as yet unknown precursors are assumed to contribute; (2) Delayed neutron yields of bromine and iodine precursors are measured in several fission reactions, as are the total contributions of non-halogen elements to the four longest periods; (3) Following the implications of the work under (1), the group is looking for delayed neutron precursors among the nuclides of the alkalies and alkaline earths; (4) Absolute delayed neutron yields are determined in fission of ^{232}Th and ^{238}U by 14 MeV neutrons by comparison of neutron and fission rates with a reference reaction as fission of ^{235}U by thermal neutrons.

1. INTRODUCTION

Work on delayed neutrons in low-energy fission was initiated at this laboratory several years ago when a Triga reactor had been ordered. Our programme is to search for new delayed neutron precursors, to study the decay properties of precursor nuclides, and to measure their contributions to the delayed neutron periods by means of rapid chemical separations. We began with some computations, comparing delayed neutron yields with fission yields of precursor nuclides [1, 2], which served for planning our experimental work. One conclusion was that the delayed neutron yields reported for fission reactions induced by 14 MeV neutrons are much higher than expected for the known precursors. We tried to eliminate this discrepancy by experiments at our Cockcroft-Walton accelerator. Results of these studies and of the computations have been presented at several meetings [1, 3, 4] and will be summarized here. Work at the reactor could be started only very recently and is at an early stage. Thus all quantitative deductions as relative abundances or contributions to period yields are still rather crude estimates.

---

* Report on work done by G. Benedict, W. Eckhardt, H. J. Fiedler, W. Grimm, G. Herrmann, G. Luthardt, P. Patzelt and H. D. Schüssler.

2. COMPARISON OF OBSERVED DELAYED NEUTRON YIELDS WITH CALCULATED FISSION YIELDS OF NEUTRON PRECURSORS

The absolute yield, Y_n, of a delayed neutron period in a fission reaction i is the sum of the neutron yields of k precursor nuclides j contributing to that period:

$$Y_{n(i)} = \sum_{j=1}^{k} P_{n(j)} \; Y_{c(ij)} \qquad (1)$$

The individual contributions depend upon the neutron emission probability, P_n, and the cumulative fission yield, Y_c, of the precursors. Taking neutron yields observed for a certain period in various fission reactions and the corresponding fission yields of the precursors known or predicted to contribute, Eq. (1) may be solved for the P_n-values by least-squares analysis. This comparison should lead to small mean deviations in P_n and Y_n if the delayed neutrons originate mainly from the precursors introduced into Eq. (1).

Absolute delayed neutron yields have been measured in a number of low-energy fission reactions [5]. Cumulative yields of precursor nuclides have not yet been determined, but have to be estimated by multiplying mass yields Y_A by fractional cumulative yields f_c, i.e. $Y_c = f_c Y_A$. Accurate mass yields have been reported for the fission chains of interest or can be interpolated in mass-yield curves [6]. Hence the estimation of fractional cumulative yields is the problematical part of such a comparison. This quantity is equal to the sum of the fractional independent yields, f_i, of the nuclide in question and of all its precursors in the fission chain. The fractional independent yields are distributed within a fission chain according to a Gaussian distribution characterized by Z_p and c [7]. Z_p is the abscissa of the maximum of that curve, c gives its width:

$$f_{i(Z)} = (c\pi)^{-\frac{1}{2}} \exp\left[\frac{-(Z-Z_p)^2}{c}\right] \qquad (2)$$

with $f_{c(Z)} = \sum^{Z} f_{i(Z)}$ and $c \approx 2(\sigma^2 + 1/12)$, σ is the root-mean-square width of the charge distribution [7]. Only for the thermal neutron induced fission of ^{233}U, ^{235}U and ^{239}Pu, both Z_p and c can be interpolated reasonably well from experimental data [7, 8], but even then it has to be assumed that no local discontinuities in Z_p and c occur as were observed in the closed-shell region around mass number 132 [9, 10]. For the remaining reactions, f_c-values have to be extrapolated in a more or less arbitrary way.

We have reported previously [1, 3] on the results of such a comparison based on five fission reactions, viz. fission of ^{233}U, ^{235}U and ^{239}Pu by thermal, and of ^{232}Th and ^{238}U by fission neutrons. More recently, the comparison was repeated with seven reactions [4] including the fission of ^{241}Pu by thermal and of ^{240}Pu by fission neutrons. Also, an approach with eleven reactions was tried using, in addition, the fission of ^{232}Th, ^{235}U, ^{238}U and ^{239}Pu by 15 MeV gamma rays for which delayed neutron yields have been published recently [11]. The use of seven reactions leads to improved fits, but no further improvement is noted with eleven reactions [4].

We shall not discuss here the numerous variations tested but are restricting ourselves to that set of parameters which gives the best fit; the results are not, however, very sensitive to the input data. In this case, fractional cumulative yields for fission of ^{233}U, ^{235}U and ^{239}Pu were estimated using c = 0.80 from Z_p-functions constructed from available fractional yields [6] with the same c-value which is close to the average value c = 0.86 ± 0.15 recommended by Wahl [12]. These three fractional cumulative yields were then plotted on a probability scale versus $(A_f - 2.8\ Z_f)$; A_f and Z_f are the mass and charge number of the fissioning compound nucleus. A straight line was then drawn through the points and fractional yields for the remaining fission reactions were read from that line. This straight-line correlation was found empirically to hold for fission products whose fractional yields are known in a number of fission reactions [3]. It is a consequence of the equal-charge-displacement rule introduced by Glendenin et al. [14] for predicting Z_p-values.

Table I shows the neutron emission probabilities obtained in this way assuming that only halogen precursors contribute. The results are compared with P_n-values measured by Aron et al. [15], and with values deduced from relative delayed neutron yields in the bromine and iodine fractions reported by Perlow and Stehney [16] and corroborated, except for ^{139}I, by us as will be shown below. While the calculated P_n-values of the bromine precursors compare favourably with experimental data, those of the iodine precursors are much higher than the experimental values. This may be explained by contributions of non-halogen precursors which are noticeable in the 6 and 2 sec period. In spite of these discrepancies, the observed delayed neutron yields in eleven low-energy reactions are well reproduced by using the calculated P_n-values, as demonstrated by Fig. 1 in which only very few points are really dropping out. Hence the neutron emission probabilities derived in this way may be used as apparent P_n-values of the halogen precursors for estimating unknown delayed neutron yields, starting with an estimate of their cumulative fission yields in the manner described above.

Next, the least-squares analysis was extended to three components in the 22, 6 and 2 sec period introducing the many possible precursors prospected by Pappas [17]. Unknown half-lives were extrapolated from known values of isotopes by plotting log $T_{\frac{1}{2}}$ versus mass number. If the answer was ambiguous, the precursor was assigned to two periods. It should be emphasized that only main contributors can be indicated by this approach. Several prospective precursors gave negative P_n-values and/or large standard deviations of P_n and Y_n. Those precursors which fit reasonably well are listed in Table II, which is compiled from more detailed tables published elsewhere [4]. The table gives the P_n-values of all three precursors and, in the last column, the estimated contribution of the third precursor to the periods in fission of ^{235}U by thermal neutrons. For comparison, the P_n-values of the halogen precursors calculated without introducing a third precursor are given, too. It should be noted that Table II is based on eleven fission reactions, in contrast to Table I.

To the 22 sec period, only ^{136}Te may contribute appreciably. This precursor would reduce the P_n-value of ^{137}I to the observed value of 3.0%. The same effect would occur on the P_n-value of ^{138}I if ^{136}Te would belong to the 6 sec period, in disagreement with a recent estimate of its

TABLE I

NEUTRON EMISSION PROBABILITIES
OF HALOGEN DELAYED NEUTRON PRECURSORS

Precursor nuclide	Neutron emission probability P_n (%) calculated[a]	observed[b]	observed[c]
^{87}Br	2.63 ± 0.05	3.1 ± 0.6	2.6 ± 0.5
^{88}Br	6.0 ± 1.0	6.0 ± 1.6	5.8 ± 1.6
^{89}Br	5.2 ± 1.1	7 ± 2	12 ± 3
^{90}Br	23 ± 3		15 ± 4
^{137}I	5.3 ± 0.6	3.0 ± 0.5	3.0 ± 0.5
^{138}I	7.3 ± 0.8	2.0 ± 0.5	2.2 ± 0.5
^{139}I	21 ± 3		4.5 ± 1.5
			11 ± 3[d]

[a] By least-squares analysis of seven fission reactions assuming that only halogen precursors contribute.
[b] ARON et al. (1964)[15].
[c] From relative neutron yields of PERLOW and STEHNEY[16] (1959), normalized at ^{87}Br and ^{137}I, respectively.
[d] From relative neutron yields reported in this work.

half-life, given as about 33 sec [18]. None of the other precursors inserted into the 6 sec period reduces the P_n-value of ^{138}I to the observed value of 2.0% and none should contribute more than a few percent to the period yield. It is interesting that ^{85}As, assigned to the 2 sec period on the basis of a fine-structure in the mass-yield curve [19], fits better the 6 sec period than the 2 sec period. On the whole, the fits of the 22 and 6 sec period are not much influenced by a third precursor. In contrast to that, the fits of the 2 sec period are considerably improved, as previously [3], with ^{94}Rb, ^{97}Sr, ^{142}Cs or ^{143}Cs as third precursors. Both caesium nuclides would also reduce the P_n-values of the halogen precursors to the observed values. Hence a search for delayed neutron precursors among the alkalies and alkaline earths was suggested [3].

Least-squares analyses with four components were tried but the results were not encouraging. Obviously the errors of the input data are too large for this purpose.

Several authors [5, 20] have pointed out that the observed delayed neutron yields in fission by 14 MeV neutrons are much higher than expected because, with increasing excitation of the fissioning nucleus, the fission chain length and, hence, the neutron yield should decrease instead

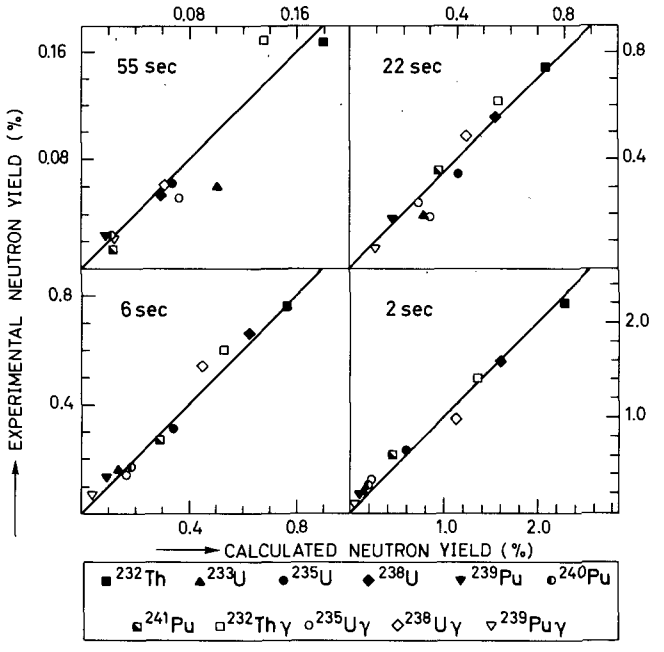

FIG. 1. Comparison of observed delayed neutron yields with yields calculated from cumulative fission yields of the halogen precursors and their neutron emission probabilities derived in this work. The fission reactions are: Fission of ^{233}U, ^{235}U, ^{239}Pu, and ^{241}Pu by thermal neutrons, of ^{232}Th, ^{238}U, and ^{240}Pu by fission neutrons, and of ^{232}Th, ^{235}U, ^{238}U, and ^{239}Pu by 15 MeV gamma rays.

of increase as reported. This qualitative argument can be stressed by an estimation of the expected yields using apparent P_n -values of the halogen precursors and their calculated cumulative fission yields [3]. We have repeated these computations with different approaches to the cumulative yields. The method which led to the best reproduction of available yield data in medium-energy fission follows a proposal of Coryell et al. [21]: The Z_p-value for the chain A is calculated from its Z_p -value in thermal neutron induced fission of ^{235}U by the formula:

$$\Delta Z_{p(A)} = 0.5(Z_c - 92) - 0.21(A_c - 236) + 0.19(\nu_A - \nu_A^r)\,(\nu_t / 2.46) \qquad (3)$$

The first and second term on the right correct for the effect of charge and mass number, Z_c and A_c, of the compound nucleus whereas the last term, which is modified compared to Coryell's formula [21], corrects for the effect of excitation energy via the neutron emission. Here ν_t is the average number of fission neutrons emitted in the reaction in question, and ν_A^r and ν_A are the number of neutrons emitted from the initial fragments of mass $A + \nu_A$ in the reference reaction [13, 23] and in the fission reaction at moderate excitation [8, 24, 25], respectively. From the Z_p-values, the fractional cumulative yields of the halogen precursors were then estimated using a charge distribution with c = 1.2. These fractional yields were finally multiplied by appropriate P_n -values taken from Table I and by mass yields from a recent compilation [6]. It should be mentioned that

TABLE II

CALCULATED NEUTRON EMISSION PROBABILITIES, P_n, OF NON-HALOGEN DELAYED NEUTRON PRECURSORS*

Period	Precursor	P_n-value (%) 3rd Precursor	Br	I	Contribution in $^{235}U(n_{th},f)$, (%)
22 sec	-	-	6.2	5.3	-
	^{136}Te	4 ± 2	6.0	2.9	28
6 sec	-	-	5.3	7.6	-
	^{85}As	8 ± 4	2.8	7.4	8
	^{93}Rb	0 ± 2	5.6	6.9	≤20
	^{135}Sn	85 ± 12	4.9	5.8	2
	^{136}Te	8 ± 3	7.8	≤2.5	56
	^{137}Te	2 ± 2	6.0	5.5	6
2 sec	-	-	27	18	-
	^{85}As	≤1	47	17	≤1
	^{86}As	-3 ± 30	36	16	≤8
	^{94}Rb	9 ± 5	31	13	24
	^{97}Sr	14 ± 8	36	12	17
	^{142}Cs	8 ± 2	22	11	41
	^{143}Cs	30 ± 8	13	11	60

* By least-squares analysis of eleven fission reactions.

the experimental data on the width of the charge distribution in medium-energy fission are contradictory: Several authors [8, 26, 27] found the same width as in low-energy fission, i.e. c = 0.8 to 0.9; others [28, 29] observed a broader distribution.

Table III shows the period yields calculated in this way and the observed values [30-36]. The calculated yields are, on the average, lower by a factor of two to three with increasing deviations in the 2 sec period. In some cases, as in the 55, 22, and 6 sec period in fission of ^{232}Th and ^{238}U, discrepancies persist even if chain yields are used which represent the upper limits of the cumulative fission yields.

3. DELAYED-NEUTRON STUDIES BY MEANS OF RAPID CHEMICAL SEPARATIONS

Several delayed neutron studies by means of rapid chemical separations [37] are now in progress on the 100 kW reactor and Cockcroft-Walton accelerator of our laboratory. Similar experimental arrangements are

TABLE III

OBSERVED AND CALCULATED DELAYED NEUTRON YIELDS IN FISSION REACTIONS INDUCED BY 14-MeV NEUTRONS

Target		Delayed-neutron yield (%)				References	
		55 sec	22 sec	6 sec	2 sec	rel.	absol. yield
^{232}Th	obs.	0.34	1.20	1.32	3.33	a	b,c
	calc.	0.11	0.41	0.32	0.67		
^{233}U	obs.	0.095	0.25	0.11	0.76	d	d
	calc.	0.068	0.16	0.082	0.10		
^{235}U	obs.	0.13	0.47	0.53	1.04	a	b,f
	calc.	0.066	0.26	0.16	0.27		
^{238}U	obs.	0.15	1.14	1.16	2.80	a	b,f,g
	calc.	0.058	0.34	0.30	0.65		
^{239}Pu	obs.	0.083	0.32	0.29	0.61	e	c
	calc.	0.029	0.15	0.078	0.11		

[a] MAKSYUTENKO (1958) [30]. [b] MAKSYUTENKO (1959) [33].
[c] SHPAKOV et al. (1962) [35]. [d] MAKSYUTENKO (1963b) [32].
[e] MAKSYUTENKO (1963a) [31]. [f] McGARRY et al. (1960) [34].
[g] BUZKO (1966) [36].

being used at both installations. Fig. 2 shows schematically the arrangement at the reactor. A rapid pneumatic system [38] is built into one of the beam holes. The sample, a solution, encapsulated in a small polystyrene or glass vial, and weighing about 5 g, is put into a shielded stand-by position from where it is shifted to the irradiation position by applying vacuum. For short irradiations, the reactor can be pulsed from 50 W to 250 MW with a pulse half-width of 40 msec. Such a pulse gives at the irradiation position an integrated thermal neutron flux of 7×10^{13} n cm^{-2} compared to a flux of 4×10^{11} n cm^{-2} sec^{-1} during long irradiations.

The Cerenkov radiation produced during a pulse is utilized to start, via photodiodes, a programmer which controls the following cycle: It opens a valve of a vessel filled with nitrogen at 1.5 to 3 atm pressure, transferring the sample in within 0.15 sec to the separation apparatus shown in the right hand side of Fig. 2. There the sample is smashed as it hits the walls of a polycarbonate container. The solution is immediately sucked through a thin layer of a preformed precipitate, followed by a washing solution injected with a syringe. The precipitate takes up the desired element by isotopic or ion exchange [39] which proceeds, in favourable cases, so rapidly that individual elements can be isolated nearly quantitatively within one or two seconds. The decay of the neutron activity is followed with ^{3}He-detectors embedded in paraffin, using a

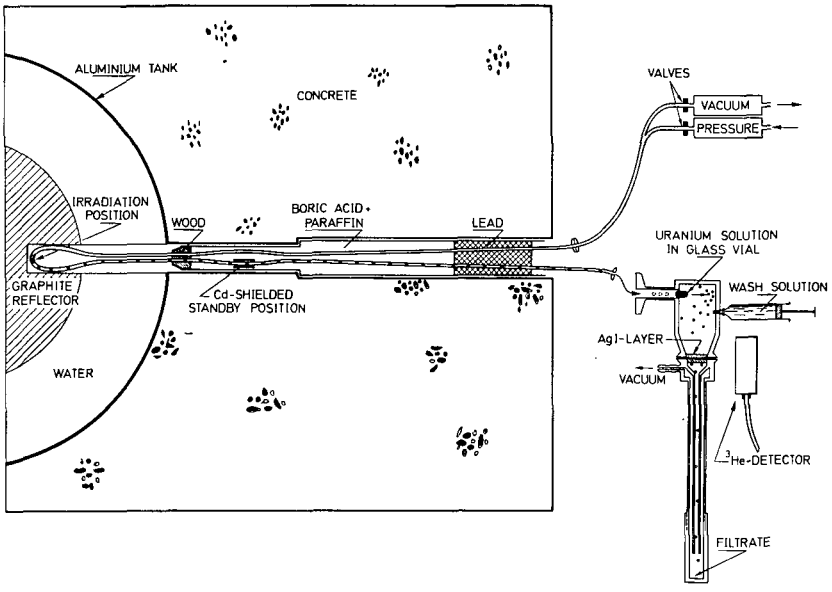

FIG. 2. Arrangement for studies on delayed fission neutrons by rapid chemical separations at the Mainz Triga reactor. The left part shows the pneumatic system installed into a beam hole, the right part on enlarged scale the apparatus for separations by exchange with preformed precipitates, e.g. of iodine nuclides by exchange with preformed silver iodide layers.

multichannel analyser in the multiscaler mode controlled by an electronic programmer.

The experiments with 14.5 MeV neutrons reported here were carried out with fluxes of about 5×10^{9} n cm^{-2} sec^{-1}. Due to an improvement of the target system, fluxes of 6×10^{10} n cm^{-2} sec^{-1} were recently attained in routine operation.

The main delayed neutron precursors, isotopes of bromine and iodine, can be simultaneously separated by exchange with silver chloride [39]. Hence by counting the delayed neutron activity remaining in the filtrate, the total contribution of non-halogen precursors to the various periods can be measured [1-4]. In a typical run, several micrograms of ^{235}U are irradiated in 2 cm^{3} 0.5N nitric acid containing sulphur dioxide as reducing agent, 0.1 mg each of bromide and iodide as carriers and ^{82}Br and ^{131}I as radioactive tracers. The preformed precipitate consists of 35 mg of silver chloride on an area of 3.1 cm^{2}. As washing solution, 3 cm^{3} of 0.5N nitric acid are used. When the counting of the neutron decay-curve is completed, the tracer nuclides are counted in the filtrate by gamma-spectrometry to correct for a breakthrough of a small fraction of halogen precursors due to the very short contact between solution and precipitate. Detailed tests have ascertained that tracer and radioisotope behave identically during the whole procedure and that no appreciable fractions of other elements are 'co-separated' on the silver chloride layer [39]. For mutual normalization of various runs and for comparison with the neutron decay-curve of unseparated samples, ^{99}Mo is isolated and counted as fission monitor. In experiments with 14 MeV neutrons,

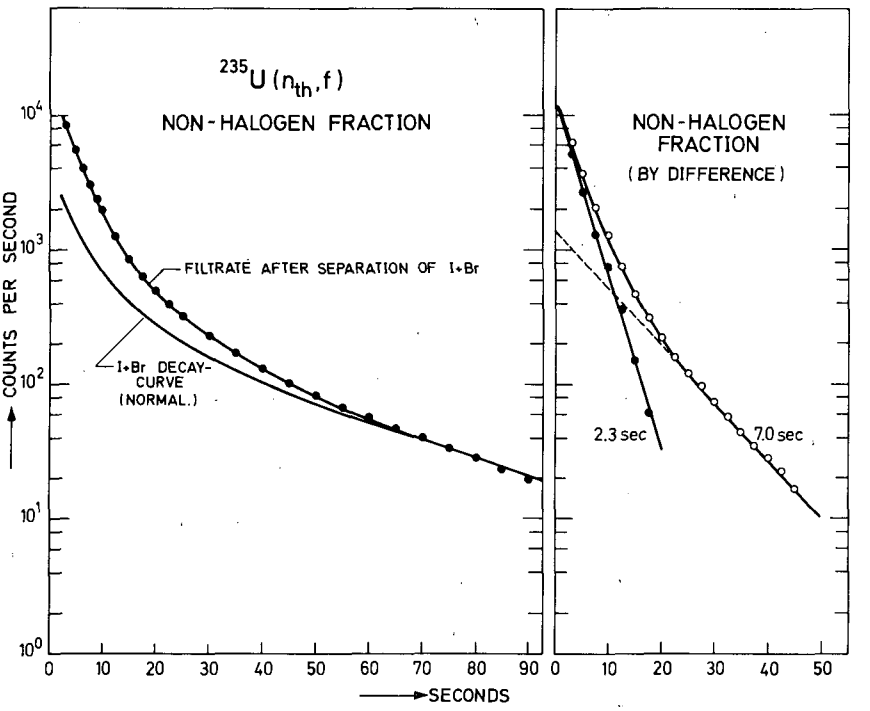

FIG. 3. Decay curve of non-halogen delayed neutron precursors in fission of ^{235}U by thermal neutrons. The counting rates plotted in the left part were measured in the filtrate remaining after bromine and iodine nuclides were removed by exchange with silver chloride. After subtraction of residual halogen activities, the curve plotted at right is obtained showing the decay of the non-halogen delayed neutron precursors.

about one gram of natural uranium or thorium were irradiated in nitric acid solution.

This technique was applied to the fission of ^{235}U by thermal neutrons and of ^{232}Th and ^{238}U by 14 MeV neutrons. Fig. 3 shows the neutron decay curve of a ^{235}U sample after a pulsed irradiation and after most of the halogen precursors were removed. The remaining halogen activity can be corrected for by means of a composite neutron decay curve of both halogens, obtained by counting the silver chloride layer instead of the filtrate and adjusted to the curve measured in the filtrate according to the ^{82}Br, ^{131}I, and ^{99}Mo data. The difference of both curves, shown in the right part of Fig. 3, corresponds then to the decay curve of the non-halogen precursors. This curve consists of two components of 2.0 to 2.5 and 6 to 7 sec half-life. Their initial activities can be compared with period activities deduced from the decay curve of an unseparated sample after normalization to the same number of fissions. In some cases, the original decay curve was first analysed for initial activities by computer analysis using half-lives reported for unseparated samples [5], and then the appropriate corrections for the contribution of halogen precursors were made.

TABLE IV

CONTRIBUTIONS OF NON-HALOGENS
TO THE DELAYED NEUTRON YIELDS OF THE 6-sec AND 2-sec PERIOD

Target	Neutron-Energy	Contribution of non-halogens (%) 6 sec	2 sec
^{235}U	thermal	10 ± 5	30 ± 10
^{238}U	14 MeV	19 ± 6	40 ± 10
^{232}Th	14 MeV	22 ± 6	48 ± 10

Table IV gives the total contributions of non-halogen precursors to the various periods which follow from our experiments. The 55 and 22 sec period are not listed because their residual activities could always be explained, according to the tracer data, by residual amounts of halogen precursors. We estimate that, in fission of ^{235}U by thermal neutrons less than 3%, in the other two reactions less than 5% of both periods originate from non-halogens. With more extended chemical treatment, Williams and Coryell [40] set an upper limit of 0.5% for the contribution of non-halogens to the 55 sec period in thermal neutron induced fission of ^{235}U. In the shorter periods, the contributions of non-halogens are comparable in magnitude within each period for all three reactions. Our results for ^{235}U corroborate the findings of Cowan and Orth [41] who concluded from volatilization studies that at least 80% of the delayed neutrons observed in this reaction originate from halogen precursors. The contributions of non-halogens found here for the fission of ^{232}Th and ^{238}U by 14 MeV neutrons are much too low to account for the discrepancy between observed and expected delayed neutron yields discussed above. If unknown precursors do cause the high observed yields, then they should contribute 60 to 80% of the total yield, as follows from Table III.

Iodine precursors can be separated selectively by isotopic exchange with silver iodide in presence of 5 to 10 mg of bromide as hold-back carrier. The yield is about 90% with less than 2% contamination by bromine precursors [39]. Fig. 4 shows a neutron decay-curve of the iodine fraction isolated from ^{235}U after a pulsed irradiation with thermal neutrons. The resulting half-lives and relative delayed neutron yields agree, as indicated in Fig. 4, with the values reported by Perlow and Stehney [16], except for the 2.1 sec period whose contribution is higher in our results. As mentioned above, our value is more compatible with the results of the least-squares analyses described in Section 2. The most interesting part of Fig. 4 is, of course, the insert with the initial part of the decay curve. Here a previously unknown, strong iodine precursor of about 0.8 sec half-life is clearly observed. This should be ^{140}I.

The decay curve of the bromine precursors can be obtained as demonstrated in Fig. 5. From a composite curve of bromine and iodine precursors, the decay curve of the iodine precursors is subtracted after normalization via the tracer and ^{99}Mo data. The half-lives and relative

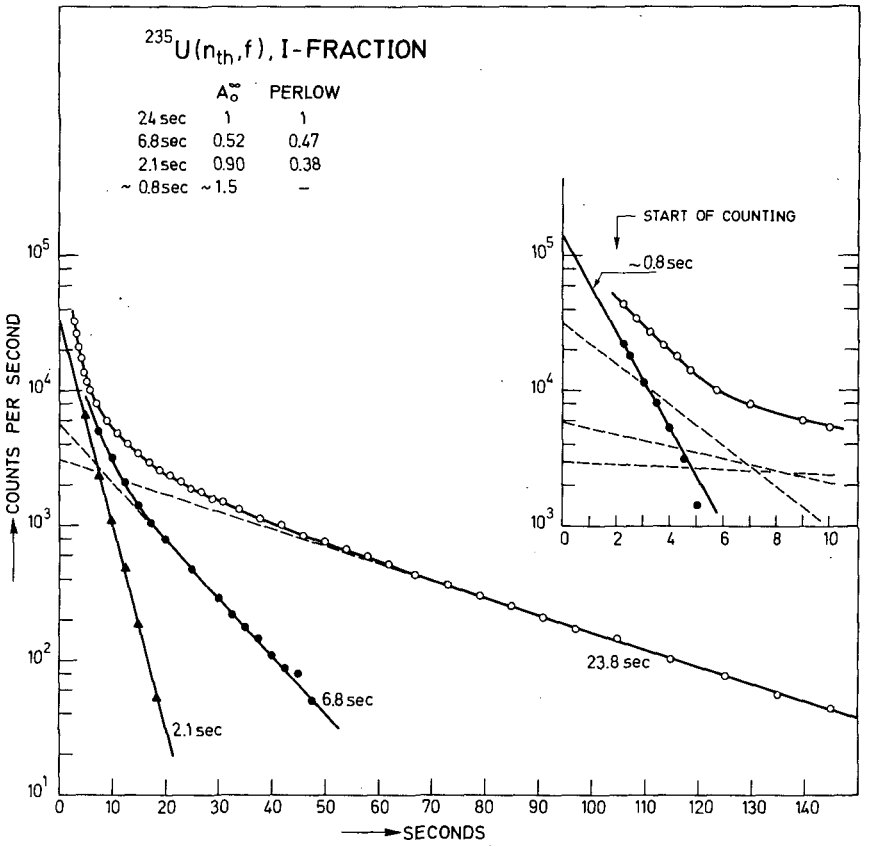

FIG. 4. Decay curve of iodine delayed neutron precursors in fission of ^{235}U by thermal neutrons, isolated by exchange with silver iodide. The insert shows the initial part of the curve. The resulting relative delayed neutron yields are compared with values reported by Perlow and Stehney [16].

yields of the bromine precursors deduced from the differences agree, as Fig. 5 shows, with the results of Perlow and Stehney [16]. Only the half-life of ^{90}Br deviates somewhat from their value of 1.6 ± 0.6 sec but our value has probably an error of similar magnitude.

An advantage of our technique is that the delayed neutron activities in the bromine and in the iodine fraction can be correlated to each other. From data shown in Fig. 5 we conclude that ^{137}I contributes 68%, ^{88}Br 32% to the halogen delayed neutron activity in the 22 sec period in thermal neutron induced fission of ^{235}U. This result compares fairly well with an iodine contribution of (57 ± 11)% obtained by Keepin [5] in a computer analysis of the neutron decay curve of unseparated samples. Since we do not find any appreciable content of non-halogen precursors in that period, we can infer from the period yield, 0.346 neutrons/100 fissions [5], that ^{137}I contributes 0.234, and ^{88}Br 0.112 neutrons per 100 fissions. By multiplying these numbers by the relative yields of iodine and bromine precursors given in Figs 4 and 5, absolute delayed neutron yields of all halogen precursors can be derived; these are listed in the upper part

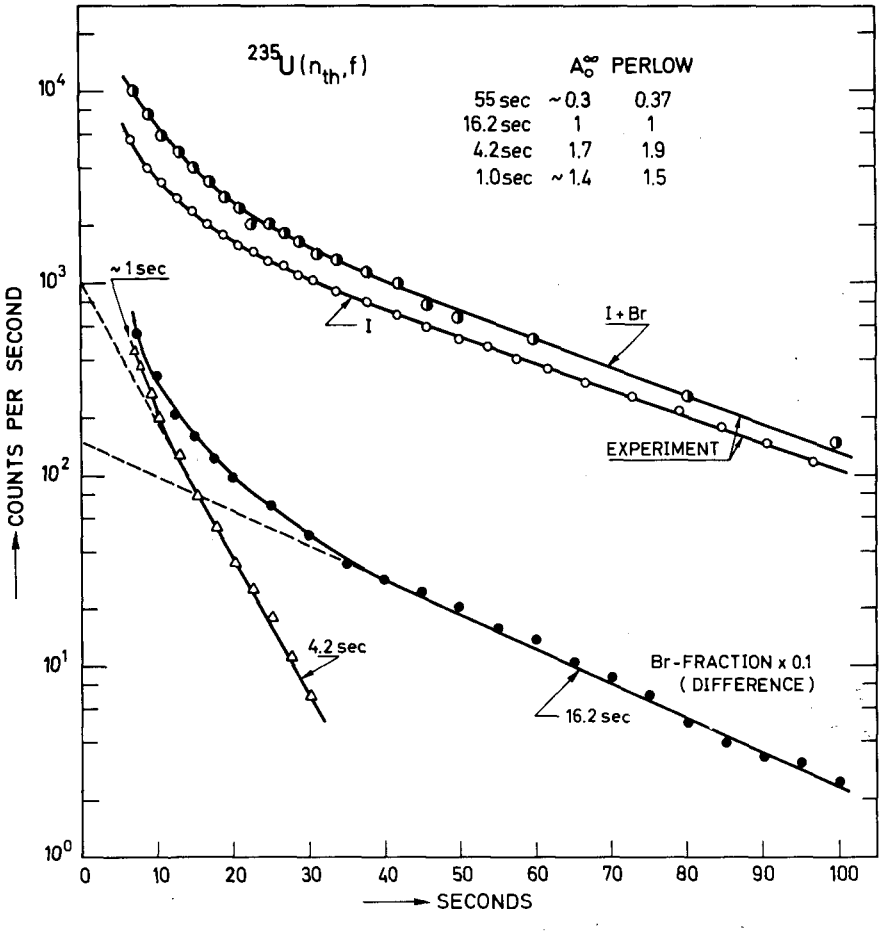

FIG. 5. Decay curve of bromine delayed neutron precursors in fission of ^{235}U by thermal neutrons, obtained by subtracting the decay curve of the iodine precursors from the composite curve of bromine and iodine precursors which were simultaneously isolated by exchange with silver chloride. Again the relative yields are compared with those of Perlow and Stehney.

of Table V. In the lower part, the same individual yields are given as fractions of the period yields. If we now add the contributions of non-halogen precursors taken from Table IV, we obtain in all four periods, within the limits of error, 100%. This shows the consistency of the results derived from different sets of experimental data.

Finally the neutron emission probabilities of the halogen precursors can be estimated by comparing their absolute delayed neutron yields given in Table V with their cumulative fission yields calculated as given in Section 2. The results, which are necessarily rather crude, tend to confirm the experimental P_n-values of the bromine precursors listed in Table I. For the iodine precursors, however, they are much higher than the experimental values of Aron et al. [15], e.g. 5.3% instead of 3.0% [15] for ^{137}I. Renormalization to 5.3% for that precursor would nearly double the P_n-values of the iodine precursors given in the last

TABLE V

DELAYED NEUTRON YIELDS FROM INDIVIDUAL PRECURSORS IN FISSION OF ^{235}U BY THERMAL NEUTRONS

Scale	Precursor	Period			
		55 sec	22 sec	6 sec	2 sec
Absolute[a]	Br	0.056	0.112	0.194	0.157
	I	-	0.234	0.122	0.211
	Total	0.056	0.346[b]	0.316	0.368
	Period yield[c]	0.052	0.346	0.310	0.624
Relative[d]	Br	107	32	63	25
	I	-	68	39	34
	Non-halogens	≤0.5[e]	≤5	10	30
	Rb			~10	
	As				~10[f]
	Alkalies				~20
	Total	107	100[b]	112	89

[a] Neutrons/100 fissions, based on relative neutron yields of Br- and I-precursors and their contributions to the 22-sec period, as reported in this work.

[b] Normalized.

[c] KEEPIN, WIMETT and ZEIGLER (1957)[49].

[d] Relative to the period yield (= 100).

[e] WILLIAMS and CORYELL (1966)[40].

[f] DEL MARMOL and NÈVE DE MÉVERGNIES (1967)[19].

column of Table I, and would bring them closer to the values resulting in the least-squares analyses listed in the second column.

As pointed out in Section 2, a search for delayed neutron precursors among the alkalies seemed to be of interest. A rapid separation of both caesium and rubidium, or only of caesium, can be achieved by exchange with preformed ammonium phosphomolybdate [39, 42]. The sample is irradiated in 0.5N nitric acid in presence of hold-back carriers for the halide ions and, if only caesium is desired, for rubidium. Chemical yields of the alkalies and contamination by halogens are monitored by adding appropriate tracers. A neutron decay-curve obtained in such an experiment with ^{235}U is shown in Fig. 6. After correcting for the halogen contamination by subtracting their composite decay curve, the curve plotted in the right hand side of Fig. 6 results. It shows two components of 2.3 and 5.9 sec half-life, contributing about 20% and 10% to the 2 sec

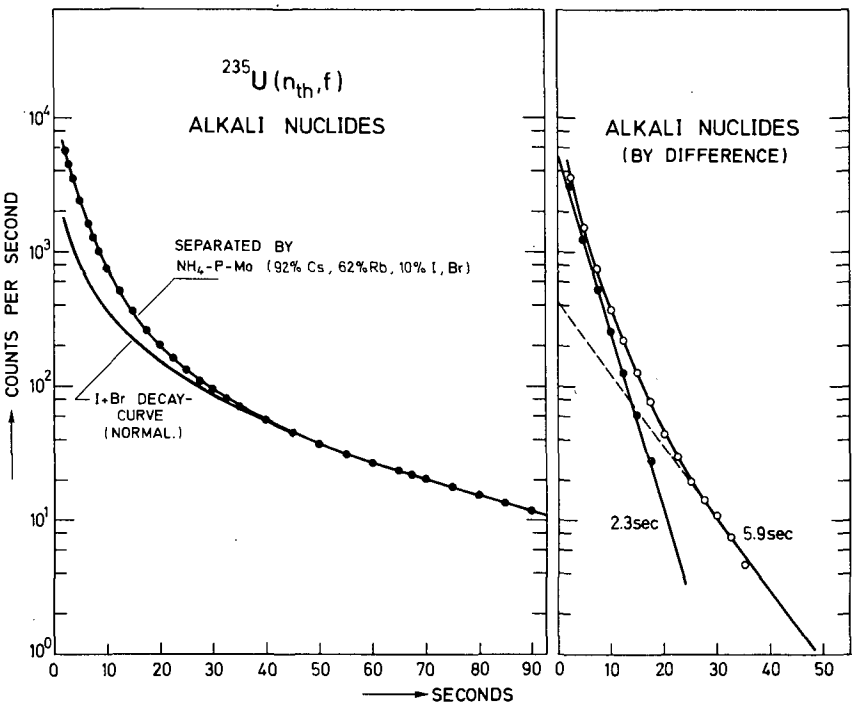

FIG. 6. Decay curve of alkali delayed neutron precursors in fission of ^{235}U by thermal neutrons. The counting rates plotted on the left were measured in an ammonium phosphomolybdate layer after exchange with the given fractions of caesium and rubidium nuclides. After subtraction of the halogen contamination the curve, plotted on the right, is obtained showing the decay of alkali delayed neutron precursors.

and 6 sec periods, respectively, in the fission of ^{235}U by thermal neutrons, as follows from a comparison with decay curves of unseparated samples.

A 6 sec delayed neutron precursor has been discovered among the rubidium isotopes by Stehney and Perlow [43] but the intensities found in our experiments are much higher than expected from their data. A contribution of caesium precursors is unlikely, because no isotope of this half-life has been observed in fission [44], and no 6 sec component appears in the neutron decay-curve of a pure caesium fraction. The most probable assignment is, thus, ^{93}Rb with a P_n-value of about 1%, following from its neutron and fission yields. The 2 sec component may be assigned, according to published half-lives [44], to ^{94}Rb, ^{142}Cs or ^{143}Cs. Since this component is also observed in a pure caesium fraction, one of the caesium isotopes should be a main contributor. Assuming that half of the 2 sec component originates from ^{94}Rb, half from one of the caesiums, we estimate P_n-values of about 3% for ^{142}Cs and about 5% for ^{94}Rb and ^{143}Cs.

It is interesting to compare the total contributions of non-halogen precursors measured in this work with the contributions of the individual precursors identified so far. As Table V shows, the 6 sec ^{93}Rb may account for the non-halogen fraction in that period, and the 2 sec alkali precursors and ^{85}As, whose contribution was estimated by del Marmol

[19], may explain the non-halogen fraction in the 2 sec period. This remarkable balance may be fortuitous because all the data entering have still considerable errors. Nevertheless it may be concluded that the main contributions to the four longest delayed neutron periods have now been identified.

With regard to separation time, the techniques described here can certainly be improved by using thinner precipitate layers giving shorter suction times, This would, of course, reduce the chemical yields. Separation times of about 1 sec might be achieved in this fashion. Even faster separations are conceivable via the gas phase by stopping fission recoil atoms in methane, where the halogens react to volatile methyl halides [45] with about 15% yield [46], which can be increased by a factor of two to three if methyl iodide is used as medium [47]. Rapid separations of methyl iodide and bromide in flowing methane by selective adsorption have been reported [48]. Therefore it seems to be possible to isolate even the halogen precursors expected to contribute to the 0.2 sec period.

4. ABSOLUTE DELAYED NEUTRON YIELDS IN FISSION OF ^{232}Th AND ^{238}U BY 14 MeV NEUTRONS

Since the high absolute delayed neutron yields in fission of ^{232}Th [33, 35] and ^{238}U [33, 34, 36] by 14 MeV neutrons cannot be explained by strong contributions of unknown precursors, we remeasure these yields using a novel technique which involves no absolute counting of neutron or fission rates: the neutron yields are determined by comparison with a reference reaction for which absolute delayed neutron yields are accurately known, as fission of ^{235}U by thermal neutrons. Both the samples produced by the fission reaction in question, x, and by the reference reaction, r, are counted in the same neutron counter, and from both samples ^{99}Mo is isolated and counted in the same beta-counter. In both reactions, the initial counting rates, I_n^0, of the delayed neutron periods are thus related to the initial counting rate, I_{Mo}^0, of the fission monitor ^{99}Mo. This correlation is calibrated in terms of absolute delayed neutron yields, Y_n, by the experiments with the reference reaction. One has, of course, to take into account that the fission yields, Y_{Mo}, of ^{99}Mo differ in both reactions:

$$Y_{n(x)} = Y_{n(r)} \frac{R_x}{R_r} \frac{Y_{Mo(x)}}{Y_{Mo(r)}}, \qquad (4)$$

with $R = I_n^0 / I_{Mo}^0$. As reference reactions, fission of ^{235}U by thermal neutrons and, in early runs [1], of ^{232}Th by unmoderated Be-D-neutrons were used. In the latter case, the average neutron energy should be comparable to that of fission neutrons. Absolute delayed neutron yields of the reference reactions were taken from Keepin et al. [49]. Fission yields of ^{99}Mo were averaged from published values for the fission of ^{232}Th [50-52] and ^{238}U [53-55] by 14 MeV neutrons, of ^{232}Th by fission neutrons [51, 56-59], and of ^{235}U by thermal neutrons [54, 60, 61] which agree in each case to within a few percent.

The measurements were performed in two steps. First, the absolute yields of the 55, 22, and 6 sec periods were measured in long irradiations.

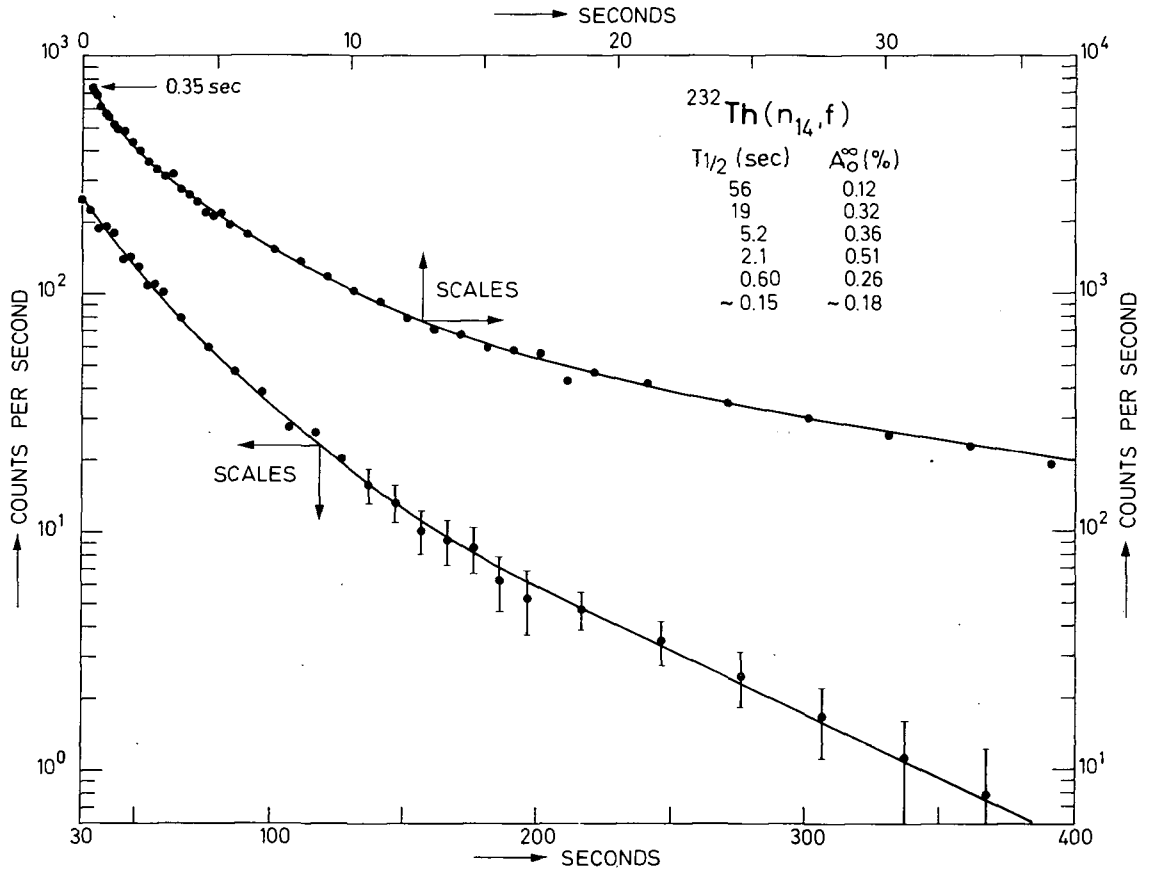

FIG. 7. Delayed neutron decay curve in fission of ^{232}Th by 14 MeV neutrons, recorded without chemical treatment after a 6 sec irradiation. The insert shows the periods and their absolute yields (neutrons/100 fissions) derived from this decay curve.

Then the yields of the shorter periods were determined relative to those values in 6 sec irradiations. In the bombardments with 14 MeV neutrons, samples of several grams of ^{238}U (99.7%) or ^{232}Th metal were placed in a pneumatic system directly below the target and transferred after irradiation to the neutron counter set in a shielded room about eight metres from the target. The accelerator was switched off during the counting operation. Six BF_3 counting tubes embedded in paraffin were used as counter. The data were registered by a multichannel analyser. Irradiation and counting were repeated several times, and the corresponding counts were summed. For the reference reaction, 50 mg of ^{235}U (90%) were irradiated with Be-D-neutrons slowed down in paraffin, the thermal neutron flux was about 5×10^8 n cm^{-2} sec^{-1}. After several cycles, the samples were dissolved, and ^{99}Mo was isolated by standard procedures. The ^{99}Mo samples were counted with an end-window beta-counter. The results were corrected, as usual, for self-absorption, chemical yields, etc. Decay curves were analysed by the least-squares method using a computer. In the case of the neutron data, this analysis was performed with the periods reported by Keepin et al. [49] for the reference reactions and by Maksyutenko [30] for the reactions in question.

TABLE VI

ABSOLUTE YIELDS OF DELAYED NEUTRON PERIODS IN FISSION OF ^{232}Th AND ^{238}U BY 14-MeV NEUTRONS

Period	Absolute yields (neutrons/100 fissions)[a]			
	^{232}Th		^{238}U	
	measured	expected[b]	measured	expected[b]
55 sec	0.12 ± 0.02[c]	0.11	0.060 ± 0.012	0.058
	0.13 ± 0.03[d]			
22 sec	0.35 ± 0.07[c]	0.41	0.37 ± 0.06	0.34
	0.40 ± 0.13[d]			
6 sec	0.32 ± 0.08[c]	0.32	0.48 ± 0.12	0.30
	0.51 ± 0.22[d]			
2 sec	0.56	0.67	0.76	0.65
0.5 sec	0.28		0.39	
0.2 sec	0.20		0.18	
Total	1.9 ± 0.5		2.2 ± 0.6	

[a] Quoted with ± 2σ-errors of the mean values.

[b] Based on cumulative fission yields of halogen precursors and their neutron emission probabilities, see Table III.

[c] By comparison with fission of ^{235}U by thermal neutrons.

[d] By comparison with fission of ^{232}Th with 3-MeV neutrons.

In the short irradiations, the pneumatic system was initiated automatically when the accelerator was switched off. The first count could be started 0.3 sec after irradiation. Fig. 7 shows a neutron decay-curve summed from several short bombardments of ^{232}Th with 14 MeV neutrons. These curves have not yet been fully analysed due to problems arising from the rather low statistical accuracy. The half-lives and neutron yields given in Fig. 7 are results of a preliminary analysis of that particular curve.

The resulting absolute delayed neutron yields in fission of ^{232}Th and ^{238}U by 14 MeV neutrons are summarized in Table VI. The shortest periods are listed without errors because of the preliminary nature of these values. Conclusions on the absolute yields, however, are not sensitive to the uncertainties because the total yields of these short periods would not change much if the individual yields are varied. As noted previously [3] for the four longest periods, we can not corroborate the unexpectedly high delayed neutron yields of about 7 neutrons/100 fissions [33-36] compared to 4.96 and 4.12 neutrons per 100 fissions found in fission of ^{232}Th and ^{238}U, respectively, by fission neutrons [49]. Our yields indicate a decrease rather than an increase of the delayed neutron emission with increasing excitation energy of the fissioning nucleus. Our results are in marked agreement with the expected values derived in Section 2, and are shown again in Table VI. We shall continue these measurements making use of the high fluxes of 14 MeV neutrons now available at this laboratory.

ACKNOWLEDGEMENTS

We wish to thank Professor F. Strassmann for his continued interest, and the staff of the Triga research reactor and the Cookcroft-Walton accelerator at this laboratory for their co-operation. We are indebted to the Bundesministerium für wissenschaftliche Forschung as well as to the Fonds der Chemischen Industrie for financial support of this work.

REFERENCES

[1] FIEDLER, H.J., HERRMANN, G., paper presented at the "Discussions on Nuclear Chemistry", Oxford, Sept. 1962.

[2] FIEDLER, H.J., Dissertation, Mainz (Nov. 1963).

[3] HERRMANN, G., FIEDLER, H.J., BENEDICT, G., ECKHARDT, W., LUTHARDT, G., PATZELT, P., SCHÜSSLER, H.D., Physics and Chemistry of Fission (Proc. Symp. Salzburg 1965) 2, IAEA, Vienna (1965) 197.

[4] PATZELT, P., SCHÜSSLER, H.D., HERRMANN, G., Proc. Symp. Why and How Should we Investigate Nuclides Far Off the Stability Line?, Lysekil, Aug. 1966, proceedings to be published in Ark. Fys. (in press).

[5] KEEPIN, G.R., Ch. 4, Physics of Nuclear Kinetics, Addison-Wesley, Mass. (1965).

[6] HERRMANN, G., Habilitationsschrift, Mainz (June 1961), rev. ed. Radiochim. Acta, to be published.

[7] WAHL, A.C., FERGUSON, R.L., NETHAWAY, D.R., TROUTNER, D.E., WOLFSBERG, K., Phys. Rev. 126 (1962) 1112.

[8] WOLFSBERG, K., Phys. Rev. 137 (1965) B 929.

[9] STROM, P.O., LOVE, D.L., GREENDALE, A.E., DELUCCHI, A.A., SAM, D., BALLOU, N.E., Phys. Rev. 144 (1966) 984.

[10] STROM, P.O., DELUCCHI, A.A., GREENDALE, A.E., BALLOU, N.E., LOVE, D.L., SAM, D., Paper presented at the 151st meeting Am. Chem. Soc., Pittsburgh (March 1966).

[11] NIKOTIN, O.P., PETRZHAK, K.A., Atomn. Energ. 20 (1966) 268.
[12] WAHL, A.C., Review paper presented at the 151st meeting Am. Chem. Soc., Pittsburgh (March 1966).
[13] APALIN, V.F., GRITSYUK, Yu.N., KUTIKOV, I.E., LEBEDEV, V.I., MIKAELYAN, L.A., Nucl. Phys. 55 (1964) 249.
[14] GLENDENIN, L.E., CORYELL, C.D., EDWARDS, R.R., in Radiochemical Studies: The Fission Products (CORYELL, C.D., SUGARMAN, N., Eds) McGraw-Hill, New York (1951) 489.
[15] ARON, P.M., KOSTOCHKIN, O.I., PETRZHAK, K.A., SHPAKOV, V.I., Atomn. Energ. 16 (1964) 368; English transl. Soviet J. atomic Energy 16 (1965) 447.
[16] PERLOW, G.J., STEHNEY, A.F., Phys. Rev. 113 (1959) 1269.
[17] PAPPAS, A.C., Int. Conf. peaceful Uses atom. Energy (Proc. Conf. Geneva, 1958) 15, UN, New York (1958) 373.
[18] WUNDERLICH, F., Radiochim. Acta (in press).
[19] DEL MARMOL, P., NÈVE DE MÉVERGNIES, M., J. inorg. nucl. Chem. 29 (1967) 273.
[20] AMIEL, S., Physics and Chemistry of Fission (Proc. Symp. Salzburg, 1965) 2, IAEA, Vienna (1965) 171.
[21] CORYELL, C.D., KAPLAN, M., FINK, R.D., Canad. J. Chem. 39 (1961) 646.
[22] LEACHMAN, R.B., Int. Conf. peaceful Uses atom. Energy (Proc. Conf. Geneva, 1958) 15, UN, New York (1958) 229.
[23] TERRELL, J., Phys. Rev. 127 (1962) 880.
[24] WHETSTONE, S.L., Phys. Rev. 133 (1964) B 613.
[25] WHETSTONE, S.L., BRITT, H.C., Phys. Rev. 133 (1964) B 603.
[26] NETHAWAY, D.R., LEVY, H.B., Phys. Rev. 139 (1965) B 1505.
[27] McHUGH, J.A., Rep. UCRL 10673 (1963).
[28] PATE, B.D., FOSTER, J.S., YAFFE, L., Canad. J. Chem. 36 (1958) 1691.
[29] WOOGMAN, N.A., POWERS, J.A., COBBLE, J.W., PHYS. Rev. 152 (1966) 1088.
[30] MAKSYUTENKO, B.P., Zh. eksp. teor. Fiz. 35 (1958) 815; English transl. Soviet Phys. JETP 35 (1959) 565.
[31] MAKSYUTENKO, B.P., Atomn. Energ. 15 (1963) 157; English transl. Soviet J. atomic Energy 15 (1964) 848.
[32] MAKSYUTENKO, B.P., Atomn. Energ. 15 (1963) 321; English transl. Soviet J. atomic Energy 15 (1964) 1042.
[33] MAKSYUTENKO, B.P., Atomn. Energ. 7 (1959) 474; German transl. Kemenergie 3 (1960) 590.
[34] McGARRY, W.I., OMOHUNDRO, R.J., HOLLOWAY, G.E., Bull. Am. phys. Soc. 5 (1960) 33.
[35] SHPAKOV, V.I., PETRZHAK, K.A., BAK, M.A., KOVALENKO, S.S., KOSTOCHKIN, O.I., Atomn. Energ. 11 (1961) 539; English transl. Soviet J. atomic Energy 11 (1962) 1190.
[36] BUZKO, M., Atomn. Energ. 20 (1966) 153.
[37] HERRMANN, G., Review paper, Why and How Should We Investigate Nuclides Far Off the Stability Line? (Proc. Symp. Lysekil, Aug. 1966), Proceedings to be published in Ark. Fys. (in press).
[38] HÜBNER, K., Atomkemenergie 10 (1965) 169.
[39] ECKHARDT, W., HERRMANN, G., SCHÜSSLER, H.D., Z. analyt. Chem. 226 (1967) 71.
[40] WILLIAMS, E.T., CORYELL, C.D., Nuclear Applic. 2 (1966) 256.
[41] COWAN, G.A., ORTH, C.J., Int. Conf. peaceful Uses atom. Energy (Proc. Conf. Geneva, 7, UN, New York (1958) 328.
[42] FIEDLER, H.J., ARCHER, N., Z. analyt. Chem. 226 (1967) 114.
[43] STEHNEY, A.F., PERLOW, G.J., Bull. Am. phys. Soc. 6 (1961) 62; and private communication (1961).
[44] HERRMANN, G., Radiochim. Acta 3 (1964) 169.
[45] DENSCHLAG, H.O., HENZEL, N., HERRMANN, G., Radiochim. Acta 1 (1963) 172.
[46] DENSCHLAG, H.O., Dissertation, Mainz (July 1965).
[47] AMIEL, S., PAISS, Y., Rep. IA-1096 (Feb. 1967).
[48] SILBERT, M.D., TOMLINSON, R.H., Radiochim. Acta 5 (1966) 217.
[49] KEEPIN, G.R., WIMETT, T.F., ZEIGLER, R.K., Phys. Rev. 107 (1957) 1044.
[50] VLASOV, V.A., ZYSIN, Yu.A., KIRIN, I.S., LBOV, A.A., OSYAEVA, L.I., SELCHENKOV, L.I., Rep. Glavnoe Upravlienie po Ispolzovaniyu Atomnoi Energii pri Sovete Ministrov SSSR Moskva (1960); English transl. AEC-tr-4665 (1960).
[51] BROOM, K.M., Phys. Rev. 133 (1964) B 874.
[52] LYLE, S.J., MARTIN, G.R., WHITLEY, J.E., Radiochim. Acta 3 (1964) 80.
[53] STEVENSON, P.C., HICKS, H.G., ARMSTRONG, J.C., GUNN, S.R., Phys. Rev. 117 (1960) 186.
[54] TERRELL, J., SCOTT, W.E., GILMORE, J.S., MINKKINEN, C.O., Phys. Rev. 92 (1953) 1091.

[55] JAMES, R.H., MARTIN, G.R., SILVESTER, D.J., Radiochim. Acta 3 (1964) 76.
[56] TURKEVICH, A., NIDAY, J.B., Phys. Rev. 84 (1951) 52.
[57] IYER, R.H., MATHEWS, C.K., RAVINDRAN, N., RENGAN, K., SINGH, D.V., RAMANIAH, M.V., SHARMA, H.D., J. inorg. nucl. Chem. 25 (1963) 465.
[58] CROOK, J.M., VOIGT, A.F., Rep. ISC-558 (1963).
[59] WYTTENBACH, A., VON GUNTEN, H.R., DULAKAS, H., Radiochim. Acta 3 (1964) 118.
[60] REED, G.W., TURKEVICH, A., Phys. Rev. 92 (1953) 1473.
[61] FORD, G.P., GILMORE, J.S., Rep. LA-1997 (1956).

EMISSION DE NEUTRONS DIFFERES DANS LES REACTIONS NUCLEAIRES INDUITES PAR DES PARTICULES DE HAUTE ENERGIE

H. GAUVIN
INSTITUT DE PHYSIQUE NUCLEAIRE,
FACULTE DES SCIENCES DE PARIS ET D'ORSAY,
ORSAY, FRANCE

Abstract — Résumé

EMISSION OF DELAYED NEUTRONS IN NUCLEAR REACTIONS INDUCED BY HIGH ENERGY PARTICLES. A review of recent results on delayed neutrons from nuclear reactions at high energy is presented. A survey of new precursors, identified or expected in light nuclei, and obtained by spallation and fragmentation reactions, is followed by a more careful examination of the fission reactions. At medium and high energies, two problems have been considered: characteristics of the delayed neutron emission and identification of new precursors. At present, the unambiguous characterization of short-lived precursors represents one of the most important problems. Using an on-line mass spectrometer, isotopes of rubidium and caesium, produced by fission in a uranium target bombarded by a 150 MeV proton beam, have been separated and analysed. Systematic research resulted in the identification of the following precursors: isotopes 93, 94, 95, 96 of rubidium, and 142, 143 of caesium. The results are discussed. The general characteristics of emission of delayed neutrons accompanying the ^{238}U fission by protons at 150 MeV, 1 and 2,8 GeV energies, and ^{232}Th and ^{209}Bi fission at 150 MeV are examined. The following features have been considered: the total emission cross-section, the relative yields in fission, groups and their relative abundances. The abundances of delayed neutrons are compared to the calculated fission yields of the identified or expected precursors for the reaction ^{238}U + p (150 MeV) and for thermal fission of ^{235}U.

EMISSION DE NEUTRONS DIFFERES DANS LES REACTIONS NUCLEAIRES INDUITES PAR DES PARTICULES DE HAUTE ENERGIE. Une revue d'ensemble est présentée des résultats récemment obtenus sur l'émission de neutrons différés dans les réactions nucléaires à haute énergie. Après un rappel des nouveaux précurseurs identifiés ou probables dans la région des noyaux légers, obtenus par réactions de spallation et de « fragmentation », les réactions de fission sont plus particulièrement examinées. A moyenne ou haute énergie, deux problèmes ont été abordés dans ce domaine: caractéristiques de l'émission de neutrons retardés, identification de nouveaux précurseurs. La caractérisation sans ambiguïté de précurseurs à vie courte constitue actuellement l'un des problèmes les plus importants. Par spectrométrie de masse «en ligne» sur un faisceau de protons de 150 MeV, les isotopes de rubidium et de césium produits par fission dans une cible d'uranium ont été sélectivement séparés et analysés. Une recherche systématique a permis d'identifier comme précurseurs les isotopes 93, 94, 95 et 96 de rubidium et les isotopes 142 et 143 de césium. Ces résultats sont discutés. Les caractéristiques générales de l'émission de neutrons différés qui accompagne la fission par protons de ^{238}U à 150 MeV, 1 et 2,8 GeV et de ^{232}Th et ^{209}Bi à 150 MeV sont examinées. On envisage successivement les sections efficaces totales d'émission, les rendements relativement à la fission, les groupes de périodes et leurs abondances relatives. Les abondances de neutrons différés sont confrontées aux rendements de fission calculés de précurseurs identifiés ou possibles dans les cas de ^{238}U + p (150 MeV) et de la fission thermique de ^{235}U.

INTRODUCTION

Les travaux que suscite l'émission de neutrons différés tendent à se développer actuellement vers la production sélective et l'identification de nouveaux précurseurs, en particulier des précurseurs à vie courte. Les résultats qui ont été et pourront être obtenus sont d'un intérêt essentiel, tant pour une meilleure interprétation de l'activité de neutrons différés

produite dans les réactions de fission induite à différentes énergies que pour les études spectroscopiques de la structure nucléaire de noyaux très excédentaires en neutrons, loin de stabilité.

Dans cette double perspective les réactions induites par des particules d'énergie élevée ont apporté récemment une contribution importante.

Bien que les réactions de fission restent la source de production la plus étendue de précurseurs encore inconnus les réactions à haute énergie relevant d'autres processus d'interaction (spallation-fragmentation) ont apporté des résultats nouveaux dans le domaine des noyaux légers. Lorsqu'on évoque l'émission de neutrons différés dans les réactions à énergie élevée il ne paraît pas possible de ne pas mentionner ces résultats, même s'ils ne s'insèrent pas directement dans les préoccupations de cette réunion. Aussi seront-ils rappelés rapidement avant d'aborder les réactions de fission.

REACTIONS AUTRES QUE LA FISSION

Les réactions de spallation ou les processus dits de «fragmentation» à très haute énergie, suivant les noyaux cibles bombardés, peuvent donner lieu à la formation de noyaux légers très excédentaires en neutrons, mais néanmoins stables vis-à-vis de l'émission de particules. En raison des énergies élevées des transitions β^- même pour des noyaux peu éloignés de la stabilité, les conditions énergétiques nécessaires, mais non forcément suffisantes (cas de ^{13}B par exemple), peuvent être réalisées pour que certains noyaux légers soient effectivement précurseurs de neutrons différés.

Les périodes des précurseurs ^{9}Li, ^{16}C, ^{17}N sont suffisamment bien connues et distinctes pour que la détection des neutrons différés, très sélective en présence d'autres activités, constitue une signature de la production de ces noyaux [1]. Envisagée sous cet angle, leur identification sans ambiguïté permet alors d'étudier le mécanisme des interactions nucléaires responsables de leur formation [1-3].

Mais dans ce domaine, les études de la structure nucléaire conduisent à rechercher des noyaux légers liés pour lesquels $N \gg Z$. C'est ainsi que le nouvel isotope ^{8}He a été mis en évidence et qu'il a été caractérisé en tant que précurseur de neutrons retardés. L'hélium-8 a été produit dans les interactions avec des noyaux légers, soit par des protons de 2,2 GeV [4], soit par un rayonnement de freinage d'une énergie maximale de 220 MeV [5]. Sa période est de 122 ± 2 ms et l'embranchement vers l'émission de neutrons est de 12%. Sa période proche de celle du ^{9}Li a été l'un des obstacles à sa mise en évidence comme précurseur par détection des neutrons. Une émission de neutrons différés avec une période de $11,4 \pm 0,5$ ms a été observée par bombardement de noyaux de masse égale ou supérieure à 15 par des protons de 2,2 GeV [6]. Diverses considérations sur les nucléides susceptibles d'être produits ont conduit à attribuer l'origine de cette activité au ^{12}Be et la probabilité d'émission de neutrons a été estimée à environ 7%.

Enfin, récemment Poskanzer et al. [7], en bombardant une cible de ^{238}U par des protons de 5,3 GeV, ont mis en évidence à l'aide de détecteurs semi-conducteurs et d'un identificateur de particules les

fragments liés ^{11}Li, ^{14}B et ^{15}B. L'énergie maximale des transitions β^- serait de l'ordre de 20 MeV et les auteurs estiment que ces nouveaux isotopes seraient tous précurseurs de neutrons différés (^{15}B à près de 100%). L'instabilité de ^{11}Li avait été supposée dans l'attribution au ^{12}Be de l'activité des neutrons différés de 11,4 ms de période, signalée ci-dessus. Sa mise en évidence repose le problème de cette attribution. Pour des noyaux précurseurs de masse plus élevée, on doit rappeler que l'émission de neutrons retardés a été observée dans les réactions de spallation du cuivre par des protons de 170 MeV [8]. Les précurseurs à N > 28 auraient des périodes de l'ordre de 18 s et 8 s. L'existence de cette activité n'a toutefois pas été confirmée aux hautes énergies [1].

REACTIONS DE FISSION

Lorsque la fission de noyaux lourds est provoquée par des nucléons incidents de haute énergie, la situation devient beaucoup plus complexe qu'à basse énergie. Le noyau fissionnant n'est plus unique, mais plusieurs noyaux très diversement excités, voisins du noyau cible et résultant de processus nucléaires divers (interaction directe, évaporation) sont susceptibles de subir la fission.

D'un point de vue phénoménologique, la fission à énergie élevée est caractérisée par la formation, le plus fréquemment, de deux fragments de masses égales, bien que des processus de rupture très asymétrique subsistent. L'énergie disponible étant plus élevée, la désexcitation des noyaux avant la fission ou des fragments eux-mêmes après la fission, par évaporation de neutrons, conduira à la formation de produits plus proches de la stabilité ou même déficients en neutrons.

Toutefois, pour des énergies incidentes très élevées, au-dessus du GeV, Friedlander et al. [9] ont montré que les courbes de dispersion des charges (en N/Z) semblaient se dédoubler, et qu'à un pic correspondant aux produits de fission déficients en neutrons se juxtaposait un deuxième pic dans la région des noyaux excédentaires en neutrons.

Cette évolution est présentée à la figure 1, où sont portés les rendements (mesurés ou calculés) par rapport à la fission des isotopes de césium, dans les cas de la fission thermique de ^{235}U[1] et de la fission de ^{238}U par des protons de 150 MeV[2] et de 2,8 GeV[3]. La figure 2 présente les rendements des isotopes du rubidium, à l'exception de la distribution, pour l'instant inconnue, dans la fission de ^{238}U par des protons de 150 MeV. Ces distributions en fonction du nombre de masse pour les isotopes de Rb et Cs peuvent sous un angle simplement descriptif rendre compte de l'évolution, en fonction de l'énergie incidente, de la formation des précurseurs de neutrons différés connus ou prévus de Z voisin de 37 et 55 dans les domaines de masses ~ 90 et ~ 140. Par rapport à la fission thermique, on observe à haute énergie que la masse la plus probable est décalée vers la stabilité de ~ 2 unités de masse pour Rb

---

[1] Rendements calculés d'après la courbe des rendements de masses de Farrar et Tomlinson [10], une distribution gaussienne des charges avec un paramètre c = 0,86 [11] et les Z_p empiriques de Wahl et al. [12].

[2] Les sections efficaces de production des isotopes de césium et de rubidium ont été déterminées par Amarel et al. [13]; σ_f = 1420 mb [14].

[3] Rendements déduits des résultats de Friedlander et al. [9], avec σ_f = 830 mb [15].

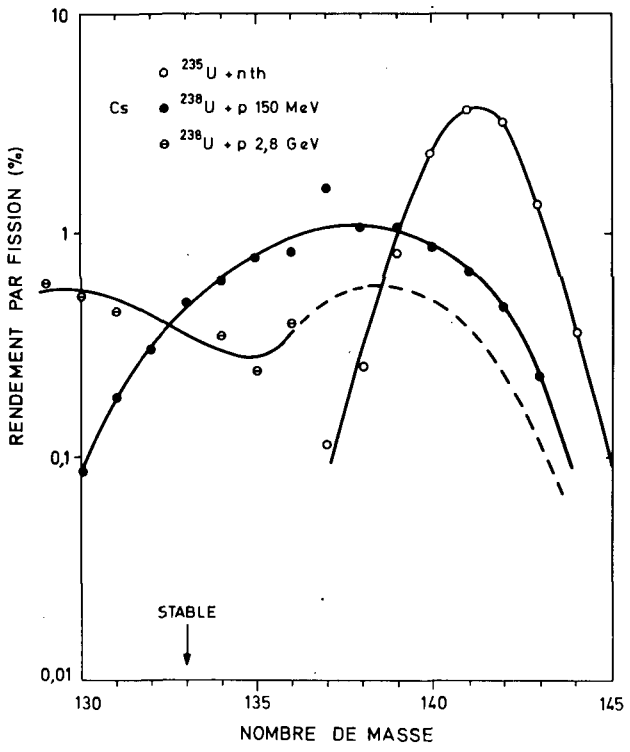

FIG. 1. Rendements par rapport à la fission des isotopes de césium dans les cas ^{235}U + n th et ^{238}U + p (150 MeV et 2,8 GeV).

et de ~ 3,5 unités pour les isotopes de Cs. Mais, de la symétrie des distributions en A à basse énergie, on évolue à énergie moyenne vers une dissymétrie qui favorise les noyaux excédentaires en neutrons pour conserver à haute énergie un pic dans la région des A élevés.

Abstraction faite des interprétations sur les mécanismes de fission que suscite cette évolution, les figures 1 et 2 montrent que la formation de précurseurs persistera à moyenne et haute énergie.

Les problèmes qui ont été ainsi abordés à énergie incidente élevée sont, d'une part, l'étude des caractéristiques de l'émission de neutrons différés, d'autre part, l'identification de précurseurs.

a) Identification de précurseurs Rb et Cs

Parmi les nombreux précurseurs qui restent inconnus, ceux de courte période (< 2 s) contribuent de façon importante à l'émission de neutrons différés observée dans la fission (plus de 50% de l'activité totale) et leur identification nécessite la mise en œuvre de méthodes de séparation à la fois sélective et très rapide. Ces conditions peuvent être effectivement réalisées par spectrométrie de masse «en ligne» sur un faisceau de particules incidentes. Un spectromètre de masse a été ainsi installé à Orsay sur le faisceau externe de protons de 150 MeV [13]. Les isotopes de Rb et Cs produits par fission dans une cible de ^{238}U portée à

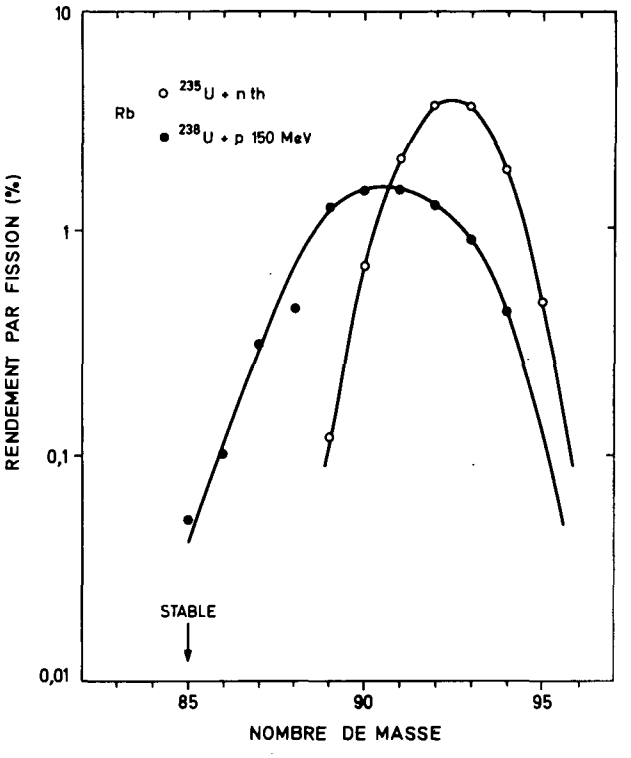

FIG. 2. Rendements par rapport à la fission des isotopes de rubidium dans les cas $^{235}U + n$ th et $^{238}U + p$ (150 MeV).

haute température ont pu être sélectivement séparés par ionisation de surface et les masses 83 à 98 du rubidium et 128 à 144 du césium isotopiquement analysées [13].

Nous avons recherché l'existence de précurseurs éventuels parmi les isotopes 92, 93, 94, 95 et 96 de Rb et les isotopes 141, 142, 143 et 144 de Cs, pour lesquels, en dehors de toute autre restriction, les conditions énergétiques peuvent être remplies (d'après les tables de Seeger [16]) pour le peuplement d'états excités instables vis-à-vis de l'émission de neutrons des émetteurs Sr et Ba [17].

Aucune activité due à des neutrons n'a été détectée pour ^{92}Rb, ^{141}Cs et ^{144}Cs. Par contre, l'émission de neutrons différés a été observée pour les isotopes 93, 94, 95 et 96 de Rb, activité qui ne peut pas être attribuée à des photoneutrons. Les périodes qui ont été déterminées sont en très bon accord avec les mesures de décroissance β^- (tableau I). La figure 3 présente une courbe de décroissance de l'activité due aux neutrons différés, enregistrée pour ^{94}Rb.

Une faible activité a été enregistrée pour ^{142}Cs et ^{143}Cs. Les conditions expérimentales permettent néanmoins de considérer ces isotopes comme précurseurs mais il n'est pas possible pour l'instant d'apporter une confirmation par détermination des périodes.

Le rubidium-93 qui a été ainsi caractérisé comme précurseur de 5,9 s de période est très probablement l'isotope observé par

TABLEAU I. PERIODES DES ISOTOPES DE RUBIDIUM ET CESIUM PRECURSEURS DE NEUTRONS DIFFERES

Isotope	$T_{\frac{1}{2}}$ (s)	
	Comptage β^-	Comptage des neutrons différés
Rb-92	4,43 ± 0,05	Pas d'activité
Rb-93	5,88 ± 0,05	6,3 ± 0,7
Rb-94	2,63 ± 0,04	2,74 ± 0,06
Rb-95	0,36 ± 0,02	0,35 ± 0,05
Rb-96	0,28 ± 0,05	0,21 ± 0,02
Cs-141		Pas d'activité
Cs-142		Activité
Cs-143	1,60 ± 0,14	Activité
Cs-144	1,06 ± 0,10	Pas d'activité

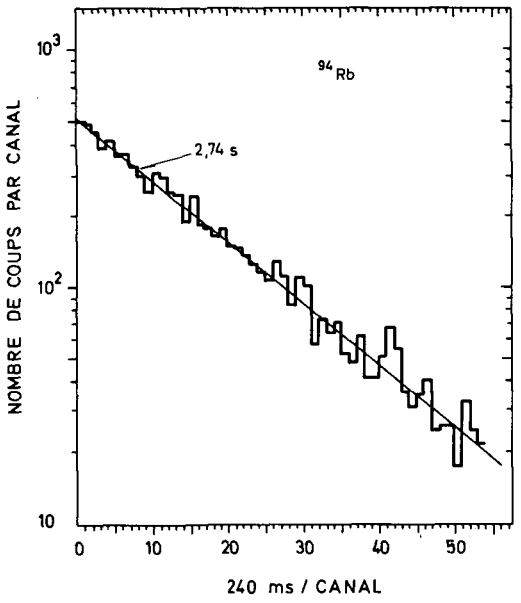

FIG. 3. Courbe de décroissance de l'activité des neutrons différés pour ^{94}Rb.

Stehney et Perlow [18] et Tomlinson [19], formé par accumulation à partir d'un parent Kr (2 s).

Les probabilités relatives d'émission de neutrons pour les isotopes 93, 94, 95 et 96 de Rb ont pu être estimées respectivement à 0,1, 1, 0,6 et 1 en supposant une même efficacité de détection. Les probabilités absolues ne peuvent pas être déterminées présentement mais il semble

que l'embranchement pour ^{94}Rb soit important. Compte tenu des conditions expérimentales de collection des ions et de détection des neutrons, une valeur de l'ordre de 10% pourrait être avancée, avec les réserves qui s'imposent. Par contre, pour ^{142}Cs et ^{143}Cs, les probabilités d'émission sont beaucoup plus faibles, d'un facteur au moins égal à 50, par rapport à ^{94}Rb. Qualitativement, cette diminution s'accorderait avec les prévisions de Keepin [20] et Pappas et Rudstam [21].

Toutefois, si les énergies disponibles $Q_\beta - B_n$ sont réellement égales pour ^{94}Rb et ^{142}Cs comme l'indiqueraient les tables de Seeger [16], la probabilité d'émission très faible pour ^{142}Cs suggère que le peuplement interdit d'états excités instables de l'émetteur Ba ou la désexcitation compétitive par transitions γ deviennent des facteurs prépondérants devant le seul critère énergétique $Q_\beta - B_n$. On rappellera que Stehney et Perlow [18], par séparation des gaz rares, n'ont pas trouvé d'activité de neutrons attribuable aux isotopes de Xe. L'absence d'activité pour ^{144}Cs, envisagé cependant comme précurseur, souligne également le problème posé par les isotopes lourds dans ce domaine de masses.

Ces premiers résultats montrent que l'analyse des produits de fission par spectrométrie de masse «en ligne» ouvre de grandes possibilités pour l'identification de précurseurs et, d'une façon plus générale, pour l'étude des isotopes à vie courte, en particulier lorsqu'elle sera étendue à des éléments autres qu'alcalins. Les études telles que la détermination des spectres d'énergie des neutrons retardés, des probabilités d'émission, etc., bien que posant des problèmes délicats, devraient devenir néanmoins beaucoup plus accessibles.

b) Caractéristiques de l'émission de neutrons différés dans la fission à moyenne et haute énergie

Les travaux effectués dans ce domaine sont assez limités. Ils concernent la fission par protons de ^{238}U à 1 et 2,8 GeV [1] et à 150 MeV [22] ainsi que la fission de ^{232}Th et ^{209}Bi à 150 MeV [22].

En raison de l'évolution signalée plus haut qui tend à défavoriser la formation de produits de fission très excédentaires en neutrons dans la fission de noyaux de $Z > 90$ par des protons d'énergie élevée, on pourrait s'attendre que l'émission de neutrons retardés présente des caractéristiques assez distinctes de celles que l'on observe à basse énergie.

Dans le cas de noyaux de $Z < 90$, la fission devient possible pour des énergies incidentes moyennes (> 30 MeV pour le bismuth). A 150 MeV, la rupture, le plus fréquemment en deux fragments de même masse, ne paraît intervenir, après les cascades nucléoniques, que sur des noyaux très appauvris par de longues chaînes d'évaporation de neutrons [23]. On n'envisage donc pas dans ces conditions que la formation de précurseurs soit possible. La section efficace de fission du bismuth bombardé par des protons de 150 MeV est suffisamment notable (126 mb) pour que des informations expérimentales aient pu être apportées sur cette question.

Sections efficaces d'émission de neutrons retardés

Pour les trois éléments étudiés, ^{238}U, ^{232}Th, ^{209}Bi, aux énergies incidentes indiquées plus haut, la fission est accompagnée de l'émission de neutrons retardés.

TABLEAU II. GROUPES DE NEUTRONS RETARDES ET RENDEMENTS DANS LA FISSION DE L'URANIUM-238 A DIFFERENTES ENERGIES INCIDENTES

U-238	$T_{\frac{1}{2}}$ (s)		σ (mb)			Abondance relative			
Groupe	156 MeV	$\bar{E}_n$ = 2 MeV[a]	156 MeV	1 GeV[a]	2,8 GeV[a]	$\bar{E}_n$ = 2 MeV[a]	156 MeV	1 GeV[a]	2,8 GeV[a]
1	53,85 ± 1,15	52,38 ± 1,29	0,34 ± 0,08	0,17	0,20	0,013	0,052	0,038	0,046
2	20,27 ± 1,13	21,58 ± 0,39	0,89 ± 0,21	0,62	0,60	0,137	0,137	0,14	0,14
3	5,22 ± 0,34	5,00 ± 0,19	1,45 ± 0,39	0,8	1,1	0,162	0,224	0,18	0,27
4	2,08 ± 0,20	1,93 ± 0,07	2,40 ± 0,60	1,8	1,4	0,388	0,370	0,41	0,33
5	0,460 ± 0,060	0,490 ± 0,023	0,96 ± 0,26	1,1	1,0	0,225	0,148	0,23	0,22
6	0,160 ± 0,020	0,172 ± 0,009	0,45 ± 0,13			0,075	0,069		
σ_n totale (mb)			6,50 ± 0,7	4,5 ± 0,4	4,3 ± 0,9				
σ_f[a] (mb)			1420	1050	830				
n_f (%)			0,46	0,43	0,52	4,12			

[a] Voir texte.

Les tableaux II, III et IV regroupent les résultats obtenus respectivement pour des cibles de ^{238}U, de ^{232}Th et de ^{209}Bi, sur les périodes des différents groupes de neutrons et les sections efficaces correspondantes. Les résultats obtenus par Keepin et al. [24] par neutrons de fission ($\overline{E}_n \simeq 2$ MeV) sur ^{238}U et ^{232}Th sont également donnés.

TABLEAU III. GROUPES DE NEUTRONS RETARDES ET RENDEMENTS DANS LA FISSION DU THORIUM-232 A DES ENERGIES INCIDENTES DIFFERENTES

Th-232	$T_{\frac{1}{2}}$(s)		σ (mb)	Abondance relative	
Groupe	156 MeV	$\overline{E}_n$ = 2 MeV[a]		$\overline{E}_n$ = 2 MeV[a]	156 MeV
1	56,49 ± 0,30	56,03 ± 0,95	0,25 ± 0,06	0,034	0,087
2	19,00 ± 0,37	20,75 ± 0,66	0,48 ± 0,12	0,150	0,163
3	5,6 ± 1,4	5,74 ± 0,24	0,67 ± 0,20	0,155	0,228
4	2,00 ± 0,34	2,16 ± 0,08	1,11 ± 0,29	0,446	0,393
5	0,300 ± 0,020	0,571 ± 0,042 0,211 ± 0,019	0,38 ± 0,11	0,172 0,043	0,128
σ_n totale (mb)			2,90 ± 0,35		
σ_f^a (mb)			900		
n/f (%)			0,32	4,96	

[a] Voir texte.

TABLEAU IV. GROUPES DE NEUTRONS RETARDES ET RENDEMENTS DANS LA FISSION DU BISMUTH-209 A 156 MeV

Bi-209 Groupe	$T_{\frac{1}{2}}$ (s)	σ (μb)	Abondance relative
1	55,83 ± 1,09	4,19 ± 0,10	0,183
2	15,59 ± 1,8	2,80 ± 0,84	0,122
3	1,49 ± 0,38	4,34 ± 1,6	0,189
4	0,200 ± 0,006	11,6 ± 3,6	0,506
σ_n totale (μb)		22,93 ± 3,10	
σ_f^a (mb)		126	
n/f (%)		0,02	

[a] Voir texte.

Les sections efficaces totales d'émission de neutrons sont faibles, particulièrement pour ^{209}Bi à 150 MeV. On notera que pour ^{238}U elles paraissent à peu près indépendantes de l'énergie incidente.

Les rendements n/f relativement aux sections efficaces de fission[4] constituent une donnée plus intéressante. Pour l'uranium, quelle que soit l'énergie incidente, le rendement ~ 0,45% est dix fois plus faible qu'à basse énergie. Pour le thorium la diminution est un peu plus sensible. Ces résultats, attendus, traduisent essentiellement le déplacement ou la déformation des courbes de distribution des charges vers la stabilité. Le rendement n/f = 0,02% pour le bismuth donne à ce noyau une position très différente de celle de l'uranium et du thorium. Pour des noyaux à seuil élevé de fission, tout au moins pour le bismuth, la formation de produits de fission très excédentaires en neutrons est pratiquement exclue, ainsi qu'on pouvait l'envisager. L'émission de neutrons différés, qui reste à un niveau très faible, apporte ici une indication expérimentale.

Signalons que l'émission de neutrons différés pouvant provenir de produits de fission a été décelée dans le bombardement du plomb par des protons de 1 et 3 GeV [1]. Les rendements trop faibles n'ont pas permis une analyse de cette activité.

Groupes de périodes et abondances relatives

A 1 et 3 GeV Dostrovsky et al. [1] ont fixé, dans l'analyse des courbes de décroissance, les périodes moyennes observées à basse énergie. A 150 MeV nous avons, suivant la procédure décrite en détail par Keepin et al. [24], déterminé pour U, Th et Bi le nombre de composantes et leurs paramètres qui rendent compte au mieux des résultats expérimentaux suivant les critères habituels: convergence de l'analyse, valeur de la variance pondérée. La résolution des courbes de décroissance demande six composantes pour l'uranium, cinq pour le thorium et quatre pour le bismuth. Dans ce dernier cas, il est intéressant de remarquer que la courbe de la distribution des masses à 150 MeV pointée sur la masse 100 exclut toute contribution de précurseurs de masse ~ 140 ($N \geq 84$). On sélectionne ainsi uniquement des précurseurs identifiés ou possibles de la région des isotopes du brome. Cet effet est particulièrement net sur le groupe 2 d'où est éliminé la composante de 24 s attribuée à ^{137}I, et où l'on ne retrouve que la période de ~ 16 s attribuée à ^{88}Br. La période de 0,2 s, par son abondance relative importante, pose un problème particulier. Des expériences sur des cibles d'or et de tantale, pour lesquelles les sections efficaces de fission très faibles à 150 MeV [26] excluent toute détection de neutrons différés résultant de la fission, montrent cependant une décroissance bien résolue par la période de 0,176 s du ^{9}Li. De plus, les sections efficaces d'émission de neutrons différés relatives à cette période sont très voisines pour Ta, Au, Bi.

---

[4] σ_f (^{238}U) = 1420 mb à 150 MeV [14];
σ_f (^{238}U) = 1050 mb à 1 GeV [15];
σ_f (^{238}U) = 830 mb à 2,8 GeV [15];
σ_f (^{232}Th) = 900 mb à 150 MeV [25];
σ_f (^{209}Bi) = 126 mb à 150 MeV [14].

TABLEAU V. COMPARAISON DES SECTIONS EFFICACES MESUREES ET CALCULEES D'EMISSION DE NEUTRONS DIFFERES DANS LA FISSION DE L'URANIUM-238 PAR DES PROTONS DE 150 MeV

(Groupe) $T_{\frac{1}{2}}$ (s)	Précurseur - identifié -(probable)	$T_{\frac{1}{2}}$ (s)	σ cumulative calculée du précurseur dans la chaîne (mb)	Probabilité d'émission P_n (%)	σ_n(mb) calculée (± 30%)		σ_n(mb) mesurée
(1)	^{87}Br	54,5	11,6	3,1[a]	0,35		0,34 ± 0,08
53,85							
(2)	^{88}Br	16,3	8	6[a] (7)[b]	0,48 (0,56)	0,64 (0,82)	0,89 ± 0,21
20,27	^{137}I	24	5,2	3[a] (5)[b]	0,16 (0,26)		
(3)	^{89}Br	4,4	4,3	7[a]	0,30		
5,22	^{93}Rb	5,9	14	(1)[c]	0,14	0,50	1,45 ± 0,39
	^{138}I	6,3	3	2[a]	0,06		
	^{90}Br	1,6	1,40	(17)[d]	0,24		
	^{94}Rb	2,67	7	(10)[c]	0,70		
(4)	(^{85}As)	2,15	0,6	11[e]	0,07		
2,08	(^{92}Kr) (^{93}Kr)	~ 1,5	2,70 1			1,06	2,40 ± 0,60
	^{139}I	2	1,40	(2,5)[d]	0,03		
	^{143}Cs	1,6	3,5				
	(^{135}Sb)	1,9	0,42	(4)[d]	0,02		
	^{142}Cs	~5	8				
	^{95}Rb	0,35	4	(6)[c]	0,24		
(5)	(^{87}As)	< 1,5					
0,460	(^{91}Br)	~0,5	0,4				0,96 ± 0,26
	(^{140}I)	~0,5					
(6)	^{96}Rb	0,23	0,6	(10)[c]	0,06		
0,160	(^{92}Br)	~0,2	0,2				0,45 ± 0,13

[a] Probabilités d'émission expérimentales P_n de Aron et al. [31].

[b] Voir texte.

[c] P_n estimées pour les isotopes de Rb (voir texte).

[d] Déduit du tableau VI.

[e] D'après del Marmol [32].

TABLEAU VI. COMPARAISON DES RENDEMENTS MESURES ET CALCULES D'EMISSION DE NEUTRONS DIFFERES DANS LA FISSION THERMIQUE DE L'URANIUM-235

(Groupe) $T_{\frac{1}{2}}$ (s)[a]	Précurseur -identifié -(probable)	$T_{\frac{1}{2}}$ (s)	Rendement absolu de la chaîne	Rendement cumulatif du précurseur dans la chaîne	Rendement absolu du précurseur	P_n (%)	Rendement absolu en neutrons différés calculé (± 25%)		mesuré[a]
(1) 55,72	^{87}Br	54,5	2,5	0,95	2,37	3,1[b]	0,073		0,052 ± 0,005
(2)	^{88}Br	16,3	3,55	0,87	3,09	6[b]	0,185	0,309	0,346 ± 0,018
22,72	^{137}I	24,4	6,25	0,66	4,12	3[b]	0,124		
	^{89}Br	4,4	4,73	0,61	2,89	7[b]	0,203		
(3)	^{93}Rb	5,9	6,51	0,65	4,23	(1)[c]	0,042	0,317	0,310 ± 0,036
6,22	^{138}I	6,3	6,68	0,54	3,61	2[b]	0,072		
	^{142}Cs	~5	5,8	0,60	3,48				
	^{90}Br	1,6	5,77	0,29	1,67		~0,280[d]		
	^{94}Rb	2,67	6,55	0,29	1,90	(10)[c]	0,190		
	(^{85}As)	2,15	1,30	0,55	0,72	11[e]	0,079		
							(0,050)[f]		
(4)	(^{92}Kr)	~1,5	6,03	0,30	1,81		~0,007[g]	~0,619	0,624 ± 0,026
2,30	(^{93}Kr)		6,52	0,10	0,65				
	^{139}I	2	6,43	0,29	1,87		~0,047[d]		
	^{143}Cs	1,6	5,70	0,24	1,37				
	(^{135}Sb)	1,9	6,45	0,06	0,39		~0,016[f]		

(Groupe) $T_{\frac{1}{2}}$ (s)[a]	Précurseur -identifié -(probable)	$T_{\frac{1}{2}}$ (s)	Rendement absolu de la chaîne	Rendement cumulatif du précurseur dans la chaîne	Rendement absolu du précurseur	P_n (%)	Rendement absolu en neutrons différés calculé (± 25%)		mesuré[a]
(5) 0,610	(^{87}As)	< 1,5	2,5	0,07	0,17				
	(^{91}Br)	~0,5	5,97	0,08	0,48				0,182 ± 0,015
	(^{140}I)	~0,5	6,25	0,08	0,50				
(6) 0,230	^{95}Rb	0,35	6,55	0,07	0,46	(6)[c]	0,028	0,034	0,066 ± 0,008
	^{96}Rb	0,23	6,40	0,01	0,06	(10)[c]	0,006		
	(^{92}Br)	~0,2	6	0,01	0,06				

[a] Résultats de Keepin et al. [24].

[b] Probabilités d'émission expérimentales P_n de Aron et al. [31].

[c] P_n estimées pour les isotopes de Rb (voir texte).

[d] D'après les rendements relatifs de Perlow et Stehney [33].

[e] D'après del Marmol [32].

[f] D'après Tomlinson [19].

[g] D'après Stehney et Perlow [18].

On peut donc penser que le précurseur responsable de la période de ~ 0, 2 s pourrait être réellement ^{9}Li mais formé par un processus distinct de la fission. La production de fragments légers dans les interactions à haute énergie [27] a été observée par de nombreux auteurs et certains l'attribuent à un processus dit de «fragmentation». Si l'on rejette ainsi ce groupe 4, on peut considérer que les trois groupes restants pour le bismuth correspondent chacun à un précurseur unique produit par fission: le groupe 1 à ^{87}Br, le groupe 2 à ^{88}Br et, d'après les possibilités limitées offertes par les courbes de dispersion des charges, le groupe 3 (1, 5 ± 0, 4 s) à ^{94}Rb, bien que la période soit un peu différente.

Contrairement à ce qui pouvait être envisagé, les différents groupes de périodes et leurs abondances relatives dans la fission de l'uranium à 150 MeV, 1 et 3 GeV se révèlent proches de ceux que l'on observe dans la fission induite à basse énergie. En fait, les abondances relatives se situent entre les cas extrêmes des noyaux composés fissionnants ^{234}U et ^{239}U [24] à $E^* < 10$ MeV. Cette observation et le bon accord entre les valeurs des périodes elles-mêmes a conduit [1, 22] à considérer que seule la fission de noyaux à faible énergie d'excitation était responsable de l'émission de neutrons différés. Qualitativement, cette interprétation est en accord avec les observations sur le bismuth qui montrent que toute contribution propre à des processus de fission à haute énergie d'excitation reste négligeable.

Comparaison des abondances absolues des groupes de neutrons différés et des rendements prévisibles

Les résultats expérimentaux assez nombreux sur la fission de ^{238}U à 150 MeV (sections efficaces cumulatives, rendements indépendants et cumulatifs partiels) [13, 28] et quelques données déduites de travaux [29,30] sur la fission du bismuth ont été utilisés pour déterminer les courbes de dispersion des charges pour les masses ~ 90 [22]. Dans le domaine de A ~130-140, pour la fission de ^{238}U, il a été fait appel à la courbe de distribution des charges établie par Pappas et Hagebø [28].

Les rendements prévisibles de précurseurs identifiés ou possibles ont pu être ainsi confrontés avec les sections efficaces d'émission de neutrons différés. Pour les groupes 1 et 2 de l'uranium, ceci a permis d'estimer les probabilités d'émission de neutrons pour ^{87}Br, ^{88}Br et ^{137}I respectivement à 3, 7 et 5%, valeurs qui sont en bon accord avec les déterminations expérimentales de Aron et al. [31]: 3,1, 6 et 3%. Cette confrontation a été étendue à tous les groupes, d'une part pour la fission de ^{238}U par des protons de 150 MeV (tableau V) et d'autre part pour la fission thermique de ^{235}U (tableau VI) en tenant compte des nouveaux précurseurs identifiés. Dans ce dernier cas, il semble que l'on puisse assez bien expliquer les rendements absolus des groupes 1 à 4 et partiellement le groupe 6 par les isotopes 95 et 96 de Rb. Le groupe 5 reste toutefois entièrement inexpliqué. Les seuls isotopes de Br et I mentionnés dans le tableau VI rendent compte de 62% de l'activité due aux neutrons et les isotopes de Rb de 17%. Ces derniers apportent donc une contribution très notable, en particulier ^{94}Rb qui apparaît comme un précurseur important.

En retenant les mêmes précurseurs, le tableau V montre des divergences dès le groupe 3 entre les sections efficaces d'émission de neutrons mesurées et calculables dans le cas de la fission de ^{238}U à 150 MeV. Si l'on envisage des précurseurs inconnus pour expliquer le désaccord des groupes 3 et 4, a fortiori leur contribution devra apparaître dans la fission thermique de ^{235}U, mettant en cause l'accord, peut-être apparent, qui est observé. Il semble plus probable d'expliquer les divergences observées à 150 MeV par l'imprécision des sections efficaces cumulatives calculées des précurseurs envisagés, en particulier pour les précurseurs à grand N/Z.

CONCLUSION

L'émission de neutrons retardés dans la fission de noyaux lourds de $Z > 90$ induite par des protons de moyenne et haute énergie présente des caractéristiques générales peu différentes de celles observées à basse énergie. Cette émission peut être interprétée comme la manifestation du processus de fission asymétrique de noyaux faiblement excités. En dehors de l'intérêt que présente sa persistance pour une analyse plus compréhensive de la fission à haute énergie, un tel mécanisme permet d'aborder les problèmes plus spécifiques liés à la recherche de nouveaux précurseurs et à leur étude.

D'après le tableau VI il semble que c'est dans le domaine de période $\leq 0{,}6$ s que la caractérisation de produits de fission précurseurs est surtout déficiente. La mise en évidence de tels précurseurs encore inconnus demande des méthodes de séparation rapide et sélective. A cet égard, les premiers résultats présentés ici montrent que les techniques de spectrométrie de masse «en ligne» apparaissent comme les plus fertiles.

La confrontation des rendements observés et calculés de l'émission de neutrons retardés avec les précurseurs nouvellement identifiés constitue un test et un guide utiles. Après les essais présentés par Amiel [34] d'une part et Herrmann et al. [35] d'autre part, les résultats encourageants pour les groupes 1 à 4 dans la fission thermique de ^{235}U que présente le tableau VI suggèrent d'étendre ces comparaisons à d'autres noyaux fissiles.

REFERENCES

[1] DOSTROVSKY, I., DAVIS, R., Jr., POSKANZER, A.M., REEDER, P.L., Phys. Rev. 139 B (1965) 1513.
[2] DOSTROVSKY, I., GAUVIN, H., LEFORT, M., Rapport interne 66 E 03, Institut de physique nucléaire, Orsay (1966).
[3] POMORSKI, L., TYS, J., VOLKOV, V.V., Physics Lett. 23 (1966) 369.
[4] POSKANZER, A.M., ESTERLUND, R.A., McPHERSON, R., Phys. Rev. Lett. 15 (1965) 1030.
[5] NEFKENS, B.M.K., SUTTON, D.C., THOMPSON, M.N., Nucl. Phys. 88 (1966) 523.
[6] POSKANZER, A.M., REEDER, P.L., DOSTROVSKY, I., Phys. Rev. 138 B (1965) 18.
[7] POSKANZER, A.M., COSPER, S.W., HYDE, E.K., CERNY, J., Phys. Rev. Lett. 17 (1966) 1234.
[8] RUDSTAM, G., SVANHEDEN, A., PAPPAS, A.C., Nature 188 (1960) 1178.
[9] FRIEDLANDER, G., FRIEDMAN, L., GORDON, B., YAFFE, L., Phys. Rev. 129 (1963) 1809.
[10] FARRAR, H., TOMLINSON, R.H., Can. J. Phys. 40 (1962) 943, 1017; Nucl. Phys. 34 (1962) 367.

[11] WAHL, A.C.,«Mass and charge distribution in low-energy fission», Physics and Chemistry of Fission (Proc.Symp. Salzburg, 1965) I, IAEA, Vienna (1965) 317..
[12] WAHL, A.C., FERGUSON, R.L., NETHAWAY, D.R., TROUTNER, D.E., WOLFSBERG, K., Phys. Rev. 126 (1962) 1112.
[13] AMAREL, I., BERNAS, R., CHAUMONT, J., FOUCHER, R., JASTRZEBSKI, J., JOHNSON, A., KLAPISCH, R., TEILLAC, J., Proc. Lysekil Symp., 1966, Ark. Fys. (sous presse).
[14] KOWALSKI, L., Thèse, Paris (1963); Annls Phys. 9 (1964) 211.
[15] FRIEDLANDER, G., « Fission of heavy elements by high-energy protons », Physics and Chemistry of Fission (Proc. Symp. Salzburg, 1965) II, IAEA, Vienna (1965) 265.
[16] SEEGER, P.A., Nucl. Phys. 25 (1961) 1.
[17] AMAREL, J., BERNAS, R., FOUCHER, R., JASTRZEBSKI, J., JOHNSON, A., TEILLAC, J., GAUVIN, H., Physics Lett. (sous presse).
[18] STEHNEY, A.F., PERLOW, G.J., Bull. Am. phys. Soc. 6 (1961) 62.
[19] TOMLINSON, L., J. inorg. nucl. Chem. 28 (1966) 287.
[20] KEEPIN, G.R., J. nucl. Energy 7 (1958) 13.
[21] PAPPAS, A.C., RUDSTAM, G., Nucl. Phys. 21 (1960) 353.
[22] GAUVIN, H., SAUVAGE, L. (à paraître).
[23] Le BEYEC, Y., LEFORT, M., PETER, J., Nucl. Phys. 88 (1966) 215.
[24] KEEPIN, G.R., WIMETT, T.F., ZEIGLER, R.K., J. nucl. Energy 6 (1957) 1.
[25] STEINER, H.M., JUNGERMAN, J.A., Phys. Rev. 101 (1956) 810.
[26] STEPHAN, C., Thèse, Paris (1966).
[27] LEFORT, M., Annls Phys. 9 (1964) 249.
[28] PAPPAS, A.C., HAGEBØ, E., J. inorg. nucl. Chem. 28 (1966) 1769.
[29] GOECKERMANN, R.H., PERLMAN, I., Phys. Rev. 76 (1949) 628.
[30] JODRA, L.G., SUGARMAN, N., Phys. Rev. 99 (1955) 1470.
[31] ARON, P.M., KOSTOCHKIN, O.I., PETRZHAK, K.A., SHPAKOV, U.J., Atomn. Energ. 16 (1964) 368.
[32] Del MARMOL, P., Proc. Lysekil Symp., 1966, Ark. Fys. (sous presse).
[33] PERLOW, G.J., STEHNEY, A.F., Phys. Rev. 113 (1959) 1269.
[34] AMIEL, S., «Delayed neutrons and photoneutrons from fission products», Physics and Chemistry of Fission (Proc. Symp. Salzburg, 1965) II, IAEA, Vienna (1965) 171.
[35] HERRMANN, G. et al., «Comparison of observed delayed-neutron abundances with calculated fission yields of neutron precursors », Physics and Chemistry of Fission (Proc. Symp. Salzburg. 1965) II, IAEA, Vienna (1965) 197.

DISCUSSION

On the papers by Roeckl et al., Day et al., Amiel et al., Herrmann, and Gauvin

The results reported by Talbert on the observations of delayed neutron emission from ^{91}Kr and ^{92}Kr were discussed at length at the panel. The following, main points have been abstracted:

The Soreq group, in the course of its investigations, was able to separate by radiochemical methods (1 sec separation time) a large amount of krypton. The decay half-lives of both isotopes in question have been determined (8.5 sec for ^{91}Kr, 2 sec for ^{92}Kr), the gamma rays have been measured but no delayed neutron activity was detected. A theoretical upper limit for delayed neutron emission from these isotopes was estimated and was found to be extremely low. It could probably not be detected by experimental means.

Theoretical considerations show that it is improbable that there will be any delayed neutron emission from these isotopes as the energy of the suitable excited level in their daughters is too low to permit the emission of delayed neutrons. Also, looking at the angular momenta (spin and parities) involved in the beta decay of ^{91}Kr followed by a neutron, decay to the ground state of ^{90}Rb is forbidden.

In the discussion, Talbert made additional remarks about the experiment and results described in his paper. Some of these remarks are summarized below.

In the paper, only the multiscale plot of ^{92}Kr is given. For ^{91}Kr, the statistics were too low to enable the construction of such a diagram for the exact determination of the half-life. The data did permit of an approximate determination of half-life ^{91}Kr (8.0 sec ± 20%).

With the present knowledge of the system used in the experiments it was not possible to determine the relative yields. The processes inside the fission sample and in the transit to the ion source are not fully investigated. The only normalization can be in terms of the activity received at the collector. In this respect, the intensity of neutrons emitted from ^{91}Kr (40% above background) and ^{92}Kr (equal to background) was at least an order of magnitude lower than the intensity observed with ^{93}Kr (60 × background).

It might have been possible that some neutrons were derived from photo-production in the apparatus. The neutron detector was checked with a very strong gamma source whose gamma rays were of an intensity and energy much higher than could be expected in the collector plate; no extra neutrons were counted above background.

It is difficult to discount the evidence supporting neutron emission which results from analysis the long-lived gamma spectra from the collector plates for the presence of (A - 1) activities. In the plates for masses 91, 92, and 93, there was firm evidence of ^{90}Rb and ^{91}Sr, respectively. Since the collector plate for mass 88 showed no trace of activity from the mass 87 decay chain, there is no other explanation for the (A - 1) activities in the other plates besides neutron emission.

GAMMA LINES USED IN THE ANALYSES WERE

^{90}Rb	2.9 min	607 keV
		836 keV
^{91}Sr	9.7 h	555 keV
		650 keV
		750 keV
		1025 keV
		1410 keV
^{92}Sr	2.7 h	235 keV
		430 keV
		1380 keV
^{39}Y	10.1 h	265 keV
		935 keV

In the discussion it was also pointed out that from the reactor technology point of view the discovery of new delayed neutron precursors with very low yields does not have much significance. There are probably as much as 40 delayed neutron precursors with yields between 10^{-6} and 10^{-7} delayed neutrons per fission since the process of neutron emission can occur marginally even in nuclei close to stability. For the reactor kinetics, only those precursors which contribute at least 0.1% to the total delayed neutron yields (10^{-5} delayed neutrons per fission) are of interest.

Looking at the energy spectra in Amiel's paper (his Fig. 17), the top figure (a) represents the first two groups. Comparing it with the second figure (b) and with old energy measurements of Batchelor, it seems that the two peaks at 500 keV and 300 - 400 keV would belong to the 55 sec ^{87}Br, which would indicate some fine structure. Such a conclusion cannot be drawn yet on the basis of the preliminary results. The new improved shuttle rabbit will produce (with different irradiation and delay times) much more data. The higher efficiency detectors mentioned in Amiel's paper will help.

It is satisfying to observe that in general the outline concerning the energy spectra as measured by the Soreq group shows the same form as the old data by Batchelor et al. [1]. The Soreq measurements are extended to higher energies. The detector system is calibrated by using the Van de Graaff accelerator at different energies.

Amiel reported on some estimates based on $Q^{\beta} - \beta^{n}$ using the Zeldes Mass formula [2]. It would be interesting to use Swiatecki's formula [3], which would probably be a better one where the fission product masses are concerned. This formula accounts for more physical properties than any formula up to now.

It would be even better to extend the past use of the few available mass formulas and to take all mass formulas in this region, including Swiatecki's to investigate the region where neutron emission may take place: this is

projected in Israel and elsewhere. In this way a more up-to-date initial selection can be obtained that can also be used later in making predictions. It would at the worst guide research towards the cases where good values of decay energies and mass values would be desirable.

The question of charge distribution in these regions is still open. Around the 50 proton shell region, the Soreq group used the Z_p values of Wahl [4]. The latest charge dispersion studies of Strom et al. [5] at the US Naval Radiological Defence Research Laboratory, San Francisco, provide the indication that the width of the charge dispersion curve is mass dependent in this region. It appears from studies in Oslo that the influence of the 50 proton shell on the charge distribution is not as large as was expected. The most probable charge seems to follow up along the 50 proton shell at the beginning but it cuts through at a rather early stage. These effects were not taken into account in Amiel's paper and might change the calculated yields considerably. On the other hand, the data [6] recently obtained with Ewald's mass spectrometer, where physical measurements of charge dispersion were done, disagree entirely with the data of Strom et al. There is at present complete uncertainty as to the final outcome. In the mass spectrometer studies, however, the passage of heavy masses (like fission fragments) through gases may cause many experimental difficulties among which the varying of the mass of a species as a result of chemical reactions at very high kinetic energies might be mentioned.

The data presented by the Ewald group at Lysekil for the masses in the range from 139 to 142 are in disagreement with radiochemical and X-ray data. The radiochemical data are very dependable in this range since the fission chains are very simple, without isomers etc. On the narrowing effect of the width of the charge dispersion details are given by Wunderlich at Munich [7]. He has measured some iodine yield in the region of interest. These data show that there is an effect, though it is not as strong as suggested by Strom et al. The width, however, cannot be determined only using yields of iodine isotopes; the results, therefore, depend on the use of certain assumption.

The iodine decay curve given in Herrmann's paper shows a much higher yield (by a factor 2.5) of 2 sec delayed neutron precursors than was found in measurements by Perlow and Stehney [8]. In the discussion, it was queried if this could be explained by invoking contamination by rubidium or some other element.

In the Mainz experiments, possible rubidium contamination was carefully avoided. The Mainz group uses a completely different kind of chemistry (simpler) than that used by Perlow and Stehney. The chemical yields for short-lived isotopes could be different in Perlow's procedure because of some slow steps in the reactions involved. The completeness of the reduction was checked using longer-lived species of iodine. By irradiating the samples for a longer time, strong ^{134}I and ^{135}I activities were obtained. The same procedure as for short-lived species was used and it was found that the percentage of iodine which can be absorbed in the filtrate is in the region of a few percent.

According to the findings of the Oslo-Uppsala group the width of the charge dispersion curve seems to increase with energy. For 170 MeV proton induced fission the width of this curve does increase by 25 to 30% as compared to that for thermal fission. Accordingly the increase of the width of the charge dispersion could not be very large when going from

thermal to 20 MeV neutrons. Hence the same charge dispersion can be used. The formula for Z_p (given by Coryell et al. [10]) used and partly modified by the Mainz group may be further improved by taking into account pre-fission neutrons.

Another problem discussed at the panel can be stated as: 'How would the estimates of the most probable charge and width of the charge dispersion influence the P_n-results, particularly in the regions around the closed shells ?'

In Mainz a study is planned in which the absolute delayed neutron yields (for iodine only) are measured in many fission reactions. A check on charge dispersion can be obtained from such data, but the results will be strongly dependent on the underlying assumptions.

The neutron emission probability, P_n, should be a physical constant for a given species, independent of how it is formed in fission. Only the presence of isomers which may be produced in various abundances in different fission reactions can, in special cases, apparently, influence the P_n-values. Ten years ago the constancy of P_n was pointed out and used as one of the main criteria on which precursors have been predicted. The constancy of P_n, or at least the fact that it is characteristic for the fission product — irrespective of where is comes from — gives a guide to the selectivity and is thus useful in establishing which precursors satisfy all data (14 MeV, thermal, etc.). The approach of the Mainz group is good in that they took all possible reactions, looked at the P_n-values, and did a least squares fit; they threw out any set of precursors for which the P_n varied too widely, as this would mean that something was wrong with the set of precursors assumed. In this respect, the ^{252}Cf data are extremely interesting since the bromine and arsenic isotopes are completely or nearly eliminated from the scene.

The reactor physicists have previously not been interested in P_n-values. However, these values are important to radiochemists, to workers involved with nuclear structures and, today, for those involved in the construction of certain types of advanced reactor. As far as the reactor people are concerned, however, the main data needed are already available: the periods and abundances divided into a small number of groups. They would like to reduce the existing six groups to two or three, and this can be done reasonably well; these groups are, of course, just as artificial as the present six group interpretation. Increasing the number of groups to seven or eight does not improve the standard deviation of the fit parameters (this being a statistical measure of how well the available data points can be fitted to a chosen number of periods).

For theoretical studies of delayed neutron emission, it is of great interest to concentrate on detailed studies of nuclear structure, the investigation of individual species, their decay schemes, branching ratios and abundances. This would finally lead to better P_n-values which would also serve the reactor physicists.

A problem that occurs in the type of measurements carried by the Mainz group can be summarized as follows. After pulsed irradiation, the contribution of the short-lived nuclei is enhanced. If the separation is done very rapidly after irradiation, the total intensity may not have had time to form. This can be checked by separating the desired product after some delay, 1 or 2 sec. Longer delays cannot be introduced since

the intensity would become too low. Such measurements were made, but they must be extended to obtain good final values for relative intensities and contributions.

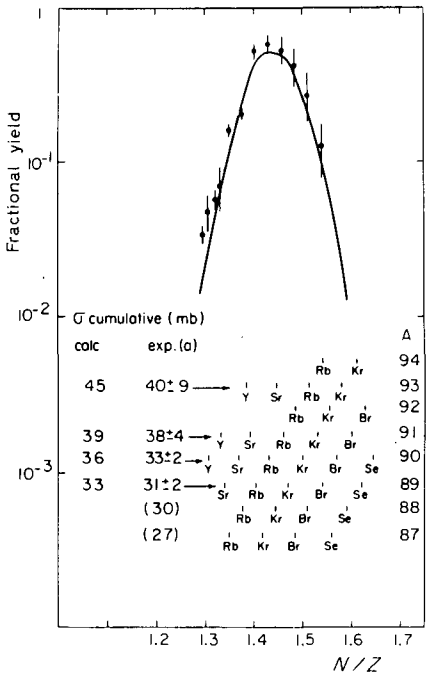

FIG.A. A comparison between cumulative cross-sections of precursors and experimental cross-sections for delayed neutrons in delayed neutron fission by 150 MeV protons.

In Gauvin's paper the experimental cross-sections for delayed neutrons emitted during uranium fission by 150 MeV protons are compared with the cumulative cross-sections of known precursors. In the region of mass 90 Amarel's results were used (Fig. A). In the region of mass 140 the curve given by Pappas was used as a basis for the calculations. It was noted that Amarel's results do not fit Pappas' curve for masses above 138 (caesium isotopes). In the case of bismuth fission at 150 MeV a charge-distribution curve centred on N/Z = 1.36 [11] was drawn from certain experimental results [12]. This enabled the P_n-values for ^{87}Br to be calculated. Table V in Gauvin's paper shows that there is reasonable agreement for the first two periodic groups with the P_n-values for ^{87}Br, ^{88}Br and ^{137}I, near to those obtained by Aron [13]. For the other groups, agreement is much less good. This may be due to the charge-distribution curves for the high values of N/Z. The mass yield curve in the 170 MeV proton-induced fission of uranium-238 has been well determined by the Oslo-Uppsala group [9]. On the basis of independent yield measurements, estimated neutron emission, etc. and the results on energy deposition calculation by the Monte Carlo method (Metropolis et al.) and compared with range measurements, the mass yield curve can be visualized as resulting from a mixture of the following different fission modes taking place in the target (each with its typical characteristics concerning charge

distribution, charge dispersion and mass distribution):

(a) a very high energy deposition – symmetric fission with single-peaked mass yield curve;
(b) a low energy deposition – asymmetric fission with double peaked mass yield curve; and
(c) a "hybrid" type of the above modes caused by medium and high energy deposition and large pre- and/or post-fission neutron emission.

In the same manner, we could consider the charge distribution to be the result of two types, one corresponding to the (fast) symmetric fission mode (unchanged charge distribution rule), and another corresponding to the (slow) asymmetric fission mode (equal charge displacement rule).

The result in high energy induced fission would be that delayed neutron emitters in the heavy mass region will be produced mainly by a type of asymmetric fission, while in the light mass region large contributions from a type of symmetric fission will additionatly enter the picture. Thus the production path of delayed neutron precursors in high energy induced fission will be rather complicated. A precursor (e.g. ^{87}Br) would then be the result of at least two processes, as suggested by the higher relative abundance of the first group (Table II of Gauvin's paper: 0.052 to 150 MeV). At any rate there is no doubt that the contribution made by low excitation energy fission prevails quite distinctly in the formation of precursors with higher N/Z values (Table II), so that it is possible to estimate the share of low excitation energy fission in the overall process at 150 MeV (about 25 to 30%) [13].

The question of the formation of precursors in the fission of nuclei with a high excitation energy is raised. Here the resultant emission of delayed neutrons would be disguised and treated as coming from low energy fissions. If the available excitation energy is not dissipated by evaporation of neutrons before fission, the fission fragments will be in a highly excited state and will de-energize themselves preferentially by neutron emission. The fission products resulting from this "cooling" process will then be much closer to the stable state and, under these conditions, precursor formation cannot be expected.

According to experimental observations, the fission of ^{209}Bi induced by 150 MeV protons results in a high delayed neutron relative yield contributing to the 0.2 sec period. Since the peak of the mass distribution curve of bismuth fission lies in the region between 90 and 100 mass units, it was suggested in the discussion that the precursors of the these 0.2 sec delayed neutrons could be bromine or rubidium isotopes.

Several conditions speak against this possibility. One line of reasoning is the following: Table IV of Gauvin's paper shows a decrease in yield when going from the first to the second period. At low energy fission, the yield of bromine precursors is seen to increase by a factor of two when comparing the second group with the first, and further increase by a factor of two is observed when moving from the second to the third period. In high energy fission, a decrease of the yield seems to continue when moving from the first to other periods since the Orsay group did not observe any delayed neutrons in the 4 sec period. Extrapolating these observations, the probability that bromine would be a precursor of the 0.2 sec period is very small. Some experiments on gold and tantalum have been made; the 0.2 delayed neutron period was also observed but no bromine precursors

have been found, which may be expected by reason, inter alia, of the very weak cross-sections of gold and tantalum for fission by 150 MeV protons.

Other delayed neutron precursors in the case of ^{209}Bi fission might be light nuclei, ^{9}Li, ^{12}Be, ^{16}C or even ^{8}He, although at present there is no experimental proof for these precursors being formed in the ^{209}Bi fission. Another possible explanation might be that the high energy proton bombardment of bismuth includes the (p, xp) reaction (x could be 3 or 4); this would shift the n/p ratio to higher values and might result in short-lived precursors. This explanation also looks very unlikely since the (p, xp) reactions for bismuth preserve the outer closed shell of 126 neutrons and because in any event, it would mean $x > 5$.

The similar results obtained for ^{209}Bi, ^{197}Au, ^{181}Ta (i.e. the same observed half-life of 0.2 sec, same neutron emission cross-section of $\sim 12\ \mu$b) suggest that the precursor responsible is generated by a process other than fission. Since the half-life value seems to indicate ^{9}Li, the hypothesis that this light particle is emitted by a "fragmentation" mechanism, brought into play at higher energies, may be put forward. The observed cross-section is rather in line with this hypothesis.

From the theoretical standpoint, the low yield of delayed neutron precursors from the ^{209}Bi fission is not surprising. Moving from ^{235}U to ^{209}Bi, the peak of the charge distribution curve would probably be shifted by 1 to 1.5 units closer to the stability line, and this would indicate a drop in delayed neutron yield, which is in fact observed (n/F = 0.02%). It would be very instructive to investigate in detail the charge distribution curve of bismuth fission. A charge distribution curve such as was used, centred on N/Z = 1.36, explains the formation of ^{87}Br and ^{88}Br.

In Gauvin's paper, the P_n-values for rubidium isotopes are given. During discussion, the question was raised how dependent these data are.

The relative probabilites among the four rubidium isotopes, ^{93}Rb, ^{94}Rb, ^{95}Rb and ^{96}Rb have been estimated. The essential assumption was that the efficiency of the neutron detection was the same in all four cases. This assumption is questionable since the neutron detector does not have a uniform response and it is possible that energy of the neutrons from different rubidium isotopes varies substantially. For ^{94}Rb, the value of (10 ± 5)% was obtained. Details and reservations are given in the paper. The conditions under which it is possible to make a selective separation are better established now and should give more precise values.

There are several factors which influence the goodness of data; for example, the dependability of the ion collection, the counter efficiency, etc. If a detector with a uniform response to the neutrons of different energies were available, it would be easier to give better values of P_n. Despite the reservations expressed in Gauvin's paper on the relative P_n-values, a qualitative comparison with the figures put forward by Pappas may be made. These show that for a given element fluctuations of the P_n-value as a function of A can be considerable. The Orsay results do not indicate a systematic increase of P_n with A. The relative P_n-values estimated appear to be consistent with the conclusions which can be drawn from Pappas' figures.

REFERENCES

[1] BATCHELOR, R., HYDER, H.R. McK., J. nucl. Energy 3 (1956) 7.

[2] ZELDES, N., GRONAU, M., LEV, A., Nucl. Phys. 63 (1965) 1.

[3] SWIATECKI, W.J., Phys. Rev. 122 (1956) 97; unpublished results summarized by HYDE, E.K., Review of Nuclear Fusion, University of California (Berkeley) Rep. UCRL-9036 (1960).

[4] WAHL, A.C., NORRIS, A.E., FERGUSON, R.L., Phys. Rev. 146 (1966) 931.

[5] STROM, P.O., LOVE, D.L., GREENDALE, A.E., DELUCCHI, A.A., SAM, D., BALLOU, N.E., Phys. Rev. 144 (1966) 984; STROM, P.O., et al., paper presented at 151 th meeting Am. Chem. Soc. Pittsburgh (March 1966).

[6] OPOWER, H., KONECNY, E., SIEGERT, G., Z. Naturforsch. 20a (1965) 131; KONECNY, E., SIEGERT, G., Z. Naturforsch. 21a (1966) 192.

[7] WUNDERLICH, to be published in Radiochimica Acta.

[8] PERLOW, G.J., STEHNEY, A.E., Phys. Rev. 113 (1959) 1269.

[9] PAPPAS, A.C. and coworkers; see paper to this Panel.

[10] CORYELL, C.D., KAPLAN, M., FINK, R.D., Canad. J. Chem. 39 (1961) 646.

[11] Le BEYEC, Y., LEFORT, M., PETER, J., Nucl. Phys. 88 (1966) 215.

[12] GAUVIN, H., SAUVAGE, L., (to be published).

[13] ARON, P.M., KOSTOCHKIN, O.I., PETRZHAK, K.A., SHPAKOV, V.I., Atomn. Energ. 16 (1964) 368.

ЗАПАЗДЫВАЮЩИЕ НЕЙТРОНЫ ОТ ИЗОТОПОВ УРАНА, ТОРИЯ-232 И ПЛУТОНИЯ-239

Б.П.МАКСЮТЕНКО
ФИЗИКО-ЭНЕРГЕТИЧЕСКИЙ ИНСТИТУТ,
ОБНИНСК,
СССР

Abstract — Аннотация

DELAYED NEUTRONS FROM URANIUM ISOTOPES, THORIUM-232 AND PLUTONIUM-239. Relative delayed neutron yields were measured for the fission fractions after the fission of different uranium isotopes, thorium-232 and plutonium-239. The energy of the bombarding neutrons was varied over the range 5 to 8 MeV. The experimental data for five groups of delayed neutrons were obtained and are presented as the ratio of the i-th group of delayed neutrons to the first group (55 sec). The results are discussed from the point of mass distribution of fission fractions and precursors.

ЗАПАЗДЫВАЮЩИЕ НЕЙТРОНЫ ОТ ИЗОТОПОВ УРАНА, ТОРИЯ-232 И ПЛУТОНИЯ-239. Измерены относительные выходы запаздывающих нейтронов, полученных из осколков деления после деления изотопов урана, тория-232 и плутония-239.

Энергия бомбардируемых нейтронов, изменялась в области 5 – 8 Мэв. Проверялись экспериментальные данные для пяти групп запаздывающих нейтронов. Результаты представлены в виде отношения i-й группы к первой (период полураспада 55 сек) и обсуждены с точки зрения массового распределения осколков деления и предшественников.

I. ТЕХНИКА ЭКСПЕРИМЕНТА И РЕЗУЛЬТАТЫ

Измерены относительные выходы запаздывающих нейтронов при делении тория-232, урана-235, урана-238 и урана-233 нейтронами с энергией от 5 до 8 Мэв. Результаты для первых трех изотопов были опубликованы ранее [1].

Нейтроны указанной энергии получались в результате реакции $D(d, n)He^3$ на генераторе Ван-де-Граафа от цирконий-дейтериевой мишени толщиной 20 мг/см^2.

Фон нейтронов после выключения ускоряющего напряжения длился около пяти секунд и соответствующие каналы при обработке отбрасывались. Детектирование осуществлялось десятью пропорциональными BF_3-счетчиками, соединенными параллельно и окруженными полиэтиленом. Для регистрации использовался временной анализатор. Распределение ширин каналов: 60 – по одной секунде и 60 – по 10 секунд. Кривые распада, соответствующие каждой энергетической точке для данного эксперимента, представляют сумму по каналам от цикла, состоящего из 10 – 40 измерений. Эти суммарные кривые обрабатывались на электронно-счетной машине при заданных значениях периодов полураспада.

Все использованные образцы – металлические, за исключением урана-233 (порошок). Вес последнего ~16 г, тория-232 ~100 г и остальных ~50 г (ф 30 – 35 мм). Образец урана-235 – 90% обогащения.

Результаты измерений представлены в таблицах I – V и на рисунках 1 – 4.

Точки на рисунках отнесены к максимальной энергии нейтронов использованного спектра.

ТАБЛИЦА I. ТОРИЙ-232.

Период полураспада (сек)	Отношение выходов при энергии нейтронов:								
	5 Мэв	6 Мэв	6,2 Мэв	6,4 Мэв	6,6 Мэв	6,8 Мэв	7,25 Мэв	7,7 Мэв	7,75 Мэв
55	1	1	1	1	1	1	1	1	1
24	2,385 ±0,072	2,54 ± 0,08	3,18 ± 0,18	2,329 ± 0,043	2,423±0,056	2,23 ± 0,07	1,969 ± 0,045	1,85 ± 0,05	1,474 ± 0,087
15,5	2,42 ±0,10	2,32 ± 0,09	1,43 ± 0,25	2,319 ± 0,063	2,288±0,083	2,29 ± 0,08	2,113 ± 0,065	2,12 ± 0,07	2,38 ±0,13
5,2	4,87 ±0,16	4,79 ± 0,16	8,07 ± 0,45	4,44 ±0,10	4,370±0,13	3,54 ± 0,11	3,70 ±0,11	3,04 ± 0,09	2,47 ±0,21
2,2	10,13 ±0,34	10,71 ± 0,26	7,74 ± 0,80	10,84 ±0,20	10,10 ±0,27	11,66 ± 0,27	6,94 ±0,21	8,87 ± 0,20	7,91 ±0,52

Примечание: фон во всех измерениях $(1 \div 3) \cdot 10^{-3}$.

ТАБЛИЦА II. УРАН-235.

Период полураспада (сек)	Отношение выходов при энергии нейтронов:						
	5 Мэв	6 Мэв	6,3 Мэв	6,6 Мэв	6,9 Мэв	7,22 Мэв	7,76 Мэв
55	1	1	1	1	1	1	1
24	3,45 ± 0,20	2,83 ± 0,03	3,50 ± 0,10	3,83 ± 0,09	3,30 ± 0,63	3,70 ± 0,04	3,424 ± 0,053
15,5	1,91 ± 0,26	2,32 ± 0,04	2,17 ± 0,12	1,04 ± 0,12	2,03 ± 0,09	1,94 ± 0,04	1,775 ± 0,073
5,2	4,23 ± 0,43	4,26 ± 0,17	5,31 ± 0,20	4,60 ± 0,20	4,83 ± 0,14	3,80 ± 0,12	4,03 ±0,13
2,2	8,40 ± 0,86	10,23 ± 0,92	9,49 ± 0,39	3,20 ± 0,38	7,44 ± 0,28	6,76 ± 0,47	6,49 ±0,32

ТАБЛИЦА III. УРАН-238.

Период полураспада (сек)	Отношение выходов при энергии нейтронов:									
	5 Мэв	6 Мэв	6,4 Мэв	6,6 Мэв	6,8 Мэв	6,9 Мэв	7,1 Мэв	7,25 Мэв	7,5 Мэв	7,76 Мэв
55	1	1	1	1	1	1	1	1	1	1
24	7,56 ± 0,17	6,93 ± 0,31	7,95 ± 0,18	7,19 ± 0,32	12,31 ± 0,37	8,42 ± 0,24	8,30 ± 0,20	7,95 ± 0,15	8,08 ± 0,14	7,32 ± 0,42
15,5	3,55 ± 0,16	3,81 ± 0,15	2,60 ± 0,16	3,76 ± 0,32	0,59 ± 0,23	3,16 ± 0,20	3,54 ± 0,19	24,0 ± 1,4	20,6 ± 1,2	3,74 ± 0,42
5,2	10,7 ± 0,3	9,18 ± 0,66	10,2 ± 0,3	11,48 ± 0,54	13,3 ± 0,6	11,63 ± 0,39	10,39 ± 0,32	8,68 ± 0,25	8,64 ± 0,22	7,04 ± 0,73
2,2	27,3 ± 0,7	30,69 ± 0,78	19,2 ± 0,6	24,9 ± 1,3	45,7 ± 3,4	24,39 ± 0,81	25,16 ± 0,70	14,0 ± 0,5	13,3 ± 0,43	28,0 ± 2,0

ТАБЛИЦА IV. УРАН-233.

Период полураспада (сек)	Отношение выходов	Период полураспада (сек)	Отношение выходов
	$E_n = 5,6$ Мэв		$E_n = 6,4$ Мэв
55	1	55	1
24	1,35 ± 0,05	24	1,137 ± 0,056
15,5	1,75 ± 0,08	15,5	1,786 ± 0,086
5,2	1,84 ± 0,12	5,2	1,58 ± 0,14
2,2	5,66 ± 0,15	2,2	5,48 ± 0,28
	$E_n = 6,0$ Мэв		$E_n = 6,8$ Мэв
55	1	55	1
24	1,408 ± 0,053	24	1,17 ± 0,05
15,5	1,602 ± 0,082	15,5	1,69 ± 0,08
5,2	2,35 ± 0,15	5,2	2,19 ± 0,13
2,2	4,22 ± 0,36	2,2	4,14 ± 0,27
	$E_n = 6,2$ Мэв		$E_n = 7,2$ Мэв
55	1	55	1
24	1,25 ± 0,07	24	1,50 ± 0,05
15,5	1,70 ± 0,11	15,5	1,56 ± 0,07
5,2	2,09 ± 0,18	5,2	2,74 ± 0,16
2,2	4,99 ± 0,37	2,2	3,17 ± 0,11

В действительности, полученные цифры не являются отношением выходов групп. Так как использованный спектр нейтронов достаточно широкий, найденные в результате разложения кривых распада отношения выходов i-й группы к первой $R_{i\text{э}}$ есть

$$R_{i\text{э}} = \int_{E_{min}}^{E_{max}} a_i(E)\sigma_f(E)\Phi(E)dE \Big/ \int_{E_{min}}^{E_{max}} a_1(E)\sigma_f(E)\Phi(E)dE$$

где $\sigma_f(E)$ – сечение деления при заданной энергии E,
$\Phi(E)dE$ – поток нейтронов,
$a_i(E)$ – абсолютный выход i-й группы запаздывающих нейтронов при делении нейтронами с энергией E.

И поскольку это отношение испытывает резкое изменение, мы можем сделать обратное заключение: отношение выходов испытывает резкое изменение.

Было проверено, не является ли наблюдаемое резкое изменение отношения выходов следствием причин математического, а не физического характера. С этой целью проведено разложение трех кривых распада (6; 6,2; 6,4 Мэв) запаздывающих нейтронов от тория-232 при заданных значениях периодов полураспада, варьируя последние по таблицам случайных величин при заданных значениях ошибок (всего проделано

ТАБЛИЦА V. ПЛУТОНИЙ-239.

Период полураспада (сек)	Отношение выходов	Период полураспада (сек)	Отношение выходов
	$E_n = 5{,}5$ Мэв		$E_n = 7{,}5$ Мэв
55	1	55	1
24	3,51 ± 0,12	24	3,14 ± 0,12
15,5	1,84 ± 0,14	15,5	2,11 ± 0,16
5,2	3,70 ± 0,20	5,2	2,20 ± 0,24
2,2	7,74 ± 0,35	2,2	11,04 ± 0,48
	$E_n = 6{,}5$ Мэв		$E_n = 7{,}8$ Мэв
55	1	55	1
24	3,650 ± 0,091	24	3,81 ± 0,11
15,5	1,94 ± 0,13	15,5	1,80 ± 0,15
5,2	3,31 ± 0,23	5,2	3,78 ± 0,27
2,2	9,37 ± 0,57	2,2	6,28 ± 0,66
	$E_n = 7{,}0$ Мэв		
55	1		
24	3,18 ± 0,11		
15,5	1,77 ± 0,16		
5,2	4,30 ± 0,27		
2,2	6,17 ± 0,39		

10 вариантов). При этом характер отношения выходов (скачки) сохранялся во всех вариантах для каждой группы, а отношение пикового значения к пьедесталу сохранялось в пределах от 6% до 0,8% для различных групп. Наблюдалось небольшое общее смещение всех трех точек (для любой группы) вверх и вниз, за исключением случая, где у двух средних групп отклонения от заданных периодов составляли +2 и − 3 среднеквадратические ошибки. Общее отклонение было большим. Этот математический эксперимент подтверждает, что наблюдаемая особенность обязана своим появлением причинам физического характера, а не способу разложения кривой распада, если последний применяется одинаковым образом.

Результаты показывают, что наблюдалась структура уже применявшегося спектра и, поскольку не имелось никаких теоретических предпосылок, такая работа является оправданной в качестве первого приближения для установления не известных до сих пор закономерностей.

Наблюдается одинаковый характер изменения отношения одних и тех же групп разных элементов и изотопов. Более близкое сходство имеет место отдельно для элементов с четным массовым числом (торий-232 и уран-238) и нечетным (плутоний-239, уран-235 и уран-233). Сходное поведение проявляют группы с периодами 24 сек и 5,2 сек у каждого элемента.

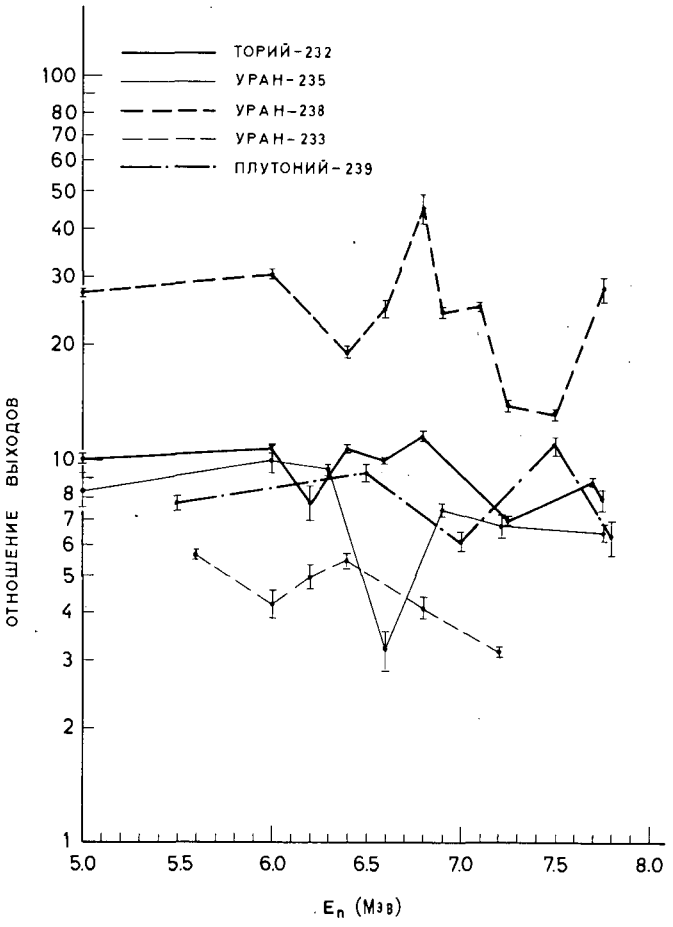

Рис.1. Группа T = 2,2 сек.

II. ОБСУЖДЕНИЕ РЕЗУЛЬТАТОВ

Как уже указывалось ранее, использованный спектр нейтронов шире наблюдаемой структуры; и мы не гарантированы, что она сохранится в том же виде при лучшем разрешении. Кроме того, пока не измерены абсолютные выходы запаздывающих нейтронов в соответствующих энергетических точках, интерпретация этого явления была бы преждевременной.

Может быть более важными, существенно затрудняющими интерпретацию, проблемами являются идентификация осколков-предшественников и распределение заряда и масс в делении.

Если осколки-предшественники одинаковы для всех изотопов всех элементов, то результаты работы Кокса [2] заставляют усомниться в правильности химической идентификации, проведенной Перлоу и Стени [3], за исключением брома-87 и иода-137. Исключая эти два последних

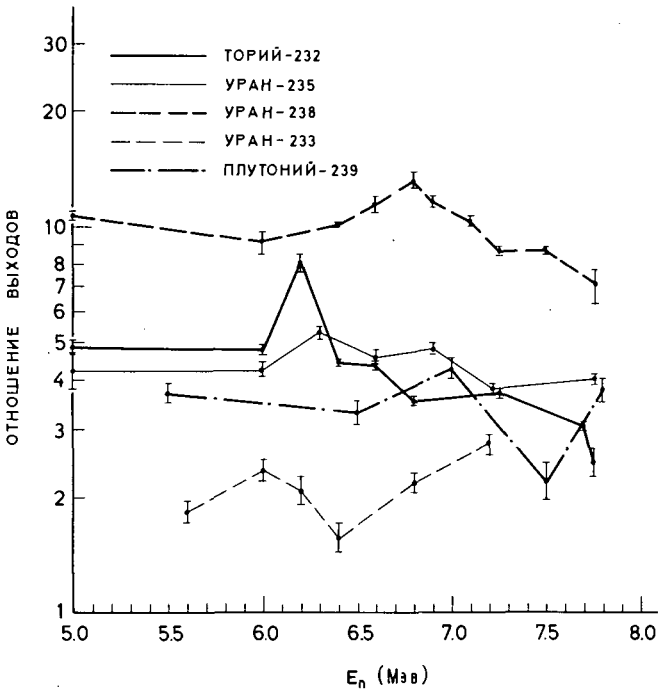

Рис.2. Группа T = 5,2 сек.

изотопа, мы не гарантированы даже в том, что какой-то осколок-предшественник принадлежит к легкому или тяжелому пику в распределении масс. С другой стороны, математическое разложение кривой распада также не гарантирует того, что мы выделяем все существующие группы. Частный результат, полученный Кипиным [4], что шесть экспонент дают наилучшее приближение к кривой распада, не есть доказательство того, что число шесть является роковым. В этом случае просто уже не работает критерий Гаусса.

Оценивая с этой точки зрения полученный результат, мы можем сказать, что если некоторые из выделенных групп представляют смесь двух или более вкладчиков, то скачок принадлежит либо одному предшественнику, либо нескольким.

Обнаружено изменение в отношениях выходов масс для урана-235 в той же области энергий [5]. Изменение этого отношения для предсказываемой теоретически области осколков-предшественников показано на рис. 5 (здесь, как и для запаздывающих нейтронов выход массы-87 принят за единицу при любой энергии). Везде наблюдается только уменьшение отношения выходов масс и нигде не проявляется увеличение, встречающееся для некоторых групп запаздывающих нейтронов. Выход любой группы запаздывающих нейтронов определяется парциальным выходом осколка-предшественника данной массы и данного заряда и вероятностью излучения нейтрона из этого осколка. Трудно предположить, что последняя может зависеть от энергии нейтронов, вызывающих деление, поскольку β-распад происходит только с основного уровня и структура уровней дальнейших членов цепочки определяется только исходным

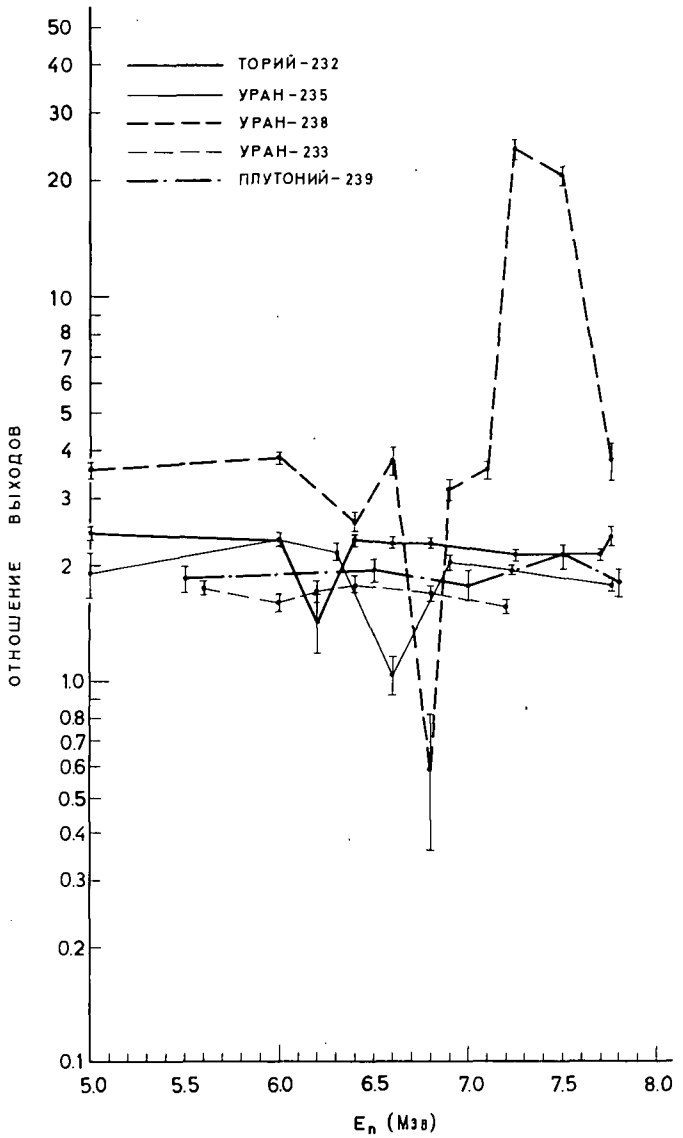

Рис.3. Группа T = 15,5 сек.

ядром. Если осколок был возбужден, избыток энергии должен быть излучен в виде γ-квантов. Ситуация могла бы измениться при наличии изомерии. Однако, как показал Кипин [6], это не имеет места. Если же вероятность излучения нейтрона постоянна для данного осколка-предшественника (т.е. не зависит от энергии нейтронов, вызывающих деление), то полученный результат можно трактовать, как резкое изменение парциальных сечений выходов осколков-предшественников. Так как в отношениях выходов соответствующих масс наблюдается только

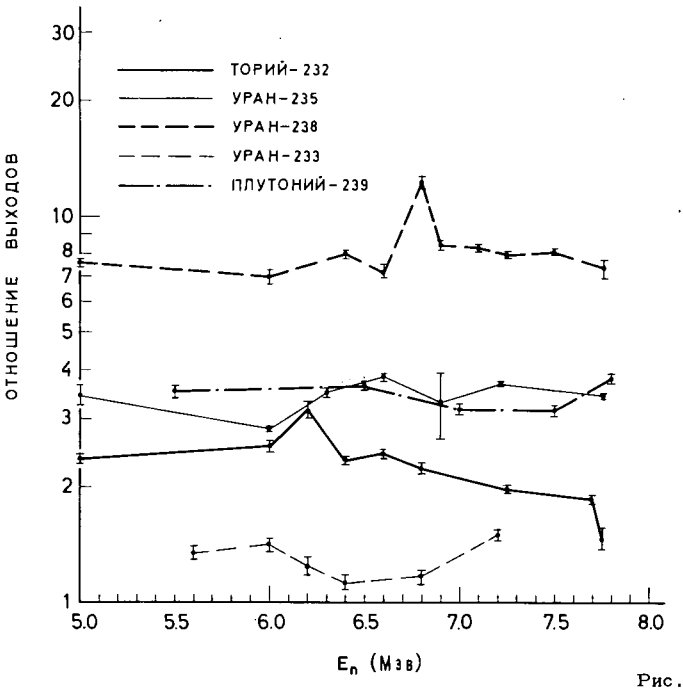

Рис.4. Группа T = 24 сек.

уменьшение, эффект увеличения этого отношения следовало бы приписать либо резкому изменению распределения заряда, либо это может быть связано с излучением мгновенных нейтронов. Теоретические расчеты вероятности излучения нейтрона у разных авторов [6, 7] в среднем отличаются в 5 – 6 раз (а иногда и более). Это показывает, что данные для масс и распределения заряда, полученные экстраполяцией, не очень надежны.

В заключение, несколько слов об оценке абсолютных выходов. Мы еще их не определяли. Однако, существование скачка в отношениях выходов позволяет сделать грубую оценку. Напишем наблюдаемую реакцию в виде:

$$\begin{matrix} A+1 & \xrightarrow{n} & A \\ \downarrow f & & \downarrow f \end{matrix}$$

где A – массовое число данного изотопа. Экспериментально измеренный абсолютный выход запаздывающих нейтронов i-й группы в какой-либо точке ступеньки в сечении деления $a_{i\,э}$; может быть представлен через абсолютные выходы запаздывающих нейтронов обоих ядер $a_{i,\,A+1}$ и $a_{i,\,A}$ и соответствующие парциальные сечения деления σ_{A+1} и σ_A

$$a_{i\,э} = a_{i,\,A+1}\sigma_{A+1} + a_{i,\,A}\sigma_A$$

аналогично для первой группы:

$$a_{1\,э} = a_{1,\,A+1}\sigma_{A+1} + a_{1,\,A}\sigma_A$$

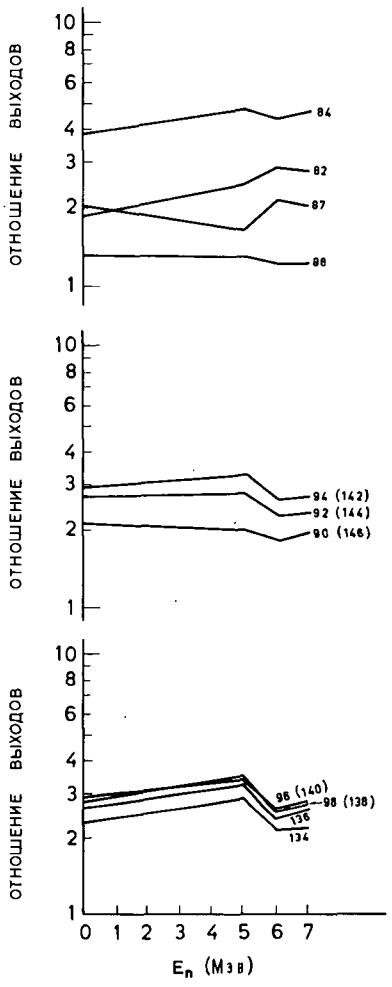

Рис.5. Отношения выходов масс для предсказываемой теоретически области осколков-предшественников.

Тогда экспериментально измеренное отношение выходов есть

$$\left(\frac{a_i}{a_1}\right)_э = \frac{\left(\frac{a_i}{a_1}\right)_{A+1} + \left(\frac{a_i}{a_1}\right)_A XZ}{1+XZ}$$

где

$$X = \frac{a_{1,A}}{a_{1,A+1}} \quad \text{и} \quad Z = \frac{\sigma_A}{\sigma_{A+1}}$$

Отсюда можно определить X:

$$X = \frac{\left(\frac{a_i}{a_1}\right)_{A+1} - \left(\frac{a_i}{a_1}\right)_э}{\left[\left(\frac{a_i}{a_1}\right)_э - \left(\frac{a_i}{a_1}\right)_A\right] Z}$$

Так как X должно быть положительной величиной, то либо

$$\left(\frac{a_i}{a_1}\right)_{A+1} > \left(\frac{a_i}{a_1}\right)_э > \left(\frac{a_i}{a_1}\right)_A$$

либо

$$\left(\frac{a_i}{a_1}\right)_{A+1} < \left(\frac{a_i}{a_1}\right)_э < \left(\frac{a_i}{a_1}\right)_A \qquad (1)$$

Значение $\left(\frac{a_i}{a_1}\right)_{A+1}$ может быть оценено, учитывая плавную зависимость этой величины между ступеньками в сечении деления экстраполяцией. Длина экстраполяции (в энергетической шкале невелика, ядро имеет уже достаточно высокую энергию возбуждения и не видно причин для резкого изменения этого хода. Если построить зависимость a_i/a_1 от A по данным Кипина для спектра деления, то значение $(a_i/a_1)_A$ может быть получено для A = 235 и A = 233. В большинстве случаев соотношение (1) не выполняется (вообще мы должны предположить, что соответствующие скачки больше измеренных $R_{iэ}$). Если сделать предельно-возможное в данном случае предположение, что $a_{i,A} = 0$, можно получить нижнюю границу значения X:

$$X \geq \left\{\frac{(a_i/a_1)_{A+1}}{(a_i/a_1)_э} - 1\right\} \frac{1}{Z}$$

Для некоторых групп такая оценка является разумной и показывает, например, для урана-233 и урана-235: $X_{233} > 3$ и $X_{235} > 0{,}8$. Несмотря на все неточности, связанные с такой оценкой, видно, что в точках, где наблюдается скачок в относительных выходах, происходит увеличение абсолютного выхода первой группы вдвое и больше. Возможно, это обстоятельство объясняет и наблюдаемое увеличение выходов (во всяком случае не уменьшение!) при делении ядер нейтронами с энергией ~15 Мэв.

Видно, что наблюдаемый эффект связан с пороговыми процессами. Для интерпретации этих явлений следует изучать распределение заряда и излучение мгновенных нейтронов в этой области.

ЛИТЕРАТУРА

[1] МАКСЮТЕНКО, Б.П., Бюллетень Информационного Центра по ядерным данным. Вып. третий, Государственный Комитет по использованию атомной энергии СССР (1966) 75.

[2] COX, S., FIELDS, P., FRIEDMAN, A., SJOBLOM, R., SMITH, A., Phys. Rev. 112 (1958) 960.
[3] PERLOW, G.I., STEHNEY, A.F., Phys. Rev. 113 (1959) 1269.
[4] KEEPIN, G.R., Physics of Nuclear Kinetics, Addison Wesley Co., 1965.
[5] ВОРОБЬЕВА, В.Г., ДЬЯЧЕНКО, П.П., КУЗЬМИНОВ, Б.Г., ТАРАСКО, М.З., Ядерная физика 4 (1966) 325.
[6] ПАНПАС, А., Труды второй международной конференции по мирному использованию атомной энергии, Женева 2 Избранные доклады иностранных ученых, М, Атомиздат, 1959, стр. 308.
[7] КИПИН, Г.Р., Атомная энергия 4 (1958) 250.

ЗАПАЗДЫВАЮЩИЕ НЕЙТРОНЫ ПРИ ДЕЛЕНИИ ЯДЕР НЕЙТРОНАМИ С ЭНЕРГИЕЙ ОТ 15 ДО 21 МЭВ

Б.П.МАКСЮТЕНКО, Р.РАМАЗАНОВ, М.З.ТАРАСКО
ФИЗИКО-ЭНЕРГЕТИЧЕСКИЙ ИНСТИТУТ,
ОБНИНСК,
СССР

Abstract — Аннотация

DELAYED NEUTRONS FROM NUCLEAR FISSION BY NEUTRONS WITH ENERGIES OF 15 TO 21 MeV. Relative delayed neutron yields were measured for the fission of uranium isotopes in the fissioning range of 15 to 21 MeV. The results of the fission of uranium-235 and -238 were compared for this energy range, and the correspondence of the uranium-235 curve at this energy with that for uranium-233 in the energy range 5 to 8 MeV is discussed. The yields were assessed in the case of processes (n, 3nf) and (n, nf), and it was found that the first reaction is the more dependent on the energy of the incident neutrons producing the fission.

ЗАПАЗДЫВАЮЩИЕ НЕЙТРОНЫ ПРИ ДЕЛЕНИИ ЯДЕР НЕЙТРОНАМИ С ЭНЕРГИЕЙ ОТ 15 ДО 21 Мэв. Измерялись относительные выходы запаздывающих нейтронов при делении изотопов урана в области деления 15 – 21 Мэв. Сравнивались также результаты деления U-235 и U-238 в этой энергетической области и дается обсуждение соответствия кривой для урана-235 при этой энергии с кривой для урана-233 в области от 5 – 8 Мэв.

Оценивались выходы в случае процессов (n, 3nf) и (n, nf) и установлено, что первая реакция больше зависит от энергии нейтронов, вызывающих деление.

Вслед за исследованием изменения отношения выходов групп запаздывающих нейтронов, вызванным реакцией (n, nf), было начато изучение отношения выходов в области энергий 15 ÷ 21 Мэв. Условия проведения опыта и метод обработки данных были те же, что и в предыдущем случае.

Это исследование могло бы показать, является ли найденная закономерность в поведении отношения выходов уникальной, связанной только с реакцией (n, nf), или же она вообще связана с пороговыми процессами. Естественно, при этом были сомнения, связанные с тем, что мы имеем дело с областью, где складываются результаты отношения выходов запаздывающих нейтронов от двух-трех предыдущих ядер цепочки деления, и такие резкие изменения могли бы быть смазаны.

Не меньший интерес представляло и следующее обстоятельство. При делении нейтронами такой высокой энергии ядра урана-235 последним из делящихся ядер цепочки

$$^{236}U_f \xrightarrow{n} {}^{235}U_f \xrightarrow{n} {}^{234}U_f \xrightarrow{n} {}^{233}U_f$$

является уран-233. В то же время при делении ядра урана-233 нейтронами с энергией 5 ÷ 8 Мэв последним ядром в цепочке

$$^{234}U_f \xrightarrow{n} {}^{233}U_f$$

также является уран-233. Эти два результата также полезно было бы

ТАБЛИЦА I. УРАН-235

Период полураспада (сек)	Отношение выходов
	E_n = 18,5 Мэв
55	1
24	2,070 ± 0,048
15,5	1,711 ± 0,068
5,2	3,27 ± 0,11
2,2	5,68 ± 0,22
	E_n = 19,5 Мэв
55	1
24	2,01 ± 0,13
15,5	2,25 ± 0,18
5,2	2,06 ± 0,27
2,2	12,01 ± 0,61
	E_n = 20,0 Мэв
55	1
24	3,54 ± 0,13
15,5	2,36 ± 0,16
5,2	4,17 ± 0,25
2,2	10,61 ± 0,50
	E_n = 21,0 Мэв
55	1
24	4,17 ± 0,08
15,5	1,93 ± 0,10
5,2	4,94 ± 0,18
2,2	7,59 ± 0,34

ТАБЛИЦА II. УРАН-238

Период полураспада (сек)	Отношение выходов
	E_n = 18,0 Мэв
55	1
24	5,06 ± 0,12
15,5	2,57 ± 0,13
5,2	6,73 ± 0,22
2,2	15,64 ± 0,45
	E_n = 19,0 Мэв
55	1
24	4,75 ± 0,12
15,5	2,53 ± 0,15
5,2	6,61 ± 0,24
2,2	16,3 ± 1,0
	E_n = 19,5 Мэв
55	1
24	4,58 ± 0,27
15,5	3,19 ± 0,32
5,2	5,43 ± 0,51
2,2	25,7 ± 1,3
	E_n = 20,0 Мэв
55	1
24	5,85 ± 0,22
15,5	3,62 ± 0,24
5,2	8,21 ± 0,39
2,2	24,47 ± 0,93

сравнить. Результаты измерений представлены в табл. I и II и на рис. 1 – 4. Видно, что необходимо еще провести измерения в некоторых дополнительных точках. Это в настоящее время делается и часть материалов уже находится в обработке. Однако уже и сейчас проявляются наиболее характерные черты поведения отношения выходов. Видно, что изменения отношения выходов групп запаздывающих нейтронов в районе ступеньки, где идет реакция (n, 3nf) – еще больше по абсолютной величине, чем там, где идет реакция (n, nf). Кривые, описывающие изменение отношения выходов запаздывающих нейтронов каждой данной группы (по отношению к первой) в зависимости от энергии, у обоих элементов подобны. Мы пытались сравнить изменения отношения выходов в случае процессов (n, 3nf) и (n, nf), совмещая начала соответствующих ступенек в сечении деления (при этом точки в сечении деления при 5,5 Мэв и 20 Мэв совпадают). Из-за небольшого количества точек, имеющихся в настоящее время в области 18 – 21 Мэв (рис. 5 – 8) детальное сравнение затруднительно, оно будет проведено после дополнительных

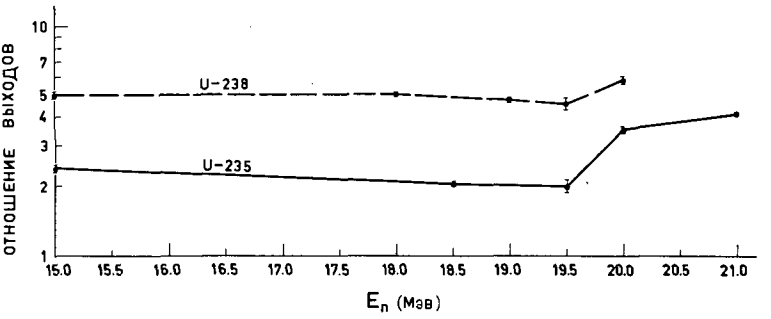

Рис.1. Группа T = 24 сек (уран-235 и уран-238).

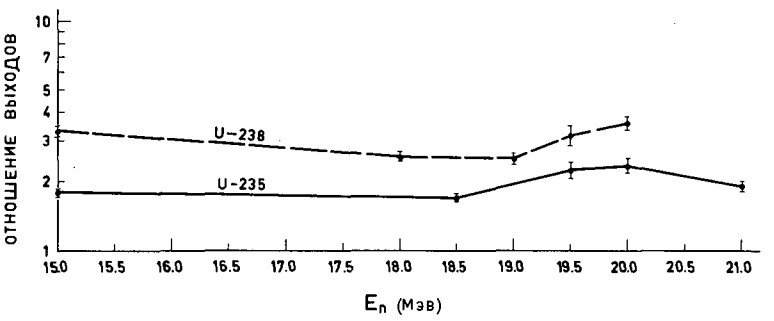

Рис.2. Группа T = 15,5 сек (уран-235 и уран-238)

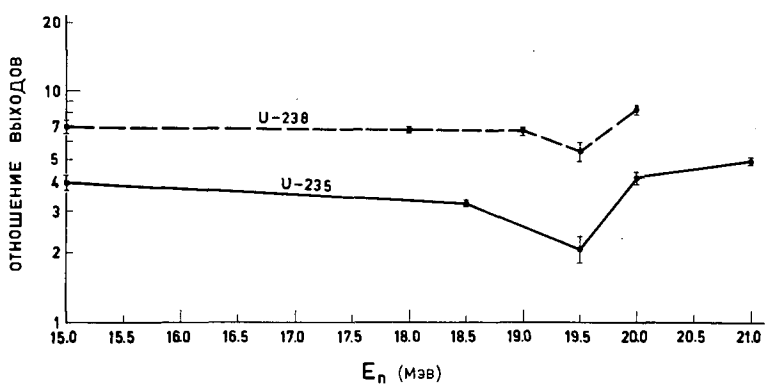

Рис.3. Группа T = 5,2 сек (уран-235 и уран-238)

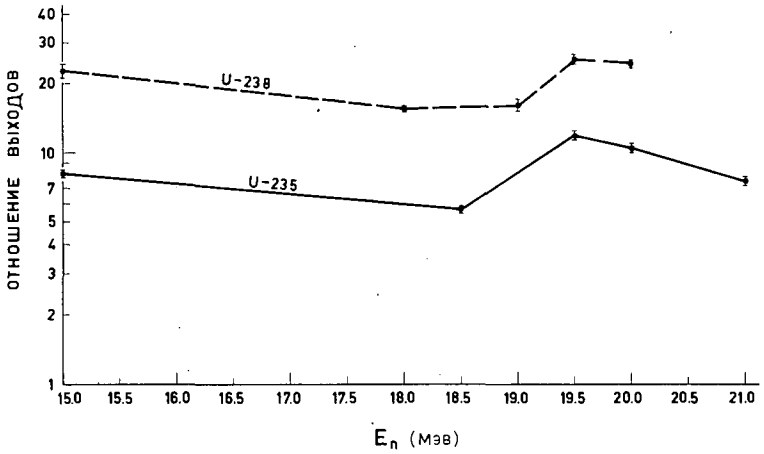

Рис.4. Группа T = 2,2 сек (уран-235 и уран-238)

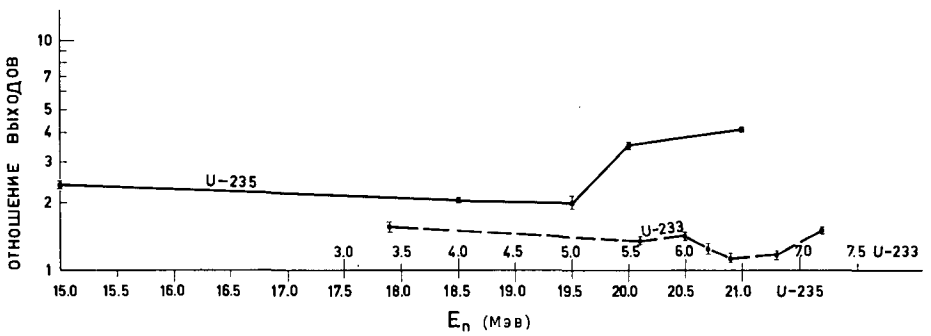

Рис.5. Группа T = 24 сек (уран-235 и уран-233)

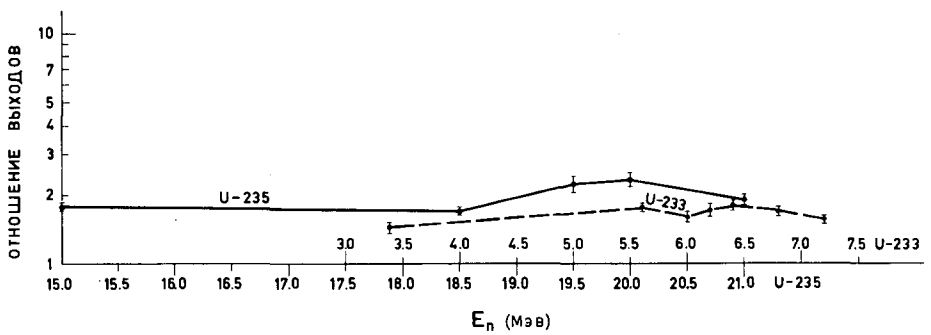

Рис.6. Группа T = 15,5 сек (уран-235 и уран-233)

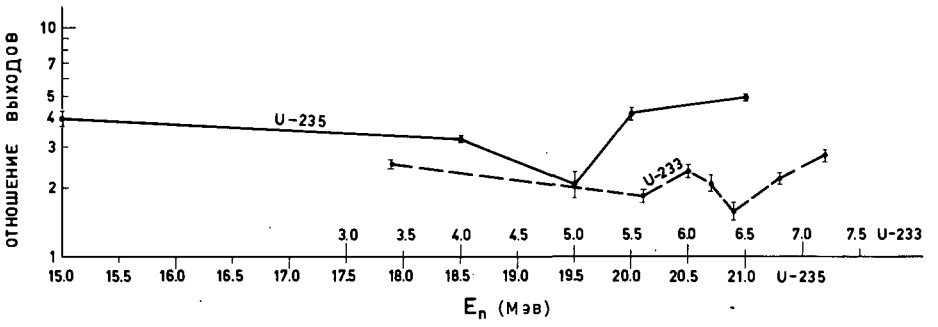

Рис. 7. Группа T = 5,2 сек (уран-235 и уран-233)

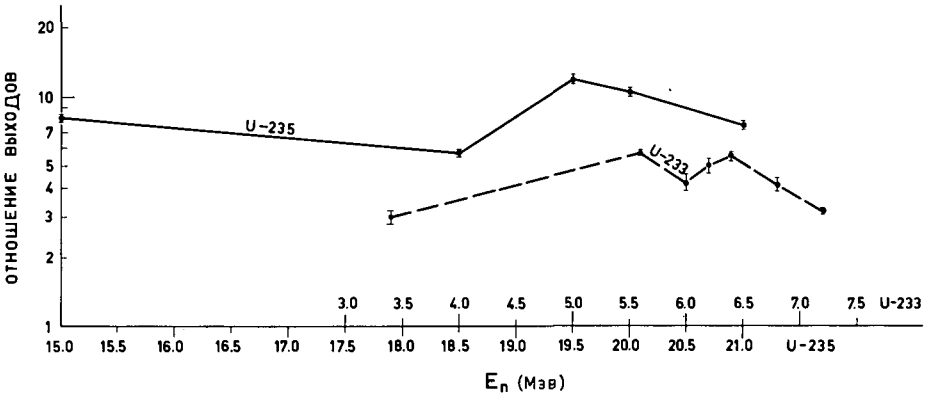

Рис. 8. Группа T = 2,2 сек (уран-235 и уран-233)

исследований. Возможно, что из-за разной ширины переходной области в обоих случаях потребуется перенормировка масштаба по энергии. Видно только, что эти изменения более резкие, чем в случае реакции (n, nf).

Мы можем здесь сделать те же замечания, что и в случае влияния реакции (n, nf) на изменение отношения выходов запаздывающих нейтронов. Пока неясно, как изменится эта структура при измерениях с тонкой мишенью. Мы не имеем данных по выходам масс в этой области энергий. Очевидно, эти последние вместе с результатами измерений относительных выходов с лучшим разрешением и значениями абсолютных выходов позволяет прояснить физические основы наблюдаемой закономерности.

DISCUSSION

On the papers by Maksyutenko, and Maksyutenko et al.

Comparing the thermal fission with fission due to high energy (14 or 15 MeV) neutrons, it was expected that the yield of delayed neutrons would decrease. However, results reported by Maksyutenko [1] indicated an increase by a factor of 1.5 to 2.0. The results of the Herrmann group indicate no increase, and Keepin's preliminary results show a decrease.

This discrepancy was discussed at length. Maksyutenko's view is summarized as follows: Some of the data presented by him are somewhat old (1958), from the times when even fission cross-sections were not properly known, and they enter into his calculations. Keepin predicted an approximately five-fold decrease of the yield for ^{235}U. It might be possible to have an experimental error of a factor of $1\frac{1}{2}$ to 2 in view of the poor knowledge of fission cross-sections in earlier times; an error of a factor of 10 is well-nigh impossible. There are other recent data in addition to those given by the Maksyutenko group. In February 1966, data of the group working in Budapest were published, confirming the results of McGarry [2]. The Maksyutenko results compare well with the McGarry data with differences of only 30-50%. In no case was a decrease of the yield at higher energy found, this excluding the possibility of a strong decrease of yield with increasing energy. It is impossible at the present time to rely on theoretical interpretations even though the calculations are rather exhaustive. There is, for example, a contradiction between two sets of facts. Firstly, the mass distribution curves for thermal neutrons and 15 MeV neutrons are known. The yield masses of the precursors generally decrease with increasing energy, and this would result in a decrease of yield. In addition, the total displacement of the charge when moving toward higher charge also predicts a decrease of the yields.

Secondly, there are the factors which indicate a shift in the opposite direction. The yield of mass 87 at 15 MeV does increase compared to the thermal energy yield. It should be pointed out that only the relative yields have been determined. In the thermal region, the ratio of the second to the first group is approximately 6 : 1. In the 14 MeV region, this ratio falls to 4 : 1. With this in mind, an estimation of the absolute yields shows an increase. So far only a small number of experimental results are available. The results of the Petrzhak, Spakhov [3] and the Budapest group indicate that there is no decrease in yield.

In experiments of yields for thermal and 15 MeV neutrons, the Maksyutenko group did not observe the theoretically predicted decrease of the yield. The experimental errors could not be higher than 30%, including uncertainties in fission cross-section. Opinions from various participants on this problem can be summarized as: At mass 87, and this applies both for ^{235}U and ^{238}U, there is no difference in mass yields going from thermal to 14 MeV neutron energy (new data). But there is a difference in Z_p. The empirical values in the high energy range are not known, but it is certain that the chains get shorter by about 0.7 units. This indicates that the yield must decrease, at least for the first group. In the second group the question of how many precursors contribute (although most are known) to this group is still open; tellurium-236 might

still be included. Even the imprecise data we have now indicate a drop of the yield. The decrease observed in preliminary measurements by the Soreq group are of the order of 10 to 20%. In no case did they find an increase. Even without exact data, we could say rather confidently that, if there is any effect, the shortening of the chains of these particular precursors (without considering any new precursors which might be discovered in this period, and which would be in the valley or on the tails of the mass distribution curve) would result in a decrease of yield. The Los Alamos group also made experimental measurements, with an absolute detector calibration and fission monitoring, and it is firmly believed that the yield does not increase. More measurements have to be done in other laboratories to obtain more experimental data.

In the continuation of the discussion, new results presented by Maksyutenko were examined in detail. Some of the conclusions are summarized below.

The process of the emission of delayed neutrons should be treated in several stages. Firstly one should consider how the nucleus is fissioned and what the numbers are of protons and neutrons in the fission products. Secondly one should observe the number of neutrons that are emitted from each fission fragment. We also do not know how the charge changes and this complicates the situation. For a more detailed evaluation, a good value for Z_p would be necessary in this energy region (the measurements will be very difficult to perform) and the distribution of the numbers of neutrons from different fission fragments should be known. The data are at present not precise enough.

The lack of knowledge is even more deplorable if one goes to the next threshold, the (n, 2n) and (n, 3n) fission. The problem is that the fissioning compound nucleus is different to the target nucleus. Coming to the first (n, n') fission in ^{238}U, it is no longer a ^{239}U excited fission. There we have nuclei which have less neutrons (with the same proton number), and nobody knows anything about the fission of such nuclei.

The irregularities appear at the points where the fission cross-section curve has a step. These steps are connected with the second nucleus of the chain, with the nucleus which is formed at low excitation energy. These are threshold processes and it is possible that they are connected not only with energy but also with spin, angular momentum and other properties. This effect is observed in the transition area , where nothing is known about spin. It is amazing that the effect continues to high energies where there is a second, third or even fourth nucleus of the fission chain.

There are some measurements of the peak-to-valley ratio in the mass distribution curve with changing excitation energy. There are some peaks when going to the second and third chance fission. In ^{99}Mo, for example, these peaks are broad and not very high. This would indicate that some unexpected effects occur. There must be a strong effect on the charge distribution and on the P_n -value. This could possibly be found from a mass distribution curve which is determined by purely physical methods, methods which must be sensitive enough to see the change in mass distribution in a narrow energy region.

The Maksyutenko group did a theoretical estimation of the charge distribution, and values for the rise of other groups as compared to the first one could be obtained.

The spin values could substantially influence the yields. Going from one threshold to another, the spin will change drastically. In an even-even nucleus, the spin is zero in the ground state; after emitting one neutron, the spin will be 9/2, 5/2 or something similar.

This might be reflected in the fission products themselves. Some measurements of the ratio of high to low spin as a function of energy have been performed. At high energy, this ratio increases as expected, at low energy it probably decreases. The fission of different uranium isotopes with protons, deuterons and α-particles has been studied, but not with neutrons at high energies. If there is an increase of the high spin isomer, this might influence the emission of delayed neutrons.

The prompt neutron emission from the fragments must also be considered. It does not follow the standard pattern, particularly if the fragments are in a state of high spin. With so many parameters involved, all estimations are really wild guesses.

One way to find out more about the situation is to make a study of heavy ion reactions, in which a very high angular momentum is introduced and the influence of the angular momentum is more evident. This would require the production of ^{238}U (or a higher isotope) by irradiating the lower-Z nuclei with heavy ions, and the subsequent measure of delayed neutrons.

Second chance fission does not suddenly take over from the ordinary fission, i.e. there is not a step transition from one to the other. At a certain energy, there is coexistence of second chance fission occurring with higher excitation, and the fission of one-mass-unit-larger nuclei still occurring in the range of 7 MeV.

Fission neutron emission seems to be a phenomenon that is very sensitive to the energy of the bombarding particle and the models are still not understood. In the region of other types of excited nuclei, where the knowledge is still poorer, where the odd-even relationships are different, it is hard to predict fission dynamics.

REFERENCES

[1] MAKSYUTENKO, B.P., Atomn. Energ. 7 (1959) 474.
[2] McGARRY, W.I. et al., Bull. Am. Phys. Soc. II 5 1 (1960) 33.
[3] SPAKHOV, V.I., PETRZHAK, K.A., BAK, M.A., KOVALENKO, S.S., KOSTOCHKIN, O.I., Atomn. Energ. 11 (1961) 539.

WORK IN GREECE ON DELAYED NEUTRONS

N.G. CHRYSOCHOIDES, A.J. NICOLITSAS *,
N.N. PAPADOPOULOS, C.C. ZIKIDES AND
C.A. MITSONIAS
DEMOCRITUS NUCLEAR RESEARCH CENTRE,
ATHENS, GREECE

Abstract

WORK IN GREECE ON DELAYED NEUTRONS. At present, two programmes on delayed neutron research are in progress in Greece.

DELAYED NEUTRON ENERGY SPECTRUM MEASUREMENTS. In an experiment at the 1 MW Democritus reactor, the energy of the delayed neutrons from ^{235}U fission is measured by the time-of-flight technique and β-n-coincidence using a special fast system for irradiation of the sample. The beta particle preceding the emission of the delayed neutron is used as a start pulse while the delayed neutron provides a stop signal. A maximum flight time of approximately 100 nsec is allowed over a flight distance of approximately 30 cm (longer flight paths could be used for better energy resolution, but this would decrease the efficiency of detecting the delayed neutron). To avoid false measurements due to other beta particles which do not correspond to delayed neutrons, an anti-coincidence system is used to cancel the measurement whenever two beta particles come in a time interval shorter than 100 nsec. Coincidences due to delayed neutrons are relatively rare in comparison with chance coincidences or β-γ-coincidences. The spectrum obtained in a first run of measurements is discussed. An attempt will be made to measure the spectrum of each individual group by varying the irradiation time and the measuring time. Various irradiation, transfer and measuring times can be obtained with the existing experimental set-up. A minimum transfer time of 300 msec can be achieved. Very thin foils (a few mg/cm^2) are used to minimize the beta-particle absorption in the sample.

DELAYED NEUTRON GROUP RELATIVE ABUNDANCES AND PERIODS. In a second experiment, measurements to determine the relative abundances and periods of the delayed neutrons for various fissile materials are now under way. The arrangement for delayed neutron group measurement allows the sample to be transferred in a minimum time of approximately 800 msec. Accordingly, delayed neutrons of quite short half-lives can be detected. The experimental facility permits of very accurate repetition of each cycle of measurement which results in good statistical accuracy. In earlier work, measurements of delayed neutron precursor relative abundance for ^{235}U fission by thermal neutrons have been performed using the radiochemically known half-lives of iodine and bromine.

DELAYED NEUTRON ENERGY SPECTRUM MEASUREMENTS

1. INTRODUCTION

In the present experiment, the delayed neutron energy is measured by a fast time-of-flight coincidence technique using the beta particle preceding each delayed neutron as a start pulse and the neutron itself as a stop pulse.

A special irradiation facility is used to irradiate a thin fissionable foil in a reactor neutron beam.

---

* Now at Queen Mary College, London, England

Transportation time of the irradiated foil from irradiation to measuring position can be as short as 300 msec; thus, short half-life groups can be detected.

Irradiation, waiting and counting times can vary within certain limits. In this way the overall energy spectrum or the individual group energy spectrum can be emphasized.

A block diagram of the experimental set-up is given in Fig. 1. The irradiation facility consists mainly of a special collimator which enables a foil to be irradiated in a reactor neutron beam for a certain pre-set time, after which the neutron beam is completely cut off and the foil moved to the measuring position.

The automatic system is designed to achieve accurate repetition of the various movements and functions of the system in each cycle of measurements. Finally, the detecting and counting units consist mainly of fast electronics which enable the rapid events to be followed within a flight time up to 120 nsec.

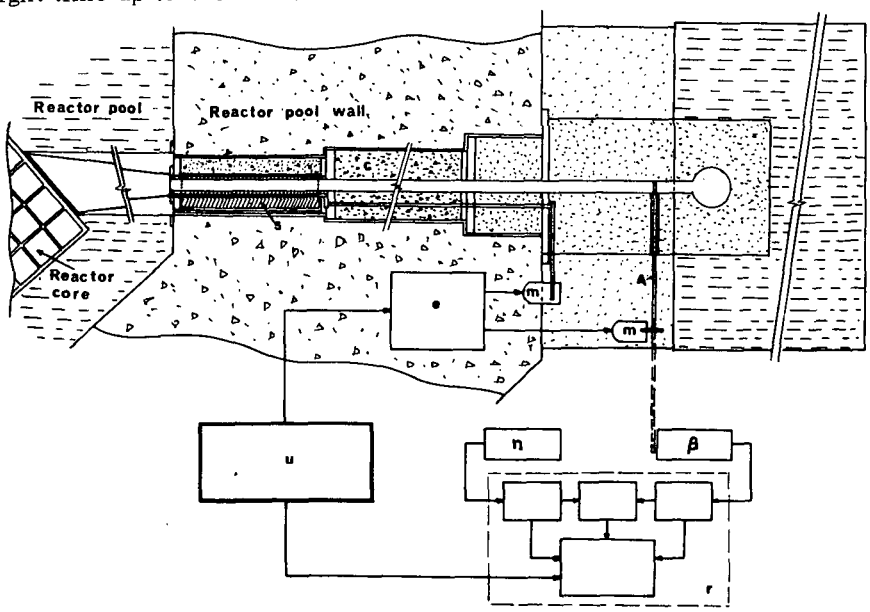

FIG. 1. General layout of the experimental set-up.
C - collimator; s - shutter; u - automatic controller; e - electrically operated valve; m - shutter and arm moving mechanisms; A - arm; n, β - neutron and beta detectors; r - counting and recording system.

2. DESCRIPTION OF THE EXPERIMENTAL SET-UP

The experimental facility is installed in one of the neutron beam tubes of the Democritus Reactor, a 1 MW, swimming-pool type of reactor.

2.1. Irradiation facility and automatic system

A detailed description of the irradiation facility and the automatic system is given in Ref. [1].

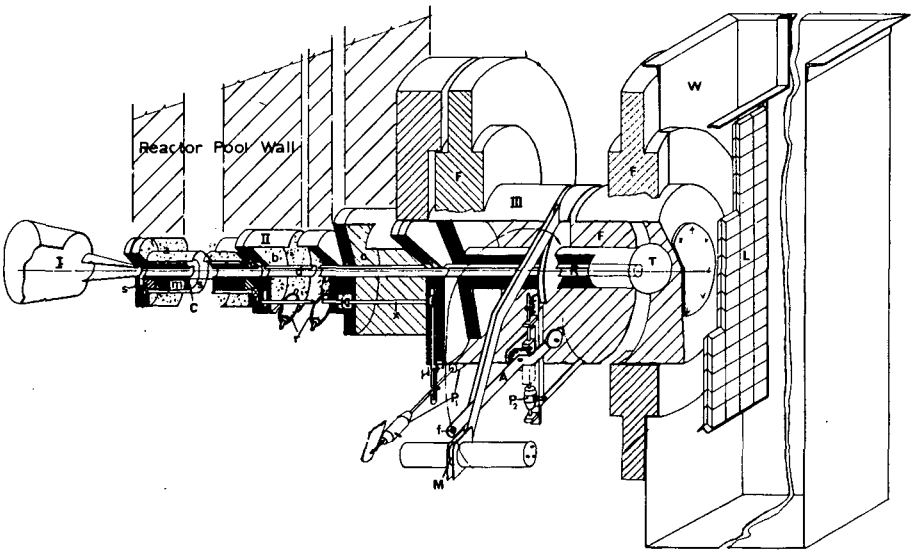

FIG.2. The collimator. I - aluminium cone; IIa, b, c, - main collimator; III - external shielding; d - collimator channel; s - shutter; m - masonite; C - cadmium sheets; S - stainless steel; r- rollers; x - shaft; F - paraffin; W- water tank; L - lead wall; T - neutron trap; R - irradiation position; M - measuring position; $F_{1,2}$ - pistons; A - arm; f - foil.

The irradiation facility, Fig. 2, comprises three main parts: the aluminium cone (I), the main collimator (II) and the external shielding (III).

Parts (I) and (II) fit into the reactor neutron beam tube while part (III) is outside the reactor wall. A neutron beam shutter, located in part (II), completely cuts off the neutron beam and gamma rays when in its closed position.

The automatic system comprises the air supply, electrically operated valve system and the automatic control unit. The functions of the automatic system are to actuate the shutter and arm mechanisms at the appropriate moments to keep the irradiation, waiting and counting periods constant for the pre-set periods of time, and finally to give the necessary visual checks on the operation of the various parts of the system.

2.2. Electronic equipment

A block diagram for the electronic units is given in Fig. 3. This part of the experimental set-up consists of the detectors, the measuring and the recording units.

2.2.1. Detectors

Two beta detectors in 4π geometry and four neutron detectors in radial geometry are used (see Fig. 4). The distance between the two beta counters can be as small as 2 mm while the distance of the neutron counters from the centre of the foil can vary from 10 cm upwards.

Nuclear Enterprises plastic scintillators, NE-102A, 5 cm in diameter, are used in both cases. The main advantage of the above

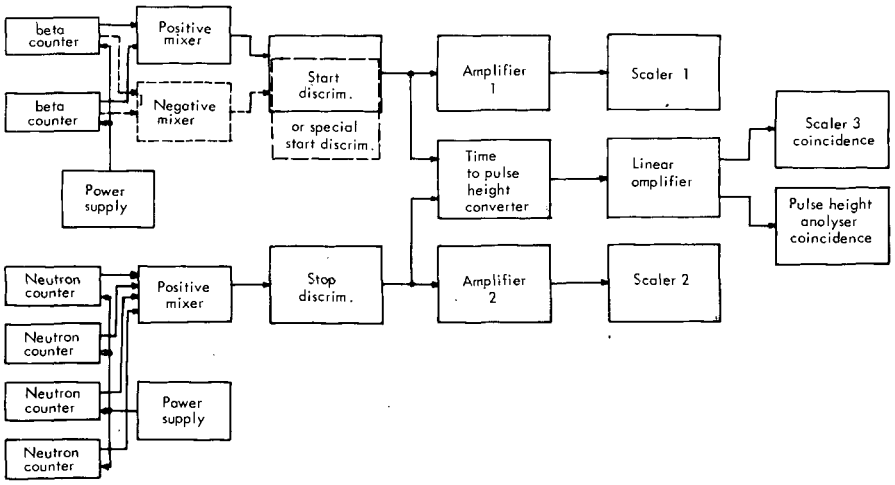

FIG. 3. Block diagram diagram of electronics.

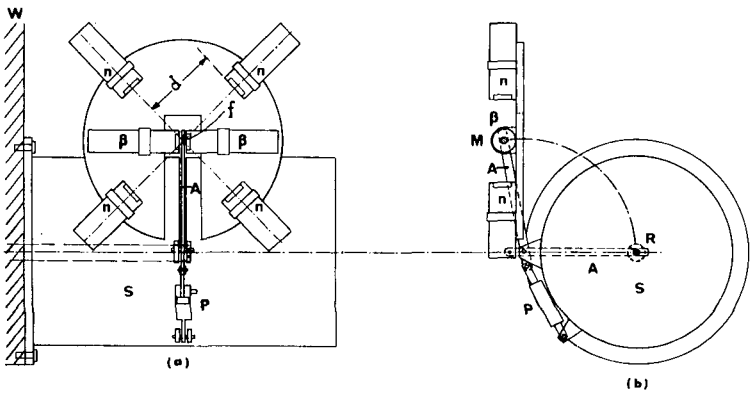

FIG. 4. Positions of the detectors. W - reactor wall; n - neutron detectors; β - beta detectors; A - arm; P - piston; S - shielding; R - irradiation position; M - measuring position; f - foil; d - flight distance.

scintillators is their short rise time (about 3 nsec). Rise time is very critical in the determination of the energy resolution of the system (see 3.1.2). On the other hand, discrimination with NE-102A scintillators between various radiations such as gammas, betas and neutrons is very difficult and thus the background problem becomes important. A proper choice of the plastic scintillator thickness has to be made. The neutron scintillators should be thin enough to minimize the neutron flight distance error and thick enough to have a relatively high sensitivity. A thickness of 15 mm is being used. The beta scintillators have a thickness of 1 mm, which makes them relatively insensitive to gamma rays.

56AVP photomultipliers are used together with the plastic scintillators. These photomultipliers have a rise time of about 3 nsec, with an output

pulse high enough to be used without amplification and with a large range of high voltage adjustment.

2.2.2. Electronic units

The idea of using a coincidence system in the present experiment derives from the fact that each delayed neutron accompanies a beta particle and the neutron emission from the excited nucleus is practically instantaneous.

The operational principle of the electronic system is as follows.

Each discriminator connected to the beta and neutron counters produces, after the arrival of a pulse, a longer pulse of duration t_1 nsec with a delay of t_2 nsec (Fig. 5). These pulses are introduced to the time-to-pulse height converter. The pulses from the beta and neutron counters are the start and stop pulses, respectively. When the stop pulse arrives with a delay of t_3 nsec after the start pulse, where $t_3 < t_1$, then a voltage ramp of duration $t_1 - t_3$ is produced which gives a pulse height, h, corresponding to the time of neutron flight. This output pulse is recorded, after suitable amplification, by a calibrated multichannel analyser.

Three scalers are connected through appropriate amplifiers to measure the beta, the neutron and the coincidence pulses. This information is necessary for the estimation of the random coincidences.

A more detailed description of the main electronic units is given below.

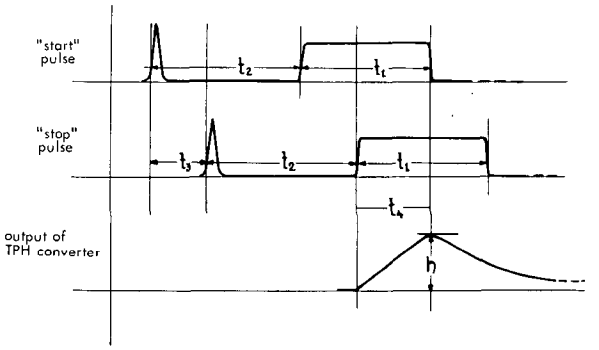

FIG. 5. Input and output pulses of the discriminator TPH convertor. t_1 - maximum allowed flight time (resolving time); t_2 - delay time; t_3 - time-of-flight; t_4 - ($= t_1 - t_3$) coincidence time.

Mixers. Two positive pulse mixers are used for the signals from the neutron and beta photomultipliers. An additional negative mixer for the beta photomultiplier is necessary for the operation of the special discriminator. The circuit diagrams of the two types of mixers are given in Fig. 6a, b.

Start or stop discriminators. These discriminators can receive at their inputs positive pulses of short rise time of the order of 2 nsec and of a height of 0.2 V up to 2 V. Output pulses have a constant duration of 120 nsec and a height of 0.7 V. The circuit diagram of the discriminator is given in Fig. 7.

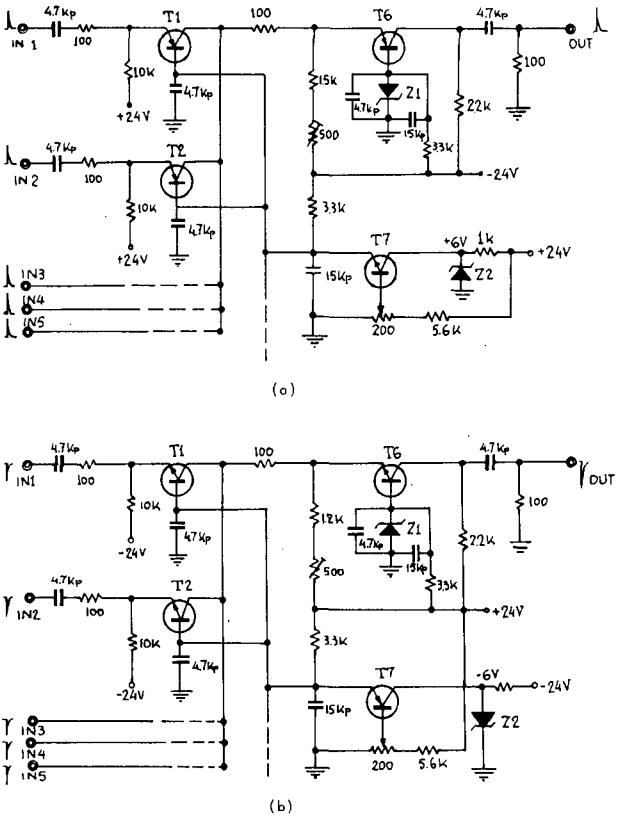

FIG. 6. Positive (a) and negative (b) mixers.

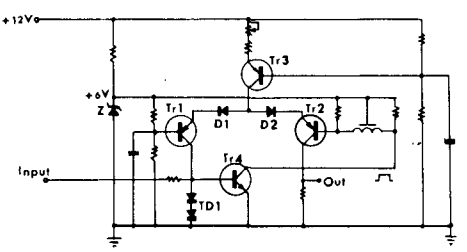

FIG. 7. Start or stop discriminator.

Special start discriminator. This is not a simple discriminator but a special anti-coincidence circuit with one input. The purpose of building such a circuit is to avoid beta-neutron coincidences due to beta particles not associated with delayed neutrons when a very high beta rate is being detected by the beta counters.

Since coincidences between neutrons and neutron-associated beta particles are to be detected within a time of 120 nsec in the presence of

a high background of randomly occurring beta particles and gamma rays, there is a possibility that a beta particle or gamma ray will give a start pulse before the beta particle associated with the delayed neutron, is detected. This could result in a false coincidence if a neutron is then detected within the next 120 nsec. The special discriminator is designed to block the start discriminator's output when two separate pulses excite its input in a time of less than 120 nsec.

Apart from this special function, the discriminator acts as a normal discriminator, identical to the start or stop discriminators, having exactly the same output characteristics.

A complete description of this special discriminator and its function is given in Ref. [2].

Time-to-pulse height converter. The function of this unit is to convert the time difference between the pulses from the output of the two discriminators into a pulse of corresponding height. A detailed circuit of the converter is given in Fig.8.

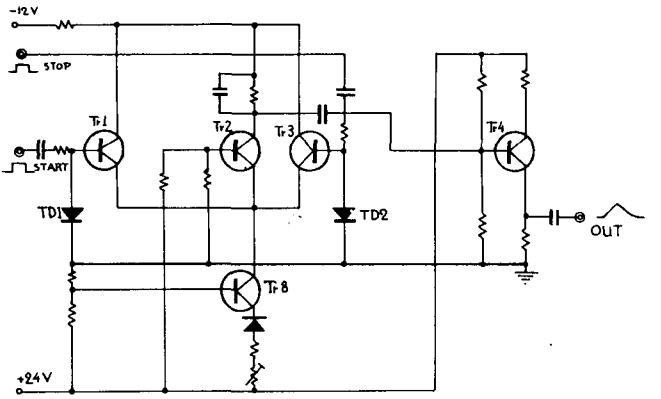

FIG. 8. Time to pulse height converter.

3. EXPERIMENTAL PROCEDURE

Certain theoretical calculations that are necessary for the evaluation of the experimental limitations are given below. The calibration of the units is also described.

3.1. Calculations

3.1.1. Foil thickness

The foil must be so thin that beta particles associated with delayed neutrons will not be absorbed in the foil. From the existing data [3] the $(Q_\beta - B_n)$ value is 2.04 MeV for the first delayed neutron group going up to 9.1 MeV for the sixth group. Since the average energy of the various delayed neutron groups is expected to be well below 1 MeV, the beta particle energy associated with delayed neutrons must be well above 1.04 MeV even for the first group. Thus, relatively thick foils can be

used without a significantly high absorption of the beta particles associated with neutrons.

In the present experiment 90% enriched uranium-235 is used as fissile material. The target consists of a U-Al alloy, with 14% of uranium by weight. Two foils have been used so far: one had a surface density of 20.6 mg/cm^2, a total surface of 1.76 cm^2 and a total ^{235}U content of 4.56 mg; the second had a surface density of 43.7 mg/cm^2, a total surface of 3.95 cm^2 and a total ^{235}U content of 21.8 mg.

3.1.2. Resolution and flight distance determination

The energy resolution of the system is determined by the rise time of the detecting and electronic units, the neutron flight distance and its energy. Since the above rise time is limited to 3 nsec by the rise time of the scintillation counters, the energy resolution depends on the flight distance and the neutron energy.

The relation between energy resolution and flight time is:

$$\frac{\Delta E}{E} = \frac{2\Delta t}{t} = \frac{6}{t} \qquad (1)$$

with E in keV, t in nsec and $\Delta t = 3$ nsec.

The relation between energy resolution and flight distance is:

$$\frac{\Delta E}{E} = 0.261 \frac{\sqrt{E}}{d} \qquad (2)$$

where d is in centimetres.

From Eqs (1) and (2), a family of curves can be obtained (Fig. 9). In these curves the energy resolution and the corresponding flight time versus neutron energy are plotted for various flight distances. The rapid improvement of the energy resolution for lower neutron energies and longer flight distances is obvious from the curves. However, for the long flight distances that are required for better resolution in certain energy regions the efficiency of the neutron counting system decreases considerably. In such cases the provision of more neutron counters would be advantageous.

3.1.3. Foil activity

The saturation activity of the irradiated foil, determined by its mass and the neutron flux, should be high enough to ensure good counting statistics for a reasonable irradiation time and low enough to keep the ratio of random to true coincidences below certain limits.

The activity of the foil is derived from its fission rate:

$$F = \frac{N_0 \sigma_f}{A} \varphi m$$

where N_0 is Avogadro's number, σ_f the fission cross-section of ^{235}U, A the atomic mass number of ^{235}U, φ the neutron flux, and m the mass of the foil.

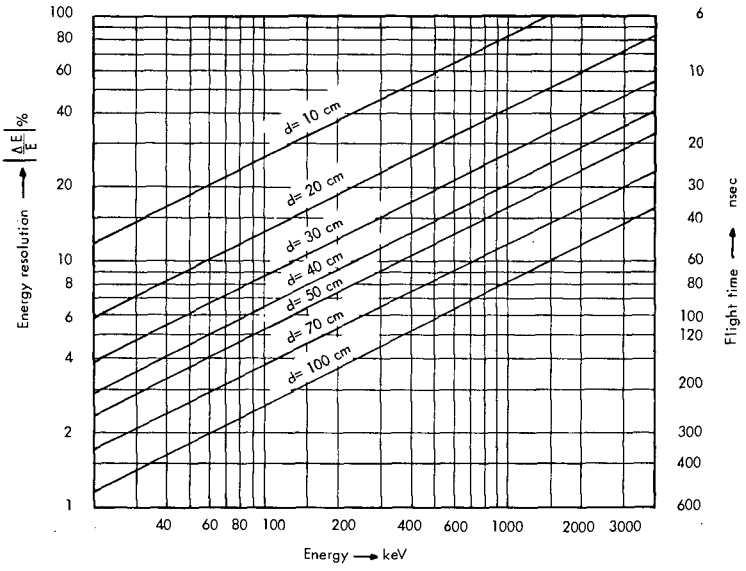

FIG. 9. Calculated energy resolution for the system.

3.1.4. Delayed neutron counts at neutron counters

The total number of delayed neutrons emitted from a foil over a time interval t_1 to t_2, following saturation irradiation is:

$$N_d = F\nu\beta \sum_i \frac{\alpha_i}{\lambda_i} \left(e^{-\lambda_i t_1} - e^{-\lambda_i t_2}\right)$$

where F is the fission rate, ν the number of neutrons emitted per fission, β the fraction of fission neutrons emitted which are delayed, α_i the relative abundance of each delayed neutron group, λ_i the decay constant of the ith group, and t_1 the waiting and $t_2 - t_1$ the counting times, respectively.

For the experiment, for foils 1 and 2 the values of m were $m_1 = 4.56$ mg and $m_2 = 21.8$ mg, respectively, and $\varphi = 2.6 \times 10^7$ n cm^{-2} sec^{-1} $t_1 = 1$ sec and $t_2 = 200$ sec. In Table I are shown the total numbers of delayed neutrons, N_{d1} and N_{d2}, for each of the foils, that should be counted by four neutron detectors for various flight distances assuming 50% total detecting efficiency.

TABLE I. NUMBER OF DELAYED NEUTRONS AT VARIOUS FLIGHT DISTANCES FOR TWO DIFFERENT FOILS

Flight distance, d(cm)	10	20	30	40	50	70	100
Count for 4.56 mg foil, N_{d_1}	994	248	110	62	40	20	10
Count for 21.8 mg foil, N_{d_2}	4770	1190	535	298	190	98	48

3.1.5. Count rate at beta counters

The equilibrium beta count rate at saturation is about four times the fission rate [7].

The beta decay of the irradiated foil was fed to a multichannel analyser. The gamma ray contribution to the beta count rate, in spite of its higher emission rate, is negligible, because of the low gamma efficiency of the beta detector.

The number of β-n-coincidences due to beta particles not associated with delayed neutrons depends on the probability, as determined by the interval distribution, that two betas will appear during the resolving time interval. To decrease this probability the beta count rate should be kept sufficiently low.

From this consideration, and with the existing count rate, it appears that it is unnecessary to use a special start discriminator which rejects the 'false' β-n-coincidences, and which therefore is more complicated in its operation: a normal start discriminator can be used.

3.2. Calibrations

Neutron detector calibration. NE-102A plastic scintillators give a light output pulse from neutron-produced recoil protons which is much smaller than the light pulse for gamma-produced recoil electrons for the same neutron or gamma energy.

The ratio of light outputs of electrons to protons of the same energy was found to be about 5/1 for an energy of 1 MeV and about 8/1 for an energy of 0.2 MeV [4-6]. Since the lowest delayed neutron energy is expected to be in the region of 100 keV, the HT and the discriminator setting of the neutron detectors should be adjusted to measure pulses from a gamma source above 15 keV. This adjustment of the low-level setting of the neutron detectors was made by using an ^{241}Am source giving gamma ray energies of this order of 15 keV.

Beta detector calibration. Discriminator and HT settings for beta detectors were adjusted to permit the detection of beta particles associated with delayed neutrons by using standard beta sources of known energy.

4. RESULTS AND CONCLUSIONS

As a preliminary estimate a measurement of relatively short duration was made consisting of 110 runs, each one of 490 sec. Although the statistical accuracy of this measurement was not very satisfactory, an approximate picture was obtained of the results to be expected. Irradiation, waiting and counting times were adjusted to 290, 1 and 199 sec, respectively. This time sequence was chosen to obtain the total energy spectrum of delayed neutrons. In Fig. 10 the number of the coincidences obtained is plotted against the channel number which has a linear correspondence to the time-of-flight.

In the short time-of-flight region of the curve a peak is clearly seen. This is due to the β-γ coincidences associated with the fission process. This peak, being outside the delayed neutron energy region under investigation, is not considered in the evaluation of the measurement.

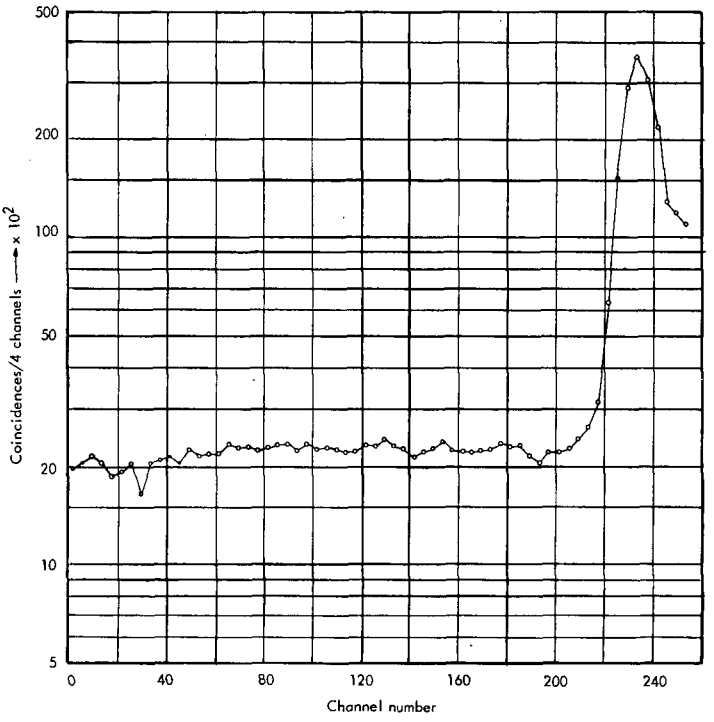

FIG. 10. Time-of-flight spectrum.

Analysis of the curve obtained is performed after allowing for the random coincidences, which can be considered to be equally distributed in time.

The number of random coincidences per channel for the total counting time is given by:

$$N_r = \frac{2\tau(N_\beta - N_c)(N_n - N_c)}{t_c n_c}$$

where τ is the resolving time of the coincidence system, t_c the total counting time, n_c the number of analyser channels used, and N_β, N_n, N_c are the total number of counts obtained in the beta, neutron and coincidence counting systems, respectively, for the whole counting period.

The delayed neutron energy spectrum is derived from the time of flight spectrum, Fig. 10, by evaluating the number of β-n-coincidence counts in channel intervals $|\Delta c|$ at various c, corresponding to energy intervals ΔE, at various E, divided by ΔE, where:

$$E = \left(\frac{54d}{265 - c}\right)^2$$

$$\Delta E = \left(\frac{0.261}{d}\right) E^{3/2}$$

where c = 265 - 2.37 t (from experimental calibration curve)
$\Delta c = 2.37\ \Delta t = 7.1$, and E is the neutron energy (keV), d the flight distance (cm), c the channel number, and t the flight time (nsec).

Using the above formula the shape of the curve, Fig. 10, will change completely. Correction will also be applied for variation of the detector efficiency with energy and of the flight distance due to the finite dimensions of the neutron scintillators and the foil.

Evaluation of the data obtained is in progress.

ACKNOWLEDGEMENTS

The authors would like to express their deep appreciation to Dr. G.R. Keepin who persuaded two of them, two years ago, to start work on delayed neutron spectra, after long stimulating discussions. They would also like to acknowledge the great assistance of the reactor staff and especially of Mr. E. Mavroyannakis for the design of the irradiation facility and Mr. L. Bassiakos for his active participation during the performance of the experiment. Finally, they would like to thank Dr. C. Mantakas for his assistance during the design and construction of the electronic equipment.

DELAYED NEUTRON GROUP RELATIVE ABUNDANCES AND PERIODS

5. INTRODUCTION

Delayed neutron precursor abundances and half-lives are being investigated in the Democritus Reactor.

A special facility has been built for the irradiation and transportation of the fissionable material. The detecting, counting and recording units are interconnected through an electronic controller to ensure accurate repetition in time of the various functions of the system.

Irradiation of fissionable materials can be accomplished either in a thermal neutron spectrum, or in an epithermal and fast neutron spectrum by putting the sample in cadmium capsule.

Analysis of the accumulated data, corresponding to delayed neutron decay characteristics for various fissionable materials, is made using an IBM-360/40 computer.

6. EXPERIMENTAL SET-UP

A block diagram of the experimental set-up is given in Fig. 11.

Detectors. Plastic scintillators NE-401 and BF_3 counters are used for neutron detection. BF_3 counters have a better discrimination against gammas. Four detectors are used in both cases in a radial geometry around the sample (Fig. 12); 3 cm of lead and 12 cm of paraffin is placed

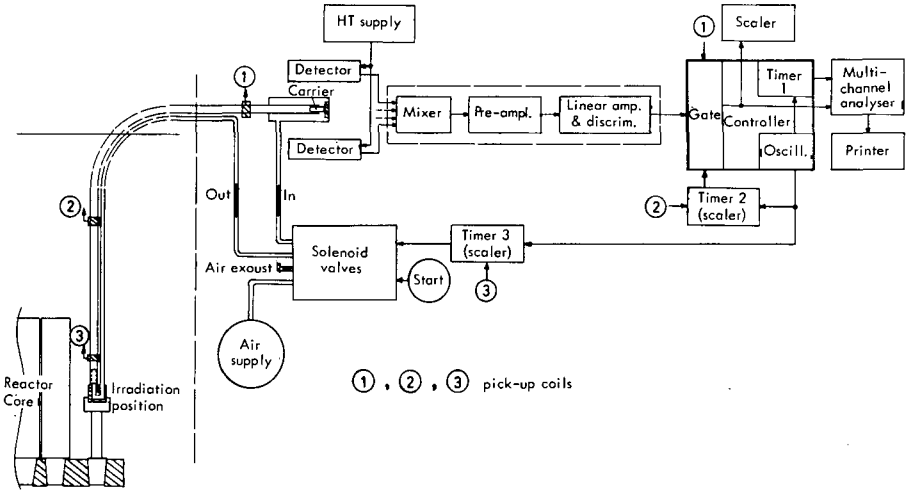

FIG. 11. Experimental assembly.

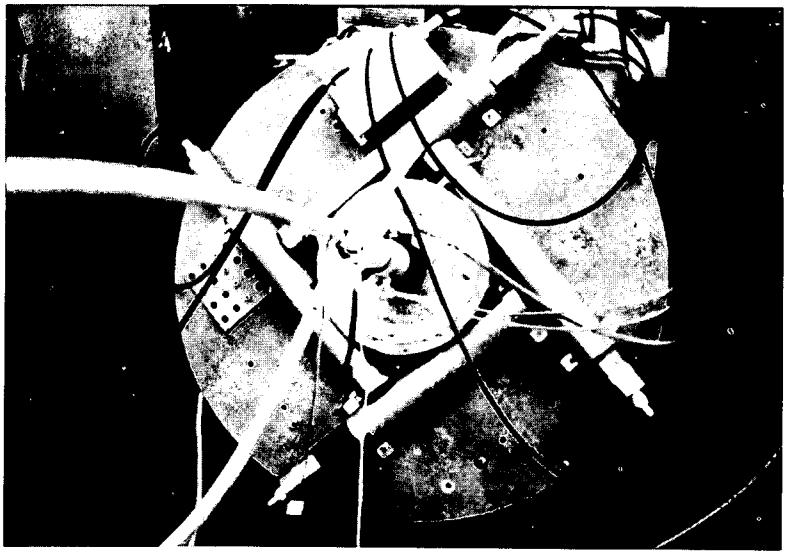

FIG. 12. Arrangement of the detectors.

between the sample and the counters to reduce the gamma background and to thermalize the delayed neutrons. Measurements were also taken with an additional 10 cm of lead in front of the detectors to reduce gamma background. This is more necessary with plastic scintillators.

Irradiation facility. The irradiation facility consists of a long bent aluminium tube for transporting the sample carrier, which is moved by compressed air. The usual minimum transfer time is 800 msec, which can, however, easily be reduced to 350 msec by using a low-friction

carrier of Teflon. The lower part of the tube, near the reactor core, is identical to a fuel element nose and it can be placed at any position of the reactor grid plate. Three coils along the tube are used to detect the position and the movement of the carrier and to give the necessary signals to the controller.

Sample carrier. The normal sample carrier is made of polyethylene and holds the capsule containing the fissionable material. A small magnet is also placed in the carrier to generate electrical impulses as it passes through the pick-up coils.

Electronic units. The signal from the detectors, after appropriate amplification and discrimination, is fed to the input of a 512 channel analyser. The three timers incorporated in the controller are used. Their function is to control the activation, the waiting and the counting times, and to give the necessary signals to operate various parts of the system at the appropriate moments. All bar one of the electronic units are standard and unmodified. The exception is the controller, which was specially built to satisfy the requirements.

7. EXPERIMENTAL PROCEDURE

A programme for investigating delayed neutron precursor abundances and half-lives for various fissionable materials is in progress.

In a first series of experiments, measurements were made to determine relative abundances of delayed neutron precursors in ^{235}U fission by thermal neutrons.

The measurements were obtained by irradiating 7.6 g of natural uranium in a thermal neutron flux of 10^{10} n cm^{-2} sec^{-1}. Irradiation time was extended to 300 sec for saturation of the longest delayed neutron group. Counting time was adjusted to start 2 sec after and stop 256 sec after the end of the irradiation. To ensure good statistical accuracy, accumulated measurements of several runs were used for each set of data.

The first four groups (out of the six recognized delayed neutron groups) were analysed into seven sets using radiochemically known half-lives of ^{87}Br (54.5 sec), ^{88}Br (16.3 sec), ^{89}Br (4.4 sec), ^{90}Br (1.6 sec), and ^{137}I (24.4 sec), ^{138}I (6.3 sec), ^{139}I (2.0 sec). A least-squares method of analysis was used.

Corrections were made for the dead time of the detectors and the background.

The results obtained apply to relative abundances of delayed neutrons. A comparison of these results was made with the corresponding relative abundances derived from a nine group absolute abundance analysis [2] and the agreement was found to be very satisfactory.

ACKNOWLEDGEMENTS

The authors would like to acknowledge with appreciation the assistance of the reactor staff during the performance of the experiment and especially Mr. S. Polygenis and Mr. V. Lymberiadis for their participation in the experiment.

REFERENCES

[1] MAVROYANNAKIS, E.G., ZIKIDES, C.C., CHRYSOCHOIDES, N.G., "Democritus" 1967 (to be published in J. sci. Instrum).
[2] MANTAKAS, C., NICOLITSAS, A.J., CHRYSOCHOIDES, N.G., Nucl. instrum. Methods 49 (1967) 161.
[3] KEEPIN, G.R., Physics of Nuclear Kinetics, Addison-Wesley, Mass. (1965) 96.
[4] KRAUS, D., LANDE, K., LEBOY, E., SELOVE, W., Rev. sci. Instrum. 29 (1958) 1142.
[5] GETTNER, M., SELOVE, W., Rev. sci. Instrum. 31 (1960) 450.
[6] BATCHELOR, R., GILBOY, B.W., PARKER, B.J., TOWLE, H.J., Nucl. Instrum. Methods 13 (1961) 70.
[7] Physics and Chemistry of Fission (Proc. Symp. Salzburg, 1965) in 2 Vols., IAEA, Vienna (1965).
[8] NICOLITSAS, A.J., CHRYSOCHOIDES, N.G., KOUVARAS, N., ZIKIDES, C.C., j. sci. Instrum. 42 (1965) 42.

BANDSAW - A PROPOSAL FOR REMEASURING DELAYED NEUTRON ENERGIES, YIELDS AND HALF-LIVES IN AFSR-TYPE REACTORS†

G.S. BRUNSON AND R.J. HUBER**
ARGONNE NATIONAL LABORATORY,
IDAHO FALLS, IDAHO,
UNITED STATES OF AMERICA

Abstract

BANDSAW - A PROPOSAL FOR REMEASURING DELAYED NEUTRON ENERGIES, YIELDS AND HALF-LIVES IN AFSR-TYPE REACTORS. Traditionally, delayed neutrons have been measured by means of a 'rabbit' experiment in which a sample of the fissionable isotope is irradiated in a neutron flux and rapidly transferred to a neutron counting geometry. Here we consider attacking the problem by means of a 'long foil' sample in the form of an endless tape passing bandsaw fashion through the 'glory hole' of a small reactor such as the Argonne Fast Source Reactor. This new approach in a field that has not really been examined since the Los Alamos work was completed nearly ten years ago, has a number of advantages: It permits of delayed neutron counting under steady-state conditions; there is a chance of observing very short-lived delayed neutrons that might have been overlooked in a rabbit experiment; and it provides by a very wide margin the best look yet at delayed neutron energies. An endless uranium bearing sample tape runs at a constant speed through the glory hole of AFSR and then through a neutron counting geometry located as closely as possible to the reactor core. At various tape speeds the various delayed neutron groups attain their maximum emphasis. The design of a suitable uranium bearing tape and the best detector arrangement using a ^{3}He-filled proportional counter operating into a multichannel pulse-height analyser are discussed in detail. Such a system would enable the calculation of relative yields, and the data can be re-analyzed for delayed neutron energies. The same equipment used with a gamma spectrometer can be used to analyse the energies of early fission fragment decay gammas. This is of particular value in the calculation of delayed photo-neutron production in reactors containing beryllium or heavy water. Obviously, the overwhelming quantity of data produced by Bandsaw does offer considerable advantage in determining yields and decay constants. Nevertheless, the outstanding advantage of the method is that it permits steady-state measurement of delayed neutron spectra. The most suitable sites for performing the experiment are reactors of the AFSR type. However, ^{235}U might be investigated in almost any university reactor thermal column if cadmium tubing is used to define the region of irradiation.

INTRODUCTION

The purpose of this paper is to examine a fresh approach to the problem of delayed neutron yield, period, and energy measurements. Traditionally, delayed neutrons have been measured by means of a "rabbit" experiment in which a sample of the fissionable isotope is irradiated in a neutron flux and rapidly transferred to a neutron counting geometry. The difficulty of this method is that the parameters describing the rapid decay at early times must be determined from relatively little data. We consider attacking the problem by means of a long foil sample in the form of an endless tape passing bandsaw fashion through the glory hole[1] of a small reactor such as

† Work done under the auspices of the USAEC.
* Now at International Atomic Energy Agency, Vienna.
** Now at General Instruments, Salt Lake City, Utah, USA.

the Argonne Fast Source Reactor [1]. This new approach, in a field that has not really been examined since the Los Alamos work [2] was completed nearly ten years ago, has a number of advantages: [1]

(a) It permits delayed neutron counting under steady-state conditions.
(b) There is a chance of observing very short-lived delayed neutrons that might have been overlooked in a rabbit experiment.
(c) It provides by a very wide margin the best look yet at delayed neutron energies.

Present information on delayed neutron energies is very unsatisfactory, and the published results are both old and discordant [3]. With the advent of plutonium reactors in which there is a large fraction of ^{240}Pu, better delayed neutron energy data is increasingly important. There could be a considerable effect on calculated β_{eff}, depending on whose data are used. Burgy et al. [3], place most of the delayed neutrons above the ^{240}Pu threshold. Batchelor [3], on the other hand, places most delayed neutron energies at the borderline with respect to the threshold and does not estimate the energies for groups five and six.

DESCRIPTION OF THE EXPERIMENT

The experimental arrangement is shown schematically in Fig. 1. An endless uranium bearing sample tape of length L runs at a constant speed v through the glory hole of AFSR and then through a neutron-counting geometry at a distance D from the edge of the core. The expected delayed neutron production rate, R(v), per gram of tape sample at the counter position is given by the expression

$$R(v) = \overline{FR} \sum_{i=1}^{N} Y_i \frac{(1 - e^{-\lambda_i d/v}) e^{-\lambda_i D/v}}{(1 - e^{-\lambda_i L/v})} \qquad (1)$$

where $\overline{FR}$ is the fission rate per gram of fuel averaged along the sample path, Y_i is the absolute delayed yield per fission of the ith group, and d is the core diameter. This equation considers the reactor flux to be rectangular in shape. A more realistic shape, e.g. cosine, will make a minor change in the form of this equation but has no tangible effect on the value of the experiment. The denominator accounts for residual precursors left from earlier passes through the core. Figure 2 shows R(v) versus v and the contribution of each of Keepin's [2] six delayed neutron groups for a specific case in AFSR. The arrows indicate the velocities at which the various delayed neutron groups attain their maximum emphasis (Best Look Point) measured as a percentage of the total delayed neutron production rate. The only exception is group 1, for which we arbitrarily indicate the velocity at which it contributes 95% of the total delayed neutron production. Calculations indicate that the best location for the neutron detector is as close as possible to the reactor. Some small improvement might be obtained by taking differences between count rates observed simultaneously at two different distances.

---

[1] Glory hole: a small-diameter hole penetrating the entire reactor in a straight line and passing through the centre of the core.

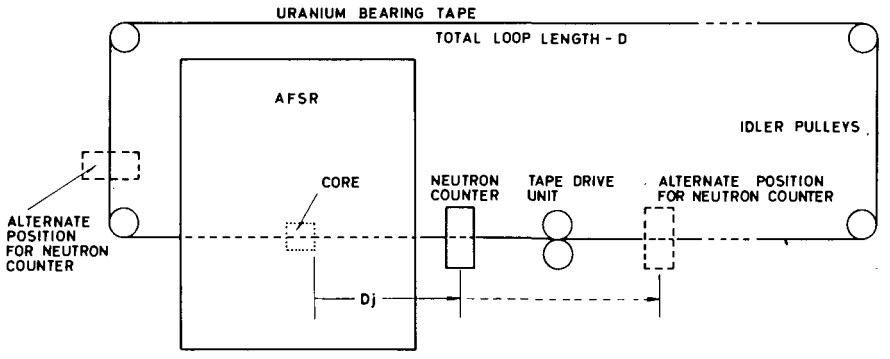

FIG. 1. Schematic diagram of EPEE experiment.

Between the 'rabbit' and 'long foil' methods, there is not much difference in emphasis that can be placed on the individual delayed neutron groups. However, with the steady-state counting of the long foil the quantity of data available is much greater. For example, Keepin [2] used 80 burst and 80 saturation irradiations to determine the delayed neutrons from fast fission of ^{235}U. The four shorter lived groups were determined from the burst irradiations; thus, his total counting time in the interval between 0.050 and about 1 sec (during which the count rate is changing rapidly) is only about $1\frac{1}{4}$ min. Yet, it is on this limited quantity of data that groups five and six depend. By contrast, the 'long foil' provides steady-state counting in any time region.

It appears that the best detector arrangement would be a ^{3}He-filled proportional counter operating into a pulse-height analyser. The ^{3}He cross-section [4] changes by less than a factor of two between 200 keV and 1 MeV, so that a computer-applied cross-section correction will produce effectively a 'long counter' response for yield measurements. In addition, it provides a method of identifying and subtracting low-energy room-return neutrons. After the relative yields have been calculated, the same data can be re-analysed for delayed neutron energies.

Substitution of a gamma spectrometer permits of the analysis of the energies of early fission fragment decay gammas. This is of particular value in the calculation of delayed photo-neutron production in reactors containing beryllium or heavy water.

ANALYSIS OF DATA

The feasibility of obtaining the various delayed neutron group yields and periods from the data generated in this experiment has been investigated. Numerous sets of synthetic data were generated by calculating the count rate versus velocity expected from the data of Keepin. Typically, over 100 different velocities were used. The expected count rates were then converted to synthetic data by adding to each expected count a number drawn from a pseudo-random distribution having an average value zero and a variance equal to the expected count. By scaling the calculated expected counts, sets of synthetic data were generated which have 'counting

TABLE I. RESULTS OF SYNTHETIC DATA ANALYSIS

Uncertainty in Keepin Data * for U-235 Fast Fission					Yield 1 7.9	Yield 2 2.3	Yield 3 8.5	Yield 4 1.7	Yield 5 6.2	Yield 6 11.5	Lambda 1 1.6	Lambda 2 2.5	Lambda 3 2.6	Lambda 4 2.6	Lambda 5 5.8	Lambda 6 9.5
Parameters for Synthetic Data					Estimated Percent Uncertainty in Specified Parameter *											
	Length Tape (m)	Data Quality	Number of Data Points	Range of Velocities m/sec												
1	100	1 %	49	0.005 - 60.0	3.7	2.3	12.6	4.8	9.4	65.6	1.0	1.7	9.6	5.3	13.1	18.5
2	∞	1 %	138	0.003 - 60.0	0.9	1.0	7.4	2.7	5.1	38.4	0.2	0.6	4.4	3.4	9.2	17.4
3	100	1 %	138	0.003 - 60.0	0.9	1.0	7.5	2.7	6.2	45.6	0.2	0.6	4.4	3.5	10.0	19.3
4	∞	0.3 %	138	0.003 - 60.0	0.3	0.3	1.8	0.7	1.3	9.8	0.05	0.2	1.2	0.8	2.4	4.6
5	∞	0.3 %	124	0.003 - 20.0	0.3	0.3	1.8	0.7	1.4	10.1	0.05	0.2	1.2	0.8	2.4	6.6
6	100	0.3 %	138	0.003 - 60.0	0.3	0.3	1.8	0.7	1.4	10.2	0.05	0.2	1.2	0.9	2.4	5.2
7	100	0.3 %	124	0.003 - 20.0	0.3	0.3	1.8	0.7	1.4	10.2	0.05	0.2	1.2	0.8	2.4	6.9
8	100	0.3 %	127	0.007 - 60.0	1.9	0.3	1.9	0.8	1.4	10.6	0.7	0.5	1.5	0.9	2.5	5.5
9	100	0.3 %	92	0.003 - 55.0	0.4	0.4	2.3	0.9	2.2	15.8	0.07	0.2	1.5	1.1	3.6	7.6
10**	50	0.3 %	138	0.003 - 60.0	0.3	0.3	1.8	0.7	1.5	10.8	0.05	0.2	1.2	0.9	2.5	6.0
11	50	0.3 %	127	0.007 - 60.0	1.9	0.35	1.9	0.8	1.5	11.2	0.7	0.5	1.5	0.9	2.6	6.3
12	50	0.3 %	92	0.003 - 55.0	0.4	0.4	2.3	0.9	2.2	15.8	0.07	0.2	1.5	1.1	3.6	7.6
13	25	0.3 %	138	0.003 - 60.0	0.3	0.3	1.8	0.7	1.6	12.1	0.05	0.2	1.2	0.9	2.7	7.2
14	25	0.3 %	127	0.007 - 60.0	1.9	0.35	2.0	0.8	1.7	12.5	0.7	0.5	1.5	1.0	2.9	7.6
15	100	0.1 %	138	0.003 - 60.0	0.1	0.1	0.6	0.2	0.5	3.9	0.02	0.06	0.4	0.3	0.9	1.6
16	50	0.1 %	138	0.003 - 60.0	0.1	0.1	0.6	0.2	0.6	4.3	0.02	0.06	0.4	0.3	0.9	1.8

* Values for yields refer to relative yields $\delta_{i/3}$

** Recommendsd design

statistics' of 1%, 0.3%, and 0.1%. The pseudo-random number distributions were generated by a digital computer technique based on the power residue method [5].

Equation (1) was fitted to the synthetic data by a non-linear least squares iterative technique (Gauss method) [6, 7], yielding estimates of twelve parameters (six yields and six periods) and the variance of each estimate. Application of this process to the several sets of synthetic data has given estimates of the range of tape velocities, number of data points, statistical accuracy of the counting data, and total tape length required for the experiment. The results of our analysis of the synthetic data for 16 different cases are given in Table I. The uncertainties indicated for both Keepin and Bandsaw yields refer only to the relative yields β_i/β.

There is nothing sacred about a six group analysis of delayed neutrons. We merely use it as the best information available on which to base an evaluation of this experiment. In the actual analysis of data we would have to repeat Keepin's steps in 'trying-on' various numbers of groups to best represent the data. A tape of length 50 metres, velocities covering a range of 0.3 cm/sec to 60 m/sec, and 138 points of 0.3% data constitute an experiment which could improve significantly on the current delayed neutron yield and period data.

The marked improvement in uncertainty for the longer lived groups merely reflects the overwhelming quantity of data produced by the bandsaw as compared with the rabbit. However, the outstanding advantage of this technique lies in opportunity to measure delayed neutron energies. Other determinations of delayed neutron energies have involved data 'peeling' both in time and energy to assign spectra to specific groups. In this case we can have abundant data at any desired tape speed. We can take spectra at each of the best look points and, starting with group 1, work toward group 6 peeling only with respect to energy. This should produce spectral information immeasurably better than any now available.

EXPERIMENTAL CONSIDERATIONS

The most suitable sites for performing the experiment are reactors of the AFSR type (including AFSR, HARMONIE [8] at Cadarache, TAPIRO [9], projected for Italy, and CORAL-1 being build in Spain [10]). However, ^{235}U might be investigated in almost any university reactor thermal column if cadmium tubing is used to define the region of irradiation. The ^{235}U experiment might even be performed in the Aerojet General AGN-201 reactor. At 10 watts, it has about 40% the per gram fission rate of the AFSR at 1 kW.

The AFSR is particularly suitable for a number of reasons. The shielding permits mounting counters as close as 2 m from the core and therefore, with high tape speeds, permits counting very soon after irradiation. The flux intensity and hardness are adequate for delayed neutron measurements not only with ^{235}U but also with ^{238}U and thorium. Plutonium and ^{233}U so far have not been considered because of radiological hazards. Calculations show (see Fig. 2) that for the AFSR core, more than 10^7 neutrons per second per gram of ^{235}U can be produced in a counting geometry 2 m from the core. A counting arrangement suitable for energy measurements (e.g. a 3 atm ^3He proportional counter of 2 in. dia. by 8 in. long, viewing

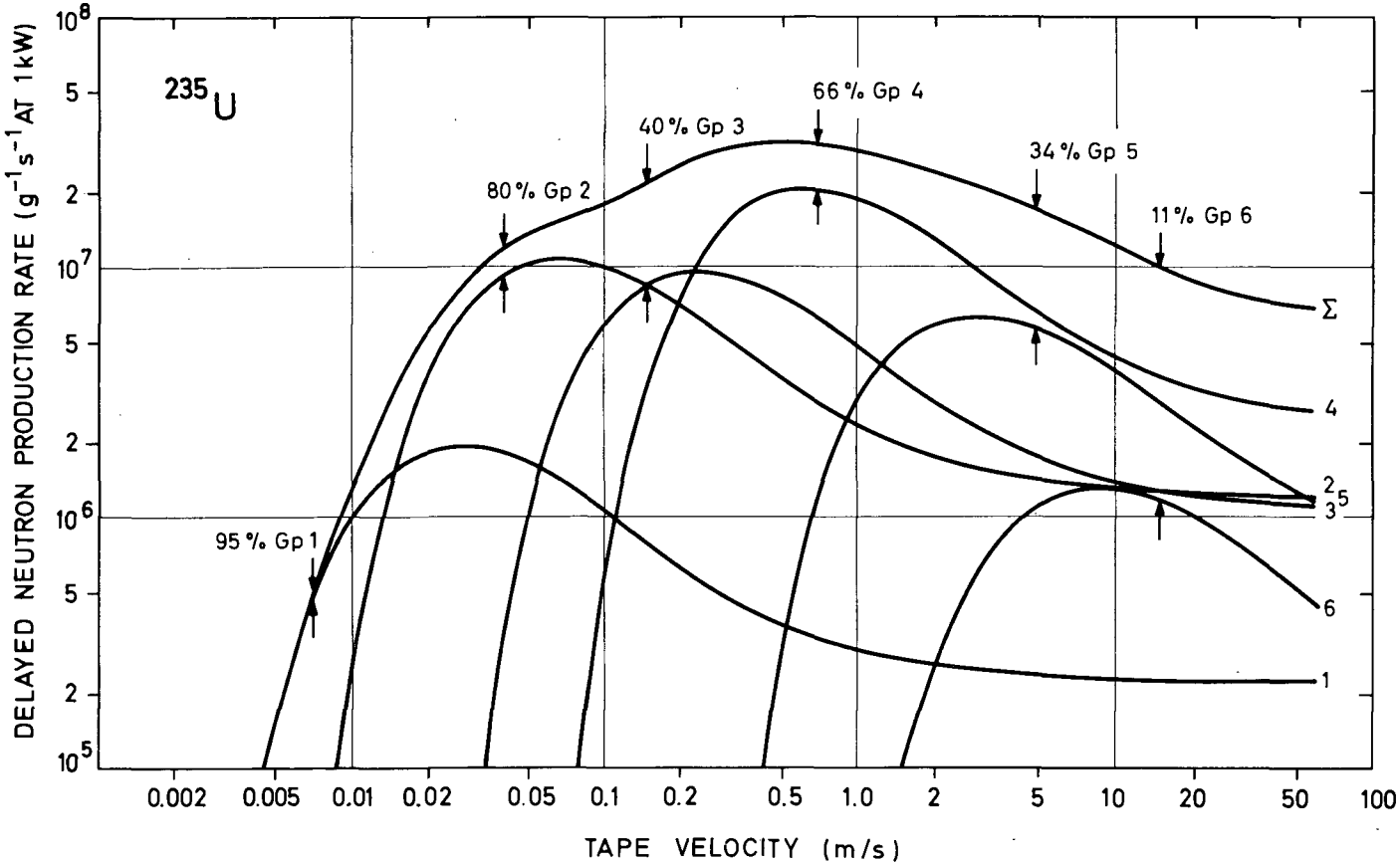

FIG. 2. Delayed neutron production rate at 1 kW reactor power, the counter located 2 metres from the core using a 50 metre tape.

a 4 in. long section of tape loaded with 0.5 g/in. of ^{235}U) is expected to yield about 100 counts/sec. This is a steady-state count rate. For ^{238}U, this rate would be reduced by about a factor of three (again for AFSR), and the rate for thorium would be down by a factor of about ten. Steps such as increasing tape loading or improving counting geometry can compensate for this lower rate.

The fabrication of a suitable uranium bearing tape appears feasible. One such design is a stainless steel tape ($\sim$ 0.4 in.$\times$ 0.025 in) loaded with 12 half-gram uranium rivets per foot. At 60 m/sec, this tape must have a tension of about 60 lb to make it follow a pulley. This is a tensile stress of about 9000 lb/in^2. This tape design, while not optimum, seems attainable without the effort necessary to produce a satisfactory uranium alloy tape.

The tape could be driven between a pair of opposed smooth tread pneumatic wheels and its velocity obtained by counting rivet heads photoelectrically. It would be guided through the glory hole by a guide assembly of aluminium bronze which is especially compatible with stainless steel. The guide would so nearly fill the glory hole as to prevent any pile-up there of uranium rivets in case of an accident.

We prefer an experiment using a 50 m tape at about 138 velocity points from 0.003 m/sec to 60 m/sec. It can be seen from Table I (comparing cases 6 and 10) that a hundred-metre tape does not improve the results much. On the other hand, going to a 25 metre tape (case 13) does show some disadvantages in determining parameters for groups 5 and 6.

Comparison of cases 6 and 7 shows an encouraging result. In case there are mechanical problems with the tape, the maximum tape velocity can be lowered to 20 m/sec with almost no loss in precision (except for group 6). The principal reason we suggest 60 m/sec as the upper limit, is the hope of seeing new short-lived groups. Similarly (comparing cases 10 and 11), cutting a few points off the lower end of the velocity range degrades group 1 results badly. Comparison of cases 10 and 12 reveals the detrimental effect of trying to reduce the number of counting velocities.

Absolute delayed neutron yields are an essential part of the experiment. An absolute fission counter would be used to determine fission rates along the sample path as a function of count rate in a high precision monitor. The absolute counter sensitivity would be obtained by stepwise counts of a known neutron source along the sample path. Even though the source neutrons differ widely in spectrum from delayed neutrons, the method of taking data in a ^3He spectrometer permits computer normalization to delayed neutron energies.

This is not a costly experiment. Ordinary pulse-height analysers are generally available. It is important to have adequate computer support for non-linear least-squares fitting of multiple parameter functions. The only specialized items required are the tape sample, the tape drive, and the ^3He detectors.

FURTHER CONSIDERATIONS

1. Consideration must be given to the effects of non-uniform tape loading. It seems that counts involving several complete circuits of the

tape will average out the loading. At very slow tape speeds non-uniformity might affect results. The reactor itself could be used to investigate loading uniformity by observing reactivity changes as the tape is moved slowly through the glory hole.

2. Attention must also be given to the problem of background due to delayed neutrons coming from sections of the tape not in the counting geometry. The AFSR is located in a low mass metal building in which it was hoped that the backscattering would be tolerable. In that case only minimal shadow shielding would be necessary to define the section of tape being counted. If on the other hand the background must be reduced, shields of ^{10}B and H (paraffin or polyethylene) would be installed. Since the counting channel as outlined above can discriminate against low energy neutrons, a reasonable number of background neutrons can be tolerated if they are back-scattered only by hydrogenous material.

3. Although one hopes for a linearly homogeneous tape and ultimately for tapes loaded with plutonium and ^{233}U, these seem remote for the present.

REFERENCES

[1] BRUNSON, G.S., Design and Hazards Report for the Argonne Fast Source Reactor (AFSR), ANL-6024 (June 1959).
[2] KEEPIN, G.R., WIMETT, T.F., ZEIGLER, R.K., Delayed neutrons from fissionable isotopes of uranium, plutonium, and thorium, J. nucl. Energy 6 1 (1957).
[3] ARGONNE NATIONAL LABORATORY, Reactor Physics Constants, ANL-5800, 2nd ed. (July 1963) 19.
[4] BROOKHAVEN NATIONAL LABORATORY, Neutron Cross-Sections, BNL-325.
[5] BROWN, R.G., Statistical Forecasting for Inventory Control, McGraw-Hill, New York (1959) 164.
[6] MOORE, R.H., ZEIGLER, R.K., The Solution of the General Least Squares Problem with Special Reference to High-Speed Computers, LA-2367 (March 1960).
[7] GIPSON, D.H., Phillips Petroleum Co., Atomic Energy Division, Program No. 40.0127.
[8] SCHMITT, A.P., CEN de Cadarache, private communication.
[9] GANDINI, A., Comitato Nazionale per l'Energia Nucleare, Italy, private communication.
[10] Nucleonics (November 1965) 28.

DISCUSSION

On the papers by Chrysochoides et al., and Brunson and Huber

The advantages of a bandsaw system as proposed in Brunson's paper, were discussed.

With a bandsaw set-up, the on-off cycle typical of any rabbit system is avoided. Data can be taken simultaneously, resulting in a higher system yield. With the proposed system and using an appropriate computer, a good separation of delayed neutron groups could be obtained.

Although the bandsaw idea was developed for an AFSR-type reactor, the same system could be used in a thermal column of any reactor. Some estimation for an AGN-201 reactor (several watts of power) was made and the results show that the bandsaw system could be used in such a reactor.

In the experiment on delayed neutron energy determination as described by Chrysochoides the main problem is the extremely high beta counting rate. The number of signals from the beta detector, which serve as start pulses for the time-of-flight measurement, is about a million times larger than the number of detected neutrons. This results in a high number of random coincidences which can even screen the true coincidences. Another problem is the high sensitivity of the neutron detectors to gamma rays.

Several possibilities for improving the experimental technique were discussed. A promising approach would be to invert the time measuring signals. The signals from the beta ray detector would be stored in a delay line, the neutron signal would be used as a start trigger, the beta ray preceding the neutron emission would be determined, and the time elapsed measured.

Using a discriminator for the beta ray signals, only those beta rays which exceed a certain energy could be used to trigger the time measurement. Such a procedure would substantially reduce the number of 'useless' beta rays which do not precede a neutron emission and only cause a high background. But the use of such a discriminator might also be dangerous since not enough is known about the distribution of energy in the emission of an electron and a neutron. Only for the 55 sec group do the measurements of Perlow and Stehney give a good value for the endpoint of the beta energy spectrum (2.1 MeV).

For the discrimination between neutron and gamma ray signals from the neutron detector, the present detectors used by the Democritus group are not very satisfactory, The boron-loaded-liquid neutron-detector would be much less sensitive to gamma rays but could not be used in this experiment since the neutron slowing-down process in such a detector is much too slow to be used in fast coincidence measurements. A suitable lead shield might improve the neutron-to-gamma ratio substantially.

SUMMARY

Aspects of delayed neutron research of interest for reactor operation

Today we are facing a great expansion in fast-breeder reactor development, and it is becoming increasingly important to have specific data on the yields, and particularly on the energy spectra of delayed neutrons. Prompt neutron numbers and spectra have been investigated rather thoroughly and are in a reasonably satisfactory state as regards reactor physics and design calculations. However, detailed measurements of delayed neutron yields and energy spectra have largely been neglected for the last ten years. But now, in order to determine detailed kinetic behaviour and control of fast power-breeder systems, reactor designers and reactor physicists have direct need for more extensive and detailed delayed neutron data, particularly the (poorly known) energy spectra.

In his paper, Keepin showed how basic delayed and prompt neutron fission data enter into detailed reactor calculations. It was shown that the most important reactor kinetics parameter is the effective delayed neutron fraction, which determines the margin of control and therefore the safety of a reactor. In ^{235}U thermal systems this fraction is often near 0.0065 (the value for pure ^{235}U) because in such systems fissions occur in ^{235}U.

Typical fast breeder systems will employ ceramic fuels such as plutonium-uranium mixed oxides or these oxides enclosed in a ^{238}U blanket designed to breed ^{239}Pu via neutron capture in the ^{238}U. In the relatively fast neutron spectra of such reactors a significant fraction of total fissions may occur in ^{238}U because of their relatively high yield per fission. The ^{238}U delayed neutrons could thus dominate the kinetic behaviour of the system, or in any case play an important role in the control characteristics of the breeder reactor.

In the years to come, there will be more work on the $^{233}U/Th$ breeding cycle. Here again, ^{232}Th has an order of magnitude higher delayed neutron yield than ^{233}U and in a fast-spectrum system both the delayed neutron yields and the relative importance of delayed neutrons from ^{233}U and ^{232}Th is of direct concern in reactor kinetics, control and safety.

The high burn-up breeder reactors (Pu-U cycle) of the future will produce not only ^{239}Pu but also ^{240}Pu, ^{241}Pu, etc. in significant quantities. The delayed neutrons from these higher neutron/proton ratio species will inevitably affect the kinetics, the safety and control characteristics of such high burn-up breeder reactors. Therefore some measurements should be made on the delayed neutron periods and abundances of these higher-mass plutonium isotopes.

In any reactor where precursors are transported out of the core region, there is a corresponding loss of reactor control. Notable cases are nuclear propulsion reactors where the coolant-propellant gas (liquid H_2 in two-phase flow) rapidly sweeps gaseous precursors out of the system, with a corresponding reduction in the reactor control margin. In very high temperature reactors, the selective diffusion of one precursor over another can result in unexpected kinetic response problems. In such cases, it is desirable to know the chemical identity of the escaping or diffusing delayed neutron precursors.

Delayed neutron data currently needed for nuclear technology applications include:

1. Gross delayed neutron spectra (steady-state or modulated)

2. Individual delay-group spectra (using time-separation techniques, including various combinations of irradiation-, wait- and observation-times to accentuate various delay groups, and then resolving individual group spectra by computer methods. Also spectrum measurements using available chemical and physical methods for separation of light and heavy fragments, halogens and non-halogens, etc.)

3. Absolute delayed neutron yields as a function of incident neutron energy (up to 14 MeV)

4. Periods and yields of delayed neutrons from fission species not yet studied in sufficient detail or not studied at all.

Nuclear structure aspects of delayed neutron research

Looking at the present knowledge of delayed neutron emission and precursors, from a nuclear spectroscopy and fission reaction point of view, rather unsatisfactory conditions are seen to exist. Further research will not be feasible before some results of crucial experiments are available.

In nuclear research, studies of delayed neutrons are important in two respects: in nuclear structure studies and in investigations of nuclear reactions. In structure problems, delayed neutron studies will be complementary to studies of delayed protons which are being done in other projects – ISOLDE, CERN, in Dubna, etc.

Study of delayed neutrons will not only give information on delayed neutron processes but will also bring results of interest in nuclear structures in general. Depending on the accuracy of the results, one might hope that some information will be gained on the matrix element, the level density function, and data on the competition between neutron and gamma emission for different types of nuclei.

The Panel showed that studies of different fission processes give valuable information on delayed neutron precursors and emitters. An opposite approach could be taken to study different fission processes by using delayed neutrons not only from different fissioning nuclei, but also at various energies from thermal to a few hundred MeV. The P_n-value of delayed neutron precursors should be characteristic for each species, independent of its formation in the fission process. Thus if the P_n-values of single precursors are available, it should be possible to estimate the yields of these precursors and also to obtain an idea of competition among the different types of fission. The yields of precursors will reflect the process in which they are produced.

The experimental results which could supply important information are:

1. Single delayed neutron spectra (group spectra are not so important for spectroscopy), as the general shape of the spectra is an indicator of the evaporation energy of the neutrons.
2. Periods and yields not only for uranium and plutonium, but also for other species such as ^{231}Pa and other elements lighter than uranium.

3. The most detailed picture possible of the spectra and if possible a knowledge of whether there are line spectra (if the resolution can be made good enough). The lower part of the spectrum and its structure may give information on level densities. It would be advantageous to know if neutrons are followed by gammas. Experimentally this means n-γ-coincidence measurements, or even better, β-γ-n-coincidence measurements. These would give information on spin and parities involved, and on the levels in the final product. The experiments will prove extremely awkward.

Experimental aspects of delayed neutron studies

The experimental approach to delayed neutron studies must be motivated by two major factors. First, there is the practical importance of delayed neutron studies for reactor design, particularly for those reactors where detailed delayed neutron yield and spectral data are necessary for understanding and predicting the dynamic behaviour. Second, there is the importance of studying delayed neutron emission as an integral part of our attempt to understand nuclear structure and the mechanism of nuclear fission. Clear objectives should be established and understood before starting any experiment.

The most interesting experimental approaches are listed below:

Aggregate experiments provide group half-lives, group abundances, and group energy spectra. These basic data are required by the reactor designers. Such systematic experimental studies have been performed by Keepin and are being extended now by different groups. With a rabbit, bandsaw or other type of conveyer, and with an adequate computer, good values could be obtained of group half-lives or abundances. Using neutron spectrometry (time-of-flight ^{3}He or n, p spectrometers with pulse-shape discrimination) the energy spectra can be measured.

For identification and characterization of delayed neutron precursors several experimental approaches could be used. One is the chemical, i.e. element, separation. Very fast chemistry techniques must be used, most of them involving the gas-sweeping techniques (which seem to be the fastest) starting with a specific chemical reaction at the target, e.g. as with antimony or arsenic hydride or rare gases. Another type of chemistry is recoil chemistry. This is 'instantaneous chemistry'. A certain compound can be labelled and then be rapidly removed and brought to the counting assembly, particularly if it is in the gaseous phase. A precipitate method was mentioned in the panel discussions and it was shown (by the Mainz group) that, if modified to provide rapid isotopic or ion exchange with preformed precipitates, the method can provide much information.

On-line mass spectrometric studies or on-line isotopic separator studies do not employ purely physical techniques. Even there chemistry does take place in a 'non-chemical' way, i.e. in the fissioning source itself. For example, surface ionization of the alkalies serves as a criterion of selectivity, as only the alkalies are emitted in an ionized form from the hot source and transported electrostatistically through the magnetic analyser. Such techniques aid quick measurement (μsec range), except that the diffusion time is still of the order of milliseconds. This method

could be extended from alkalies to other elements and could provide isotopic and elemental separation of numerous nuclei. At the same time, the on-line separator programmes are being established, both with accelerators (like ISOLDE in CERN) or near reactors (TRISTAN, SOREQ, etc.). These separators introduce the problem of chemistry that should be performed before the ion source, very fast chemistry, fast transfer, and the problem of introducing the separated element, through a very great pressure drop, into the ion source. The magnetic analysers should also be mentioned; these are not isotopic but isobaric separators, giving a separation of e/M. Such experiments give an excellent orientation as to where one should look for delayed neutron precursors and what the relative abundance of these species at different mass and half-life ranges is. They can indicate where further work should be done in order to get better nuclidic assignments and more precise nuclear data. There are other similar 'exploratory' experiments, for example, the double recoil collection from which rough information on masses and half-lives can be obtained.

By studying delayed neutrons the structure and mass of the nucleus and the different modes of decay can be obtained, this information being very valuable for the case of delayed neutron emitters since all of them are nuclides far off stability and very little is known about them. Also, delayed neutron studies can provide the answer to some problems in fission, especially for low energy fission, where nuclear structure can be responsible for certain fine structure in the mass and charge distributions of fission fragments.

ANNEX

SUMMARY OF EXPERIMENTAL DATA ON DELAYED NEUTRON PRECURSORS BASED ON REPORTS TO THIS PANEL*

Compiled by P. del MARMOL

A large amount of new evidence concerning individual delayed neutron precursors has been brought forward by the panel on delayed fission neutrons. It would appear to be helpful for future work to summarize the available experimental data concerning charge, mass and half-life attributed to and the relative contributions of individual delayed neutron precursors as presented in the literature and papers discussed during this meeting. Delayed neutron precursors predicted by various mass formulae, coupled with half-lives of gross delayed neutron decays, have not been included. Also omitted are the data concerning ^{210}Tl and nuclides of low mass number (^{8}He, ^{9}Li, ^{12}B, ^{16}C, ^{17}N) which do not appear in binary fission and were not discussed during the meeting.

It is realized that certain results are still preliminary. However, the following table is presented to give a simple indication of the pertinent literature and it can serve as basis for future improvement.

New experimental evidence has been reported during the meeting for the existence of delayed neutron precursors in the region of mass number 96 [23]; these results are not included in the table owing to the present uncertainty as to the individual elements.

To avoid excessive listing only the references of papers which led directly to charge, mass and best half-life results are given.

It was hoped that this table could be arranged to include the measured neutron emission probabilities (P_n) of individual isotopes, as they are important nuclear parameters. However their values sometimes differ widely, as they are often subject to different semi-empirical fission charge distribution calculations or are dependent on measurements of different reference isotopes. Thus it was found more realistic to send the reader to the individual papers presented at this panel for P_n-value reviews or estimations. P_n-values for bromine and iodine isotopes are the most extensively reviewed and new data are presented in Ref. [19]. P_n-values calculated by least-squares analysis of seven fission reactions by Herrmann [19] can be compared with those measured by Aron et al. [21] and Perlow and Stehney [9], noticing that in the latter case the halogen delayed neutron activities are measurements relative to ^{87}Br or ^{137}I. The agreement is good in the case of ^{87}Br and ^{88}Br; the calculated value for ^{87}Br ($P_n = 2.63 \pm 0.05$) free of interference from ^{86}Br with similar half-life is probably the best value for this isotope. Experimental P_n-values for other delayed neutron precursors are usually related to ^{87}Br with the exception of the iodine delayed neutron precursors which are correlated

* Panel Meeting on Delayed Fission Neutrons, Vienna, 24-27 April 1967.

to ^{137}I, so it is also important to have a precise value for this isotope. The value calculated by Herrmann [19] and confirmed by an experimental measurement is higher than the one measured by Aron et al. [21]. The disagreement between P_n-values of shorter-lived bromine and iodine isotopes is large, suggesting a need for further experiments in this region.

P_n-values for arsenic and antimony are given in Refs [13] and [16]. Relative P_n-values for rubidium isotopes and orders of magnitude for caesium isotopes are reported in Ref. [15]. These can be changed into absolute values through the P_n measurements of ^{93}Kr and ^{93}Rb of Amiel et al. [13]; however, one then obtains more delayed neutrons than experimentally observed, as discussed in the paper and where P_n readjustments are proposed. On the other hand Herrmann [19] found a lower P_n-value for ^{93}Rb which could lead to a better correlation.

Description of the Table

The first column presents the delayed neutron precursor in order of increasing charge and mass, followed in the second column by the references of the work that led to the assignments.

The third column gives 'best available' half-life values for the delayed neutron precursors presented. They are based on what was believed the most reliable neutron or β-decay measurements of isolated elements or isotopes. For instance in the case of ^{87}Br only values based on neutron counting were taken into consideration owing to the existence of ^{86}Br of similar half-life. In no case were these values based on predicted components of neutron gross decay curves. When more than one reference is given the weighted averages were taken ($\propto 1/\sigma^2$); the overall standard deviation was weighted in a similar way. In the case of ^{93}Rb it was not possible to choose between the two quoted values as their standard deviations did not overlap.

The fourth column gives a qualitative estimate of the individual delayed nitrogen precursor contributions to the total delayed neutrons emitted in ^{235}U thermal neutron fission. They are classified by letter symbols defined as follows:

A: Major contributor; $\geq$ 5.6 neutrons per 10^4 fissions. This limit was arbitrarily chosen so as to include ^{87}Br.

B: Minor contributor; 1 to 5.5 neutrons per 10^4 fissions.

C: Weak contributor; < 1 neutron per 10^4 fissions.

It is to be understood that these values are merely indicative owing to the sometimes large uncertainties in P_n estimates and charge distribution parameters.

The last column is reserved for comments on the evidence for attributing a certain delayed neutron precursor to a specific isotope. In the case of 'no comment' the charge and mass attributed is taken as reliable owing to agreement between results of measurements on delayed neutrons and either β-decay half-lives of known isotopes or on-line mass-separator data.

EXPERIMENTAL DATA ON DELAYED NEUTRON PRECURSORS

Assignment	Reference	Half-life (sec)	Class *	Comments
As-85	[1, 2]	2.10 ± 0.12 [1, 2]	B	As-87 excluded as its $T_{\frac{1}{2}} \leq 1.5$ s and As-85 prefered to As-86 on fission mass yield arguments [2].
Br-87	[3, 4, 5]	55.67 ± 0.20 [6, 7]	A	An upper limit of 0.5% is set by [6] to any contribution of other d.n.p. with half-lives of 55 s or longer.
Br-88	[8]	15.85 ± 0.10 [4, 7, 8, 9]	A	
Br-89	[9, 10]	4.46 ± 0.31 [7, 9]	A	Mass assignment based on *similarities in* half-life decrease of bromine and iodine isotopes [9]; independent fission yield of 4.5 s Br as measured by [7] in agreement with that expected for Br-89. Other mass assignments for these activities would lead to unrealistic results for delayed neutron abundance calculations [22]
Br-90	[9, 10]	1.6 ± 0.6 [9]	A	Mass assignment based on similarities in half-life decrease of bromine and *iodine* isotopes [9]
Kr-91	[11]	8.36 ± 0.15 [12]	C	On-line mass separator shows for Kr low neutron activity with $T_{\frac{1}{2}} \sim 8$ s at mass 91 [11]; not observed by [13] and [14].

Kr-92	[11]	1.92 ± 0.07 [12]	C	On-line mass separator shows for Kr neutron activity with $T_{\frac{1}{2}} \sim 2.0 \pm 0.15$ s at mass 92; 9.7 h Sr-91 γ-rays also observed [11]; not observed by [13]
Kr-93	[11, 13, 14]	1.18 ± 0.04 [12, 13]	B	
Rb-93	[11, 13, 14, 15, 19]	5.89 ± 0.04 [15] 5.60 ± 0.05 [13]	A [13] or B [15, 19]	
Rb-94	[15]	2.67 ± 0.04 [15]	A	A neutron activity with 2.3 s half-life observed by [19] in separated alkalies attributed to Cs with a possible contribution of Rb-94.
Rb-95	[15]	0.36 ± 0.02 [15]	B	
Rb-96	[15]	0.23 ± 0.02 [15]	B	
Sb-134	[16]	~10 s [16]	C	Observed by [16] to follow Sb chemistry and assigned to mass 134 by similarity to Sb-134 half-life [17]. However [18] observed for Sb-134 a $T_{\frac{1}{2}} < 1.5$ s and [2] could not correlate a 10 s delayed neutron half-life with Sb.
Sb-135	[1]	$1.9\ ^{+0.9}_{-0.5}$ [18]	B	Observed by [1] to follow Sb chemistry and assigned to mass 135 by similarity with Sb-135 half-life [18]. Upper limit for a $T_{\frac{1}{2}} \sim 2$ s neutron contribution by [2] does not disagree with this attribution
I-137	[3, 4]	24.4 ± 0.4 [9]	A	

* A: major contributor; ≥ 5.6 n/10^4 fissions – B: minor contributor; 1 to 5.6 n/10^4 fissions – C: weak contributor; < 1 n/10^4 fissions.

EXPERIMENTAL DATA ON DELAYED NEUTRON PRECURSORS (cont.)

Assignment	Reference	Half-life (sec)	Class*	Comments
I-138	[9]	6.3 ± 0.7 [9]	A	
I-139	[9]	2.0 ± 0.5 [9]	A [19] or B [21]	
I-140	[19]	~0.8 s [19]	A	Neutron activity observed with other iodine activities separated by isotopic exchange. Should belong to mass 140 or higher.
Xe-141	[11]	1.70 ± 0.05 [12]	C?	On line mass separator shows for Xe weak neutron activity at mass 141 [11]; Cs-141 ruled out by [15].
Cs-142	[11, 15, 19]	2.3 ± 0.2 [20]	C?	On line mass separator shows weak neutron activity for separated Cs at mass 142 [15]; also observed for separated Xe by [11] who did not exclude Xe-142 as d.n.p.
Cs-143	[15, 19]	1.60 ± 0.14 [15]	C?	On line mass separator shows weak neutron activity for separated Cs at mass 143.

A neutron activity with 2.3 s half-life observed by [19] in separated alkalies attributed to Cs-142 and/or Cs-143 and possibly in part to Rb-94.

* A: major contributor; ≥ 5.6 n/10^4 fissions – B: minor contributor; 1 to 5.6 n/10^4 fissions – C: weak contributor; < 1 n/10^4 fissions.

[1] TOMLINSON, L., J. inorg. nucl. Chem. 28 (1966) 287.
[2] del MARMOL, P., NEVE de MEVERGNIES, M., J. inorg. nucl. Chem. 29 (1967) 273.
[3] SNELL, A.H., LEVINGER, J.S., MEINERS, E.P., Jr., SAMPSON, M.B., WILKINSON, R.G., Phys. Rev. 72 (1947) 545.
[4] SUGARMAN, N., J. chem. Phys. 17 (1949) 11.
[5] STEHNEY, A.F., SUGARMAN, N., Phys. Rev. 89 (1953) 194.
[6] WILLIAMS, E.T., CORYELL, C.D., Nuclear Appl. 2 (1966) 256.
[7] SILBERT, M.D., TOMLINSON, R.H., Radiochem. Acta 5 (1966) 223.
[8] PERLOW, G.J., STEHNEY, A.F., Phys. Rev. 107 (1957) 776.
[9] PERLOW, G.J., STEHNEY, A.F., Phys. Rev. 113 (1959) 1269.
[10] SUGARMAN, N., J. chem. Phys. 15 (1947) 544.
[11] DAY, G.M., TUCKER, A.B., TALBERT, W.L. Jr., these Panel Proceedings.
[12] PATZELT, P., HERRMANN, G., Physics and Chemistry of Fission, (Proc. Symp. Salzburg, 1965) 2, IAEA, Vienna (1965) 243.
[13] AMIEL, S., GILAT, J., NOTEA, A., YELLIN, E., these Panel Proceedings.
[14] STEHNEY, A.F., PERLOW, G.J., Bull. Am. phys. Soc. II 6 (1961) 62.
[15] AMAREL, I., BERNAS, R., FOUCHER, R., JASTRZEBSKI, J., JOHNSON, A., TEILLAC, J., GAUVIN, H., Phys. Letters 24B (1967) 402.
and GAUVIN, H., these Panel Proceedings.
[16] TOMLINSON, L., these Panel Proceedings.
[17] STROM, P.O., DELUCCHI, A.A., GREENDALE, A.E., private communication to TOMLINSON, L.
[18] BEMIS, C.E., GORDON, G.E., CORYELL, C.D., J. inorg. nucl. Chem. 26 (1964) 213.
[19] HERRMANN, G., these Panel Proceedings.
[20] FRITZE, K., Can. J. Chem. 40 (1962) 1344.
[21] ARON, I.M., KOSTOCHKIN, O.I., PETRZHAK, K.A., SHPAKOV, V.J., Atomn. Energ. 16 (1964) 368.
[22] HERRMANN, G., FIEDLER, J., BENEDICT, G., ECKHARDT, W., LUTHARDT, G., PATZELT, P., SCHÜSSLER, H.D., Physics and Chemistry of Fission, (Proc. Symp. Salzburg, 1965) 2, IAEA, Vienna (1965) 197.
[23] ROECKL, E., EIDENS, J., ARMBRUSTER, P., these Panel Proceedings.

LIST OF PARTICIPANTS

AMIEL, S.	Nuclear Chemistry Department, Soreq Nuclear Research Centre, Yavne, Israel
ARMBRUSTER, P.	Institut fur Festkörper und Neutronenphysik, Kernforschungsanlage Jülich, 517 Jülich, Federal Republic of Germany
BRUNSON, G.S.	Division of Nuclear Power and Reactors, IAEA
CHRYSOCHOIDES, N.G.	Democritus Nuclear Research Centre, Aghia Paraskevi Attikis, Athens, Greece
GAUVIN, H.	Institut de physique nucléaire, B.P. No. 1, 91 Orsay, France
HERRMANN, G.	Institut für Anorganische Chemie und Kernchemie, J. Gutenberg-Universität, Johann Joachim Becher-Weg 24, 6500 Mainz, Federal Republic of Germany
KEEPIN, G.R.	Los Alamos Scientific Laboratory, University of California, P.O. Box 1663, Los Alamos, New Mex. 87544 United States of America
LOTT, M.	CEN de Fontenay-aux-Roses, B.P. No. 6, Fontenay-aux-Roses (Seine), France
MAKSYUTENKO, B.P.	Institute for Physics and Power, Obninsk, Union of Soviet Socialist Republics

del MARMOL, P.	Neutron Physics Department, CEN, Mol, Belgium
PAPPAS, A.C.	Department of Chemistry, University of Oslo, Forskningsvn. 1 Blindern, Norway
ROECKL, E.	Institut für Festkörper und Neutronenphysik, Kernforschungsanlage Jülich, 517 Jülich, Federal Republic of Germany
TALBERT, W.L., Jr.	Institute for Atomic Research and Department for Physics, Iowa State University of Science and Technology, Ames, Iowa 50010, United States of America
TOMLINSON, L.	Chemistry Division, Atomic Energy Research Establishment, Harwell, Berks, United Kingdom

SECRETARIAT

SCIENTIFIC SECRETARY	J. DOLNICAR	Division of Research and Laboratories, IAEA
EDITOR	E.R.A. BECK	Division of Publications, IAEA

IAEA SALES AGENTS

Orders for Agency publications can be placed with your bookseller or any of our sales agents listed below:

ARGENTINA
Comisión Nacional de
Energía Atómica
Avenida del Libertador
General San Martin 8250
Buenos Aires - Suc. 29

AUSTRALIA
Hunter Publications,
23 McKillop Street
Melbourne, C.1

AUSTRIA
Georg Fromme & Co.
Spengergasse 39
A-1050, Vienna V

BELGIUM
Office international de librairie
30, avenue Marnix
Brussels 5

BRAZIL
Livraria Kosmos Editora
Rua do Rosario, 135-137
Rio de Janeiro

Agencia Expoente Oscar M. Silva
Rua Xavier de Toledo, 140-1° Andar
(Caixa Postal No. 5.614)
São Paulo

BYELORUSSIAN SOVIET SOCIALIST REPUBLIC
See under USSR

CANADA
The Queen's Printer
Ottawa, Ontario

CHINA (Taiwan)
Books and Scientific Supplies
Service, Ltd.,
P.O. Box 83
Taipei

CZECHOSLOVAK SOCIALIST REPUBLIC
S.N.T.L.
Spolena 51
Nové Město
Prague 1

DENMARK
Ejnar Munksgaard Ltd.
6 Nörregade
Copenhagen K

FINLAND
Akateeminen Kirjakauppa
Keskuskatu 2
Helsinki

FRANCE
Office international de
documentation et librairie
48, rue Gay-Lussac
F-75, Paris 5e

GERMANY, Federal Republic of
R. Oldenbourg
Rosenheimer Strasse 145
8 Munich 8

HUNGARY
Kultura
Hungarian Trading Co. for Books
and Newspapers
P.O.B. 149
Budapest 62

ISRAEL
Heiliger and Co.
3 Nathan Strauss Street
Jerusalem

ITALY
Agenzia Editoriale Internazionale
Organizzazioni Universali (A.E.I.O.U.)
Via Meravigli 16
Milan

JAPAN
Maruzen Company Ltd.
6, Tori Nichome
Nihonbashi
(P.O. Box 605)
Tokyo Central

MEXICO
Librería Internacional
Av. Sonora 206
Mexico 11, D.F.

NETHERLANDS
N.V. Martinus Nijhoff
Lange Voorhout 9
The Hague

NEW ZEALAND
Whitcombe & Tombs, Ltd.
G.P.O. Box 1894
Wellington, C.1

NORWAY
Johan Grundt Tanum
Karl Johans gate 43
Oslo

PAKISTAN
Karachi Education Society
Haroon Chambers
South Napier Road
(P.O. Box No. 4866)
Karachi 2

POLAND
Ośrodek Rozpowszechniana
Wydawnictw Naukowych
Polska Akademia Nauk
Pałac Kultury i Nauki
Warsaw

ROMANIA
Cartimex
Rue A. Briand 14-18
Bucarest

SOUTH AFRICA
Van Schaik's Bookstore (Pty) Ltd.
Libri Building
Church Street
(P.O. Box 724)
Pretoria

SPAIN
Librería Bosch
Ronda de la Universidad 11
Barcelona

SWEDEN
C.E. Fritzes Kungl. Hovbokhandel
Fredsgatan 2
Stockholm 16

SWITZERLAND
Librairie Payot
Rue Grenus 6
1211 Geneva 11

TURKEY
Librairie Hachette
469, Istiklâl Caddesi
Beyoğlu, Istanbul

UKRAINIAN SOVIET SOCIALIST REPUBLIC
See under USSR

UNION OF SOVIET SOCIALIST REPUBLICS
Mezhdunarodnaya Kniga
Smolenskaya-Sennaya 32-34
Moscow G-200

UNITED KINGDOM OF GREAT BRITAIN AND NORTHERN IRELAND
Her Majesty's Stationery Office
P.O. Box 569
London, S.E.1

UNITED STATES OF AMERICA
National Agency for International Publications, Inc.
317 East 34th Street
New York, N.Y. 10016

VENEZUELA
Sr. Braulio Gabriel Chacares
Gobernador a Candilito 37
Santa Rosalía
(Apartado Postal 8092)
Caracas D.F.

YUGOSLAVIA
Jugoslovenska Knjiga
Terazije 27
Belgrade

IAEA publications can also be purchased retail at the United Nations Bookshop at United Nations Headquarters, New York, at the news-stand at the Agency's Headquarters, Vienna, and at most conferences, symposia and seminars organized by the Agency.

In order to facilitate the distribution of its publications, the Agency is prepared to accept payment in UNESCO coupons or in local currencies.

Orders and inquiries from countries where sales agents have not yet been appointed may be sent to:

Distribution and Sales Group, International Atomic Energy Agency,
Kärntner Ring 11, A-1010, Vienna I, Austria

INTERNATIONAL
ATOMIC ENERGY AGENCY
VIENNA, 1968

PRICE: US $5.00
Austrian Schillings 130.-
(£2.1.8; F.Fr. 24,50; DM 20,-)